

**Autonomic Modulation of Ventricular Repolarization in Long QT syndrome**

by

Dr. Rajkumar Mantravadi

MBBS 1994

MRCP (UK) 2002

Submitted to the

Department of Cardiovascular Sciences

for the degree of

Doctor of Philosophy

University of Leicester

2008

UNIVERSITY OF LEICESTER  
Department of Cardiovascular Sciences

This Thesis was presented

By  
Dr.Rajkumar Mantravadi

It was defended on

14<sup>th</sup> April 2008

And approved by

Prof Godfrey Smith, University of Glasgow

Dr John Mitcheson, University of Leicester

Copyright © by Rajkumar Mantravadi

2008

## **Autonomic Modulation of Ventricular Repolarization in Long QT syndrome**

Rajkumar Mantravadi, MBBS, MRCP (UK)

University of Leicester, 2008

Arrhythmias in Long QT syndrome are known to occur during autonomic activity. The changes in repolarization of the myocardium under autonomic activity are thought to influence arrhythmia mechanisms. Although autonomic modulation of the ventricle is modulated by both humoral and nervous components, yet, due to technical difficulties a detailed understanding of the underlying mechanisms of the neuronal modulation is still elusive. This work is a description of the evolution of a novel model and early results of studies pertaining to the effects of the autonomic nerve stimulation on ventricular repolarization, in the context of long QT pathophysiology. These neuro-cardiology studies were performed using a combination of isolated innervated heart preparation and optical mapping for the first time. Two important repolarization characteristics namely physiological restitution and dispersion of repolarization were studied. The early results suggest that during sympathetic nerve stimulation, physiological restitution curve show unique characteristics of a negative slope at peak heart rates, not reported by classical restitution studies. Also, the action potential duration adaptation at peak heart rates showed heterogeneity over the surface of the myocardium and in addition, exhibited some features of a possible reduction of repolarization reserve, especially during ion channel inhibition. Another set of data obtained using this novel model revealed the autonomic nerve stimulation modulated the dispersion of repolarization in a unique way, and differed from pharmacological autonomic stimulation significantly. Interestingly, preliminary data evaluating the myocardial substrate suggests heterogeneity to be at more than one level i.e. key ion channel distributions, nerve terminal distribution over the myocardium and a possible interaction between them. When the hearts were treated with key repolarization inhibitors, the dispersion of repolarization showed a generically similar response rather than a characteristic response of individual ion currents. In these studies, the substrate changes of repolarization seem to dominate that of neuromodulation of the ventricle.

## TABLE OF CONTENTS

<b>1.0</b>	<b>INTRODUCTION.....</b>	<b>1</b>
<b>1.1</b>	<b>EPIDEMIOLOGY.....</b>	<b>2</b>
<b>1.2</b>	<b>CARDIAC ION CHANNELS AND THE ACTION POTENTIAL .....</b>	<b>3</b>
<b>1.2.1</b>	<b>Normal ventricular action potential an ionic approach .....</b>	<b>3</b>
<b>1.2.2</b>	<b>Molecular mechanisms in Long QT syndrome .....</b>	<b>8</b>
	<b>IK<sub>s</sub> channel pathologies (LQT 1, LQT 5, J-LN 1, J-NL2).....</b>	<b>8</b>
<b>1.2.2.1</b>	<b>.....</b>	<b>8</b>
<b>1.2.2.2</b>	<b>IK<sub>r</sub> channel pathologies (LQT2, LQT6 and ALQTS) .....</b>	<b>10</b>
<b>1.2.2.3</b>	<b>I<sub>Na</sub> channel pathologies (LQT3, LQT9 &amp; LQT10) .....</b>	<b>11</b>
<b>1.2.2.4</b>	<b>Ankyrin –B disorder (LQT4).....</b>	<b>12</b>
<b>1.2.2.5</b>	<b>I<sub>kir 2.1</sub> abnormality (LQTS 7) .....</b>	<b>13</b>
<b>1.2.2.6</b>	<b>L-type calcium channel defect (LQT 8 or Timothy syndrome).....</b>	<b>13</b>
<b>1.3</b>	<b>ARRHYTHMIA MECHANISMS IN LQTS.....</b>	<b>15</b>
<b>1.3.1</b>	<b>Clinical concepts in Long QT syndrome.....</b>	<b>15</b>
	<b>1.3.1.1 Risk factors.....</b>	<b>17</b>
	<b>1.3.1.2 Suggestions of Autonomic involvement .....</b>	<b>18</b>
<b>1.3.2</b>	<b>Theories on the origin of TdP .....</b>	<b>20</b>
<b>1.3.3</b>	<b>Heterogeneity of Myocardium and Dispersion of Repolarization.....</b>	<b>21</b>
<b>1.3.4</b>	<b>Repolarization Reserve.....</b>	<b>22</b>
<b>1.3.5</b>	<b>Arrhythmias and Calcium in Myocardial Cytosol .....</b>	<b>23</b>
	<b>1.3.5.1 Normal Calcium Cycling.....</b>	<b>25</b>
	<b>1.3.5.2 L-type calcium current windows.....</b>	<b>25</b>
	<b>1.3.5.3 Calcium Oscillations and triggered arrhythmias in LQTS .....</b>	<b>26</b>
<b>1.3.6</b>	<b>Autonomic Nervous system and LQTS.....</b>	<b>28</b>

	1.3.6.1	Effects of sympathetic activity in the myocardial cell .....	30
	1.3.6.2	Cholinergic regulation of ventricular electrophysiology.....	31
2.0		<b>THESIS AIMS AND LAYOUT .....</b>	<b>35</b>
2.1		<b>AIMS.....</b>	<b>35</b>
2.2		<b>THESIS LAYOUT.....</b>	<b>36</b>
3.0		<b>MATERIALS AND METHODS .....</b>	<b>38</b>
3.1		<b>MATERIALS .....</b>	<b>39</b>
	3.1.1	Monophasic action potential measurement.....	40
	3.1.2	Principles of Optical Mapping.....	44
	3.1.2.1	Potentiometric dyes .....	44
	3.1.2.2	Simultaneous multiparametric optical mapping and Calcium sensitive optical dyes.....	52
	3.1.2.3	Optics .....	53
	3.1.2.4	Isolated innervated heart preparation.....	60
3.2		<b>METHODS.....</b>	<b>71</b>
	3.2.1	Measurement of APD and Motion Artifacts .....	74
	3.2.2	Nerve stimulation Protocols.....	81
	3.2.3	Protein expression Analysis .....	81
4.0		<b>APD RESTITUTION AND REPOLARIZATION RESERVE .....</b>	<b>83</b>
4.1		<b>ABSTRACT.....</b>	<b>83</b>
4.2		<b>INTRODUCTION .....</b>	<b>84</b>
	4.2.1	Brief overview of classical Restitution .....	84
	4.2.1.1	Autonomics and Restitution.....	86
	4.2.2	Relevance of Physiological Restitution.....	86
4.3		<b>METHODS.....</b>	<b>88</b>
	4.3.1	Nerve stimulation protocols and measurements .....	88
	4.3.2	Data Analysis.....	91
	4.3.3	Results .....	93
	4.3.3.1	APD adaptation during sympathetic nerve stimulation.....	93
	4.3.3.2	Physiological Restitution in LQT1 models:.....	99
	4.3.3.3	Physiological Restitution in LQT2 models:.....	100

4.3.3.4	Physiological Restitution in LQT3 models:.....	100
4.3.4	Discussion.....	108
4.3.4.1	Alterations in ion channel kinetics in APD adaptation in the context of APD restitution.....	111
4.3.4.2	Repolarization Reserve and Restitution curves.....	115
4.3.4.3	Conclusion.....	117
4.3.4.4	Limitations.....	117
4.3.4.5	Future directions.....	119
5.0	DISPERSION OF REPOLARIZATION.....	120
5.1	ABSTRACT.....	120
5.2	INTRODUCTION.....	121
5.3	METHODS.....	122
5.3.1	Stimulation protocols.....	123
5.4	RESULTS.....	124
5.4.1	Neuro-Modulation of apex-base DOR.....	124
5.4.2	Apex-base DOR under ion channel inhibition.....	131
5.5	DISCUSSION.....	136
5.5.1.1	Conclusions.....	143
5.5.1.2	Limitations.....	144
5.5.1.3	Future directions.....	145
6.0	SUMMARY AND FUTURE DIRECTIONS.....	146
	BIBLIOGRAPHY.....	149

## LIST OF TABLES

Table 1: Summary of LQTS- Genotype phenotype correlation from channelological perspective	14
Table 2: Probability criteria for clinical diagnosis of LQTS .....	18
Table 3 List of the different sets of experiments conducted in this work.....	71
Table 4: Comparisons between Activation intervals and Action Potential durations SNS vs. Pacing.....	95
Table 5: Apex-base heterogeneity of physiological restitution .....	96
Table 6 AI and APD changes in control and after HMR1556 (0.5 $\mu$ M infusion) .....	102
Table 7 AI and APD changes before and during E4031 infusion (0.01 $\mu$ M) .....	104
Table 8 AI and APD changes before and during APA infusion (10nM).....	106
Table 9: Changes in APD and DOR during Autonomic stimulation.....	127
Table 10: Neuromodulation of APEX-Base DOR during HMR 1556 (0.5 $\mu$ M).....	132
Table 11: Neuromodulation of Apex-Base DOR during E 4031 (0.01 $\mu$ M) .....	133
Table 12: Neuromodulation of APEX-Base DOR during Anthopleurin A (10nM).....	135

## LIST OF FIGURES

Figure 1: Overview of ion channels, currents, encoding genes and normal action potential contour .....	4
Figure 2: Approximate locations of effects of LQT channelopathies on Action potential.....	9
Figure 3: QT interval Measurement.....	16
Figure 4: Holter tracing of a patient with Long QT syndrome .....	16
Figure 5: Role of Autonomics on Gene-Specific Arrhythmia Triggers .....	19
Figure 6: Putative arrhythmia mechanism in LQTS .....	24
Figure 7: Electro Mechanical coupling in myocardial cell.....	27
Figure 8: Scheme of generalized neurocardiac architectural network.....	29
Figure 9: Schematic showing the regulation of intracellular calcium signaling in the heart during sympathetic activity. ....	33
Figure 10: A Schematic depiction of the various putative cholinergic pathways influencing PKA .....	34
Figure 11: Recordings of MAPs from a single catheter from one region of the heart .....	41
Figure 12: Measurements of MAP Signals.....	43
Figure 13: Scheme of a typical optical mapping system .....	45
Figure 14: Schematic representation of the function of membrane-bound dye molecule in optical mapping.....	47
Figure 15: Principles of voltage-dependent changes in emission spectra of a typical dye.....	48
Figure 16: Ultrastructural changes in a Di-4-ANEPPS molecule during Excitation.....	50
Figure 17: Schematic showing intra molecular reorientation of fast potentiometric probe like di-4- .....	51
Figure 18: Fluorescence spectra of two commonly used dyes in simultaneous optical mapping	53
Figure 19 : Tandem lens arrangement with Epi-illumination and simultaneous imaging.....	55
Figure 20: Photograph of the optical mapping apparatus .....	58
Figure 21: Scheme of optical mapping Apparatus used in this study.....	59

Figure 22: Schematic diagram showing isolated innervated heart preparation with dual Perfusion .....	66
Figure 23: Tray and Chamber assembly .....	67
Figure 24: Mounted specimen of the isolated innervated heart preparation for optical mapping	69
Figure 25: Close-up view of the heart positioned for optical mapping .....	70
Figure 26 : Schematic representation of first and Second derivatives of an action potential.....	76
Figure 27: Measurement of first and second derivatives from action potentials from a single diode.....	77
Figure 28 : Arbitrary method of separation of Apex and base regions using the graticule .....	80
Figure 29: Diagram of cardiac Action potential duration (APD) restitution curve. ....	85
Figure 30: Scheme of stimulation protocol for comparisons of APD Restitution Loops.....	92
Figure 31 : APD Samples and physiological Restitution loops.....	94
Figure 32 : Apex-base heterogeneity of Physiological Restitution curves.....	97
Figure 33 : Western blot data of two key Repolarization factors .....	98
Figure 34: Comparison between APD restitution loops without and with HMR infusion.....	103
Figure 35: Physiological Restitution under E4031 (0.01 $\mu$ M).....	105
Figure 36 : Physiological restitution under APA.....	107
Figure 37: Factors controlling APD rate adaptation with changes in Heart rate.....	114
Figure 38 : Summary of heart rate changes and electrograms during Autonomic Modulation..	126
Figure 39 : Summary of changes of DOR during Autonomic Nerve stimulation .....	128
Figure 40 : Pharmacological modulation of (apex-base) DOR .....	129
Figure 41: Dynamic changes of DOR during SNS and recovery .....	129
Figure 42: Overall DOR changes during Autonomic interventions .....	130
Figure 43 : Neuromodulation of Apex-Base DOR under $IK_s$ inhibition .....	132
Figure 44: Neuromodulation of DOR under E4031 .....	133
Figure 45: Neuromodulation of DOR under APA.....	135

## LIST OF ABBREVIATIONS

ACh	Acetylcholine
AI	Activation interval
ALQTS	Acquired Long QT syndrome
ANS	Autonomic nervous system
APD	Action potential duration
Ca <sup>2+</sup>	Calcium ions
Cai	Calcium transients
CaMKII	CaM kinase II
cAMP	Cyclic Adenosine Monophosphate
CCD	Charge couple device
CICR	Calcium induced calcium release
DADS	Delayed After Depolarization
EADS	Early After Depolarization
eNOS	Endothelial Nitric Oxide Synthase
GC	Guanosine cyclase
ICDs	Implantable Cardioverter Defibrillator
IDL	Interface data language
I <sub>K(Ach)</sub>	Potassium current activated by acetylcholine
I <sub>Kir 2.1</sub>	An inward rectifier potassium current
I <sub>Kr</sub>	Rapid type of delayed rectifier potassium current
I <sub>Ks</sub>	Slow type of delayed rectifier potassium current
I <sub>Kur</sub>	Ultra rapid type of delayed rectifier potassium current
I <sub>Na</sub>	Sodium channel
I <sub>to1</sub>	Transient outward current

JSR	Junctional sarcoplasmic reticulum
KCNE2	Potassium voltage-gated channel subfamily E member 2
KCNH2	Potassium voltage-gated channel subfamily H member 2
LED	Light emitting diode
LQTS	Long QT syndrome
LTCC	L- type calcium channel
LV	Left ventricle
M cells	Mid-myocardial cells
mAKAP	Muscle-selective A-kinase anchoring protein
MAP	Monophasic action potential
MINK	misshapen/NIK-related kinase
MiRP1	MinK-related protein
NCX	Sodium calcium exchanger
Nerve prep	Isolated innervated heart preparation
NO	Nitric oxide
PDA's	Photodiode arrays
PDE	Phosphodiesterase
PLB	Phospholamban
PMTs	Photo multiplier tubes
PP1	Protein phosphatase-1
PVTs	Polymorphic ventricular tachycardia
RyR2	Ryanodine receptor
S/N	Signal-to- noise ratio
SCN5A	Sodium channel, voltage-gated, type V, alpha subunit
SERCA2a	Sarcoplasmic reticulum ATP-ase
SR	Sarcoplasmic reticulum
TAP	Transmembrane action potentials
TdP	Torsade de pointes
TnC	Troponin C
V <sub>m</sub>	Transmembrane voltage

## **DECLARATION**

Surgeries involving isolated innervated heart preparation and optical mapping procedures were undertaken by me, at Department of Cardiovascular Sciences, University of Leicester and Department of Cell biology and Physiology, University of Pittsburgh. Western blot analysis was done by technical staff of the Cell Biology and Physiology Department University of Pittsburgh. This material has not been submitted previously for any other degree. Some results have been published /presented at international and national meetings, during the period of study, details of which are given below.

## PUBLICATIONS

### Papers

1. Autonomic nerve stimulation reverses ventricular repolarization sequence in rabbit hearts Rajkumar Mantravadi, Bethann Gabris, Tong Liu, Bum-Rak Choi, William C. de Groat, G. André Ng, Guy Salama *Circ Res.* 2007 Apr 13;100(7):e72-80. Epub 2007 Mar 15 (cover page)

### Abstracts

1. *Europace*, Vol 9, supplement 5, oct2007, ISSN 1099-5129;V1 At least two neurocardiological factors influence spatial heterogeneity and physiological actionpotential restitution on the ventricle: a novel study using innervated heart and optical mapping R.Mantravadi, G.Salama, G.A. Ng
2. *European Heart Journal* (2007) 28 ( Abstract Supplement ), 728-729.Apex-base heterogeneities of physiological APD Restitution Kinetics (RK):comparison of Sympathetic Nerve Stimulation (SNS) to pacing R. Mantravadi, WG Ortin, B.Gabris, WC De Groat, , G Salama, GA Ng
3. *European Heart Journal* ( 2007 ) 28 ( Abstract Supplement ) , 729 Sympathetic nerve stimulation dynamically reverses cardiac repolarization: optical mapping of fully innervated Langendorff rabbit hearts. R. Mantravadi, WG Ortin, B.Gabris, WC De Groat, G Salama, GA Ng
4. *Heart Rhythm* Vol 4,No 5 supplement May2007,PO1-14: Apex-Base heterogeneities of Physiological APD Restitution Kinetics (RK): Comparison of Sympathetic nerve stimulation (SNS) to Pacing R.Mantravadi, WG Ortin, B.Gabris, WC De Groat, GA Ng, G Salama. (Featured presentation)
5. *Heart Rhythm* Vol 4,No 5 supplement May2007,PO2-72: Sympathetic Nerve Stimulation dynamically reverses Cardiac Repolarization: Optical mapping of fully innervated isolated hearts. R.Mantravadi, B.Gabris, WC De Groat, GA Ng, G Salama.
6. *World Congress of Cardiology 2006*. Analysis of Action Potential Duration Restitution During Sympathetic Nerve Stimulation Versus Pacing: Effect of IKs inhibition Mantravadi R, Ng GA, Choi BR, Liu T, De Groat W, Salama G. P4397
7. *Heart Rhythm*, Action Potential Duration Restitution During Sympathetic Nerve Stimulation Versus Pacing: Effect of IKs inhibition, Mantravadi R, Ng GA, Choi BR, Liu T, De Groat W, Salama G, Publication Date: 5/2006, Volume 3.

8. Heart Rhythm, Action Potential Duration Restitution During Sympathetic Nerve Stimulation Versus Pacing, GA Ng, Rajkumar Mantravadi, Bumrak Choi, Tong Liu, William De Groat Guy Salama, Publication Date: 5/2005 , Volume: Volume 2, Pages: Issue 1S; S257

### **Oral presentations**

1. ESC Nov2007 Sympathetic nerve stimulation dynamically reverses cardiac Repolarization: optical mapping of fully innervated Langendorff rabbit hearts.
2. ESC Nov2007 Apex-base heterogeneities of physiological APD Restitution Kinetics (RK): comparison of Sympathetic Nerve Stimulation (SNS) to pacing.
3. Young investigator award finalist presentation, HR UK, Nov 2007  
At least two Neurocardiological factors modulate heterogeneity of Repolarization.
4. British Cardiac society annual scientific meeting, Glasgow, April 2006. Action Potential Duration Restitution during Sympathetic Nerve Stimulation versus Pacing: Effect of IKs inhibition

## ACKNOWLEDGMENTS

I cannot thank enough, all the people who helped me complete this phase of studentship; a phase that was enjoyable yet turbulent and was rather challenging in more ways than one. In particular, I would like to thank my advisor Dr Ng who gave me this opportunity and stood by me throughout these three years, supporting and guiding me every step of the way.

Most importantly, I would like to thank Prof Guy Salama (Department of Cell Biology and Physiology, University of Pittsburgh), who provided the state-of-the-art equipment, lab-space and enriched my scientific thought, manuscript writing and exposed me to high standards in cardiac arrhythmia research (which was like ‘learning to swim with sharks’). I would also like to thank Dr Barry London, chief of Cardiology, UPMC and Pittsburgh school of medicine and Prof De Groat, Department of Pharmacology, University of Pittsburgh, for their inputs time to time.

This project would be nothing without mentioning the warmth, friendship, knowledge and support of Bum-Rak Choi, Vasil Tumbbev, Carl Sims, Vanlata Patel, Tong Liu, Dean Tai, Seong-min Hawang, Christy Milburn, Bethann Gabris, Prakash Viswanathan and, one and only Waldo Gabriel Neuz Ortin.

I would be ungrateful indeed, if I do not thank Bill, Greg, Larry and Travis (University of Pittsburgh) for all their support with their electronics and mechanical engineering skills; their patience with me to keep my experimental juggernaut in smooth motion.

Above all, I would like to thank my dearest Ma, Dadaji and the Lord, who’s Grace, tenderness and Love gave me the strength to persevere, and made this process an incredible learning experience. I would like to offer this work to them in deep gratitude.

## 1.0 INTRODUCTION

Long QT syndrome (LQTS) is a heterogeneous group of potentially lethal diseases of cardiac ion channels. They have a common manifestation on the ECG – the prolongation of the QT interval. This is measured as the interval from the beginning of the Q wave to the end of the T wave on the ECG. Durations of more than 450 milliseconds is generally considered abnormal. Many LQT patients have symptoms and even die suddenly during perturbations of autonomic activity. Most of them die suddenly following a cardiac arrhythmia known as torsade de pointes, a polymorphic ventricular tachycardia, which often leads to ventricular fibrillation.

There is an intense ongoing effort by many research groups, all over the world, to solve this puzzle of arrhythmogenesis. The approach adopted by most groups is a multi-pronged one. Commonly, patch clamp techniques are used to characterize the ion channel biophysics and current alterations. Alongside, organ level experiments are conducted to characterize the data at an organ level using sophisticated techniques including ones described in this work. Simultaneously, in-silico models at various levels: single cell, single fiber, two dimensional tissue and three-dimensional myocardial models are developed using the ion channel biophysics data, obtained from experimental single cell studies. After validation, these models are used for further experimentation using clinical disease scenarios to assess the various triggers and risk factors.

Biomedical research in Long QT syndrome has become important in recent years as it sets the paradigm to gain insights into cardiac arrhythmia mechanisms in general. Current research approaches in this area tend to be multidisciplinary in nature as mentioned above. The aim is to gain insights into substrate alterations in disease states at many levels: genetic mutations with associated phenotype alterations of the ion channel physiology, structure and complex kinetics of various cardiac ion channels, gap junctions, wave front dynamics during arrhythmogenesis and arrhythmia termination, development of accurate in-silico models to

characterize arrhythmia states in animals and in the humans; and most importantly, to explore novel treatment modalities based on such insights to prevent and treat arrhythmia, particularly sudden death.

There are two main types of Long QT syndromes - Inherited (LQTS) and Acquired (ALQTS). So far, ten different genes and over three hundred mutations have been identified. These mutations are responsible for LQTS in 70% of affected patients (Roden 2008). ALQTS as is currently understood, results from a blockade of the rapid type of delayed rectifier current ( $I_{Kr}$ ) and is mainly drug induced. The  $I_{Kr}$  blockade prolongs the QT interval and increases the dispersion of repolarization (Chiang 2004). Inherited LQTS was first described in 1957 in a family. Several children of this family had QT prolongation on the Electrocardiogram and congenital bilateral neural deafness. These children suffered episodes of syncope and some died suddenly. The hereditary phenotypic transmission resembled that of an autosomal-recessive pattern of inheritance; and it became known as Jervell and Lange-Nielsen syndrome [J-LN] (Jervell and Lange-Nielsen 1957). In 1964, another familial disorder with an autosomal-dominant inheritance and QT prolongation but without deafness was described and was known subsequently as Romano-Ward syndrome [R-W] (Romano C 1963; Ward 1964). Of late, some recessive forms of R-W syndrome without deafness have also been described (Priori, Schwartz et al. 1998).

## 1.1 EPIDEMIOLOGY

Epidemiology of LQTS is still unclear. The incidence of Romano Ward syndrome is estimated to be around 1 in 5000 to 10,000 individuals (Moss, Schwartz et al. 1991) and is thought to be higher in certain areas, like Utah in the United States and in Finland where it is around 1 in 5000 (Naik 2007). The prevalence of Jervell and Lange-Neilson syndrome is much more infrequent and estimated to be between 1.6 and 6 per million in children aged 4 to 15 years. LQTS causes 3000 to 4000 sudden deaths in children and young adults each year in the United States (Vincent 1998) and in untreated patients there is a high mortality rate, of around 70% in 10 years (Moss, Schwartz et al. 1985).

## 1.2 CARDIAC ION CHANNELS AND THE ACTION POTENTIAL

Electrical activity of the heart precedes mechanical activity. The unit of electrical activity is called an action potential. It is governed by a highly coordinated sequence of changes in ion channel kinetics conduction. The electrical activation of the heart is the net result of depolarization of the individual cells. The opening of sodium channels is mainly responsible for the depolarization of myocardial membrane and results in the upstroke of the action potential. The resetting of the activated state to baseline occurs by bringing the membrane potential to baseline. This is called repolarization and is a more complex process governed by tandem but overlapping changes in many ion channel currents like inactivation of sodium channels, activation and inactivation of L-type calcium current, changes in potassium currents etc. The QT interval on surface electrocardiogram represents the repolarization phase of the cardiac action potential.

Changes in individual repolarizing currents affect the net repolarization of the heart. For example, a delay the sodium channel inactivation leads to prolongation of the QT interval. The  $I_{Ks}$  and  $I_{Kr}$  currents are key delayed rectifier currents, which contribute to the main part of repolarization. The  $I_{Kir2.1}$  is an inward rectifier current which contributes to the terminal phase of the repolarization. A reduction in these currents also causes prolongation of the APD/QT and cause LQTS. LQT 8 was described in 2005 and is thought to be due to a reduction of L-type calcium current.(Splawski, Timothy et al. 2005)

### 1.2.1 Normal ventricular action potential an ionic approach

It is only over the last ten years that specific gene mutations and resultant ion channel abnormalities are coming to light. Most of the affected patients have one gene mutation and only about 2% to 3% carry more than one gene mutation. The updates on the specific mutations can be found on a website of the study group on molecular arrhythmias <http://pc4.fsm.it:81/cardmoc/index.html> (cardiology). Fig.1 summarizes the different ion channels, their respective coding genes and contribution to the shape of a normal cardiac action potential.

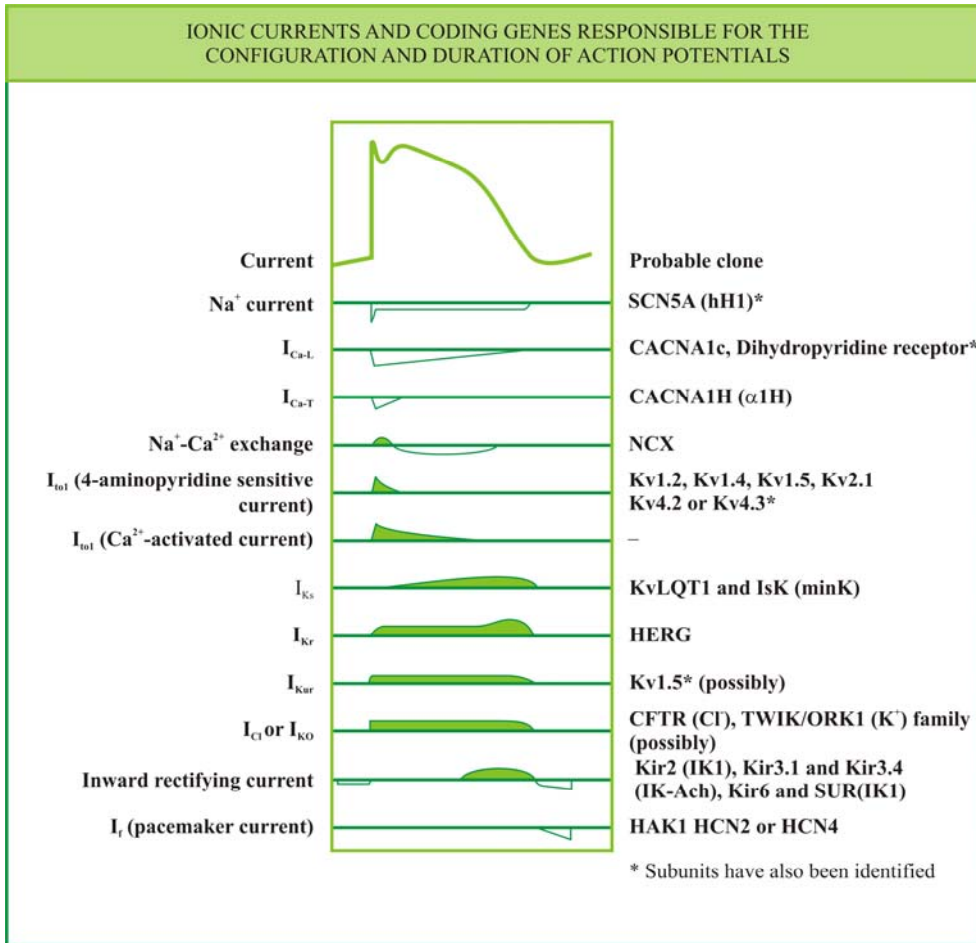


**Figure 1:** Overview of ion channels, currents, encoding genes and normal action potential contour

Key currents: **I<sub>Ca-L</sub>**: L type calcium current; **I<sub>Ca-T</sub>**: Transient calcium current seen in the atria; **I<sub>Ks</sub>**: slow type of delayed rectifier potassium current; **I<sub>Kr</sub>**: rapid type of delayed rectifier potassium current; **I<sub>Kur</sub>**: Ultra rapid delayed rectifier current; **I<sub>f</sub>** funny current; **I<sub>K1</sub>**: Inward rectifier Potassium current; **I<sub>Cl</sub>**: chloride current and **NCX**: Na<sup>+</sup>-Ca<sup>2+</sup> exchange current (modified from Cardiology, 2ed, Crawford).

Initiation of depolarization occurs in a resting myocyte from neighboring cells via intercellular channels called connexons. Sodium ions enter the cells and lift the membrane potential from -90mV to -70 mV when the sodium channels open to allow influx of sodium ions, which further increase the potential to about +10 mV (Fozzard 1992) . This rapid change of membrane voltage causes the upstroke and when it reaches the peak, about 90 % of sodium channels get into an inactivated state. The remaining channels remain activated and allow a steady slow current during the plateau phase (Grant 1995). This current is critical and any delay in inactivation may prolong the action potential duration.

The sodium channel is voltage gated and has 4 homologous domains (alpha subunits Nav), each of which has six transmembrane-spanning regions and these four domains form the pore which permits sodium ions. Among the Nav alpha subunits Nav1.5 is predominantly expressed in the mammalian myocardium. The Nav alpha subunit is encoded by SCN5A gene. Mutations of the gene are linked to arrhythmias. (for review see (Nerbonne and Kass 2005))

The plateau phase of the action potential follows the depolarization upstroke; it is produced by a balance of important currents opposing each other. The slow sodium current and inward mode of sodium calcium exchange current counter-balance out the outward potassium current to maintain the membrane voltage near 0 mV. This extends the action potential duration for effective ventricular contraction. Also during this period, the L-type calcium current is active and plays an important part in the electro-mechanical relationship of the heart. This is discussed in greater detail later in the chapter. Briefly, Voltage gated calcium channels (Cav) are assemblies of four alpha subunits and auxiliary subunits-Cav beta and or Cav alpha 2 delta subunits. Among the various alpha subunits, Cav1.2 encoded by CACNA1C gene is prominent in the mammalian myocardium.

The phase of repolarization beyond the plateau phase is denoted as phase 3 or the rapid repolarization phase. This phase is characterized by the movement of potassium ions out of the cell into the extracellular space, via different potassium channels (see below).

There are four important types of potassium channels in ventricular electrophysiology. They are  $I_{to1}$ ,  $I_{Ks}$ ,  $I_{Kr}$   $I_{K1}$  and recently, there is evidence to suggest that  $I_{K(Ach)}$  plays some role in ventricular electrophysiology in several species including human, when bound to a ligand, i.e. acetylcholine (Koumi and Wasserstrom 1994; Koumi, Sato et al. 1997) are involved in

repolarization. The inwardly rectifying cardiac  $K^+$  ( $K_{ir}$ ) channels are involved in modulation of terminal period of rapid repolarization phase.

The voltage-gated potassium channels ( $K_v$ ) are composed of four separate pore forming or alpha subunits and each containing six segments (S1-S6) of the hydrophobic aminoacids that are thought to form membrane-spanning domains. These segments are joined by loops that perform specific functions like, pore formation (by V&VI), voltage sensing (by segment IV), and channel inactivation (by loop of III& IV) (Hoshi, Zagotta et al. 1990; Zhou, Morais-Cabral et al. 2001)..  $K_v$  alpha subunits that are expressed in the human heart include  $K_v1$ ,  $K_v4$ , hERG, and KVLQT sub families. In addition, alpha subunit proteins interact with  $k_v$  channel accessory subunits like minK, KiChIP2 and MiRP1 which form functional channels with distinct kinetics. ERG1 alpha subunits and MiRP accessory subunits contribute to the formation functional cardiac  $I_{K_r}$  channels.  $K_vLQT1$  alpha subunits associate with minK accessory subunits to form  $I_{K_s}$  channels in human myocardium

Rectification deserves a special mention as it plays an important role in potassium current characteristics. Simply, in an electrical medium with constant resistance, the current is directly proportional to the voltage applied (ohm's law). This current-voltage relationship is also seen in cardiac ion channels across membranes. However, relationships are not strictly linear in ion channels, especially potassium channels, where the same change in voltage may produce much disproportionate inward or outward currents. This nonlinear relationship is called rectification. The rectifications are called inward and outward depending on the direction of the movement of the ions.  $K_{ir}$  channels are open at very negative potentials but show a reduced conductance at positive membrane potentials. This phenomenon, termed inward rectification, has also been termed anomalous rectification, because it is opposite the "normal" outward rectification that is seen in delayed rectifier  $K^+$  channels.(Nichols, Makhina et al. 1996) Rectification of potassium currents seem to be due to blocking of K channel pore by polyamines (Lopatin, Makhina et al. 1994), divalent magnesium ions, by electrochemical gradients by voltage dependent inactivation (Ishihara, Mitsuiye et al. 1989; Ashcroft 2000).

The net  $I_K$  current has three different currents which are identified by the speed of their rectification and they bring the membrane voltage back to the baseline. All potassium currents are delayed rectifier currents. The  $I_{K_s}$ ,  $I_{K_r}$  and  $I_{K_{ur}}$ , are different types of delayed rectifiers, namely

the slow, rapid and ultra rapid potassium currents (Sanguinetti 1993). The ultra rapid rectifier current is found in the atria and will not be discussed here.

The  $I_{Ks}$ , slow delayed rectifier potassium current is slow to reach its full intensity (takes tens of milliseconds). The peak is reached during the down slope phase 3 of the action potential. The current increases with adrenergic stimulation and terminates during phase 4. The  $I_{Ks}$  channel has an associated protein segment minK which, when mutated prolongs the repolarization time, seen in LQT 5. (Sanguinetti, Jurkiewicz et al. 1991; Sanguinetti 1993)

$I_{Kr}$  or rapid type of delayed rectifier potassium current reaches its peak more rapidly than the  $I_{Ks}$  current. When the current reaches its peak, it remains on a plateau until late phase 3 of the action potential. The current is inactivated by attrition and is not as responsive to adrenergic influences.

$I_{to1}$  is a transient outward current which gets activated when the membrane voltage reaches about +10 mV. This effluxes some potassium ions, and initiates repolarization. The coassembly of Kv4.3 alpha subunit and accessory subunit KiChIP2 forms  $I_{to}$  channel in humans and dogs (Rosati, Pan et al. 2001).

In this voltage milieu, two other currents come into play: the calcium dependent chloride channel ( $I_{to2}$  or  $I_{Cl(ca^{++})}$ ) and a more important sodium-calcium exchange current (NCX). The former is activated by high cytosolic calcium concentrations at the end of phase 0 and early phase 1 and causes an influx of chloride ions which lowers the voltage.

The NCX is a complex multi-phasic current, which alternately exchanges the sodium and calcium ions in opposite directions and is driven by their ionic electrochemical gradients. The NCX channel is a continuous peptide with eleven transmembrane spanning peptides with long intra-cellular loop which has the inactivation site. Segments 2,3,8,9 form a common pore to transport the ions. Being electrochemically driven, the NCX gets activated and allows sodium ions to pass into the cell during depolarization. During early repolarization, calcium is extruded out of the cell. During the plateau phase, the small gradient formed by slow sodium current causes an influx of sodium ions into the cell. But during the rapid repolarization phase (phase 3) of the action potential, there is a greater efflux of calcium ions via the NCX. About 80% of the cytosolic calcium extrusion out of the cell occurs via the NCX in each cardiac cycle. The NCX seems to play an important role in arrhythmogenesis (discussed elsewhere in this work). Also

there is data to suggest that  $\alpha_1$  adrenergic receptor activation enhances the NCX and ischaemia and hypoxia inhibit it.(Dubin 2003)

$I_{K1}$ , is a membrane voltage activated channel which maintains the baseline membrane voltage at about -90mV in addition to modulation of terminal part of rapid phase of repolarization (Nichols and Lopatin 1997). Figure 1 shows the summary of the ion currents responsible for the action potential and the respective areas of predominant role.

### **1.2.2 Molecular mechanisms in Long QT syndrome**

The Long QT syndrome is a repolarization abnormality due to malfunctioning ion channels. The molecular mechanism of the LQTS is rather complex, heterogeneous and not fully understood. A brief overview is attempted below in groups of molecular defects resulting in their respective channel dysfunction. Also for the sake of clarity, the LQTS is described in groups of individual ion channel pathologies with their individual protein subunits ( $\alpha$  and  $\beta$ ) involvement.

Some subtypes are more clinically prevalent than others. Long QT Types 1, 2, and 3 account for more than 95% of all the cases. This work deals mainly with these types. The genetics and ion channel effects are summarized in Table 1 and Figure 2.

#### **1.2.2.1 $I_{Ks}$ channel pathologies (LQT 1, LQT 5, J-LN 1, J-NL2)**

As mentioned in previous section, the  $I_{Ks}$  channels are active during the phases 2 and 3 of the action potential. Thus it is a major player in repolarization and any defective function might influence net repolarization. The Commonest form of LQTS is the LQTS1; it is associated with reduced  $I_{Ks}$  current due to reduced channel function.

At least two molecular mechanisms attempt to explain the reduced  $I_{Ks}$  channel functions in LQT1.

Deletions of one of the KCNQ1 alleles result in formation of abnormal subunits that do not co-assemble with normal subunits. This mutation results in loss-of-function and a 50% reduction in the number of functional channels. (Keating and Sanguinetti 2001)

Missense mutations produce channels with subtler structural abnormalities. These mutations, however, do not affect the co-assembly and the result is the formation of regular-

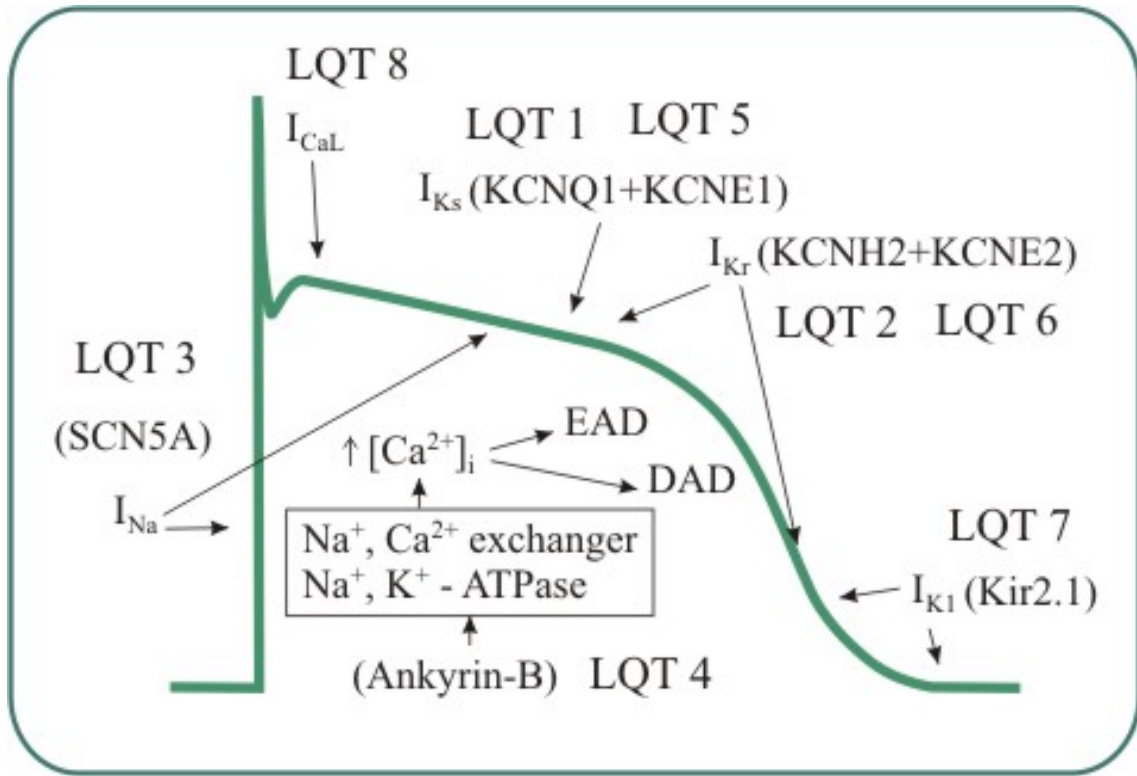


**Figure 2: Approximate locations of effects of LQT channelopathies on Action potential**

$I_{Ca-L}$ : L type calcium current;  $I_{Ks}$ : slow type of delayed rectifier potassium current;  $I_{Kr}$ : rapid type of delayed rectifier potassium current;  $I_{K1}$ : Inward rectifier Potassium current;  $Na^+$ -  $Ca^{2+}$  exchange current.  $I_{Na}$ : Sodium current. DAD: delayed after repolarization; EAD: Early after depolarization.

heterotetramers but with varying functional capacities. There seems to be a dominant negative effect in the function of this mutated channel, i.e., if the ratio of the mutant subunit to normal subunit is 1:3, despite normal co-assembly to form a tetramer, the function of the channel drops to half its normal. This seems to be the case particularly when missense mutations occur in the pore region of the channel (Schwartz, Priori et al. 2001).

### **1.2.2.2 $I_{Kr}$ channel pathologies (LQT2, LQT6 and ALQTS)**

The HERG -“human ether-a-go-go related” gene, also known as KCNH2, encodes the alpha-subunit of  $I_{Kr}$  protein which, like  $I_{Ks}$  channel protein, has 6 transmembrane spanning segments (S1–S6), a voltage sensor (S4) and a  $K^+$ -selective pore between S5 and S6 segments (Curran, Splawski et al. 1995).

Recently, a novel potassium channel gene (KCNE2) encoding minK-related peptide 1 (MiRP1), located on chromosome 21, about 70 kb from KCNE1 (minK) gene, has been cloned (Abbott GW 1999). MiRP1 encodes the beta-subunit of  $I_{Kr}$  channel protein and, co assembles with KCNH2 to form normally functioning  $I_{Kr}$ .

Mutations (mainly deletions or missense) of KCNH2 cause loss-of-function or dominant-negative effect, resulting in a reduction of the repolarizing current. Defects in biosynthetic processing or intracellular protein trafficking of mutant KCNH2 channel protein have also been recently reported.

Homozygous KCNH2 mutations in humans caused severe form of LQTS with marked QT prolongation, 2:1 atrio-ventricular block, and increased the risk of sudden death during intrauterine life and the first months after birth. However, patients with heterozygous mutations present with a less severe form of disease (Hoorntje, Alders et al. 1999).

KCNE2 (MiRP1) mutations have also been implicated in drug-associated LQTS [12]. Interestingly, the  $I_{Kr}$  current shows unique pharmacological sensitivity to methanesulfonanilide, dofetilide, D-sotalol, E 4031 and other drugs causing acquired LQTS (ALQTS).

Further, co-expression of KCNH2 with KCNE2 does appear to modulate drug sensitivity of  $I_{Kr}$  but this was only shown by some studies (Abbott GW 1999; Sesti, Abbott et al. 2000). This possibly indicates a molecular link between the congenital and acquired Long QT syndromes.

Pourrier et al (Pourrier, Zicha et al. 2003) suggested that mutations of KCNE2 played an important role in the excess prolongation of action potential in Purkinje fibres but not ventricular

muscle thus predisposing the heart to early afterdepolarisation (EADs) and polymorphic ventricular tachycardia (PVT). This observation concurs with the theories of formation of EADs and TdP (discussed below).

### 1.2.2.3 $I_{Na}$ channel pathologies (LQT3, LQT9 & LQT10)

Mutations of sodium channel genes were found to allow for complex effects on the electrophysiological phenotype both on activation and repolarization. Wang et al showed that the gene responsible for LQT3 is SCN5A (Yan, Wu et al. 2001). It encodes the alpha-subunit of the cardiac sodium channel, which has 4 homologous domains, each of which contains 6 transmembrane segments.

Unlike  $K^+$  channels, expression of a single [alpha]-subunit of the cardiac sodium channel was found to be sufficient to ‘recapitate’  $I_{Na}$  and making it functional.

The SCN5A-encoded defects generally result in a delayed inactivation of the sodium channel. These mutant channels not only have delayed inactivation kinetics but also reopen abnormally during the plateau phase of the action potential and prolong the action potential duration. Activation of these  $Na^+$  channels, remained normal (Mohler, Schott et al. 2003).

An RH and Wang XL et al recently reported a novel mechanism where a point mutation induced an altered [alpha] and [beta]-interaction; resulting in delayed inactivation of the channel. They found a novel mutation, a single A→G base substitution at nucleotide 5519 of the SCN5A cDNA, which was expected to cause a nonconservative change from an aspartate to a glycine at position 1790 (D1790G) of the SCN5A gene product. They investigated ion channel activity in human embryonic kidney (HEK 293) cells transiently transfected with wild-type (hH1) or mutant (D1790G) cDNA alone or in combination with cDNA encoding the human  $Na^+$  channel  $\beta_1$ -subunit (h $\beta_1$ ) using whole-cell patch-clamp procedures. Heteromeric channels formed by coexpression of  $\alpha$ - and  $\beta_1$ -subunits were affected: steady-state inactivation is shifted by -16 mV, but there was no D1790G-induced sustained inward current. This effect was independent of the  $\beta_1$ -subunit isoforms. Further they saw no significant effect of D1790G on the biophysical properties of monomeric  $\alpha$ - (hH1) channels. They concluded that the effects of the novel LQT-3 mutation on inactivation of heteromeric channels were due to D1790G-induced changes in  $\alpha$ - and  $\beta_1$ -interactions. (An RH 1998)

Lupoglazoff et al reported on homozygous SCN5A mutations with severe LQTS phenotype and 2:1 atrioventricular block. Some other LQT3 carriers with common mutation: 1795 insD in SCN5A gene have demonstrated bradycardia, sinus pauses or even sinus arrest. This was shown to be due to a negative shift in inactivation of the persistent inward current associated with decreased diastolic depolarization rate in the sinus node cells. Some patients have severe negative shifts in persistent sodium current; and in these patients, sinus arrest is thought to occur following failure of repolarization in the sinus node. (Lupoglazoff, Cheav et al. 2001; Veldkamp, Wilders et al. 2003).

The new genes associated with LQTS were named as recently as within the last two years. One encodes for Caveolin-3 protein (CAV3) a constituent of caveolae and the other NaV4B (SCN4B), encodes for an axillary subunit of the sodium channel protein; and mutations of both result in gain of function of the sodium channel and a phenotype resembling LQT3. (Vatta, Ackerman et al. 2006; Medeiros-Domingo, Kaku et al. 2007)

#### **1.2.2.4 Ankyrin –B disorder (LQT4)**

Recently, Ankyrin B, is a multivalent adaptor protein which is structurally unrelated to cardiac ion channels, has been shown to be involved in the pathogenesis of a rare variety of LQTS. Mohler et al in 2003 showed that defective Ankyrin-B is responsible for LQT4.

Ankyrin-B is thought to play a role in recognizing proteins such as  $\text{Na}^+$ - $\text{Ca}^{2+}$  exchanger,  $\text{Na}^+$  pump, and inositol-1, 4,5-triphosphate receptors, and in their insertions into appropriate domains of cell membranes. Two normal copies of the Ankyrin-B gene are normally required for normal  $\text{Ca}^{2+}$  signaling. A missense mutation may lead to loss-of-function. The loss of  $\text{Na}^+$  pump function is probably the major contributor to elevated  $[\text{Ca}^{2+}]_i$  transients in  $\text{AnkB}^{+/-}$  ventricular myocytes and thereby causes delayed after depolarizations (DADs) and EADs.(Mohler, Schott et al. 2003)

The mechanism of LQT4 induced arrhythmogenesis is not understood and the exact role of  $\text{Ca}^{2+}$  handling in prolonging QT and generating arrhythmias is not yet known. The increase in QT interval observed in  $\text{AnkB}^{+/-}$  mice is associated with delayed conduction. (Mohler, Schott et al. 2003; Mohler and Wehrens 2007).

#### **1.2.2.5 $I_{kir 2.1}$ abnormality (LQTS 7)**

The molecular problem in LQT 7 is believed to be a defective  $I_{K1}$  current. KCNJ2 gene encodes  $I_{K1}$  channel protein.  $I_{K1}$  is an inward rectifier current and normally does not contribute to repolarization during the plateau phase but, provides substantial current during late repolarization. A reduction in  $I_{K2.1}$  prolongs the terminal phase of the cardiac action potential. In the setting of reduced extracellular  $K^+$ , spontaneous arrhythmias occur in a  $Na^+/Ca^{2+}$  exchanger-dependent manner (Tristani-Firouzi, Jensen et al. 2002; Chiang 2004).

#### **1.2.2.6 L-type calcium channel defect (LQT 8 or Timothy syndrome)**

Timothy syndrome is a recent addition to the growing list of LQTS. The main defect seems to be a recurrent de novo mutation of the cardiac L -type calcium channel (CaV1.2) protein, encoding the transmembrane segment S6 of domain 1 (Splawski, Timothy et al. 2005). This leads to an increase the L-type calcium current, prolongs the QT interval and predisposes the heart to arrhythmias. These patients also have musculoskeletal abnormalities and mental disabilities as certain exons are expressed in multiple tissues.

**Table 1: Summary of LQTS- Genotype phenotype correlation from channelogical perspective**

Long QT types	Gene	Chromosome	Ion Channel	Effects	% LQTS patients
<b>Autosomal Dominant</b>					
<b>Ramono- Ward</b>					
LQT 1 -1991	KCNQ1 (KVLQT1)	11p 15.5	Alpha subunit of $I_{Ks}$	Reduced $I_{Ks}$ current	50 %
LQT 2- 1994	KCNH2 (HERG)	7q 35-36	Alpha subunit of $I_{Kr}$	Reduced $I_{Kr}$ current	45 %
LQT 3- 1994	SCN5A Na <sub>v</sub> 1.5	3p 21-24	Alpha subunit of $I_{Na}$	Increased $I_{Na}$ current	3 - 4 %
LQT4 - 1995	Ankyrin B	4q 25-27		increased late $I_{Na}$ ?	less than 1%
LQT5 - 1997	KCNE1 (min K)	21q 22.1-22.2	Beta subunit of $I_{Ks}$	Reduced $I_{Ks}$ current	less than 1%
LQT6- 1999	KCNE2 (MIRP 1)	21q 22.1-22.2	Beta subunit of $I_{Kr}$	Reduced $I_{Kr}$ current	less than 1%
LQT7- 2001	KCNJ 2	17q 23	Kir 2.1	Reduced $I_{Kir2.1}$ current	less than 1%
LQT8- 2004	CACNA1c	12P 13.3	Cav 1.2 (cardiac L type)	increased $I_{CaL}$ current	less than 1%
LQT9- 2006	CAV 3	3P 25	Caveolin-3	increased $I_{Na}$ current	less than 1%
LQT10-2006	SCN4B Na <sub>v</sub> B4	11q 23.3	Auxillary subunit of $I_{Na}$	increased $I_{Na}$ current	less than 1%
<b>Autosomal recessive</b>					
<b>Jervell and Lange- Nielson</b>					
JLN1 1997	KCNQ1 ( KVLQT1)	11p 15.5	alpha subunit of $I_{Ks}$	reduced IKs current	less than 1%
JLN2 1997	KCNE1 (min K)	21q 22.1-22.2	Beta subunit of $I_{Ks}$	reduced IKs current	less than 1%

The Table summarizes the chronology, the faulty gene, host chromosome location, type of inheritance, major ion channel subunit dysfunction and resultant effect on the repolarizing current. A percentage distribution of the individual LQT patients is also shown. Note: the majority of LQTS patients fall into the first two groups i.e. LQT1 and 2.  $I_{Ca-L}$ : L type calcium current;  $I_{Ks}$ : slow type of delayed rectifier potassium current;  $I_{Kr}$ : rapid type of delayed rectifier potassium current;  $I_{Kir2.1}$ : Inward rectifier Potassium current.  $I_{Na}$ : Sodium current.

## 1.3 ARRHYTHMIA MECHANISMS IN LQTS

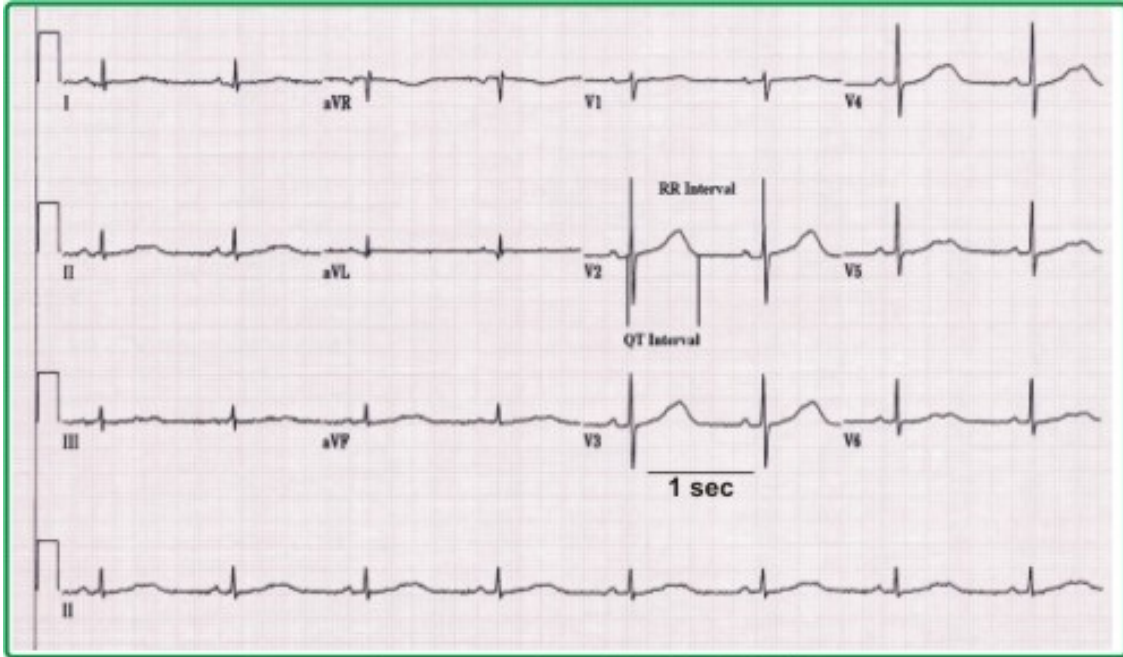
### 1.3.1 Clinical concepts in Long QT syndrome

Before a discussion is presented on the mechanisms of arrhythmogenesis in Long QT syndrome, a brief clinical overview may be helpful to set the paradigm.

Patients with LQTS often suffer from pre-syncope, syncope and if left untreated, die suddenly. A number of studies have shown that the underlying cause of symptoms in LQTS is Torsade de Pointes (TdP), a polymorphic ventricular tachycardia (Keren, Tzivoni et al. 1981; Viskin 1999), which appears to be twisted around its axis, and often degenerates to ventricular fibrillation resulting in sudden cardiac death (Poelzing, Akar et al. 2004). The link between QT intervals and deaths was shown as early as 1964. Selzer and Wray reported that QT prolongation and fibrillation occurred in patients on Quinidine.

QT interval is measured as the duration from the start of q wave to the end of T wave (figure 3) on the surface ECG.

Precordial leads seem to be more reliable for the measurement of the QT interval. Since QT interval measurement poses difficulty with its diurnal variation, with electrolyte imbalance, autonomic fluctuations, and ECG acquisition techniques accounting for intra and inter-observer variability. Since QT interval varies with heart rate, correction formulae are used to reduce the influence of these factors. The most commonly used formula is the Bazette's formula which is shown below. The utility and limitations of the formulae are not discussed in this work. Normal QT interval is  $\leq 440$ ms in both genders. QT duration of 440-460 ms in men and 440-470 ms in women are considered borderline. (Gupta, Lawrence et al. 2007)



**Bazette's correction :  $QTc: QT/\sqrt{RR}$**

**Figure 3: QT interval Measurement**

The ECG tracing illustrating the measurements of QT interval and RR intervals.

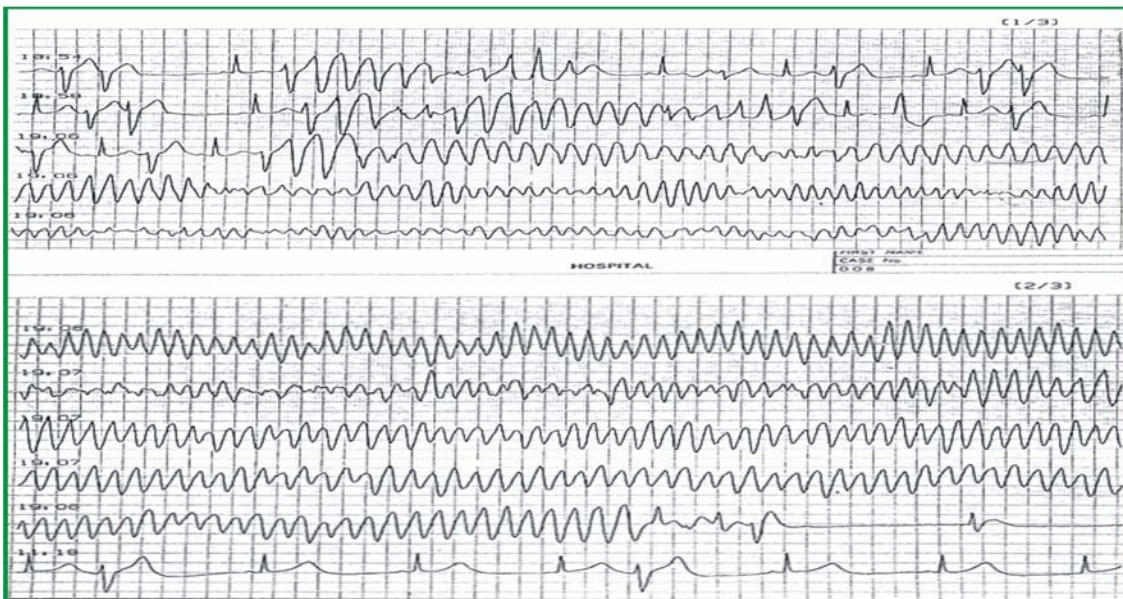


**Figure 4: Holter tracing of a patient with Long QT syndrome**

This patient was in normal sinus rhythm, developed torsade de pointes and fortunately reverted spontaneously to sinus rhythm. The patient experienced syncope at this time (with permission from Dr. AJ Moss).

### **1.3.1.1 Risk factors**

Many patients with LQTS remain asymptomatic and arrhythmia-free unless associated with certain risk factors. Most of the asymptomatic patients have at least one risk factor eg female gender. Other risk factors include: structural heart disease, electrolyte imbalance, QT prolonging drugs, family history of LQTS and/or sudden death, past history of syncope, liver impairment, bradycardia etc.(Gupta, Lawrence et al. 2007)

Also, not all patients with mutations demonstrate prolonged QT or suffer from arrhythmias, unless when they take medications prolonging their QT interval. Typically, LQTS 6 patients do not show arrhythmias in the absence of such provoking agents. This is thought to be due to decrease in the repolarization reserve, see below (Gupta, Lawrence et al. 2007)

Schwartz et al tried to simplify the picture by using a comprehensive scoring system and published a probability score to aid clinical diagnosis of LQTS in 1993 (See Table 2).

In spite of several attempts to improve the specificity of the diagnosis using ECG evidence, remains a challenge. In a recent Mayo clinic study, clinical diagnostic criteria were specific only in 41% of the cases. This limitation was attributed to miscalculation of QTc, misinterpretation of normal distribution of QTc values and misinterpretation of symptoms (Taggart, Haglund et al. 2007).

**Table 2: Probability criteria for clinical diagnosis of LQTS**

<b>Criteria</b>	<b>Point</b>
<b><u>History</u></b>	
Clinical history of syncope	
Without stress	1
With stress	2
Congenital deafness	0.5
Family history of LQTS	1
Unexplained sudden-death in a first degree-family member <30 yrs	0.5
<b><u>ECCG</u></b>	
Corrected QT interval (QTc by Bazett's formula)	
460–470 ms (males)	1
460–470 ms	2
>480 ms	3
Torsade de pointes	2
T-wave alternans	1
>3 Leads with notched T waves	1
Bradycardia (<second percentile for age)	0.5
<b>A score &lt;1=low probability; 1 to &lt;4=intermediate probability; ≥4=high probability</b>	

The Table underscores the need for a good clinical history and ECG criteria for accurate diagnosis of this condition. Mere prolongation of the LQT interval alone does not make the diagnostic probability of LQTS as a high. Redrawn from (Schwartz, Moss et al. 1993)

### **1.3.1.2 Suggestions of Autonomic involvement**

Evidence from both basic science and clinical studies strongly point to the role of autonomic involvement in arrhythmogenesis in LQTS.

Patients with genetically proven mutations causing LQTS exhibited symptoms during particular autonomic states. Schwartz et al have shown in 2001 that specific LQT genotypes have arrhythmias under a characteristic autonomic state. For example, LQT1 patients seem to have TdP and suffer syncope more during peak exercise than at rest. Later, ion channel data confirmed that the  $I_{Ks}$  current accumulates during  $\beta$  adrenergic stimulation; providing the link between the autonomic nervous system and LQTS. In LQTS3 the opposite seems to be true; where, lack of

sympathetic drive was the precipitating trigger in most patients having symptoms. In these patients, pacing to maintain a higher baseline rate and avoiding  $\beta$ -blockers have been shown to help with clinical outcomes (Schwartz 2005).



**Figure 5: Role of Autonomics on Gene-Specific Arrhythmia Triggers**

Note: LQT1, LQT2 and LQT3 have slightly different autonomic triggers. LQT1 symptoms were shown to be precipitated at peak exercise; whereas, in LQT2 symptoms occurred more frequently during acute emotional stress and in contrast the LQT3 patients had symptoms during rest. (Schwartz, Priori et al. 2001) Figure presented with kind permission of Dr. AJ Moss.

The limitations of drug treatment, including  $\beta$ -blockers, are being recognized of late. Even though,  $\beta$ -blockers have been shown to reduce the incidence of syncope and sudden death it is not sufficient in a significant number of patients. ICDs (Implantable Cardioverter Defibrillator) have shown to be very effective in reducing the incidence of sudden death but have been currently reserved for high risk patients (survivors of cardiac arrest, documented TdP or syncope on  $\beta$ -Blockers). Several other high risk groups have not yet been included for ICD treatment e.g. males with LQT3, females with LQT2 having a QT >500ms, members of family having malignant family history. (Priori, Schwartz et al. 2003)

### 1.3.2 Theories on the origin of TdP

What make the myocardium vulnerable to polymorphic ventricular tachycardia is still unclear.

There are three fundamental modes by which rhythm can be disturbed in the heart. They are- triggered activity, automaticity and re-entry. Triggered activity refers to an intracellular disturbance (generally in calcium handling) which results in electrical disturbance on the membrane which causes abnormal electrical firing and arrhythmia. Automaticity refers to repetitive organised electrical firing by a single or group of cells which initiates and maintains an arrhythmia. Re-entry refers to a substrate abnormality, which causes a normally generated impulse to propagate abnormally; especially to loop around an island of poorly conducting tissue thus providing for a sustained source of abnormally repetitive signals (Mark Anderson 2004).

There is growing evidence elucidating the characteristics of TdP. Several factors have been shown to influence the precipitation of TdP such as, prolonged repolarization times, beat-to-beat variability of the repolarization duration (Thomsen, Oros et al. 2007) and increased dispersion of repolarization. (Restivo, Caref et al. 2004)

Dispersion of Repolarization (DOR) refers to the lack of uniformity in action potentials across the myocardium. It is the difference in the action potential durations across the region of interest and subtracting the local activation times(Conrath and Opthof 2006). Increase in dispersion of repolarization encourages the propagation of early after depolarization (EADs) which results in triggering TdP via an R-on-T extra systole. Further, increased dispersion also serves a conducive-substrate for functional re-entry (Yan, Wu et al. 2001; Lankipalli, Zhu et al. 2005).

Several research groups contributed significantly to the current understanding of the TdP (Dessertenne 1961; Dessertenne 1966; Mark Anderson 2004; Restivo, Caref et al. 2004). It was initially thought that TdP was due to alternating firing of action potentials automatically, from two or more sites leading to the polymorphic character. Later experiments showed that increased dispersion of repolarization both spatially and temporally over the myocardium leads to re-entry which maintained the tachycardia (Hoffman, Cranefield et al. 1959; Fontaine 1979). Others suggested a role of triggered activity via EADs

and showed that PVTs arose mostly from Purkinje fibre myocytes or sometimes from mid-myocardial cell (M cells).

El-Sherif's group (Restivo, Caref et al. 2004) showed that the initial beat of polymorphic ventricular tachycardia consistently arose from a subendocardial site following focal activity. However, many research groups believed that repetitive subendocardial focal activity and /or re-entrant excitation were required to sustain the arrhythmia (Burashnikov and Antzelevitch 2002) rather than initiate it. There is also evidence to suggest that these arrhythmias are not substrate size dependent and even a small volume of tissue is sufficient to cause TdP via re-entrant circuits (Poelzing, Akar et al. 2004).

Experiments by Gbadebo *et al*, (Gbadebo, Trimble et al. 2002) showed that a calmodulin inhibitor could prevent TdP formation in LQT models without a change in the QT interval.

Even though, it is still unclear to what the exact underlying mechanism of TdP is and what are the substrate characteristics required to initiate and maintain TdP, there is large amount of data confirming several factors which play a contributory role in the arrhythmogenesis.

### **1.3.3 Heterogeneity of Myocardium and Dispersion of Repolarization**

Although, QT prolongation is important in the arrhythmogenesis in the LQTS it is by no means the only factor. Shimizu et al and Van opstal et al (Shimizu and Antzelevitch 2000),(van Opstal JM; Shimizu and Antzelevitch 2000) have shown that prolongation of QT interval by itself is not enough to cause TdP but dispersion of repolarization is required.

The myocardium normally does not have a homogenous distribution of all the ion channels and currents. There is a dispersion of repolarization within the myocardium. Increase in this dispersion has been shown to be the principle arrhythmogenic substrate in both acquired and congenital LQTS. (Shimizu and Antzelevitch 2000)

The potassium channels show diversity across the species (London, Baker et al. 2007) and across the ventricle. However, sodium channels have less functional diversity (Hille 1992) as compared to the potassium channels. Therefore, it is not surprising that the action potential duration are also not uniform across different regions of the heart both from endocardium to epicardium and apex to base over the surface of the ventricle. This inherent heterogeneity occurs

normally over the ventricle and contributes to the dispersion of repolarization. In human and canine hearts, M cells are thought to constitute up to 30% to 40% of the myocytes in the left ventricular free wall, which have the longest APD with smaller  $I_{Ks}$ , and larger late  $I_{Na}$  currents.  $I_{Kr}$  density appears to be similar in all cell layers (Liu and Antzelevitch 1995; Chiang 2004). Also see fig 3.

Animal models of LQT have shown that a preferential prolongation of APDs in M cells increases DOR, and causes an increase in QT at the same time. As mentioned above, increased intrinsic heterogeneity together with EAD and DAD-induced triggered activity form a vulnerable window for TdP both by triggered activity and re-entry (Antzelevitch 2007).

In LQT1 models, Chromanol 293B increased the QT interval uniformly across the wall of the myocardium thus having no effect on the DOR. However, when these hearts were treated with  $\beta$ -adrenergic agonist, the transmural DOR was dramatically increased and led to the development of TdP (Shimizu and Antzelevitch 2000). A summary of the current views on the mechanisms of arrhythmogenesis in LQTS is shown in figure 6.

Role of intercellular gap junction proteins is being increasingly recognized as important players in arrhythmogenesis. Gap junctions have been shown to be involved in impulse propagation and electrical synchronization between myocytes. (Saffitz, Davis et al. 1995) Connexin 43 (Cx43) is a principle gap junction protein, whose expression and distribution in the ventricle is linked to transmural heterogeneities in both normal and failing hearts. Drugs which decrease coupling have been experimentally shown to increase DOR and promote arrhythmias (Poelzing, Akar et al. 2004; Poelzing and Rosenbaum 2004). There is also exciting new evidence to suggest that gap junction enhancing agents reduce the DOR and suppress TdP formation in LQT3 models. (Quan, Bai et al. 2007)

#### **1.3.4 Repolarization Reserve**

As mentioned above the main pathophysiologic mechanism in LQTS is the reduction of repolarization current either due to a decrease in outward currents or due to an increase in inward current. However, there is a host of risk factors which have been shown to modify the outcomes in these patients.

It is not clear at this time, how such a diverse range of factors increase the vulnerability of the myocardium to arrhythmias. Recently, a unified approach using the concept of repolarizing reserve has emerged, to try and understand the link between the prolongation of QT interval and arrhythmogenesis. According to this view, a reduced reserve makes the myocardium vulnerable to arrhythmia. This reduction can be due to various factors, either in isolation or in combination (known as single or multiple hits).(Roden 2006) The opponents of this view had emphasized that the direct-proof-of-concept-evidence was lacking. Very recently, there has been ion channel data (both experimental and modeling) demonstrating the presence of repolarization reserve. This suggests the presence of biological redundancy in the repolarizing ion currents controlling the action potential. (Remme and Bezzina 2007)

At the clinical level, studies have shown marked phenotypic heterogeneity (in both QT-interval duration and symptoms) even though all affected family members were carriers of the same *KCNQ1* mutation (A341V) suggesting the presence of genetic or environmental modifiers of repolarization reserve (Brink, Crotti et al. 2005). Thus, the potential for QT prolongation to result in the development of torsades de pointes are ultimately determined by the net effect of all the mediators of repolarization reserve. Further discussion is attempted in chapter 3.

### **1.3.5 Arrhythmias and Calcium in Myocardial Cytosol**

The role of triggered activity in the development of arrhythmias in LQTS is being actively pursued in recent years. Calcium long has been suspected to be linked to cardiac arrhythmias. Investigations into calcium channel physiology and its role in the genesis of cardiac arrhythmias at a cellular level is being actively pursued over the last three decades. These extensive research studies have resulted in important hypotheses on the role of intracellular calcium in arrhythmogenesis.

A brief account is attempted below to summarize the role in the context of Long QT related arrhythmias.

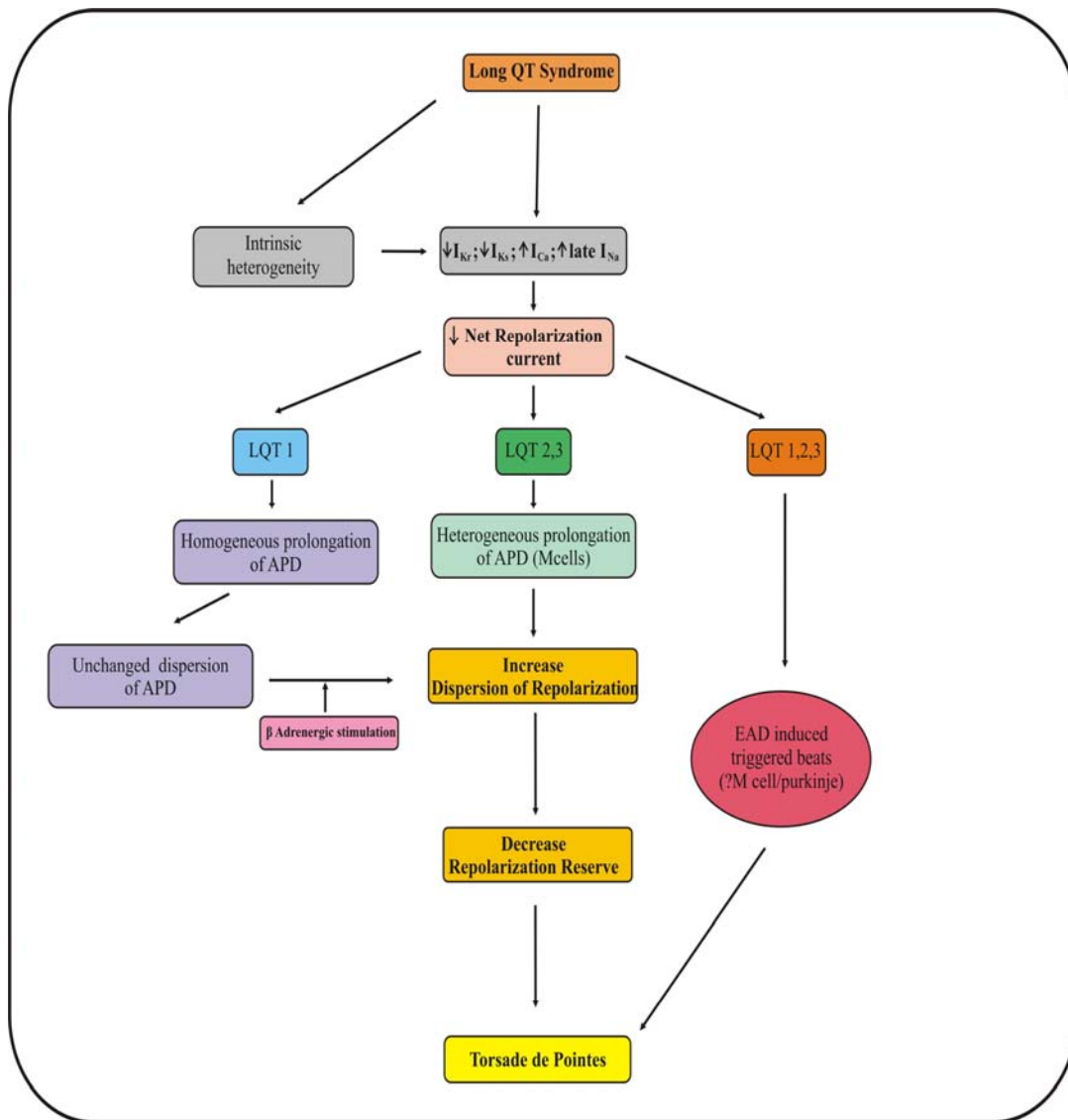


**Figure 6: Putative arrhythmia mechanism in LQTS**

$I_{Ca-L}$ : L type calcium current;  $I_{Ks}$ : slow type of delayed rectifier potassium current;  $I_{Kr}$ : rapid type of delayed rectifier potassium current;  $I_{K2,1}$ : Inward rectifier Potassium current.  $I_{Na}$  : Sodium current. (Antzelevitch 2007)

### **1.3.5.1 Normal Calcium Cycling**

During depolarization, calcium ions enter the myocytes via the L-type calcium channels. The amount of calcium which enters through this route is very small compared to that which is required for contraction. Extracellular calcium ion concentration is about 3mM. When the membrane potential reaches about -40mV, calcium channel activates and calcium ions enter the cell. When this occurs near the feet of the ryanodine receptors, this opens sarcoplasmic reticulum (SR) ryanodine calcium-release channel (and T-tubule calcium channel for deeper regions), which releases calcium ions from the calcium binding proteins, calsequestrin and calreticulin that line the SR cisternae and corbulae (the localized pouches of the SR). This is called calcium induced calcium release or CICR. The released free calcium in the cytosol binds to the actin TnC sites and in the presence of ATP a power-stroke of contraction is initiated. Thus CICR enables the myocyte to help itself with the adequate amount of calcium required for its contraction from calcium entry via the L-type calcium channel. Not all calcium released in the cytosol adheres to the TnC sites for contraction. Hence, a transient elevation of the cytosolic calcium is seen. The sodium-calcium exchanger (NCX) channel comes into play to offset this imbalance by driving the calcium out of the cell. (Dubin 2003)

During the rapid phase of repolarization, when the membrane voltage is more negative, the SR  $\text{Ca}^{2+}$ ATPase pumps get activated and sequester the  $\text{Ca}^{2+}$  ions back into the SR by using ATP. For every ATP molecule used, two  $\text{Ca}^{2+}$  ions are pumped into the sarcoplasmic reticulum. It is thought that it is the SR ATPase pump which contributes mainly to myocyte relaxation (Katz 1992; Edes 1997).

### **1.3.5.2 L-type calcium current windows**

It is beyond the scope of this thesis to describe the biophysical details of the kinetics of the L-type calcium current. It may be sufficient to say during the normal action potential the calcium channels are activated when membrane potential increases and the channels are fully open to allow extracellular calcium to enter the cell at the end of depolarization. The channel undergoes a voltage and calcium dependent inactivation during the early repolarization phase (plateau phase). As membrane potential drops the channels are closed. However, in LQTS the abnormal prolongation of the APD allows for recovery of inactivation and/or reactivation of L-

type  $\text{Ca}^{2+}$  channels. This untimely opening of  $\text{Ca}^{2+}$  window currents (-35 to 0 mV), acts as a trigger for formation of EADs during the plateau phase of the AP (Hirano, Fozzard et al. 1989) (January and Riddle 1989; Zhou, Gong et al. 1998).

### **1.3.5.3 Calcium Oscillations and triggered arrhythmias in LQTS**

In situations where ventricular repolarization is prolonged, such as LQTS, there is evidence to suggest that an exaggerated fluctuation occurs in cytosolic calcium levels. These are called  $\text{Ca}^{2+}$  oscillations.  $\text{Ca}^{2+}$  oscillations occur during high  $\text{Ca}^{2+}$  loading conditions.

An increase in  $\text{Ca}^{2+}$  influx occurs when APD is prolonged. This may cause an increase in activity of forward-mode of the NCX which in turn increases  $\text{Ca}^{2+}$  loading of the cell. This subsequently causes a high SR  $\text{Ca}^{2+}$  load and is associated with spontaneous release of SR  $\text{Ca}^{2+}$  into the cytoplasm which triggers calcium dependent transient inward currents ( $I_{\text{ti}}$ ,  $I_{\text{Cl}(\text{Ca})}$ ). When the excess cytosolic  $\text{Ca}^{2+}$  is removed by the electrogenic (forward mode)  $\text{Na}^+ - \text{Ca}^{2+}$  exchanger it sets forth  $\text{Ca}^{2+}$  oscillations in the cell and is thought to result in EADs or DADs. If the oscillations reach high levels to cause supra-threshold membrane depolarization, it may result in impulse propagation and arrhythmia (Laflamme and Becker 1996), (Franz MR 1989). This phenomenon of spontaneous release of  $\text{Ca}^{2+}$  by the overloaded SR with subsequent membrane depolarization due to currents such as NCX, calcium dependent chloride current, is referred by some groups as 'reverse coupling'.

Evidence from Volders et al (Volders PG 1997) , Szentadrassy et al (Szentadrassy, Banyasz et al. 2005), Vos et al (Vos, Verduyn et al. 1995) support the hypothesis that calcium overload in the cytosol causes calcium oscillations. They suggested this to be a dominant mechanism to trigger EADs in LQT. Volders et al showed that during EADs, the cell  $\text{Ca}^{2+}$  concentrations and cell shortening, precedes voltage changes (Volders PG 1997). There have also been several other studies in both animal models and computer simulations, which showed simultaneous changes of both Calcium and Voltage ( $V_m$ ) in the cell during EADs and DADs (Hirano, Fozzard et al. 1989; Miura, Ishide et al. 1993; De Ferrari, Viola et al. 1995; Miura, Ishide et al. 1995; Nordin 1997; Wehrens and Marks 2004; Medeiros-Domingo, Kaku et al. 2007)

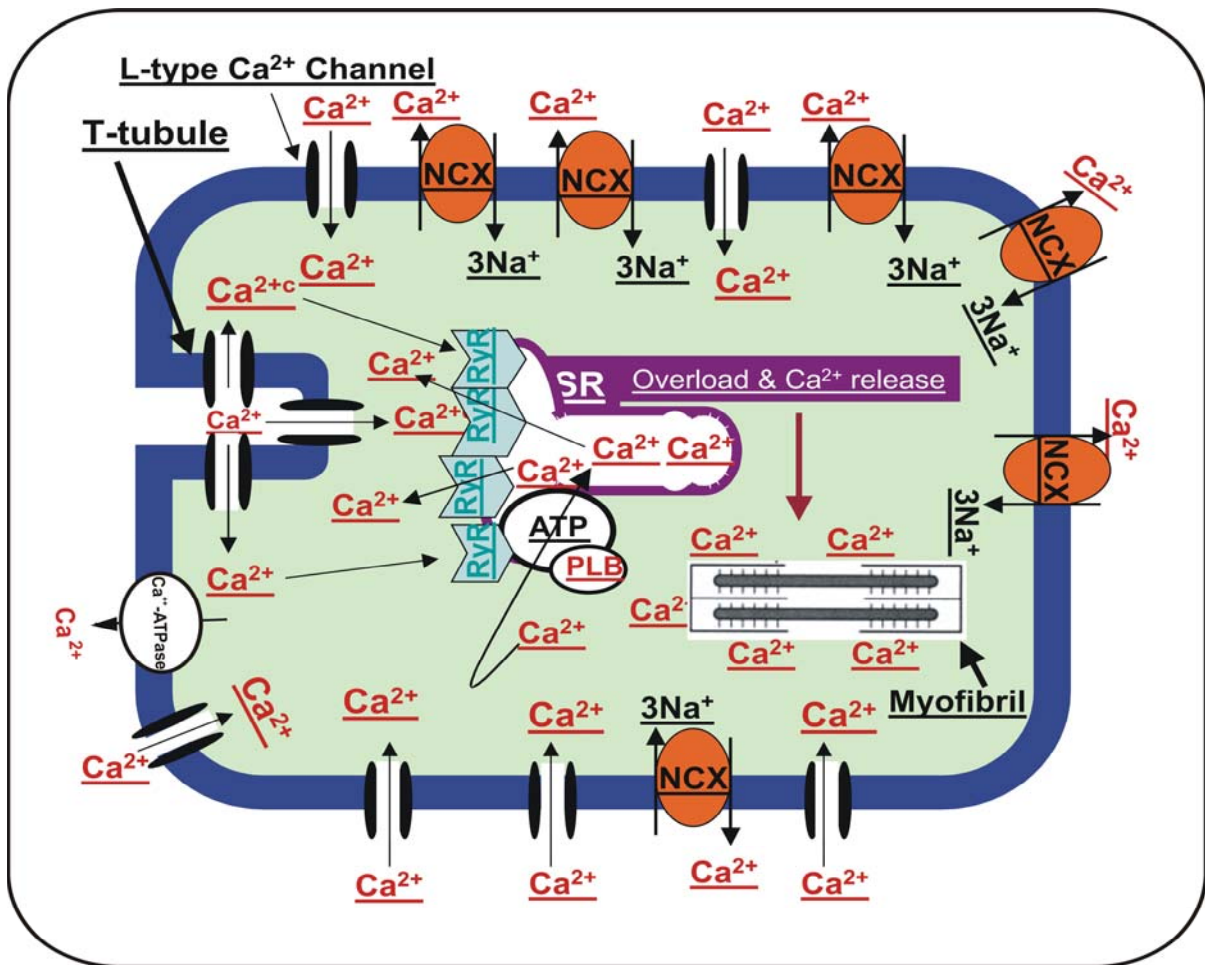


**Figure 7: Electro Mechanical coupling in myocardial cell**

Under normal conditions, AP triggers  $\text{Ca}^{2+}$  release from sarcoplasmic reticulum (SR) by voltage changes and by calcium induced calcium release mechanism (CICR). This elevation of  $\text{Ca}^{2+}$  is utilized for mechanical contraction of the muscle and then removed from cytoplasm by SR  $\text{Ca}^{2+}$  reuptake into the SR.  $\text{Ca}^{2+}$ -ATPase and  $\text{Na}^+/\text{Ca}^{2+}$  exchanger expel the calcium out of the cell. (With kind permission of Dr. Carl Sims, Youngstown State- University, USA)

### 1.3.6 Autonomic Nervous system and LQTS

As mentioned in previous section, most but not all patients of LQTS suffer symptoms and cardiac arrest during sympathetic activation, stress, emotion or following intravenous infusion of epinephrine. KCNQ1 mutation carriers have been seen to develop events about 68% of the times, during physical exercise or emotional stress and only 9% of times at rest (Schwartz, Priori et al. 2001). Further, swimming related cardiac events occur almost exclusively in LQT1 patients (Vatta, Ackerman et al. 2006). On the other hand, LQT 2 patients commonly develop TdP following auditory stimuli or startle responses (Schwartz, Priori et al. 2001). In contrast, LQTS 3 patients have an increased probability (49%) of having symptoms at rest or during sleep. Even though, there is plethora of data confirming the involvement of the autonomic nervous system in arrhythmogenesis in LQT, the role of neuromodulation is unclear and is not fully understood. This work mainly focuses on the neuronal component of the ANS and its role in some repolarization properties in LQT models.

Autonomic regulation of the heart has two distinct components. These are the neuronal and humoral components. However, these two components work in conjunction with each other. Cardiac neuro-anatomy is reported to be very complex and not fully understood. There seems to be wide inter-species and intra-species variation in the ganglionic neuroanatomy and nerve terminal distribution to the heart. A brief outline of the general neurocardiac anatomy is presented below. (Figure 8)

The autonomic neuromodulation of the heart is governed by the sympathetic system and the parasympathetic system. The sympathetic nervous system is governed by central nuclei from the thoraco-lumbar out flow system, which has its nuclei in the anteromedial horn of the spinal cord. From here, the nerve fibers run to various discrete ganglia in the chest including the stellate ganglia. The ganglia form an intercommunicating nexus between themselves. This network does not only involve the extra-cardiac intra-thoracic ganglia but also intra-cardiac ganglia. There have been several attempts to dissect out the neuroanatomy to understand their individual contributions but the clarity of functional neuro-physiology is still lacking. This has been attributed to the fact that isolation of a few ganglia changed the overall function of the network thus making it impossible to understand the role of these individual ganglia in the context of the neurophysiological hierarchy. (Armour 2004)

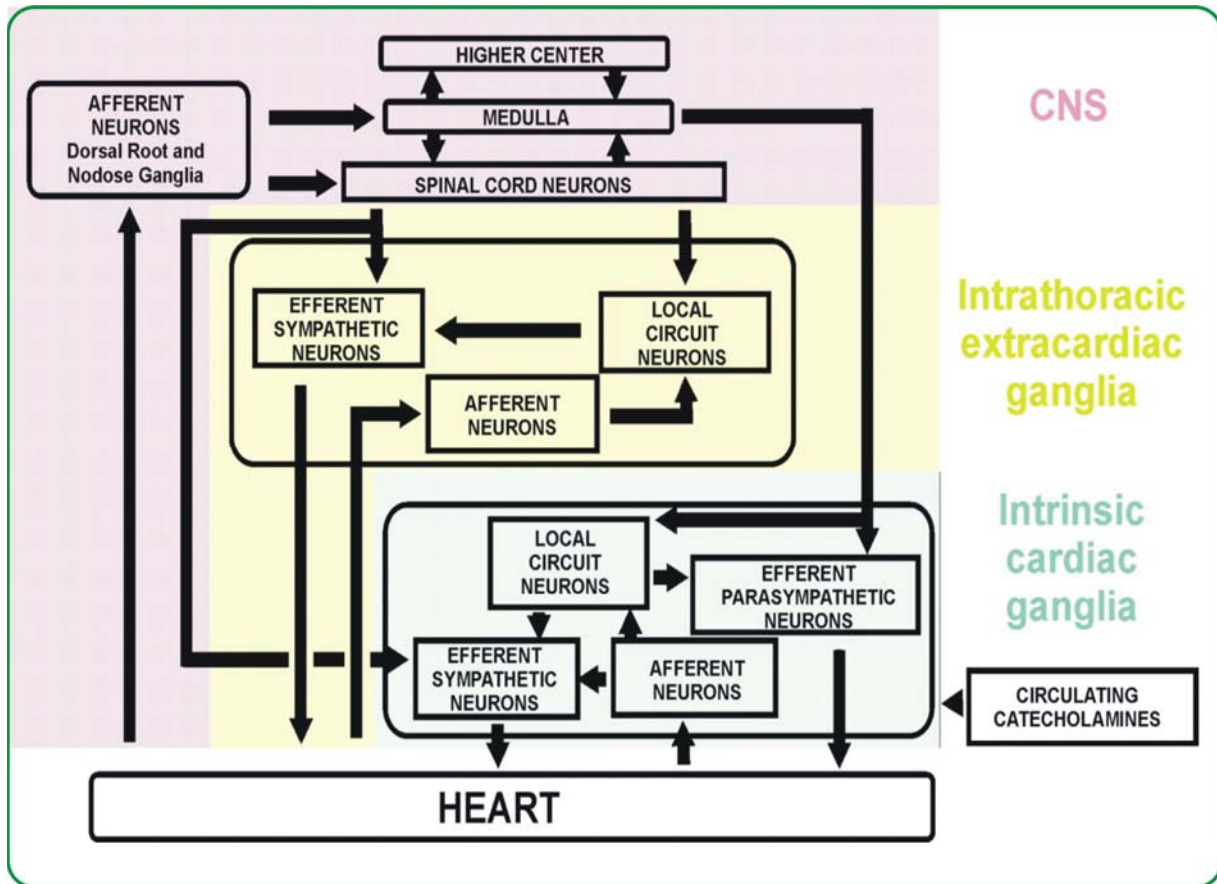


**Figure 8: Scheme of generalized neurocardiac architectural network**

The scheme summarizes the neuronal distribution related to the heart. The neuronal out flow starts from the higher centers via the cardiovascular centers in the medulla. The thoracic sympathetic out flow starts from the intermedio-lateral horns of the thoracic spinal cord. The efferents form intrathoracic ganglia which network here with the afferent arm from the heart and the local circuit neurons. The efferents from the intra-thoracic neurons innervate the heart directly and via intrinsic cardiac ganglia. The intrinsic cardiac ganglia are situated in the heart and have both afferent and efferent arms of the arc. Further, the circulating catecholamines influence the heart both directly and via the intrinsic cardiac ganglia. The parasympathetic nerves interdigitate and network with the sympathetic neurons at mainly intracardiac and to a lesser extent, in extra cardiac ganglia. (Armour 2004)

### 1.3.6.1 Effects of sympathetic activity in the myocardial cell

A short overview of the effects of the sympathetic activity in the myocardial cell is presented in this subsection.

Stimulated sympathetic nerve terminals release norepinephrine which activates the  $\beta$ -adrenoceptors in the cell membranes of excitable cells such as the pacemaker cells. The increase in heart rate with sympathetic stimulation is through increase in 'funny current'. Intracellular rise of cAMP leads to positive shift of voltage dependence of funny current and faster activation - both lead to increase in funny current and therefore faster rate of diastolic depolarisation of pacemaker cells (Wainger, DeGennaro et al. 2001). Further, sympathetically mediated phosphorylation of the cardiac sodium channels increases the number of bursts, their opening times. The electrophysiological consequences of increased phosphorylation of sodium channels are increased cell to cell conduction, higher and faster depolarization upstroke shorter action potential durations (Nathan and Beeler 1975; Murray KT 1990; Levi, Dalton et al. 1997)

Molecular biology and biochemical studies suggest that sympathetic activity increases PKA via the cyclic AMP (cAMP) pathway. PKA is thought to bind to the C-terminal portion of L-type calcium channel (at a consensus site) via phosphatases (Shimizu and Antzelevitch 2000). Recently, Marx et al experimentally showed that PKA (both catalytic and regulatory (RII) subunits), Protein Phosphatase 1 (PP1) and, Yotiao (the PKA- and PP1-targeting protein), were components of KCNQ1 macromolecular signaling complex in humans. They also showed that the channel activity was up regulated via PKA and down regulated by PP1 binding to its N-terminal domain (Marx, Kurokawa et al. 2002).

Fig.9 summarizes the intra cellular pathways following sympathetic stimulation. Briefly, the  $\beta$ -adrenoceptor is activated by sympathetic stimulation via activation of the adenylate cyclase (AC) system and specific G proteins. The cAMP, formed from adenyl cyclase, activates protein kinase A (PKA), which in turn activates L-type  $\text{Ca}^{2+}$  channel (LTCC) via A-kinase anchoring protein (AKAP), and ryanodine receptor-2 (RyR2) and  $\text{Na}^+/\text{Ca}^{2+}$  exchanger (NCX) via muscle AKAP (mAKAP). At higher sympathetic stimulation increase the cytosolic  $\text{Ca}^{2+}$  concentration, which activates  $\text{Ca}^{2+}$ /calmodulin-dependent protein kinase (CaMKII). CaMKII is thought to phosphorylate LTCC, RyR2 (to which CaMKII is directly targeted) and

phospholamban (PLB). Activation of  $\alpha$  adrenoceptor activates phospholipase C (PLC) via G proteins, which in turn activate protein kinase C (PKC  $\alpha$ ). PKC  $\alpha$  directly phosphorylates protein phosphatase inhibitor-1 (I-1), enhancing the activity of the protein phosphatase-1 (PP1) and causing hypophosphorylation of PLB. (Wehrens and Marks 2004)

Of relevance to LQT2 physiology, Gullo et al in 2003 showed that the blockade of ERG  $K^+$  channel enhances the firing rate and epinephrine secretion from rat chromaffin cells. They have also shown that blockers of ERG channels modify the excitability of single chromaffin cells and, cause a release of large amounts of catecholamine during sympathetic stress during startle reactions. This phenomenon is probably due to the lack of ERG channel-sustained feedback mechanism. This may account, in part, for the typical symptoms in LQT 2, where patients have low resting heart rates and have sudden cardiac arrest when startled (Gullo, Ales et al. 2003).

### **1.3.6.2 Cholinergic regulation of ventricular electrophysiology**

It has been known for a few decades that vagal nerve stimulation leads to release of acetylcholine (ACh) at the nerve endings. Yang et al in 1996 showed in dog sub-epicardial cells that, the negative inotropic effect of acetylcholine is due to its effect on L type calcium channel (Yang, Boyett et al. 1996). Yan et al showed ACh to be a strong inhibitor of the L type calcium current ( $I_{CaL}$ ). (Yan, Wu et al. 2001). George et al in 1970 showed that ACh increases cGMP which subsequently activates PKG (Brink, Crotti et al. 2005). Recently, it was shown that  $I_{CaL}$  is reduced by both PKG and cGMP (Sperelakis, Katsube et al. 1996). Belardinelli and Isenberg in 1983 showed that  $I_{K(ACh)}$  activation reduced APD in atrial cells which led to voltage dependent termination of  $I_{Ca2+}$  (Belardinelli and Isenberg 1983). This mechanism was earlier thought not to exist in the ventricular muscle of several species. However, recent data from cellular studies demonstrated similar electrophysiology of muscarinic activated potassium channels in ferret, canine and feline ventricular cells respectively (Belardinelli and Isenberg 1983), (Yang, Boyett et al. 1996; Knisley, Justice et al. 2000). In the human ventricles, the presence of ACh receptors and their distribution is well documented by immuno-histochemical techniques (Kawano, Okada et al. 2003).

Cholinergic activation is thought to antagonize sympathetic stimulation (accentuated antagonism) in two ways - firstly, ACh causes pre-junctional inhibition of NE release from the

sympathetic nerve terminals via M3 receptors (Loffelholz and Muscholl 1969; Kobayashi, Nagashima et al. 1987) and secondly, by post-junctional interference and inhibition of beta-adrenergic pathway of the myocardial cell. The post-junctional mechanisms of cholinergic regulation thought to occur via the mechanisms which are summarized in fig 10. Where, AC and cAMP levels in the cell are decreased directly by putative  $\alpha$  subunit of the muscarinic receptor (Hartzell 1988) and indirectly via  $\beta\gamma$  subunit of the muscarinic receptor and the inhibitory G protein (Fleming, Strawbridge et al. 1987).

George et al showed that cGMP levels increase after cholinergic stimulation (Brink, Crotti et al. 2005). Later Hartzell et al showed in 1988 that guanylate cyclase (GC) increases cGMP levels. In 1995, Balligand et al (Balligand JL 1995) showed that endothelial nitric oxide-synthase (eNOS) produces nitric oxide (NO) and this in turn mediates GC. The exact role of NO with regards to its antagonistic properties on cAMP and PKA is still unclear owing to lack of appropriate controls and technical difficulties (Vandecasteele, Eschenhagen et al. 1998; Balligand 1999).

The net effect of cGMP on cAMP and calcium channels is not fully clear. Although there is strong evidence to point to decreased PKA via phosphodiesterase II (PDEII) (Fischmeister R 1987), cGMP was shown to increase cAMP via inhibition of PDE III in guinea pig ventricular cells and a biphasic action on L-type calcium channels. (Ono and Trautwein 1991; McDonald, Pelzer et al. 1994).

There is also evidence to suggest that the  $\beta$  adrenergic stimulated L type calcium current is reduced by cholinergic stimulation and this is thought to happen by cGMP mediated reduction of PDE II via muscarinic receptor/eNOS/NO mechanisms (Fozzard 1992; Sasaki, Daitoku et al. 2000; Dittrich, Jurevicius et al. 2001; Yan, Wu et al. 2001).

Lindermann and Watanabe *et al* in 1985 showed that phospholamban (PLB) phosphorylation induced by isoprenaline is attenuated by ACh and this was supported by further experiments by Bartel et al in 1993 and Sulakha and Vo in 1995. Thus there is evidence to suggest a presence of cell level antagonism of the sympathetic pathway. Hence, the cholinergic pathway may contribute to change of intracellular calcium transient (Lindemann and Watanabe 1985; Bartel, Karczewski et al. 1993; Sulakhe and Vo 1995).

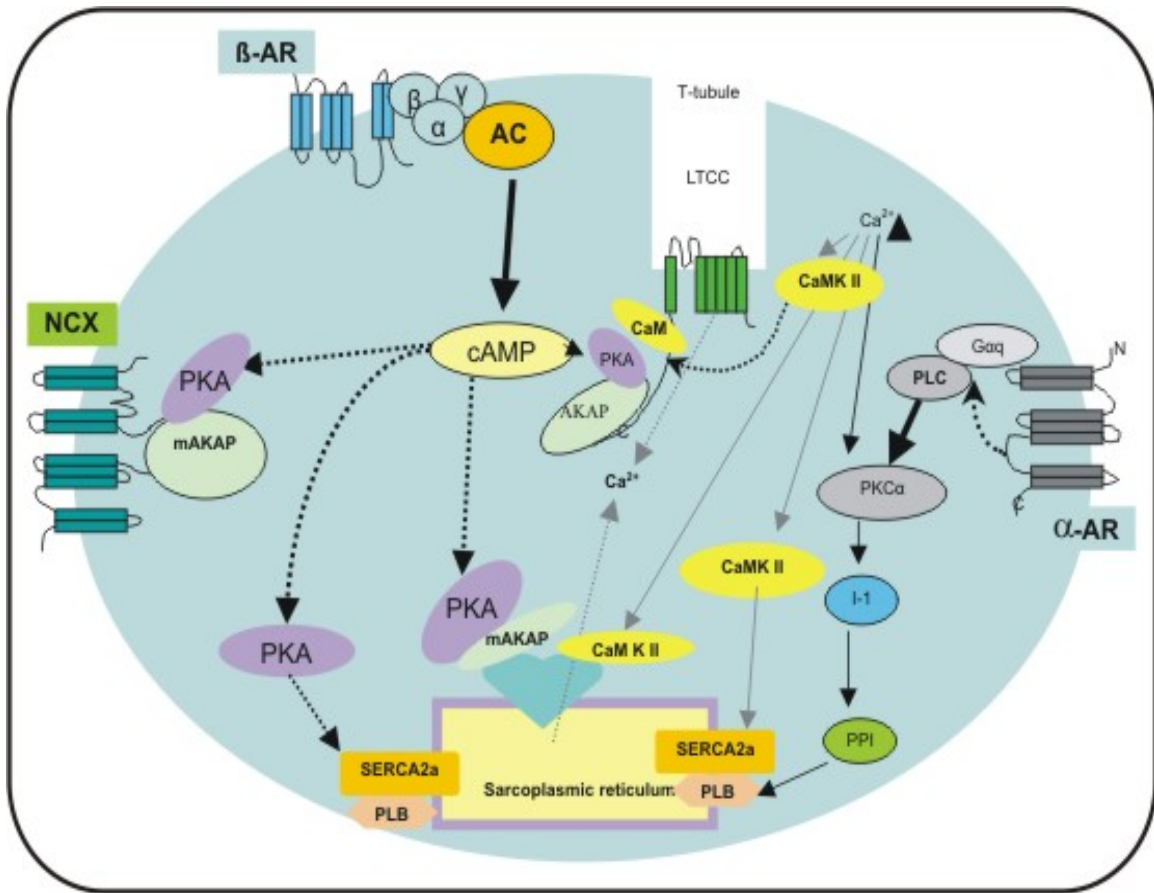


**Figure 9: Schematic showing the regulation of intracellular calcium signaling in the heart during sympathetic activity.**

Sympathetic activity activates the  $\beta$ -adrenoceptor which leads to activation of adenylate cyclase (AC) via specific G proteins. cAMP (formed from adenyl cyclase), activates protein kinase A (PKA), which activates L-type  $\text{Ca}^{2+}$  channel (LTCC) via A-kinase anchoring protein (AKAP), and ryanodine receptor-2 (RyR2) and  $\text{Na}^+/\text{Ca}^{2+}$  exchanger (NCX) via muscle AKAP (mAKAP). At higher sympathetic stimulation increase the cytosolic  $\text{Ca}^{2+}$  concentration, which activates  $\text{Ca}^{2+}$ /calmodulin-dependent protein kinase (CaMKII). CaMKII is thought to phosphorylate LTCC, RyR2 (to which CaMKII is directly targeted) and phospholamban (PLB). Activation of  $\alpha$  adrenoceptor activates phospholipase C (PLC) via G proteins, which in turn activate protein kinase C (PKC  $\alpha$ ). PKC $\alpha$  directly phosphorylates protein phosphatase inhibitor-1 (I-1), enhancing the activity of the protein phosphatase-1 (PP1) and causing hypophosphorylation of PLB. SERCA2a, sarcoplasmic reticulum ATP-aseBeta adrenoceptors; (Modified from Xander HT, Weherens and Andrew R Marks. *Novel Therapeutic Approaches for Heart failure by Normalizing Calcium Cycling*. *Nature Reviews* vol 3. july 2004)

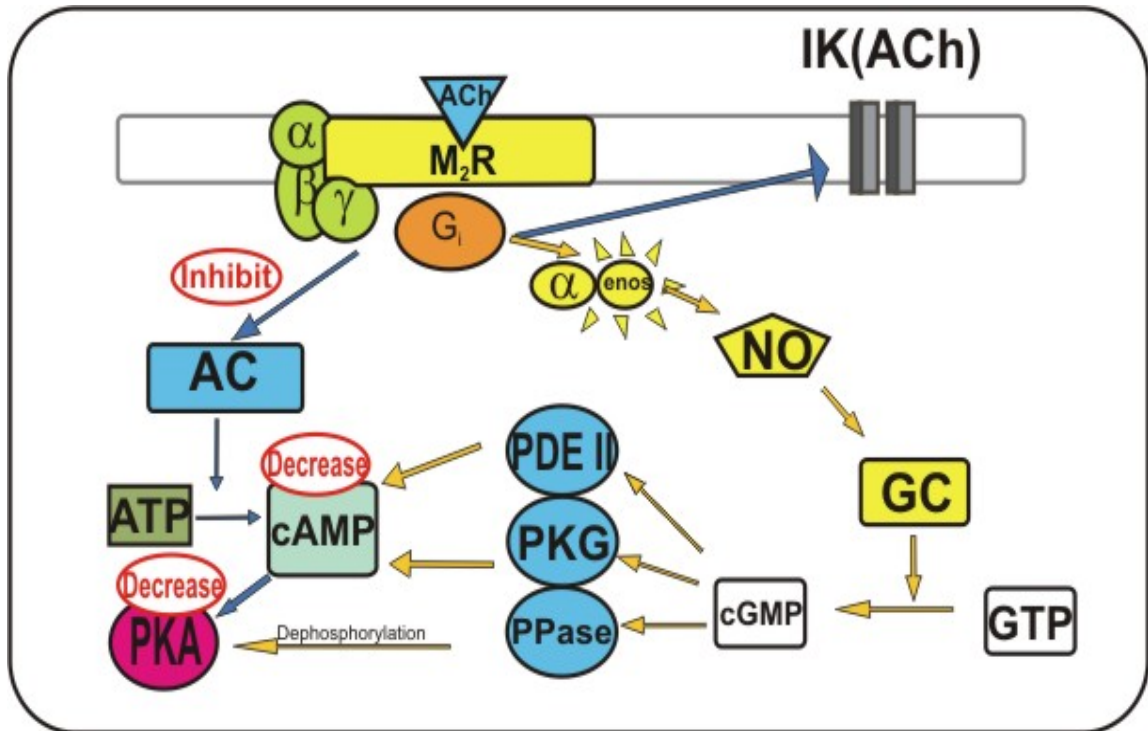


**Figure 10: A Schematic depiction of the various putative cholinergic pathways influencing PKA**

When Acetylcholine (ACh) binds to the muscarinic receptor 2 ( $M_2R$ ), Cyclic Guanosine Mono Phosphate (cGMP) system gets stimulated (adenyl cyclase system (AC) gets inhibited) via inhibitory G protein ( $G_i$ ). IK ACh is a ligand (acetyl choline) gated potassium channel which get activated via  $G_i$  protein and results in inward rectifier potassium current. eNOS or Endothelial Nitric Oxide Synthase produces nitric oxide which via Guanyl cyclase (GC) and phosphodiesterase II (PDE), Protein phosphatase (PP), cAMP- cyclic Protein kinase G (PKG) reduces cytosolic PKA, thus anatagonistic to the effects of sympathetic system. See text for details.

## 2.0 THESIS AIMS AND LAYOUT

### 2.1 AIMS

As discussed in chapter 1, syncope and sudden death in Long QT syndrome are predominantly due to polymorphic ventricular tachycardia, torsade de points and ventricular fibrillation. However, mechanisms predisposing the heart to arrhythmias are still incompletely understood. Arrhythmias in Long QT syndrome are known to occur during autonomic activity. The changes in repolarization (Dispersion of repolarization (DOR), Restitution and Repolarization reserve) of the myocardium under autonomic activity are thought to influence arrhythmia mechanisms. Although autonomic modulation of the ventricle is modulated by both humoral and nervous components, yet, due to technical difficulties a detailed understanding of the underlying mechanisms of the neuronal modulation is still elusive.

In order to address this long standing problem, the isolated innervated rabbit heart preparation was developed by Andre Ng *et al* at the Universities of Leicester and Birmingham. This preparation enables one to study the influences of sympathetic and parasympathetic nerve stimulation and humoral effects on the cardiac electrophysiology independently. Until recently, electrophysiological data using this preparation was obtained by Monophasic action potentials (MAP) recorded from the surface of the ventricle using contact electrodes. The widely used contact MAP electrodes have several inherent limitations in action potential duration measurements, especially when used to study repolarization. Optical mapping, a relatively new technique which uses voltage-sensitive dyes, offers the most accurate measurements of the action potential with a very high spatial and temporal resolution. Further adaptation of this preparation was necessary for optical mapping, a technique that uses fluorescent voltage-sensitive dyes and offers highest spatial and temporal resolution.

A combination of these two state-of-the-art techniques was hypothesized to allow the evolution of a powerful model that can simultaneously measure action potential properties from 256 sites on the ventricle during autonomic nerve stimulation.

This work aims to address above issues in three components 1) Experimental surgical research to adapt the isolated innervated heart preparation to optical mapping, 2) modification of the optical mapping set-up for stable and sustained light collection during nerve stimulation and 3) study of the effects of neuronal stimulation on dispersion of repolarization and restitution kinetics before and during ion channel inhibition, mimicking LQT pathophysiology.

## **2.2 THESIS LAYOUT**

Chapter 3 focuses on the methods. It attempts to briefly discuss the existing methods to measure action potentials under autonomic stimulations, the need for a stable accurate neurocardiological model, surgical procedure in detail, initial difficulties faced during surgical adaptation of the isolated innervated preparation with optical mapping, novel modifications like dual cannulation technique and a novel hybrid method of low dose excitation-contraction uncouplers and physical restraint of the heart has reduced motion artifacts to the minimum and maximized the accuracy of the action potential measurements.

Chapter 4 describes the relevance of physiological restitution compared to classical restitution studies in the context of LQTS. It presents the rationale for assessment of restitution during sympathetic nerve stimulation; describes the experimental protocols; presents the data and discusses the findings and interprets the data in the light of current literature. It also attempts to interpret the change in physiological restitution during ion channel inhibition in the context of reduction of repolarization reserve.

Chapter 5 describes and discusses the role neuromodulation of another important repolarization property shown to be involved in LQT arrhythmias i.e. Dispersion of repolarization (DOR). The chapter presents novel data suggesting the uniqueness of

neuromodulation of DOR in controls and further discusses its influence on the ventricle during ion channel inhibition mimicking LQT pathophysiology.

Chapter 6 summarises the work and suggests future directions.

### 3.0 MATERIALS AND METHODS

To study the electrical changes over the myocardium during autonomic nerve activation on stimulation, several methods were used over the last few decades. These methods are briefly outlined in this section. This may set the background for current work and summarize the latest technologies used in organ-level cardiac electrophysiology research.

As mentioned in the introductory chapter, anatomically and functionally complex neuronal aggregates coordinate regional cardiac electrophysiology. Data obtained thus far, about the regional control of neuronal hierarchy have been acquired by neurosurgical experiments mainly on the canine species. Also, comparative cardiac neuroanatomy has been used to compare the anatomical differences between the species. Current information about the regional neurocardiac control of the heart comes from a large data pool from heterogeneous experiments involving several animal species. They range from intra-operative stimulation of various intracardiac ganglia, selective destruction of intracardiac ganglia, regional pericardial stimulation and several other in-vitro neurophysiological studies (LazzaraR 1973; Randall 1985; WC 1986; Rosenbaum, Kaplan et al. 1991; Armour J.A. 1997; Pauza DH 2000; Arora RC 2003).

The model developed and described in this work is a result of a conjugation of two independently validated methods i.e. an isolated innervated heart preparation and optical mapping. Both these techniques had to be modified for mutual compatibility. Innervated heart preparation allows the study of electrophysiology of the heart during autonomic nerve stimulation. Optical mapping is the most accurate of all the contemporary methods to study the action potentials over a surface of the heart. It offers excellent spatial and temporal resolution. The surgical modifications and mechanical adaptations are described in detail in this chapter.

Also an attempt has been made to mention the pros and cons of the different aspects of the model and importantly, to record the failures of several initial attempts in the process of adaptation of the innervated heart preparation for optical mapping. It is hoped that this will make it easier for researchers who intend to use this model in future.

Since most of the time was spent on the shaping of the method, data acquired was a by product of the evolution of this novel neuro-cardiological model, the data is presented as preliminary data.

Further work is required to refine this model especially to optimize multi-parametric optical mapping.

### 3.1 MATERIALS

Accurate measurement of electrical activity from the heart is crucial for electrophysiological studies. Local cellular electrical activities are not clearly depicted on the surface electrocardiograms of the whole heart. This is because the signals from surface ECGs represent net averages of the regional electrical activity. There seems to be a ‘loss’ of data by the averaging process.(Fogoros 2006)

Patch-clamping techniques enable one to record transmembrane electrical activity directly. This has been an invaluable tool in the last few decades to characterize the building blocks of cellular electrophysiology. However, this approach is not as helpful for integrative biological studies as it is impossible to measure all the cells simultaneously, especially in an intact organ.(Efimov, Nikolski et al. 2004)

Local and regional electrical signals have been the studied using MAP electrodes before the turn of last century. These techniques are still used to measure local electrical signals. A short account of these methods and their limitations is presented below.

One of the most recent of the technological revolutions in contemporary electrophysiology research is that of Optical mapping. Optical modes of imaging, in combination with parameter-sensitive probes have already demonstrated their ability to overcome the problem of spatiotemporal resolution in two dimensions for a wide range of applications from single molecular events to *in vivo* whole animal physiology.(Efimov, Nikolski et al. 2004) A detailed account of this technique is presented in this chapter.

### 3.1.1 Monophasic action potential measurement

Monophasic action potentials (MAP) are waveforms of membrane electrical activity recorded from the extracellular space using electrodes. These waveforms have been shown to loyally reproduce the depolarization and repolarization of transmembrane action potentials. Burdon-Sanderson and Page, in 1882, placed one electrode on the intact epicardial surface and another on an injured site on a frog's heart. They demonstrated phasic electrical changes between two electrodes and called it the 'injury current'. (Burdon-Sanderson 1880)

Subsequently, a much less traumatic contact electrode technique was developed and first used in 1935 by Jochim *et al* (Kenneth Jochim 1935). Contact MAP electrodes have been used for both experimental studies and also clinically to study the local electrical signals from the endocardial surface of the heart in the clinical electrophysiology labs (Franz, Schottler *et al*. 1980; Franz 1999). They were basically of two types: unipolar and bipolar electrodes. The Unipolar electrode measures the local electrical activity compared to a distant reference electrode. The bipolar electrode measures the local electrical activity with an adjacent (about 5mm) reference electrode that is indifferent to the monophasic field. This aims to provide a true local signal of less than 5mm diameter by canceling out far field electrical signals (Franz, Burkhoff *et al*. 1986). Figure 11 illustrates an example of comparative MAPs.

Although transmembrane action potentials (TAP) and MAPs were shown to be identical in their morphology (Franz MR 1989), the exact mechanism of genesis of these potentials is still debated. Several theories are discussed. One thing is clear; MAP signals are not intracellular measurements of electrical activity. This is simply because of the sheer size of these electrodes (1-2mm in diameter). Older theories debated whether the signals are injury currents or simply recordings of electrical activity from intact myocardium by simple contact.

It is beyond the scope of this work to indulge in a detailed discussion of these theories. Briefly, Schutz *et al* proposed a hypothesis according to which, MAPs are a result of a voltage drop (due to differences in the resistances) between the different electrode which was thought to be in contact with injured myocardium, and the indifferent electrode in contact with the normal myocardium. Subsequent theorists felt that MAPs signals were a result of a current source from volumes of cells below the electrodes which act as electromotive generators arranged in series.

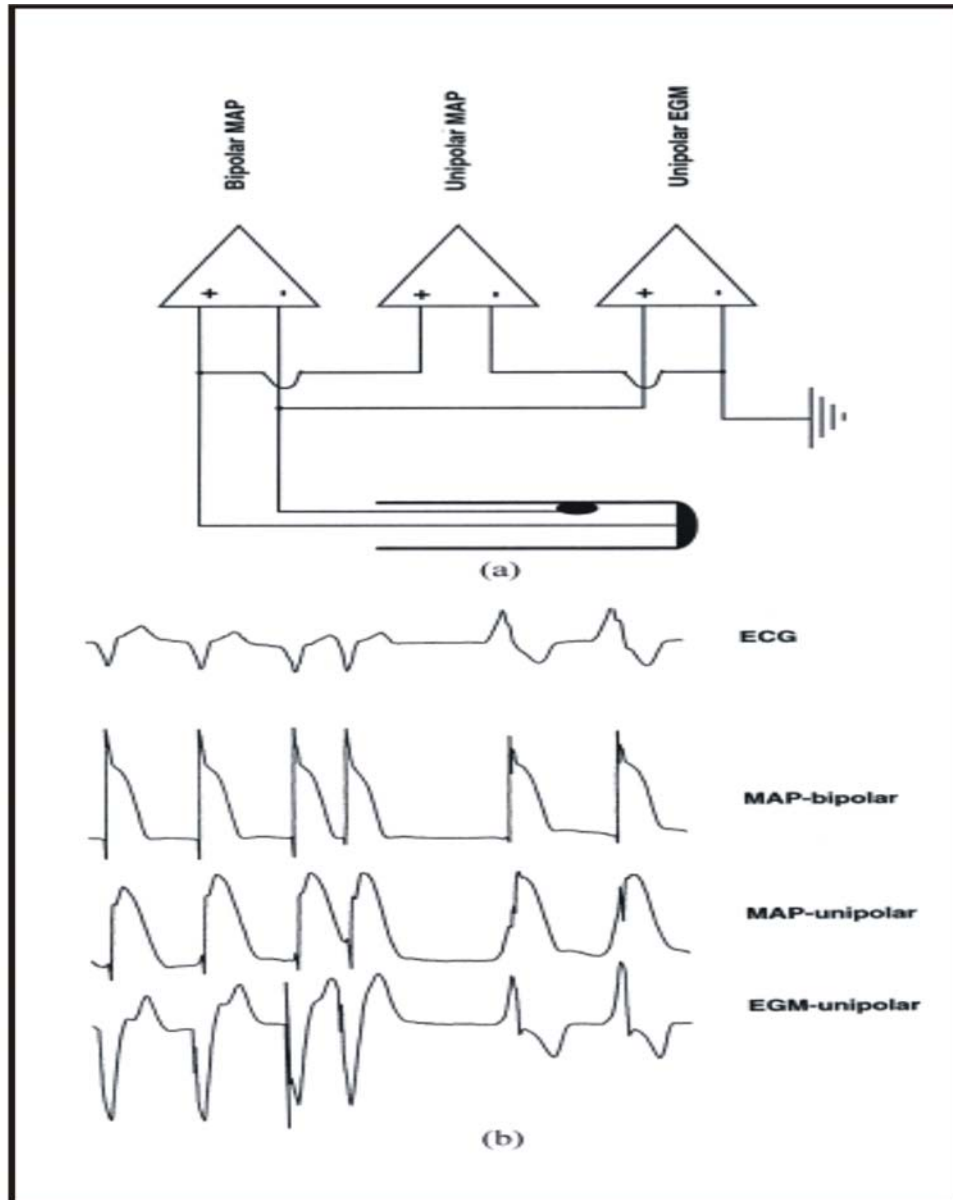


**Figure 11: Recordings of MAPs from a single catheter from one region of the heart**

Panel (a) shows a schematic diagram of the anatomy of a modern contact electrode having three channels. This electrode has three Monophasic action potential (MAP) recording circuits: The Bipolar MAP, Unipolar MAP and the Unipolar Electrogram (EGM). Panel (b) shows simultaneous local tracings from each of these channels and the rhythm strip of the surface ECGs. The Unipolar MAPs and Unipolar EGMs show significant distortions in their waveforms and durations whereas, Bipolar MAPs are more stable morphologically and change dynamically with change in cycle length (note the ectopic beat). Slightly modified from (Franz 1999)

The reader interested in the details is referred to the following articles (Franz 1991), (Franz 1999). More recently, there are reports suggesting that it is not the contact electrode or the MAP electrode which records the MAP but it is actually the non inactivating indifferent electrode (Kondo, Nesterenko et al. 2004). This group, proposes the view that MAP represents the extracellular potential difference between the active and inactive sites with in the heart rather than potential differences between the injured and normal sites

Regardless of the debate about how MAP works, MAPs have been used as standard techniques for electrophysiological measurements for many decades. Action potential durations (MAP durations) were traditionally measured by the desired percentage of repolarization (see figure below). The repolarization studies were carried out using this form of measurements. Several uses of MAP recordings have been recognized, amongst them are: effects of rate and rhythm on the action potential durations; understanding arrhythmias mechanisms especially EADs, DADs, ventricular tachycardia, mechanisms of T wave alternans etc; measurements of dispersion of repolarization; study myocardial ischaemia and related substrate changes; last but not the least- monitoring radiofrequency ablations.(Franz 1983; Moore and Franz 2007) Multi-site recordings simultaneously are also possible with MAP electrodes. Overall, MAP contact electrodes are very useful tools for measurement of local action potentials in an intact heart.

However, MAP recordings have inherent limitations. A number of studies have shown that, unless the quality of MAP recordings meets important high-quality criteria, the MAPs do not seem to match TAPs. The general criteria for acceptability are the following: amplitude of MAP not less than 10mV; rise time not more than 5ms; total absence of contamination by intrinsic deflection or QRS; smooth upwardly convex plateau; horizontal diastolic baseline; MAP waveform fidelity to changes in cycle length. (Hoffman, Cranefield et al. 1959; Franz, Burkhoff et al. 1986; Ino, Karagueuzian et al. 1988)

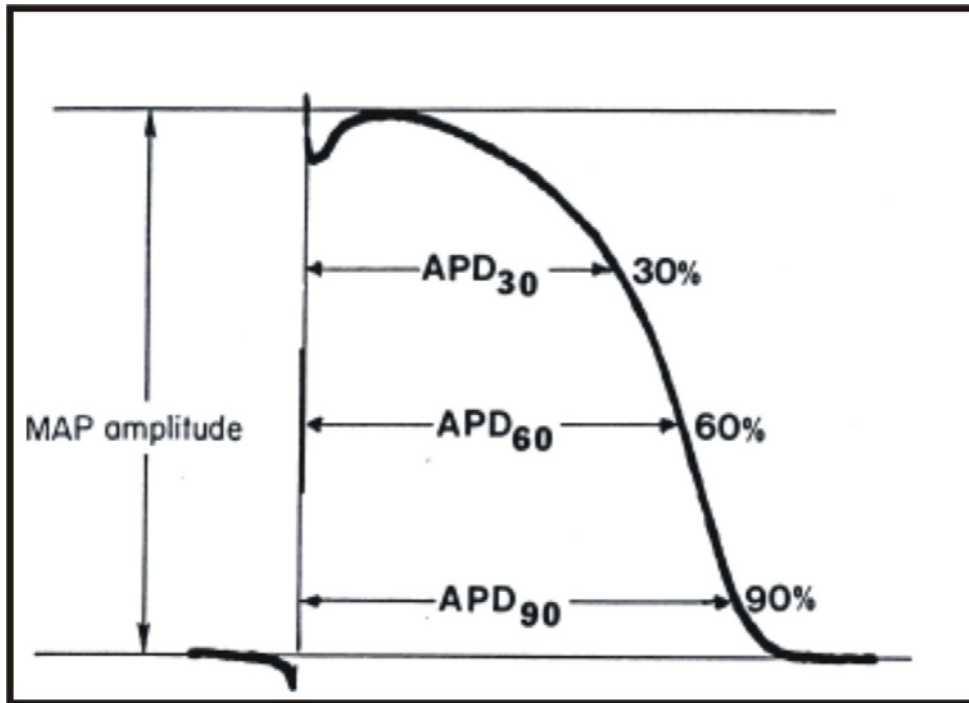


**Figure 12: Measurements of MAP Signals**

A traditional approach to measurement of Monophasic action potential (MAP) signals is shown in the figure. The Amplitude is the distance between the baseline and the tip of plateau. The duration of the MAP signal is measured along a horizontal line to the diastolic baseline, from the point of intrinsic deflection to the desired repolarization level (i.e.30%, 60%or 90%). Slightly modified from (Franz 1983)

Beating hearts pose difficulties to action potential measurements due to the physical motion itself. With contact MAP recordings, the amplitude of the MAP is dependent somewhat, on the contact pressure exerted by the electrode against the myocardium. Therefore, on a beating heart, oscillations in the amplitude, shifts in the diastolic baselines, irregularities in sustained steady contacts are some problems with MAP electrodes.

Furthermore, several other factors such as heterogeneity of the myocardium, non-uniform ventricular contractions and mechanoelectric feedback mechanisms, sensorineural nested feedback mechanisms influence the local APD, however, not enough data is available to characterize these influences on local APDs. These difficulties may reduce the accuracy of measurements (Franz, Schottler et al. 1980; Franz 1999; Armour 2004).

More recently, it was shown that it is possible to measure the action potentials accurately without actually placing an electrode to the heart, by optical techniques (Salama and Morad 1976). The relatively recent advent of optical mapping has revolutionized the measurements of

action potentials. The principles and overview of optical mapping is presented in the following subsection.

### **3.1.2 Principles of Optical Mapping**

Guy Salama showed that a dye Merocyanine 540, binds to the cardiac cell membrane without having any deleterious effect on its function, and is capable of monitoring the change in the myocardial cell membrane potential fluorometrically when excited at 540nm (Salama and Morad 1976). With the availability of better optical dyes and scanning equipment, the optical techniques have revolutionized electrophysiology research not only measuring the action potentials, but also calcium homeostasis and other cellular processes. Optical mapping has been extended from study of the electrophysiology of the heart to neurons and other tissues as well.

An optical mapping system consists of three major components: 1) the heart preparation which is stained with a voltage sensitive dye 2) Optical system which filters the light and focuses it and then collects the emitted fluoresced light from the heart preparation on to the photo-detectors and 3) photo-detector, which measures the emitted fluorescent light form the heart preparation (Figure13).

The voltage-sensitive dye molecules, when administrated via the perfusates or superfusates, bind to the myocardial cell membrane with high affinity. These molecules act as local membrane transducers and fluoresce light in proportion to the membrane voltage thus obviating the need to insert the cells/tissues with electrodes. Furthermore, this method allows much higher spatial resolution than the MAP electrodes. (Rosenbaum 2001)

#### **3.1.2.1 Potentiometric dyes**

When the dye molecules are bound to the cell membranes, two basic steps govern the function of the fluorescence of these dyes. Firstly, the dye molecules have to be excited by a specific wavelength of light from the light source. This excites the dye to a higher energy state. Secondly, the dye molecules should emit a longer wavelength of photons when their energy levels return back to resting states.

There are two kinds of potentiometric probes - a) fast response b) slow response probes

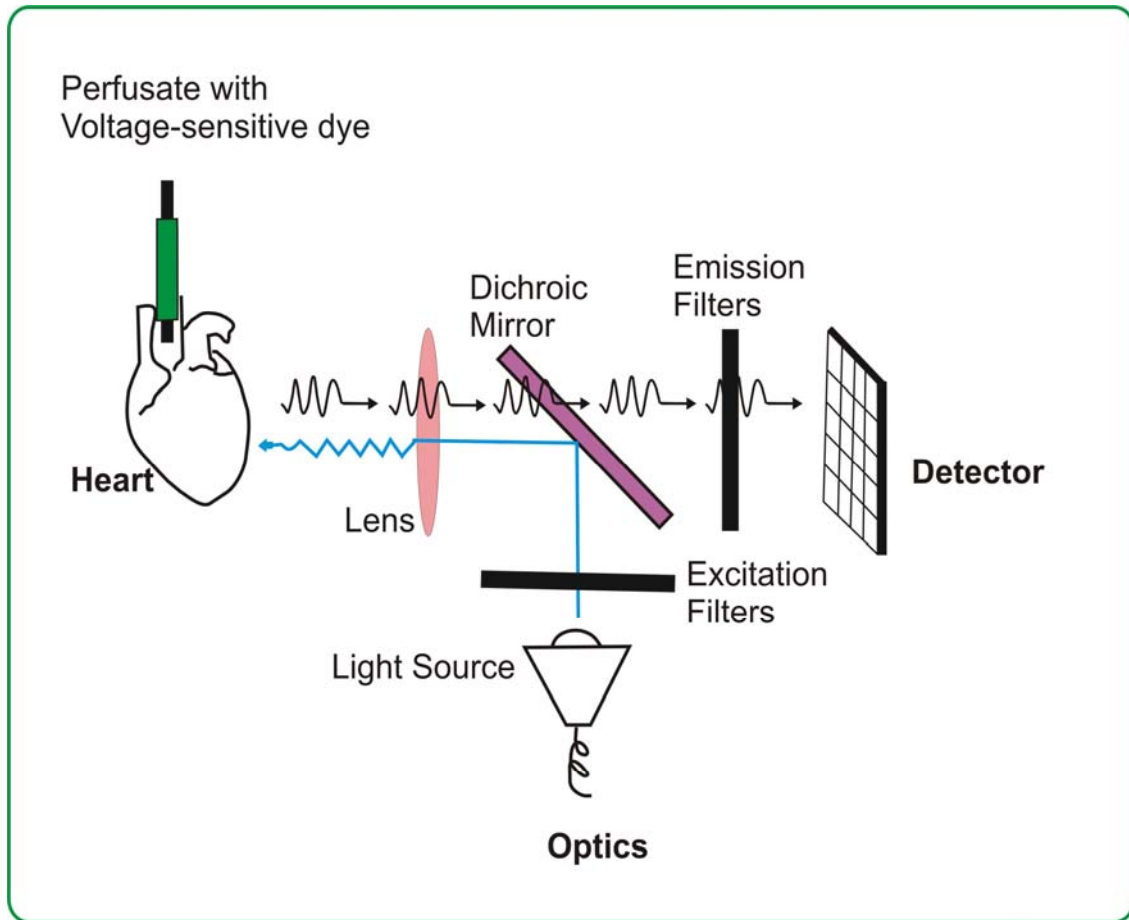


**Figure 13: Scheme of a typical optical mapping system**

The figure highlights the three essential components (in bold) of a typical optical mapping system. Heart stained with voltage sensitive dye, Optics for transmission and collection of light and the Detectors for light quantification. Excitation filter allows selected wavelength of light to pass on to the heart via a Dichroic mirror which can reflect the excitation light from the light source whilst refracting the emitted fluorescent light from the heart on to the Detector for measurement (Rosenbaum 2001).

Slow response potentiometric probes produce changes in the emission wavelength following transmembrane movement of entire molecules. These are not used in cardiac electrophysiology routinely and are not discussed here.

Fast-response probes (or electrochromic dyes) undergo electric field-driven changes of intramolecular charge distribution and produce corresponding changes in the spectral profile of intensity, or wavelength of their fluorescence emission (see figure below). These dyes are used extensively in cardiac optical mapping studies because the optical responses of fast potentiometric probes are so fast that they can detect transient millisecond potential changes on the cell membranes. For example, for an electrochromic dye to change its fluorescence it requires about  $10^{-12}$  to  $10^{-6}$  ms. This is manifold faster than the fastest electrical event i.e. depolarization which takes about  $10^0$  ms. Thus they are able to change their fluorescence with great agility.

For any given constant excitation wavelength, the voltage-sensitive dye emits a range of wavelengths depending on the membrane voltage. This is called the emission spectra. During a steep change in membrane voltage (during depolarization), there is corresponding rapid shift in the emission spectrum. This change in the emission spectrum also changes the amount of light collected by the detectors.

Therefore, by quantifying the change in light intensity one can indirectly gather information about the changes in membrane voltage. This is the fundamental principle of optical mapping. It is important to emphasize that changes in emission spectra reflects the relative changes in membrane voltage and do not correspond to absolute membrane voltage. (See figure below for a schematic representation of the principle of voltage sensitive fluorescence (Rosenbaum 2001))

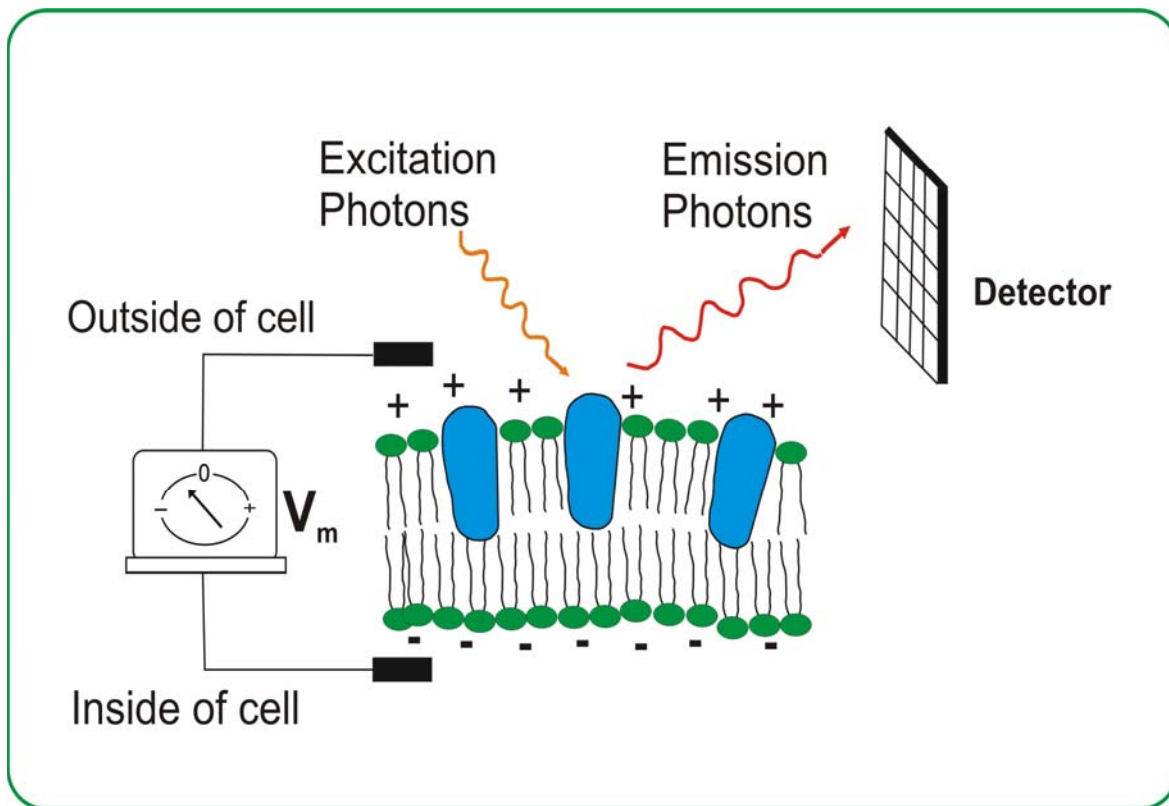


**Figure 14: Schematic representation of the function of membrane-bound dye molecule in optical mapping**

When the exciting wavelength incidents on the membrane-bound dye molecule (in blue), the dye emits longer wavelength photons. The intensity of the fluorescence varies according to the membrane voltage  $V_m$ . This emitted light from the dye when collected on the detectors is converted back into electrical signal by the photo detector (labeled as detector). Modified from (Rosenbaum 2001).

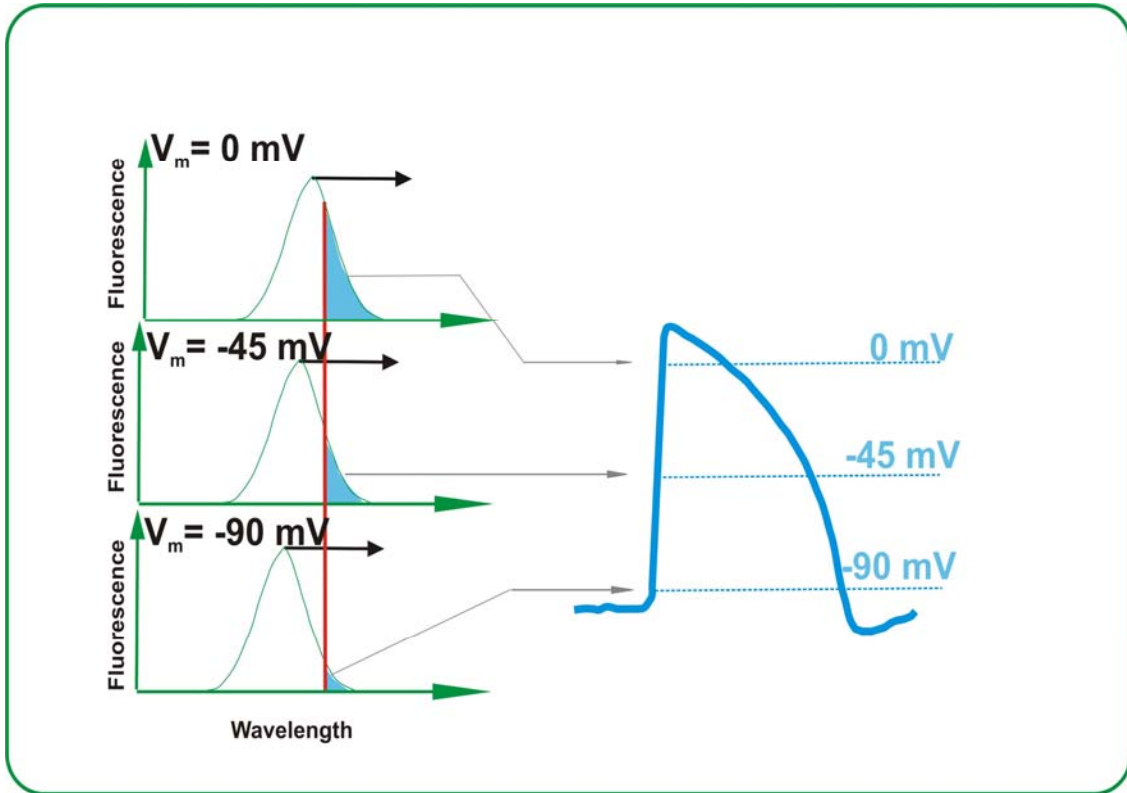


**Figure 15: Principles of voltage-dependent changes in emission spectra of a typical dye**

The schematic diagram highlights the principle behind voltage-sensitive fluorescence of typical membrane-bound electrochromic dyes. The emission spectrum of the dye molecule changes in consonance with membrane-voltage changes. As resting voltage (-90mV) increases during depolarization, the emission spectrum of the dye shifts to the right. When a long pass filter (depicted by the red line) is placed in the path of the emitted light, the amount of light striking the detector depends on the membrane voltage. This is denoted by the blue shaded area under each spectrum. Thus the voltage sensitive dyes convert membrane potential into light intensity. Modified from (Rosenbaum 2001).

A large number of potentiometric dyes are available commercially for optical mapping. Each dye has its own set of optical properties. They have unique absorption ( $\lambda Abs$ ) and emission ( $\lambda Em$ ) wavelength spectral peaks. They have different wavelengths in different media. Detailed properties of voltage-sensitive optical dyes are presented in Molecular Probes handbook (P.Haugland). There are a number of dyes available to be used and are many being developed to improve the quality of the measurements. Generally, the magnitude of their potential-dependent fluorescence change is small; fast-response probes typically show a 2–10% fluorescence change per 100 mV. (P.Haugland; Loew, Cohen et al. 1992; Girouard, Laurita et al. 1996; Baker, London et al. 2000)

The dye that has the most desirable features for cardiac electrophysiology is di-4-ANEPPS-[1-(3-sulfonatopropyl)-4-[ $\beta$ -[2(di-n-butylamino)-6-natyl]vinyl]pyridiniumbetaine] (Loew, Cohen et al. 1992). This dye exhibits large fractional fluorescence changes during an action potential (8% to 15%) with low toxicity and photobleaching destabilization. The signal amplitude and kinetics are stable for 2 to 4 hours without the need for restraining the preparation.

In isolated cells and cholesterol vesicles, di-4-ANEPPS showed large electrochromic shifts and ratiometric fluorescence measurements were found to be linear with the changes in the membrane voltage. Di-4ANEPPS is a probe of choice in a number of optical mapping laboratories studying cardiac electrophysiology.

The electrochromic mechanism of Di-4-ANEPPS has been studied by Leslie Lowe et al, (Loew and Simpson 1981; Loew, Cohen et al. 1985) who have proposed the following mechanism: The naphthylstyryl (and others) chromophore portion of the molecule undergoes a charge shift upon excitation from the ground state because of reorganisation of its electronic structure (see figure 16). The appended polar groups and non polar hydrocarbon chains of the molecule are arranged in such away that they hold the chromophore parallel to the intramembrane electrical field. The field produced inside a polarized membrane lowers the energy difference between the ground and excited states thus shifting the dye spectra to higher wavelengths. Since there is no involvement of the physical movement of the dye molecules, and the change in fluorescence occurs due to electrical charge shift, fast potentiometric response results during membrane action potential (see figure17).

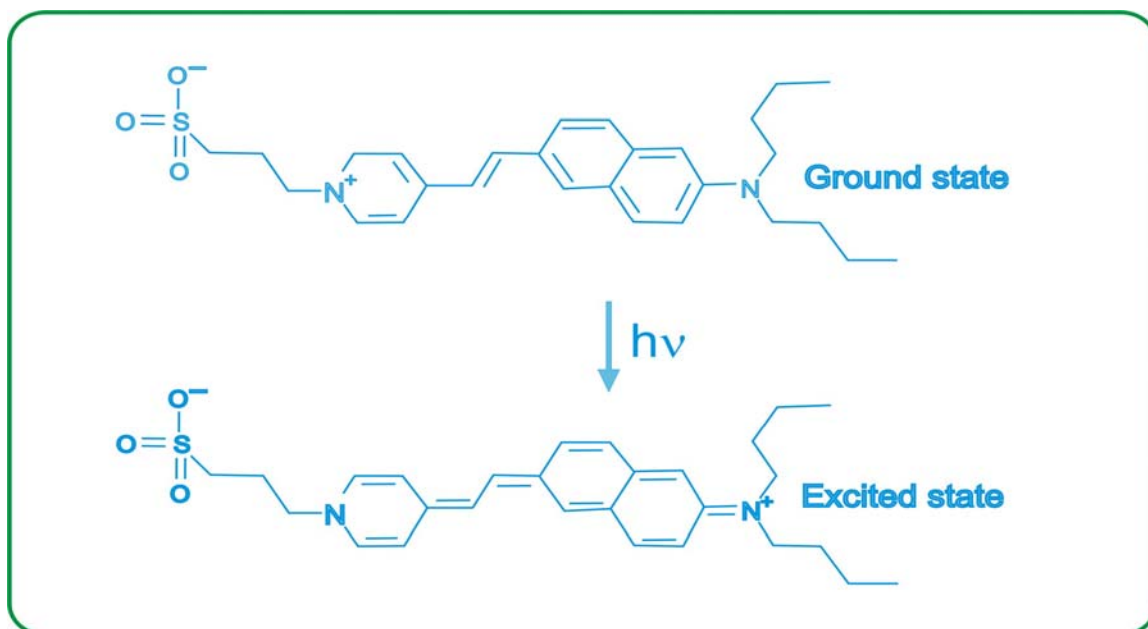


**Figure 16: Ultrastructural changes in a Di-4-ANEPPS molecule during Excitation**

The figure shows ultrastructural reorganization in the di-4-ANEPPS molecule when the light of excitation wavelength is incident on the dye molecule. The chromophore portion of the molecule undergoes a charge shift upon excitation.  $h\nu$ : light of excitation wavelength (502nm). Note: In the ground state, the chromophore has a positive charge localized near the Pyridinium end on the left and upon excitement the charge positive charge shifts to aniline moiety on the right.

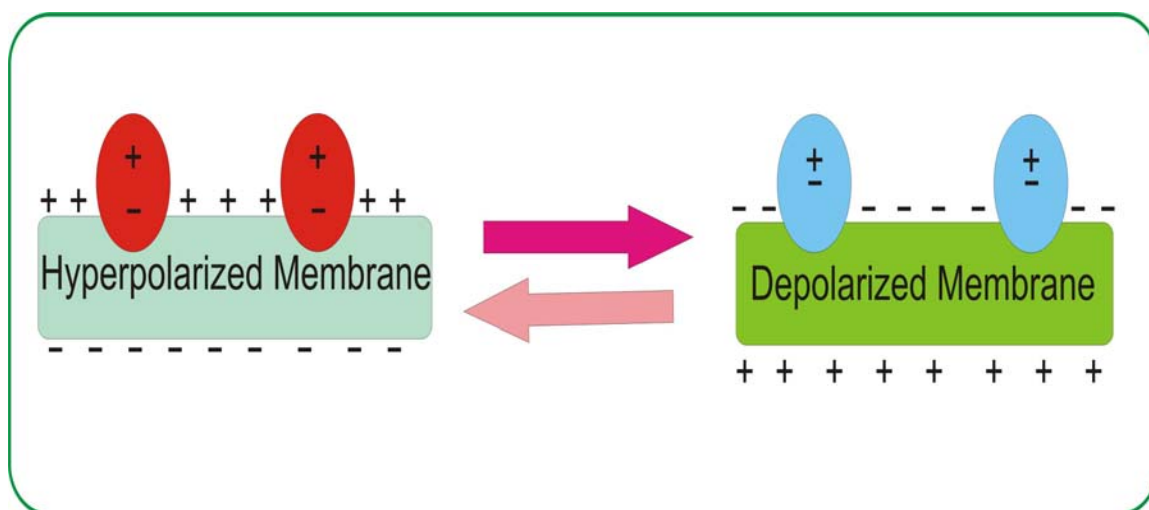


**Figure 17: Schematic showing intra molecular reorientation of fast potentiometric probe like di-4-ANEPPS**

The chromophore moiety of the dye (colored in red and blue) is aligned with the lipid molecules on the cell membrane (not shown). This unique arrangement occurs when the hydrophilic sulphonated groups and lipophilic hydrocarbon chains are engineered to append on opposite ends of the dye molecule (see Figure 16). This alignment ensures parallel charge shifts to the field of the membrane (shown in the figure). When the membrane is hyperpolarized, the energy of the dye is decreased and the wavelength shifts towards the red. When the membrane is depolarized the spectrum shifts towards the blue (M.Loew 2001).

### 3.1.2.2 Simultaneous multiparametric optical mapping and Calcium sensitive optical dyes

A brief mention is needed on the extended scope of current optical mapping. Recently, with the improvements in optics, multiparametric simultaneous optical mapping (ie simultaneous optical mapping of voltage and calcium) has been shown to be feasible. This allows one to study the roles of individual players in complex physiological / pathophysiological environments. The role of calcium in cardiac electrophysiology has been in sharp focus for some time.

Calcium cycling is probably one of the most important parts of cardiac excitation-contraction coupling. During pathological conditions, abnormalities in  $[Ca^{2+}]_i$  handling may activate  $Ca^{2+}$ -dependent currents and promote arrhythmias (Laflamme and Becker 1996),(Franz MR 1989). Calcium sensitive dyes emit spectral response when they bind to the intracellular free calcium and allow measurements of the same in different ways by using spectrophotometers, microscopes, optical cameras. The two main kinds of calcium fluorescent dyes are a) dyes excitable by UV light b) dyes excitable by visible light. Many studies have been conducted using calcium sensitive dyes.

Marban E et al was the first to measure cytosolic  $[Ca^{2+}]_i$  concentration of coronary-perfused intact ferret hearts using  $^{19}F$  NMR spectroscopy (Marban, Kitakaze et al. 1987) and at the same time Steenbergen et al used  $^{19}F$  NMR fluorescent  $Ca^{2+}$  to show the free cytosolic calcium in ischaemic intact rat hearts (Steenbergen, Murphy et al. 1987). Dyes like indo1 (Moss, Schwartz et al. 1985), bioluminescent  $Ca^{2+}$  indicator Aequorin (Kihara, Grossman et al. 1989) were developed and tested at that time. In 1995 fluorescent  $Ca^{2+}$  indicator Fluo 3 was developed (Nolan, Batin et al. 1998) and another dye- Rhod 2, was used by del Nido et al to measure fluorescence of calcium transients and calcium in sub cellular localizations in perfused rabbit hearts (Del Nido, Glynn et al. 1998; MacGowan, Du et al. 2001; Efimov, Nikolski et al. 2004).

Multiparametric optical mapping involves the imaging of voltage and intracellular calcium simultaneously and allows simultaneous measurements of APs and  $[Ca^{2+}]_i$  transients. Thus, it is an invaluable investigational tool to address fundamental questions regarding the spatiotemporal relationship of voltage and  $[Ca^{2+}]_i$  and their role in cardiac arrhythmias (Efimov, Nikolski et al. 2004). A few combinations of dyes were tested for improved safety, quality and to minimize the cross talk between the dyes (Efimov, Huang et al. 1994), (Knisley, Justice et al. 2000), (Knisley, Justice et al. 2000), (Kennth R Laurita 2001),(Zhou, Morais-Cabral et al. 2001).

Recent studies have used RH 237 as a voltage sensitive dye in combination with Rhod 2 as a calcium sensitive dye (Baker, London et al. 2000). Rhod 2 was found to have least cross talk with RH 237 and this seems to be the best combination thus far, for simultaneous mapping for  $V_m$  & Cai (Fig 18).

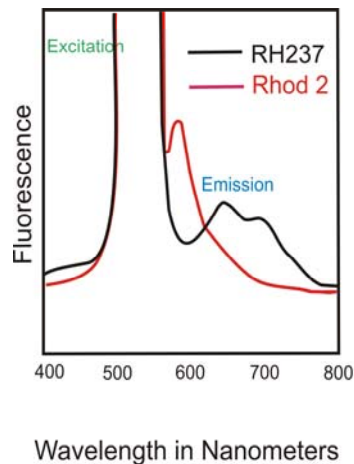


**Figure 18: Fluorescence spectra of two commonly used dyes in simultaneous optical mapping**

### 3.1.2.3 Optics

An optical action potential represents a multicellular spatial average of transmembrane potentials from cells within a small volume of tissue. A brief introduction to the general principles of optics and detectors is presented here along with some of the specific information on the equipment used in this work.

The optical potentials are optical signals which accurately represent membrane voltages but by themselves are not membrane electrical potentials. Hence, optical potentials are governed by optical principles. For example, optical magnification influences the spatial resolution of the action potentials measured across a surface. When the magnification decreases, more cells were found to contribute to the surface action potential and thereby decrease the spatial resolution. However, the signal to noise ratio (S/N), an important indicator of quality of signal, increases with decreases in magnification. This is because the proportion noise signal is reduced when more cells participate to the given optical signal. Further, at relatively low magnifications, there is a small prolongation of the rise-times of the APs. However, this effect is minimized successfully by mathematical correction to match AP rise time data obtained from

microelectrodes. For further details on optical principles in optical mapping, the reader is referred to (Girouard, Laurita et al. 1996; Kenneth R Laurita 2001; Rosenbaum 2001).

Importantly, most of the surface optical signals come from no deeper than 500 $\mu$ m into the tissue. Thus optical mapping is essentially analysis of optical action potentials from the surface of the tissue in 2-dimensions. This is because of exponential decay of the light inside the tissue and also the poor penetration of light into the tissue (Knisley 1995) .

The fluorescent light emanating from the tissue is of low intensity. In order to study the details of optical action potentials, the emitted light has to be maximally collected and focused on the detectors. The efficiency of light collection has been shown to be directly proportional to the square of the numerical aperture of the lens (NA). This is achieved by using photographic lenses for low magnification studies and microscopic lenses for higher magnification studies on specimens less than 4 mm<sup>2</sup>. For studies requiring smaller magnifications photographic lenses are used who have a NA in the range of 0.25 to 0.4. Improvements in light collection improve the signal fidelity without increasing the intensity of the excitation light.(Kenneth R Laurita 2001)

Photographic lenses are used for magnifications less than 10X, and as mentioned before have NA between 0.25-0.4. Newer versions of optical mapping setups use tandem lenses for better light collection. With this the S/N ratio was greater than single lens and was greatest at magnifications of 1.24X. Another factor which has improved light collection is that of epi-illumination. Here, the incident and emitted light is collimated by lenses (as shown in Figure 19 below) by using dichroic mirrors which selectively split beams so that the emitted light can be split between two detectors (Ratzlaff and Grinvald 1991)

The emitted fluorescent light is focused on the detectors in order to convert the light intensity into electrical signal. The main types of detectors used in optical mapping are the CCD video camera and Photodiode arrays (PDAs). Photomultiplier tubes (PMTs) which are used in laser scanning optical systems (Dillon and Morad 1981) are beyond the scope of this work. Only the PDA and CCD systems are discussed in brief here.

When photons strike a detector material electron-holes are generated. This is called the photoelectric effect. These charge carriers are converted to electric current and amplified and digitized. PDAs typically have a few hundred individual photodiodes in a typical area of about 3 cm<sup>2</sup>. The CCDs have several hundred thousand elements in a smaller surface area. In the PDAs,

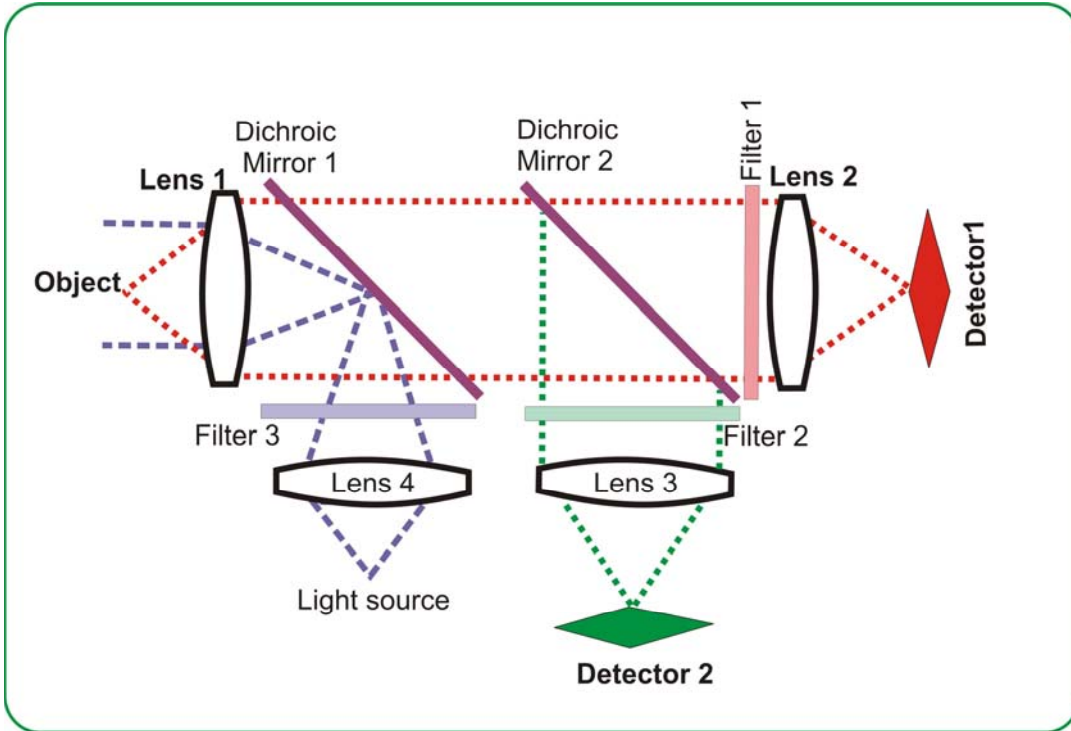


**Figure 19 : Tandem lens arrangement with Epi-illumination and simultaneous imaging**

Tandem lens method of light collection has improved brightness by about 100 fold. Excitation light from the light source is filtered (by filter 3) and reflected by Dichroic Mirror 1 which is incident on to the object (tissue with dye). The emitted light is collected and split into two wavelengths by Dichroic Mirror 2 and is further filtered by emission filters (filters 1&2) and then is focused on the photo detectors which collect light for electronic amplification and digitization. Redrawn from (Kenneth R Laurita 2001)

the impinging photons are converted to charge and further, these charges are converted to current flow and then to voltage instantaneously via a pre-amplifier using a feedback resistor.

The magnitude of the current generated is directly proportional to the intensity of the light and each photodiode is connected to its own resistor. In the CCD detectors the photo excited charge current is not immediately converted into current flow but is collected in the photodiode over a limited period of time called the integration time. Here the quantity of charge collected is directly proportional to the incident light intensity and integration time. Signal amplitude is proportional to the integration time (Kenneth R Laurita 2001) .

CCD cameras offer good spatial resolutions (number of pixels/detector) as they have large number of pixels (from 1600x1200 to 80x80 pixels). However, this reduces the rate of data acquisition thus lowering the temporal resolution. PDAs have better temporal resolution (frames/second) as they have limited numbers of pixels/detector (e.g. 16x16 pixels) and better data acquisition rate (e.g. up to 10,000 fps). The most widely used PDA (including the one used in this study) is made by Hamamatsu and has 16x16 pixels. It is beyond the scope of this work to go into the details of all available camera systems and their properties. However it is important to mention that optical mapping systems are chosen to meet study objectives. The reader is referred to (Entcheva and Bien 2006) for a review of optical systems.

The optical apparatus used for this project was designed by Guy Salama *et al* and was assembled at the machine and electronic shops of the University of Pittsburgh Cell Biology and Physiology department. See Fig. 20 and 21.

The apparatus consists of the following components as marked out in figure 20. A 100 W tungsten-halogen lamp acts as the light source, which is collimated, and the light is focused on the heart via interference filters. Fluorescence emitted from the dye-stained heart is collected via 85 mm, f1: 14 Nikon camera lens and is refracted through a 45-degree angle dichroic mirrors (made by Omega Optical, Brattleboro, VT), which separates the wavelengths of the emitted light. The dichroic mirror is importantly thin (0.8 mm) and is placed at an angle of 45 °, to reduce double image formation due to refraction. Fluorescence from the anterior surface of the heart is then focused on two 16 x 16 elements photodiode arrays (Hamamatsu Corporation, Bridgewater, NJ, 10 MW feedback resistors). The split fluorescent images are focused on the two arrays of Photodiodes perpendicular to each other after passing through respective emission interference filters. Each Diode has a sensing area of 0.95 X 0.95 mm<sup>2</sup>, with a pitch of 1.1 mm, which is the

distance from center to center of neighboring diodes. Diodes at each corner of the arrays were ignored thus optical signals were monitored from 252 out of 256 diodes. A magnification of 1 is used in rabbit hearts and each diode detected light from a  $0.95 \times 0.95 \text{ mm}^2$  area of epicardium.

The slightly varying optical pathways (due to chromatic aberration, filters and dichroic mirrors), of voltage and calcium are optimally aligned and the image is brought into sharp focus with the help of a graticule, which has the exact dimensions of the arrays (made by Graticules Ltd, Tonbridge, UK). The voltage and calcium arrays were precisely aligned, with a diode one array exactly overlapping a diode on the other array. This is achieved by manual alignment during the initial setting up of the apparatus by using light emitting diode (LED) that emits at two wavelengths close to the emissions of the two dyes. The LED was mounted on a micromanipulator, placed behind a pinhole (0.5 mm diameter), on the plane of the heart's surface. Pulsed light from the LED is focused on the  $\text{Ca}^{2+}$  array by moving the LED along the optical axis until a single diode on the  $\text{Ca}^{2+}$  array gives maximum signal. Similar procedure is performed on a diode at a matched position on the voltage array. All three axes are aligned to maximize the red LED pulses as wavelength for Rhod-2 is shorter than that for RH237 and filter setups may produce a small change in the image of calcium in relation to the voltage due to optical variance previously discussed.

The photons from the heart reach the photodiodes but have very little energy to produce a visibly tangible image. Hence, the voltage generated from photodiode arrays is amplified 1, 50, 200 or 1000 gain times using ArgoTransdata Corporation amplifiers. This signal is then digitized to 12 bit resolution, using DAP 3400/a, Micro star laboratories, Bellevue, WA and stored in the memory of a 266 MHz Pentium IV computer running Windows XP.

The analog-to-digital converter consists of 4 individual simultaneously digitizing converters, which initially digitizes 4 voltage diodes and then their spatially matched calcium diodes in an alternating fashion. This results in a diode- to-diode sampling delay between voltage and calcium signals and is sampling rate dependent; the estimated delay is in the non distorting range of 3.9 and  $1.9 \mu \text{ sec}$  at sampling rates of 2000 and 4000 frames/second respectively. The later speed is particularly useful to measure the V-C time (voltage–calcium delay).

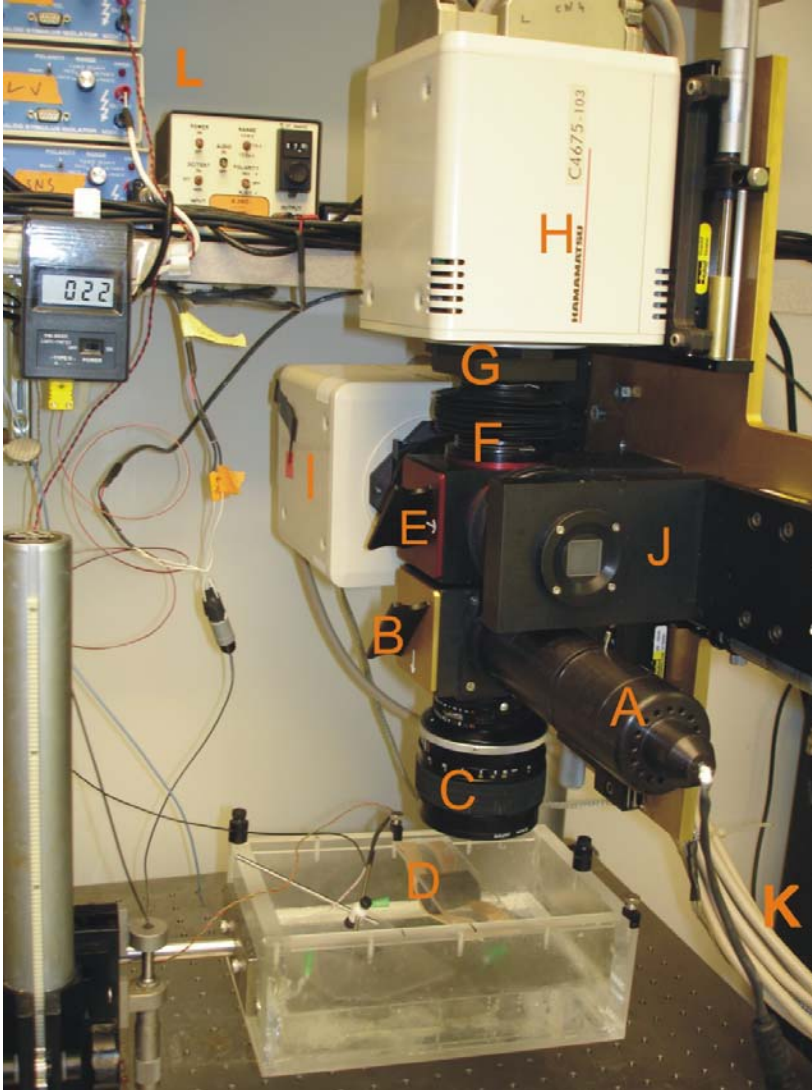


**Figure 20: Photograph of the optical mapping apparatus**

(A) the light source; (B) excitation dichroic; (C) object lens; (D) position of the object (not real object); (E) emission dichroic; (F) Focus lens for detector (H); (G) Emission filter for detector (H); (I) a second detector ; (J) Graticule for focusing the object; (K) cables carrying signals from detectors for amplification and digitization; (L) equipment for nerves stimulation and temperature probe. The detectors have photodiodes to convert the impinging photons into voltage.

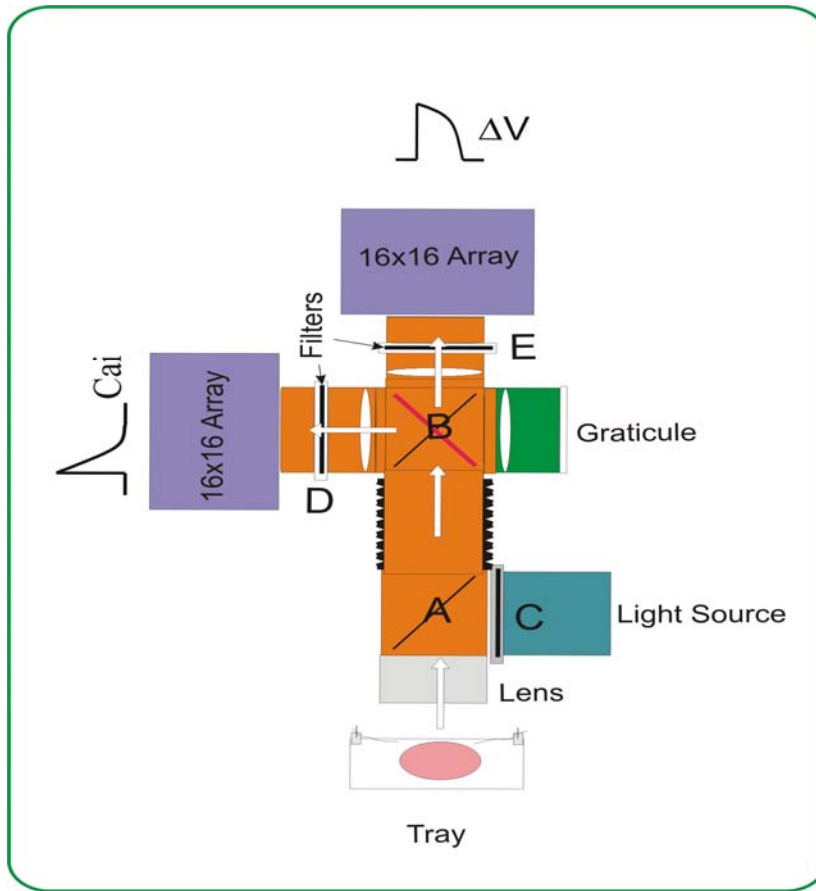


**Figure 21: Scheme of optical mapping Apparatus used in this study**

The light from the collimated light source passes through the hot mirror and is filtered by excitation band pass filter C, then is reflected on to the heart. The emitted light is passes through both excitation (A) and emission dichroics (B) and is collected by the Arrays after passing through band pass filter for calcium (D) and from a range of cutoff filters (E) for trans membrane potential measurement (see below for specifications)

A. Excitation Dichroic-575DRLP, 5 cm, 0.7 mm

B. Emission Dichroic- 635DRLP, 5 cm, 0.7 mm

C. Band Pass for Excitation-

1. 530DF50, 5 cm, 3 mm

2. 670BP10, 5 cm, 3 mm

3. Hot mirror, 54515 (from Edmund)

D. Band pass for Calcium 585BP30, 5 cm, 3 mm

E. Cutoff for Transmembrane Potential (5 cm, 2~3 mm range)

1. 570 nm

2. 610 nm

3. 630 nm

4. 715 nm

The typical scan file consists of 512 signals sampled at 2000 Hz for 2.8 seconds. The data from the ECG and two optical maps are stored from the instrumentation channels at the bottom of the arrays. The data acquisition board has a temporary (RAM) memory of 8 Mbytes which helps in uninterrupted transfer of data to the PC.

Automated analyses of the data are possible by a custom written and validated software program using Interactive Data Language (IDL). Research systems the data acquisition and hardware control were written in C language using Microsoft visual C++ 5.0. (choi 2001).

The fluorescence changes due to the action potential are small compared to the overall background fluorescence. This is in the range about 8 to 12% of the total fluorescence. Hence, it is important to selectively amplify this part of the fluorescence to measure the membrane electrical activity during the action potential. For this, a data acquisition card with fast sampling rates at 12 bit resolution in the range of 5 V is used and this enables one to measure the change of fluorescence as small as of 8% during the APs accurately. However, this does not give a good digital resolution. Therefore, the signals are amplified and baselines of signals are brought down to 0 mV by AC coupling. AC coupling brings the baseline to zero and reduces the voltage offset, which occurs due to the electronic circuit, the background fluorescence and the bias voltage. This poses a problem to measure the calcium transients as they have less background fluorescence and less offsetting. If the calcium kinetics is measured in the AC coupled mode, there is loss of accuracy of the diastolic calcium measurement. Hence calcium measurements are made in non-AC coupled mode i.e. D-C mode.

#### **3.1.2.4 Isolated innervated heart preparation**

The second major component of this work is the modification and use of a novel neuro-cardiological preparation to study the effects of nerve stimulation on cardiac ventricular repolarization properties. The novel model of combining optical mapping and isolated innervated preparation is attempted for the first time to our knowledge. Considerable amount of time and effort was required to adapt the isolated innervated preparation to optical mapping. The details of the preparation and the modifications are presented below.

In 2001, Andre Ng *et al* developed and reported this novel heart preparation to study the autonomic influences on the heart (Ng, Brack et al. 2001). It is a modified Langendorff perfused (where the myocardium is perfused in a retrograde flow via the coronary arteries) rabbit heart

with intact dual autonomic innervations. This preparation enables one to study the direct effects of both sympathetic and vagal nerve stimulation individually and together on the whole heart.

This model offers advantage over *vivo* preparations in that there is absence of confounding cardio-cerebral and other haemodynamic reflexes. It also eliminates the influences of circulating hormonal effects on the heart, as well as the necessity to use pharmacological agents to mimic the sympathetic and vagal nerve effects, which thus far, have been used in testing autonomic influences on the heart (Schwartz, Priori et al. 2001). Further, this model was used to study the effect of sympatho-vagal interactions on the heart rate of the heart (Ng, Brack et al. 2007). Recently, using this preparation, Ng *et al* have shown that the slope of APD restitution was flattened by vagal stimulation and the ventricular fibrillation threshold is increased by vagal stimulation (Ng, Brack et al. 2007). Thus, the isolated innervated heart preparation is a well validated neurocardiology tool. However, all the electrophysiological data acquired thus far, was by using contact suction MAP electrodes. This was mainly because of the difficulty with the delicate nature of the preparation and the lack of local availability of optical mapping technology.

Several modifications were necessary to adapt the 'Nerve prep' to enable the investigator to use optical mapping technology to study the ventricular electrophysiology at an organ level. A stepwise approach to surgery is presented below. Also presented in the subsequent sections, are the difficulties encountered and the limitations of this model.

### ***Isolated innervated heart preparation***

In order to obtain a preparation with a healthy heart and innervation, meticulous surgical technique is required. Special license/approval was obtained at the University of Leicester (Home office, UK) and University of Pittsburgh (IUCAC). The reader is taken through the surgery in a step-by-step manner. New Zealand white Rabbits 2.5-4 Kgs were used (Myrtle, USA).

Necessary equipment:

Necessary items for the surgical preparation were arranged before the surgery and are listed as follows a) twenty 6-8 inch 2.0 silk suture threads immersed in water; b) five 60ml syringes with tyrode solution and immersed in ice; c) 500 ml ice cold Tyrode solution in a beaker immersed in an ice tub; d) surgical instruments : four angled forceps; pair of Mayo tough cut scissors curved and straight; two toothed forceps; scalpel with 11 number BP handle; four

haemostatic forceps; curved needle with 2.0 silk thread to suture the internal mammary arteries; A Gross Anatomy Rongeur for vertebral osteotomy; e) Drugs (discussed below), Terumo surflo winged infusion set for ear vein cannulation f) small animal air ventilator for ventilation during anaesthesia; g) 'y'-junction cannula for tracheal intubation and ventilation.

#### *Pre-anaesthetic medication and reversible surgical anaesthesia*

A Modified University of Leicester protocol was used which involves parenteral administration of Medetomidine 0.25 mg/kg; Ketamine Hcl 15 mg/kg; and Propofol 0.5 mg/kg for maintenance of surgical anaesthesia. Before the incision was made, the rabbit was premedicated with Medetomidine and Ketamine by a single intramuscular injection and within five-ten minutes the rabbit was very deeply sedated and partial surgical analgesia was achieved. Then, the anterior Torso was clipped using a hair clipper and the limbs restrained.

#### *Incisions and carotid artery ligation*

On confirming the pain threshold by a pedal stimulus, a five-inch midline thoracic incision was made. The superficial layers were dissected until the trachea was reached. Then, by a gentle blunt dissection the trachea was isolated from the underlying tissues and a tracheotomy was performed and the rabbit was ventilated by a Y shaped cannula attached to the ventilator whose rate was constant at 40-50 cycles/min on a volume controlled mode delivering about 15 cc of air/cycle. Care was taken to ensure no pneumothorax was created by forceful ventilation. The surgical anaesthesia was deepened and maintained by Propofol bolus/infusion injections, intermittently with a close watch on the cardiovascular function. The carotid arteries were identified on both sides and are very carefully tied off with special attention paid to the presence of the delicate vagus nerves just below it.

A bolus of 2 ml of Propofol was administered just before tying the axillary neurovasculature to completely eliminate break through pain at this stage of the surgery.

#### *Isolation of the major arteries and Jugular veins*

Once the carotid arteries were tied off, the original midline incision was extended over the sternum and was lateralised at the level of last intercostals spaces to the mid-axillary lines on both sides. The pectoral muscles were incised and the surgical plane just below the Pectoralis minor was found parasternally and the axillary neurovascular bundles were identified and ligated. The neurovascular bundle was cut in such a way that there was only a short, well-

haemostatized sternal stump. Then, the curved forceps was used to find a plane between the pectorals and clavicular head of sternocleidomastoids. The jugular vein was tied and severed from its superior part. As a final step the intercostal vascular bundle was identified below the trapezius muscle. Although this bundle has a small artery it has a potential to cause significant decrease in the perfusion pressure when the tyrode solution is infused during the experiment and hence needs to be ligated.

#### *Terminal Anaesthesia*

Once the peripheral vasculatures were isolated, an intravenous bolus of pentobarbital was administered at the dose of 40mg/kg. Ventilation was stopped, and the subsequent steps are taken rapidly (about 2-3 min), with an aim of minimising myocardial oxygen demand.

#### *Surgery in the chest*

Bilateral mid-axillary thoracotomy was performed and costochondrectomy was extended anteriorly to the parasternal region just lateral to the internal mammary arteries. The internal mammary arteries were sealed off as proximally as possible by a 2-0 silk suture. At this time, the assistant kept the heart at near-zero temperature by packing the thorax with ice and squirting of ice-cold tyrode on the heart, which led to cold-cardioplegia. The lungs were tied off at the hila, to prevent air being sucked into the heart.

#### *Descending Aorta cannulation*

The lower thoracic aorta was identified, isolated from the tissues below and was cannulated at the level of the cardiac apex using a conical-grooved- stainless steel cannula ( diameter of 2.5 mm), which was custom made by the Machine shop, University of Pittsburgh . Again the distal aorta was sutured off to minimise blood loss.

#### *Vertebral Ostectomy*

The dual vertebral ostectomy was performed at the thoraco-lumbar and atlanto-axial region using a large sized bone cutting Rongeur. The underlying tissue was excised and the 'Nerve prep' was placed in an ice tub for mounting.

### *Vagal dissection*

Once the preparation was perfused with warm tyrode solution, the heart would start beating steadily. Vagal nerve dissection was done. The sternomastoids were lifted from their attachments on both sides and were separated from the underlying tissues. The trachea and oesophagus were cut as proximally as possible. Then the carotid sutures and vagal nerves were identified. The vagii were isolated from the carotids and the sternomastoids below in such a way that the nerves were not directly handled with forceps. The vagus nerves, once isolated were tied with a silk thread each at their proximal few millimetres. This allows easy and relatively less traumatic handling of the nerve during the experiment. The vagus nerves thrive best in its natural habitat of the surrounding tissues and kept moist with Tyrode solution.

### *Carotid cannulation*

An important step for optical mapping and dye injection was the insertion of the cannula in the ascending aorta via the carotid artery. A 5F single lumen, monitoring pulmonary wedge balloon catheter (B Braun) is advanced via a rent made in the right carotid artery and is advanced in the ascending aorta with great care with the balloon inflated at about one cm proximal to the Aortic valve. Too proximal or too distal positioning results in damaging the aortic valve which may make further experimentation impossible. Also, excessive dilation of the balloon damaged the vagus nerves at the root of the aorta and made vagus experiments impossible. However, this did not affect the sympathetic nerve stimulation responses.

### *Dual perfusion*

Another important adaptation in the surgical technique of the innervated heart preparation for optical mapping is the use of dual perfusion technique. Once the ascending aorta was cannulated, Tyrode is perfused using a second peristaltic pump (Peristar) with a speed of 30 ml/min. Perfusion rate of the other pump descending aorta may be reduced to as little as 15 ml/min, which was adequate for the spinal perfusion and hence sympathetic nerve sustenance throughout the experiments. This procedure was essential to maintain well oxygenated heart and nerves. If single perfusion method described by Ng et al (Ng, Brack et al. 2001) was used, there was significant loss of perfusion pressure when the heart was placed in position for optics especially after the physical restraints were put in place. This led to poor dye staining and more importantly, the heart rapidly became ischaemic and would fibrillate within minutes. Also, the amount of dye required to adequately stain the heart was about 10 times more. Even, with the

large flows (40-60 ml/min) required using single cannulation method; it was difficult to maintain adequate perfusion pressures when the heart was placed with the restraints.

### **Mounting the prep on the tray**

The mounting platform is an important interface-equipment between the optical recording and the nerve preparation. This helps to keep the preparation (heart and the nerves) in position during optical mapping. Any shift in position during mapping will change the orientation of the heart and thus making diode-to-diode comparison of the data difficult.

Several mounting platforms for optimal optical mapping were tried for preserving the nerve function and avoiding pressure induced ischaemia to the heart. The initial version of the tray-chamber assembly (made in the departmental machine-shop University of Pittsburgh Cell Biology, Physiology and Pharmacology (CBP)) could only achieve partial success. It consisted of two parts- a rectangular top tray which held the 'prep' in a prone position with the heart vertically hanging through a rectangular hole in the floor of the tray for optical mapping, and an optical chamber suspended from the floor of the tray at the rectangular hole. Also, the chamber has the following features a) adjustability of the heart position, in two axes (x-axis and z), crucial for focusing the heart during optical mapping; this is achieved by the interface grooves between the tray and the chamber below (see 23 figure)

Also, whole chamber –tray assembly was mounted on an adjustable stand with a magnetic base and has a tri-dimensional adjustment -callipers to allow fine mm- range adjustment in all the three axes. The 'prep' was first perfused with Tyrode solution at a rate of about 50 ml/min at 37° C.

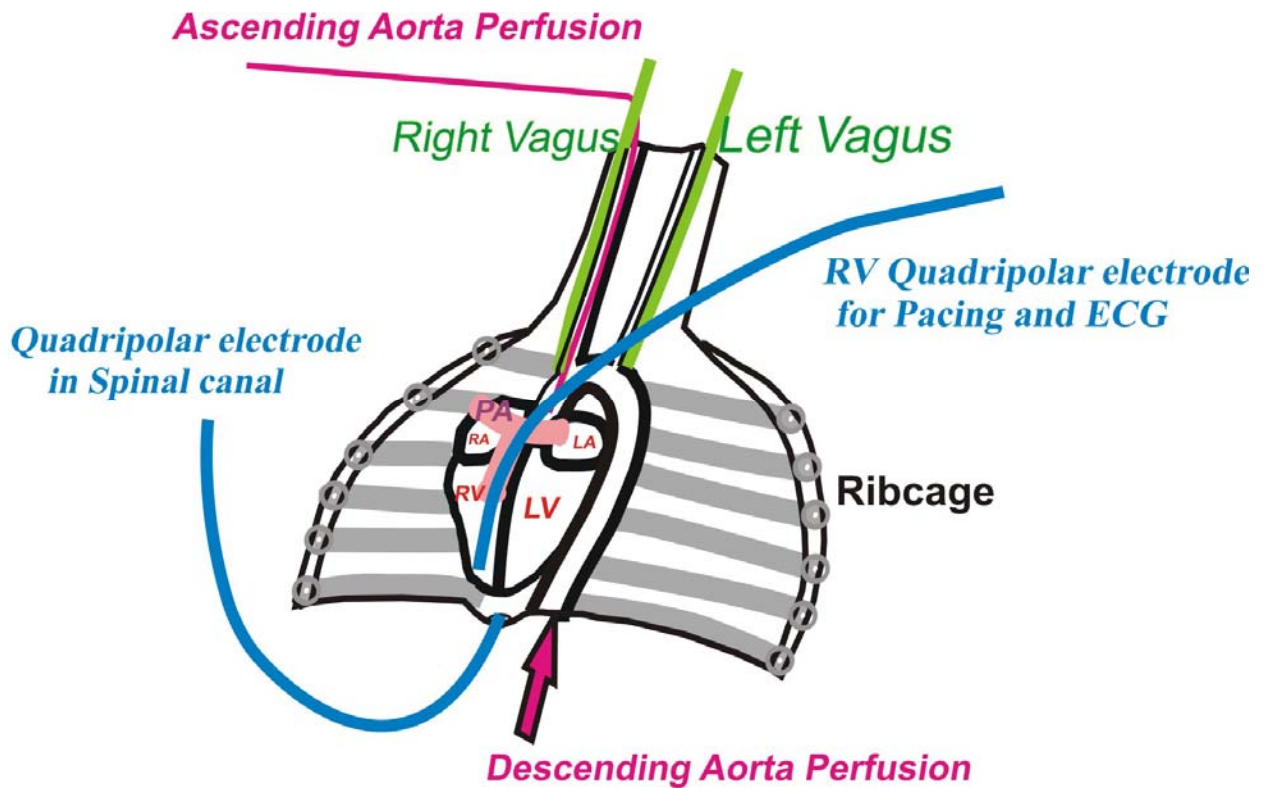


**Figure 22: Schematic diagram showing isolated innervated heart preparation with dual Perfusion**

This figure shows the important parts of the model adapted for optical mapping purposes. The myocardium of the heart is perfused by Tyrode solution via the ascending aorta cannula in the carotid artery. The balloon at the tip of this catheter holds it in place in the ascending aorta without damaging the aortic valve and coronary arteries below and the vagus nerves which go around the proximal part of the ascending aorta. The descending aorta cannula is used to perfuse Tyrode solution to the spinal cord via the spinal arteries (branches of the descending aorta). A quadripolar electrode is placed in the right ventricle to pace the heart and also collect electrograms. Another quadripolar electrode is passed into the spinal canal from below as shown in the diagram. This electrode tip is positioned at the T2 level, and is used to stimulate the thoracic out flow of the sympathetic trunk. RA: Right atrium; RV: Right ventricle; LV: Left ventricle; LA: Left atrium; PA: Pulmonary artery.

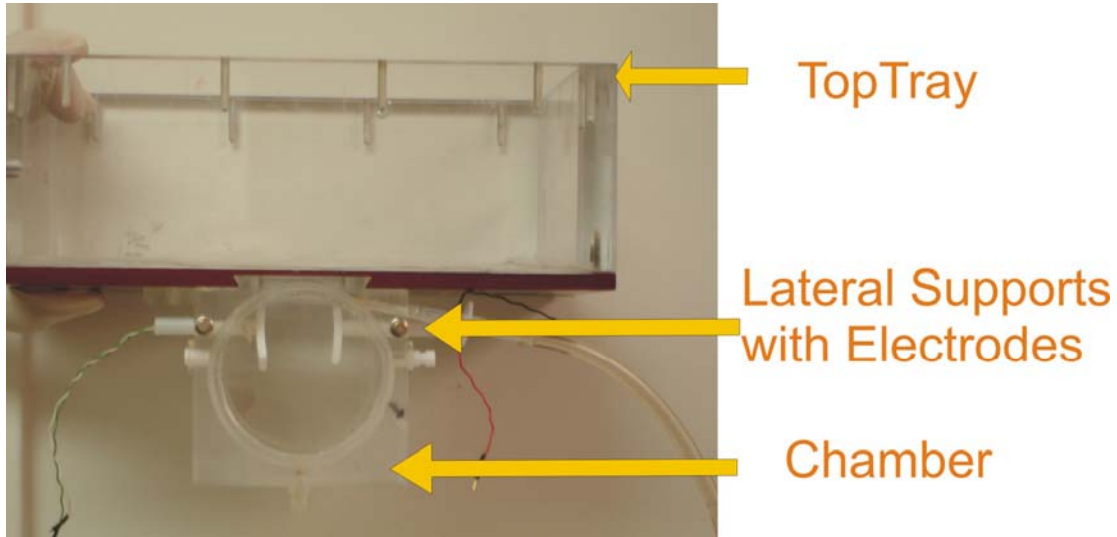


**Figure 23: Tray and Chamber assembly**

The top tray held the spine and the chest with the heart vertically suspended into the chamber. The heart was immobilized by lateral and posterior chamber supports (posterior supports not seen in this view). The lateral supports not only held the heart in place but also allowed positioning of the heart in the X-axis. The junction between the tray and the chamber was grooved and this allowed adjustment of the heart position in the Z-axis. The main limitation was that the restraints themselves caused pressure ischaemia and the nerves, especially the vagus nerves were damaged because the heart was vertically suspended and also due to the trauma of the edges of the roof aperture for suspending the heart. The sympathetic nervous system was not damaged in this mounting apparatus and some early SNS data was collected using this apparatus.

This mounting apparatus had the following disadvantages-a) the heart was suspended vertically therefore the ascending aorta was bent in two different positions making dye delivery difficult b) also the sheer weight of the suspended heart made it arrhythmogenic. This could be handled by placing sponges from below. c) the vagus nerves were damaged because of the stretch of the nerves due to suspension and also the trauma from the edges of the rectangular aperture on the floor of the tray, made for suspending the heart d) the heart was suffering ischaemic insults within a short time after mounting due to pressure exerted by the lateral and posterior restraints.

These limitations were unacceptable for stable experimentation. Further modifications were made to overcome these limitations. Decompression measures by adjusting the sizes of the apertures were made but were not effective in improving the health of the preparation.

Hence, a new assembly was devised. Since the vertical positioning of the heart was not fully satisfactory, it was abandoned and a custom made tray with more flexible immobilisers was built at the machine shop at the department of CBP University of Pittsburgh. A rectangular tray (20cmX15cm) with silica gel base was made with a groove in the top portion to position a glass slide. The grooves also had screws to fix the glass slide once positioned. The slide had dimensions 14.8 cm X 4 cm. The most important part of this modification was the attachment of two rubber slings on the lower surface of the slide. These were custom made and glued to the under surface of the sling in such a way that it allowed flexibility to position hearts of different sizes and at the same time held it well apposed to the slide above. The heart was placed between the slide and the rubber slings in such a way that the vertebral column lay below the heart and the slings. The adjustment helped to keep the heart against the slide and offered a flat surface for optical mapping. This also allowed for the adjustments of the positions of the heart/prep in order to preserve good nerve function. Further, since the distance between the slide and the lens was adjusted and fixed, focus was very easily achieved. A small left ventricular vent was also inserted at the apex to drain the excessive venous affluent (Thebesian) and kept the LV cavity decongested when it was treated with uncouplers. These manoeuvres stabilized the preparation for the entire duration of the experiments. Stability of the preparation was monitored by stability of APD shape (non triangular), durations (absence of significant shortening), maintenance of aortic pressures, reproducibility of the heart rate response to nerve stimulation and uniform dye staining. See Figures 24 and 25 below.

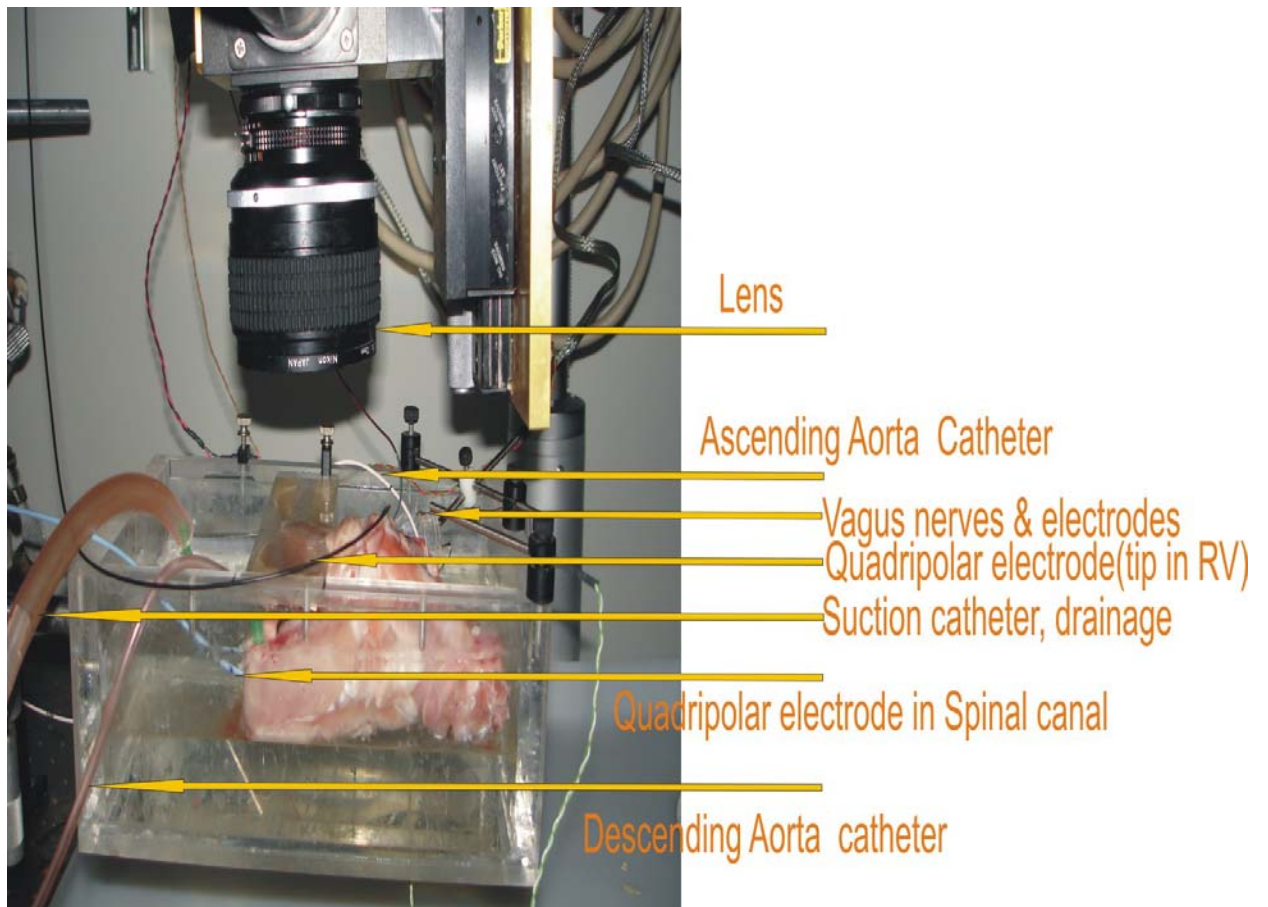


**Figure 24: Mounted specimen of the isolated innervated heart preparation for optical mapping**

The photograph shows the holding tray (not labeled) with the preparation in position for optical mapping. Compare the individual components of the preparations with the scheme shown in earlier figure. Additional needles are inserted into the prep to fix it on to the silica gel base, to prevent it from moving during nerve stimulation.

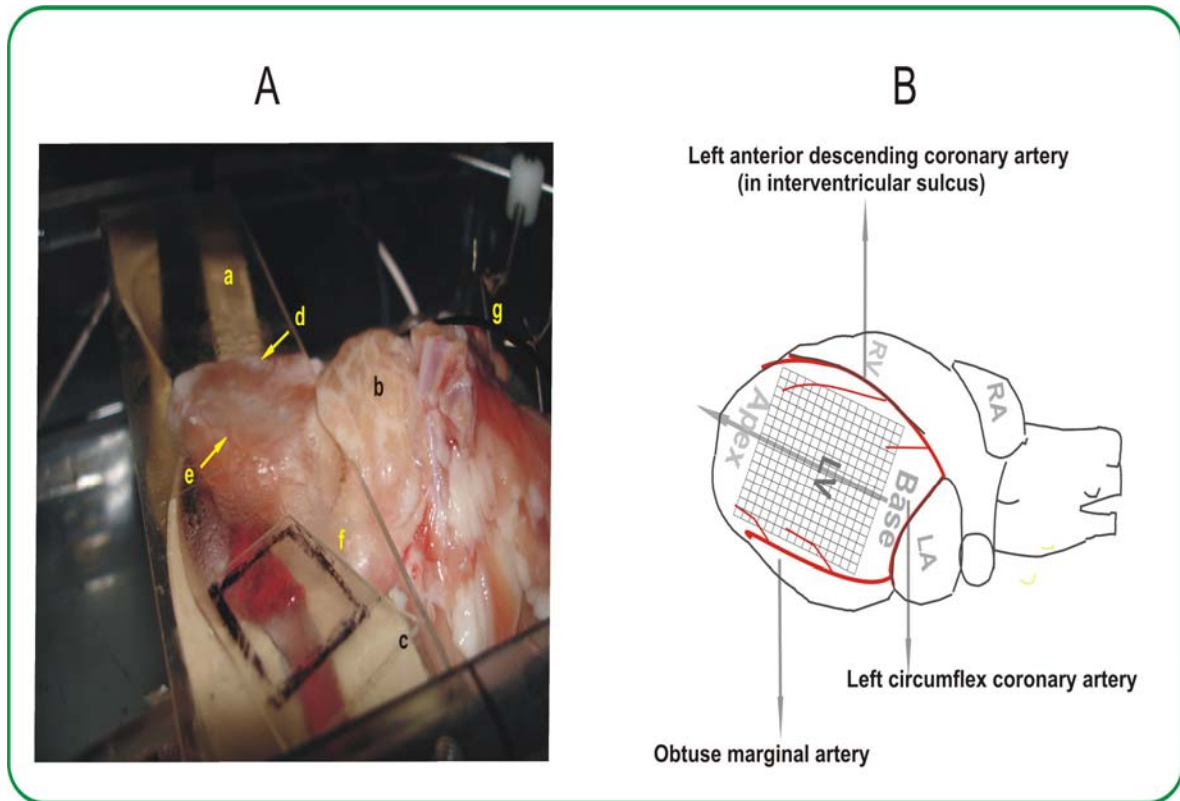


**Figure 25: Close-up view of the heart positioned for optical mapping**

Panel **A**: shows a photograph of the heart just before an experiment. a: rubber sling keeping the heart in position against the slide for optical mapping; b: Thymic pad of fat; c: aligning glass slide with exact dimensions of the graticule to fine tune the focus on regions of interest; d: left anterior descending artery; e: obtuse marginal artery; f: left Atrium; g: Vagus nerve hooked on the platinum electrode ready for stimulation. Panel **B**: schematic of the anterior surface of the heart (facing the lens) positioned for optical mapping. RA: Right Atrium; RV: Right ventricle; LV: Left Ventricle; LA: Left atrium. The grid on the LV represents the area mapped optically.

## 3.2 METHODS

Underlying general principles and the main issues pertaining to methods used in this work are discussed here. Detailed discussions about the individual experimental protocols are discussed in the respective chapters.

As mentioned earlier, this work is the study of the effects of neuronal modulation of two important repolarization properties (i.e. APD restitution and dispersion of repolarization), which have been shown to be involved in the arrhythmogenesis in Long QT syndrome. A list of all the experimental sets is shown in Table 3.

**Table 3 List of the different sets of experiments conducted in this work**

	<b>Experiments</b>
<b>1</b>	<b>APD restitution with SNS and Pacing</b>
<b>2</b>	<b>APD restitution during ion channel inhibition</b>
<b>3</b>	<b>APD &amp; DOR with SNS and VNS</b>
<b>4</b>	<b>APD &amp;DOR with SNS and VNS during ion channel inhibition</b>
<b>5</b>	<b>Western Blot analysis of Apex-Base protein expression</b>

To understand the influence of the sympathetic nerves on the ventricular repolarization two sets of experiments were conducted.

*APD Restitution measurements:* The sympathetic nerves were stimulated in normal hearts to characterize the controls at the T2 level as described in the previous sections using a quadripolar electrode in the spinal canal. The heart rates increased and reached a plateau and no further increase was noted with continued stimulation. These observations were earlier made by Ng et al (Ng, Brack et al. 2001). The hearts were optically mapped during the entire duration of heart rate change until steady state is reached and its return to the baseline. The changes in the

action potential durations were measured (see below) using custom written software programs (choi 2001).

APD Restitutions (APD vs DI) for these heart rate changes were studied during the sympathetic nerve stimulation (SNS). Since, the changes in the heart rate alone can produce the changes in the restitution curves, it was necessary to cross compare the effects of pure heart rate change on restitution without neuronal stimulation. The hearts were paced (now without SNS) via the quadripolar electrode in the right ventricle. This was done by recording the activation interval verses time course for the entire duration (AI vs. T).

When these restitution plots were superimposed, significant differences between the graphs emerged at the base of the heart but not in the apex region. This was hypothesized to be due to the differences in the ion channel and nerve ending distributions over the ventricle.

*Western blot assessment:* In order to explore above issues further and to gain a more mechanistic insight, preliminary tests were done to explore an anatomical basis for a neurocardiological synergy between  $I_{Ks}$  and regional distribution of sympathetic nerve terminals (described below). Epicardial tissue was taken from apex and base regions of the left ventricle and was analysed for the protein expression of  $I_{Ks}$  channel proteins and distribution sympathetic nerve endings. This procedure was not done by the author personally but experimental design and collection of the samples was done by him. The western blots were run by William Walker *et al*, Cell Biology and Physiology University of Pittsburgh.

Interestingly, there was evidence to suggest that the  $I_{Ks}$  protein expression and the distribution of sympathetic nerve endings are increased significantly at the base of ventricle. Thus, this data seem to be adding further strength to the hypothesis that these factors may interact more at the base of the ventricle than at the apex giving rise to the observed changes in the repolarization of the innervated heart preparation.

*Dispersion of Repolarization (DOR):* Apex to base dispersion of repolarization (DOR) and its modulation under autonomic nerve stimulation was studied in this work. For this, individual beats were analyzed during the heart rate changes obtained during autonomic nerve stimulation. Control and peak autonomic neuronal effects on APD and DOR were studied and Cross-comparisons were made with known beta-adrenergic agonist Isoproterenol (for SNS effects) and acetylcholine infusion (for VNS) on the innervated ventricle. The results are presented and discussed in the DOR chapter.

The effects of pharmacological agents were not tested for restitution studies as the AI vs. T changes with these agents were not identical to that obtained during the nerve stimulation. Also, since vagal stimulation produced a bradycardia response, restitution studies were not possible without concomitant use of programmed stimulation protocols; which was beyond the scope of this work. This aspect has been published recently. An interested reader is referred to a recent paper by Ng et al (Ng, Brack et al. 2007).

*LQT models:* Since, there is plenty of clinical data to suggest that autonomic neuro-modulation may precipitate arrhythmias in LQT substrates (see introduction); this model offers an opportunity to study the repolarization characteristics of the altered substrate (mimicking LQT pathophysiology) during neuronal stimulation.

When the control data was collected repeatedly and consistently, effects of nerve stimulation was tested in LQTS models and comparing them with the control data obtained in the same sample. LQTS1 pathophysiology has been traditionally studied by treating the heart with specific ion channel inhibitors which produce functional defects which produce repolarization abnormalities seen in various types of LQTS. Long QT1, as mentioned before, is a loss of function defect in  $I_{Ks}$  channel protein leading to prolongation of repolarization; this defect was produced by treating a normal heart (or cells) with  $I_{Ks}$  inhibitors like HMR 1556 and Chromanol 293B.

Similarly, LQT2 pathophysiology can be created in normal hearts by treating the hearts with specific  $I_{Kr}$  blockers like D sotalol or E4031. E4031 has been used extensively in LQT experiments and is also used in this study.

Since, LQT3 is a gain of function lesion; specific  $I_{Na}$  channel inactivation inhibitors were used to create LQT3 model in vitro. Sea anemone toxin Anthopleurin A (APA) and ATXII (specific antibody) are two popular agents used in LQT3 models but APA has been used more extensively including in this study. The specific use of these agents is discussed elsewhere in this work.

The repolarization changes (Restitution and DOR) during neuro stimulation in LQTS models were studied by stimulating the autonomic nerves during the perfusion of the specific inhibitors of  $I_{Ks}$ ,  $I_{Kr}$  and delayed inactivation of  $I_{Na}$  currents. This was done in three different subsets of experiments after obtaining appropriate paired control data in each group.

Accuracy of measurement of the action potential duration is critical to the study of repolarization. Several recent methods have improved the accuracy by the use of second derivative algorithms, judicious use of uncoupling agents in combination with mechanical stabilization and recent availability of novel and better uncouplers have equipped optical mappers with more tools to deal with the long standing difficulty of motion artifacts (Fedorov, Lozinsky et al. 2007; Mantravadi, Gabris et al. 2007). A brief discussion of a few aspects of this issue is in place and is attempted below.

### 3.2.1 Measurement of APD and Motion Artifacts

One of the major technical limitations faced by the optical mappers world-wide over the last few decades has been the problem of motion artifacts. The voltage-dependent signals are particularly distorted by large motion artifacts due to brisk physical contractions of the heart. Several attempts have been to reduce them and had their own advantages and disadvantages. The main attempts to solve the problem are the following-

- a) *The use of physical restraints* was popularized by Salama et al (Salama 2001). Optical chambers with lateral and antero-posterior supports were used to provide mechanical stabilization while preserving physiological conditions. Although the motion of the heart was reduced significantly (Girouard, Laurita et al. 1996), this was not ideal and the chambers also posed significant threat to the health of the heart causing pressure induced cardiac ischaemia. The balancing act of adequately restraining the heart and avoiding ischaemia is often very difficult.

When the restraining mechanical chambers were used with single cannula perfusion, a further problem was caused. The perfusion pressure of the heart reduced due to diversion of the Tyrode in to the rest of the vasculature. However, this was overcome successfully by the dual perfusion technique.

- b) *Motion subtraction techniques* are being investigated by a few groups. These approaches use mathematical corrections and image post-processing methods to reduce motion artifacts. Gustavo et al have shown that irregularities in the action potential shapes can be corrected by using image registration and image alignment algorithms. For details the reader is referred to (Rohde, Dawant et al. 2005) . Knisely et al have shown that by using

an emission ratiometric approach, one can decrease the motion artifacts. This group used dual wavelength measurement and showed that the ratio of their intensities was a superior depiction of the action potential than either of the wavelengths.(Knisley, Justice et al. 2000) Also, Stephan Rohr *et al* (Rohr and Kucera 1998) have shown that it is possible to subtract the fractional fluorescence that was estimated in long- and short-wavelength signals. Furthermore, Tai et al (Tai, Caldwell et al. 2004) have shown that one can remove motion artifact if a common contraction-dependent component can be identified and matched in decay-corrected short- and long-wavelength signals. They have shown that this method may be more effective than direct subtraction ratiometry. These techniques are relatively new, having their own limitations. To use these techniques regularly, major software modification is often required. Further, there are no uniform consensus views yet, about the relative merits and demerits of these techniques. There is no data on whether an iterative process can be used combining all these methods. For the aforementioned reasons, these methods have not been used here for motion correction. However, these techniques may be used in future studies.

- c) *2<sup>nd</sup> derivative algorithm* to measure the APD: To quantify repolarization time accurately and reproducibly from hundreds of sites over the surface of the ventricle, action potential duration was shown to be the time taken from the maximum first derivative ( $dF/dt$ ) to the second derivative ( $d^2F/dt^2$ ) at its maximum amplitude (Rosenbaum, Kaplan et al. 1991), see figure 26.

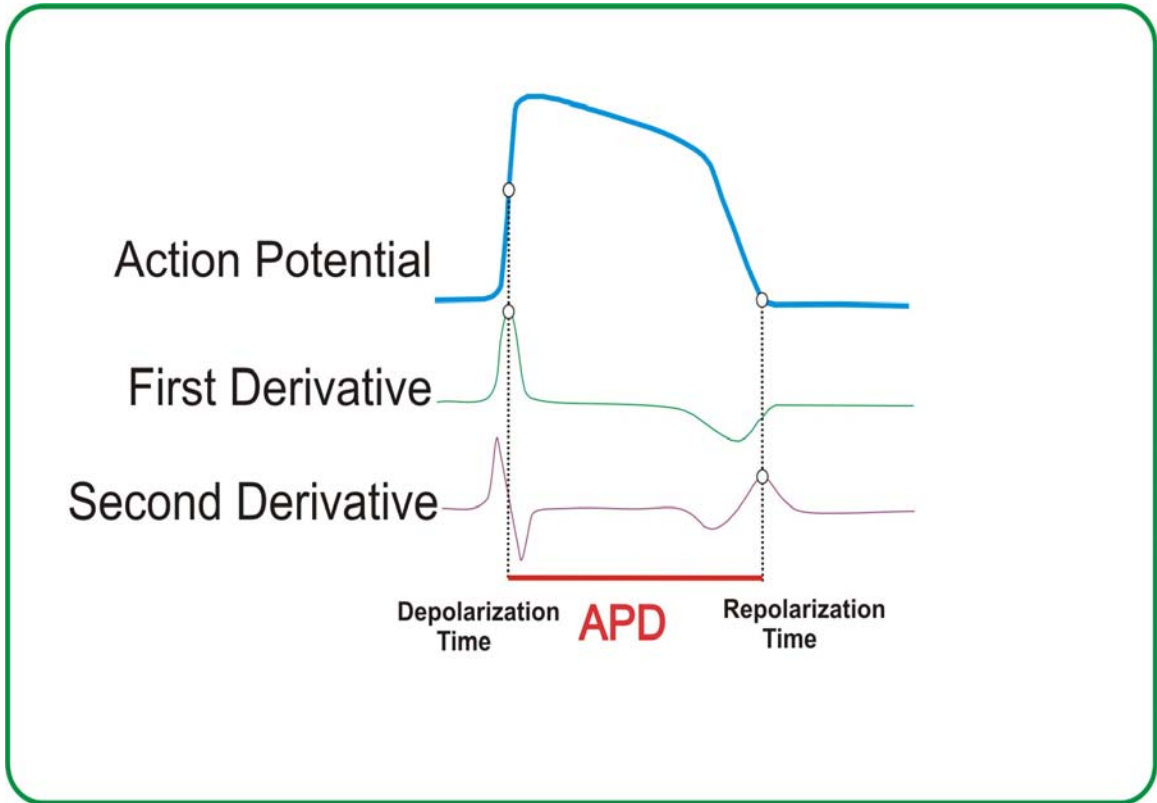


**Figure 26 : Schematic representation of first and Second derivatives of an action potential**

Depolarization time is the time at which the first derivative is at its maximum. Repolarization time is represented by the maximum second derivative deflection. The unfilled circles represent the points of first and second derivative and their corresponding points on the action potential; APD; Action potential duration.

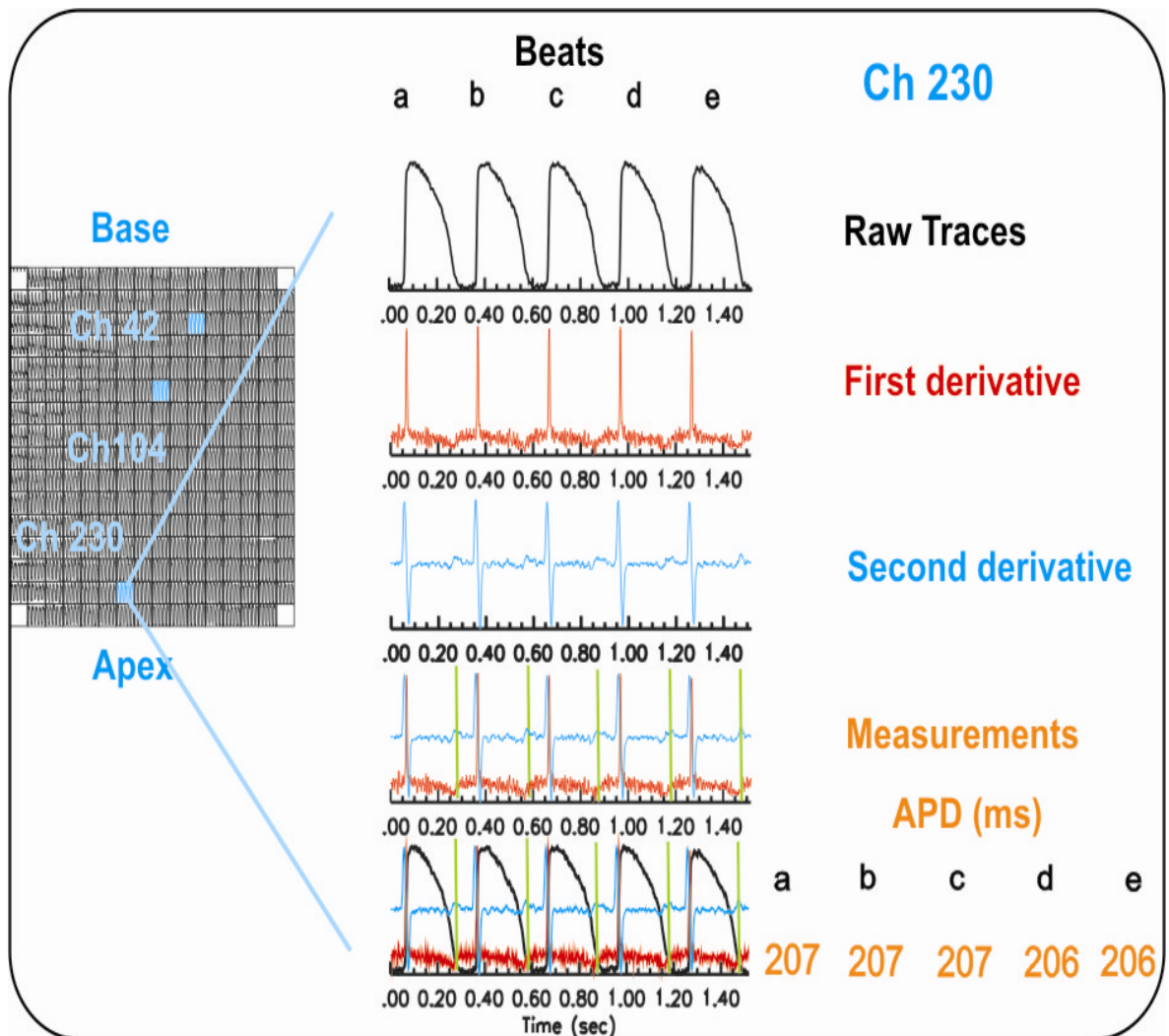


**Figure 27: Measurement of first and second derivatives from action potentials from a single diode**

This figure shows actual traces of 5 action potentials from a single diode (ch230) from the apex of the left ventricle during an experiment. The second panel in red shows the first derivative of the raw action potential traces and the third panel in blue shows the second derivative of the action potential and the last two panels show the measurements of the action potential duration using the first and second derivative algorithm. The accuracy of the measurement our experiments was very high (about $\pm 1$  ms) using frame rates of 2000/sec.

Micro electrode and simulation studies have shown that maximum second derivative signals correspond to 97% recovery of the action potentials. Hence this method has a certain advantage over measuring optical signals with absolute threshold or first derivative alone, where the maximum accuracy does not extend beyond 90-95% of the recovery. Also, the second derivative algorithm has been shown to be robust in the wake of motion artifacts. This is because the muscle contractions have slower kinetics and hence the  $d^2F/dt^2$  max is preserved during motion artifacts and baseline drifts. (Efimov, Huang et al. 1994)

- d) *Use of mechanical uncouplers* is a commonly utilized technique to reduce motion artifacts. Uncouplers are pharmacological agents that inhibit myocardial contraction with some electrophysiological consequences. Popular agents like 2,3-butane-dione monoxime(BDM), cytochalasin-D (cyto-D) have been used for about a decade or so and very recently, blebbistatin, a novel uncoupler has been reported (Fedorov, Lozinsky et al. 2007).

The mechanisms of action of these compounds are different. BDM inhibits the contraction by inhibition of myofibrillar ATPase (Blanchard, Smith et al. 1990; Liu, Cabo et al. 1993; Lee, Lin et al. 2001) in a dose and species dependent manner. Cytochalasin-D inhibits contraction by inhibition of actin polymerization (Cooper 1987). The novel uncoupler Blebbistatin, inhibits the ATPases associated with class II myosin isoforms in actin detached states (Allingham, Smith et al. 2005).

Even though uncouplers are used widely they have significant limitations. BDM has been shown to slow the conduction velocity (Verrecchia and Herve 1997), change action potential duration (Blanchard, Smith et al. 1990; Liu, Cabo et al. 1993; Baker, London et al. 2000; Lee, Lin et al. 2001) and alter APD restitution characteristics (Banville and Gray 2002). Both Diacylmonoxime and cytochalasin-D produce alterations in the calcium transients and cardiac restitution therefore making it less useful for these purposes (Banville and Gray 2002; Baker, Wolk et al. 2004; Kettlewell, Walker et al. 2004). Even though, blebbistatin has been shown to be superior to BDM and Cyto-D there is no data yet on the effect of blebbistatin on cardiac restitution (Fedorov, Lozinsky et al. 2007). There are a number of studies to suggest that cyto-D has no effect

(Biermann, Rubart et al. 1998; Lee, Lin et al. 2001) or minimal effect on action potential duration and on conduction at very low doses. Further, Cyto-D has been shown have variable effects on restitution (Hayashi, Miyauchi et al. 2003; Baker, Wolk et al. 2004; Kettlewell, Walker et al. 2004). Even in our studies, the use of cyto D was linked with a reduction in total change of APD durations during sympathetic nerve stimulation (see relevant chapters). It must be emphasized that in the above studies the stimulation protocols and dosages of cytochalasin D used were not the same.

In our studies, we used a combined approach (Mantravadi, Gabris et al. 2007) of small dose of cytochalasin-D of 2  $\mu\text{mol}$  infusion for 10 min and physical immobilization of the heart using a novel approach described in this chapter. Further, we used the second derivative algorithm to measure the APDs.

*e) Apex and Base regions*

Although there is no doubt about the existence of Apex to base heterogeneity, yet there is no clear anatomical and histological definition of the apex and base of the ventricle (Rosenbaum 2001). In the present study, the graticule was used in optical apparatus was used to consistently and clearly separate the apex and base regions. The top 8 rows of pixels were assigned to the base region and the lower 8 rows to the apex region. See figure 28.

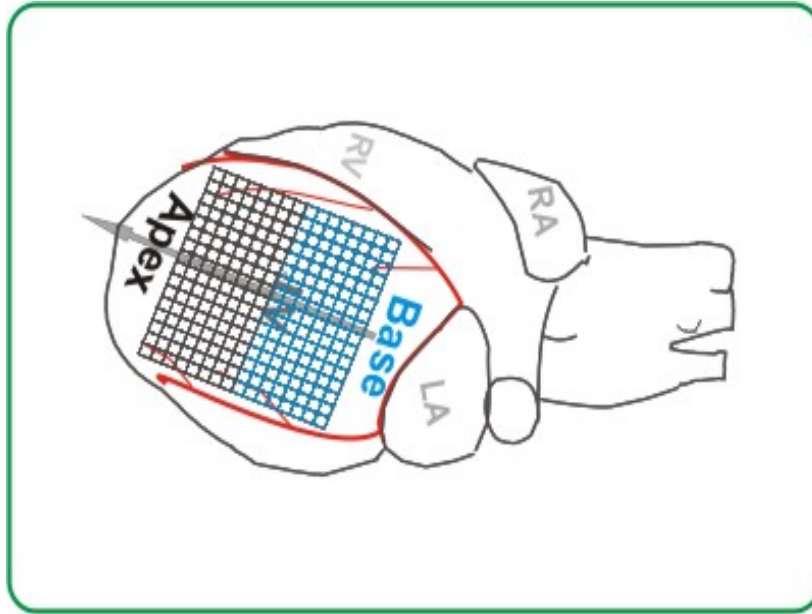


**Figure 28 : Arbitrary method of separation of Apex and base regions using the graticule**

The figure shows a method of separation of the apex and base of the heart using the graticule. The top 8 of the 16 rows of pixels are assigned to the base region and the lower 8 rows to the apex region. This allows consistency of nomenclature and strict separation for measurements. The graticule accurately corresponds to the photodiodes in focus for light collection over the surface of the ventricle. The pole regions of the heart were not included because at the base the circumflex artery, Coronary sinus and accompanying fat pads interfered with the clarity of the signals and the Apical tip was also excluded as its conical morphology did not allow stable focus without extra pressure and the tip did not cover all the pixels hence there was difficulty in uniform data collection.

### **3.2.2 Nerve stimulation Protocols**

A quadripolar electrode was inserted in the spinal canal at the 12<sup>th</sup> thoracic vertebra, and the tip was advanced to the level of the second thoracic vertebra to stimulate cardiac sympathetic outflow. From previous reports, SNS and VNS tolerated stimulation frequencies of up to 20 Hz and 15 V, without noticeable run down of the autonomic responses, measured as changes in heart rate and developed pressure. In this study, SNS were kept at a submaximal stimulation strength of 15 Hz and 15 V for 50 seconds or until the maximum change of heart rate occurred (Ng, Brack et al. 2001); then the stimulus was turned off to allow heart rate to return to baseline. Vagus nerves were stimulated individually (right or left) or simultaneously with silver chloride bipolar electrodes (15 V, 15Hz for 5 seconds) producing a drop in the heart rate to <100 bpm. A stimulus generator was custom made in the electronic shop of University of Pittsburgh to control the stimuli from 1 to 20 V and 1 to 20 Hz.

### **3.2.3 Protein expression Analysis**

In order to explain the heterogeneity of the repolarization properties, protein expression data were collected. This was an attempt to understand the neuro-cardiological factors influencing repolarization. First steps taken in this direction are presented in this work. Full characterization of all the known factors is beyond the scope of the present study. In this section, the method used in quantitative protein expression analysis is presented.

Tissues from the apex or base of rabbit hearts was disrupted using a PowerGen model 125 homogenizer (setting 5, 30 sec) in 1 ml Enhanced Lysis Buffer (ELB; 250 mM NaCl, 0.1% NP-40, 50 mM HEPES [pH 7.0], 5 mM EDTA, 0.5 mM DTT) supplemented with a cocktail of protease and phosphatase inhibitors. The extract was rocked for 15 min at 4<sup>0</sup>C, cellular debris was removed by centrifugation (12 000 x g, 5 min) and supernatant containing the protein extract was stored at -80°C. Protein concentrations were determined by the Bradford method (Bio-Rad

protein assay, Bio-Rad). Cell lysates were fractionated by sodium dodecyl sulfate-polyacrylamide gel electrophoresis (SDS-PAGE), transferred to polyvinylidene difluoride (PVDF) membranes (Immobilon-P, Bedford, MA, USA), and incubated overnight at 4<sup>0</sup>C with a KCNQ1 (H-130): sc-20816 rabbit antibody (Affinity Bioreagents, Golden, CO, USA) that was directed against KCNQ1 (diluted 1:1000) or mouse  $\beta$ -actin or Tyrosine hydroxylase (Sigma, St. Louis, MO, USA, diluted 1:20,000), followed by horseradish peroxidase-conjugated second antibody (Sigma). The antigen-antibody complex was visualized with Millipore Immobilon<sup>TM</sup> Western Chemiluminescent HRP substrate. Digitized fluorograms were quantified by using NIH Image 1.6 Software.

## **4.0 APD RESTITUTION AND REPOLARIZATION RESERVE**

### **4.1 ABSTRACT**

Action potential duration (APD) restitution is the property of the myocardium, which describes the relationship of the diastolic interval (DI) of a heartbeat to the APD of the subsequent beat. Restitution kinetics (RK) has been shown to be linked to the vulnerability to arrhythmias. To understand restitution kinetics in both experimental and modeling studies, researchers have used various protocols based on programmed stimulation of the heart. RK have not been studied during heart rate changes with sympathetic nerve stimulation. This was mainly due to technical limitations. Until lately, there was no heart model with intact autonomic innervations and a technique to continuously measure the action potentials accurately and simultaneously over the different sites on the myocardium. Combining the isolated innervated heart preparation with optical mapping allows one to study this. Analysis of physiological RK showed important differences in its characteristics from classical restitution studies. Briefly, studies on classical restitution kinetics suggests that the slope of the restitution during peak heart rates, tend to be steep and when this slope is greater than one, it makes the myocardium vulnerable to arrhythmias and vice versa. Contrary to classical restitution studies, during sympathetic nerve stimulation, physiological restitution curves had a negative slope at peak heart rates. At peak heart rates, the diastolic interval actually increased while the APD continued to shorten. To understand the influence of heart rate with and without SNS, we compared the restitution kinetics during pacing of the heart (without SNS) with the heart rate change acquired during earlier SNS. The restitution loops formed by pacing alone were significantly different from that of SNS at the base of the ventricle but not at the apex. This difference was abolished when the hearts were treated with agents known to prolong repolarization (HMR 1553, E- 4031 and Anthopleurin A) suggesting that the difference observed may indicate the repolarization reserve reported by other groups.

## 4.2 INTRODUCTION

### 4.2.1 Brief overview of classical Restitution

Electrical restitution is a property of the myocardial substrate, which describes the electrical recovery of the heart from the previous beat. Several studies have shown that restitution kinetics are linked with arrhythmogenesis (see below).

Electrical restitution curve was originally defined by Bass et al as the description of the recovery time course of action potential that occurs from the most premature beat to the one with the longest coupling interval attainable, each following a previous steady state beat (Bass 1975). Boyett and Jewell further qualified the property of restitution as a function, not of the extra stimulus response interval but rather of the preceding diastolic interval (Boyett and Jewell 1980). With time, the protocols for the study of restitution evolved from the ‘classical’ steady state – extra stimulus application, to dynamic restitution, where the myocardium was paced with serially increasing or decreasing cycle lengths (Koller, Riccio et al. 1998). Broadly, restitution represents the adaptation of the action potential and diastolic intervals to changing time course of heart rate, by the application of either an extra stimulus to the myocardium (Standard Restitution) or simply changing the pacing interval (Dynamic Restitution).

According to the restitution hypothesis, if the slope of APD restitution curve  $>1$ , the myocardium becomes unstable and is vulnerable to oscillations and wave breaks, facilitating fibrillation. At peak heart rates, when the curve is steep, small changes in diastolic interval can cause large changes in APDs (Figure 29). Several studies have supported this observation both in mathematical models and in experimental studies (Nolasco and Dahlen 1968; Karma 1994; Cao, Qu et al. 1999; Gilmour and Chialvo 1999).

Restitution kinetics is influenced by several factors like sympathetic states (see below); cardiac memory, where the APD characteristics in a train of beats are influenced by preceding APDs (Gilmour, Otani et al. 1997; Fox, Riccio et al. 2002; Watanabe and Koller 2002); conduction velocity of the tissue and ion channel kinetics.

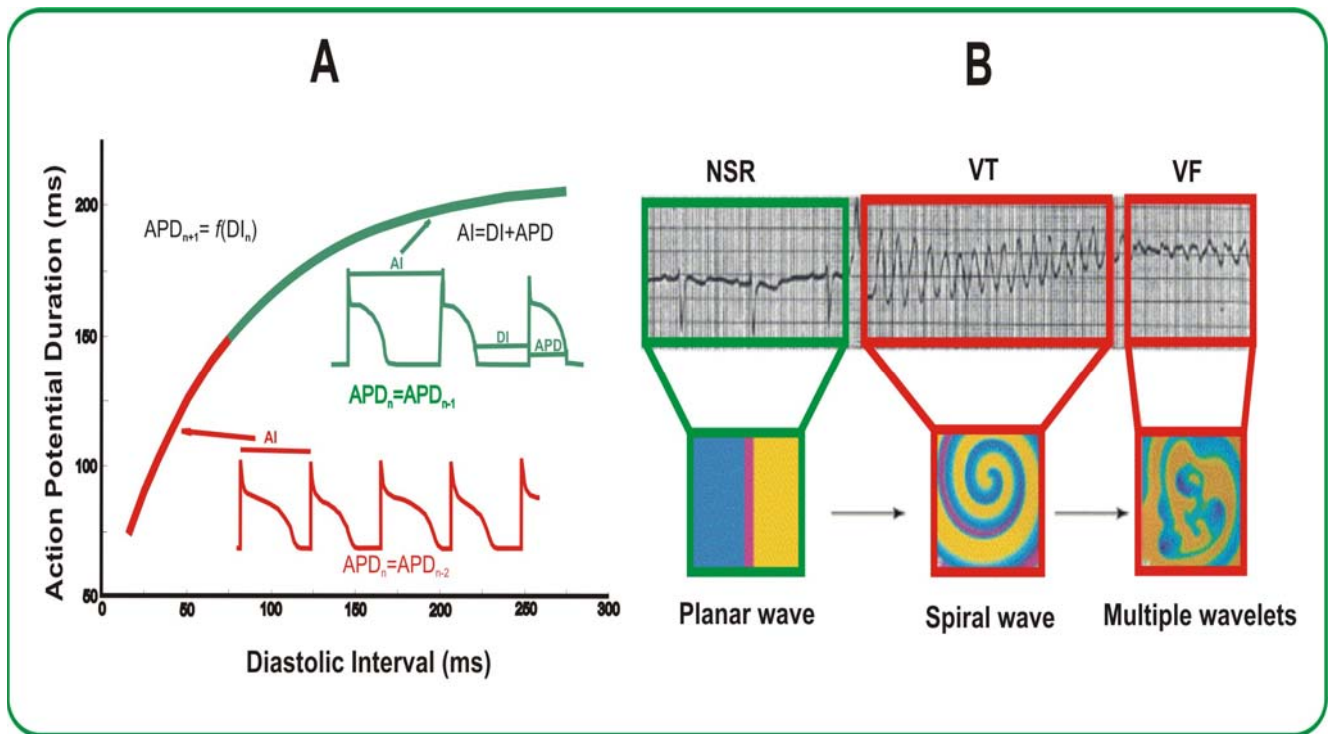


**Figure 29: Diagram of cardiac Action potential duration (APD) restitution curve.**

The figure was drawn as a scheme to illustrate the restitution hypothesis. Normally, at higher activation intervals or lower heart rates, depicted in green in panel A, the myocardial substrate is stable. Wave-front analysis of this is a planar wave. This normally corresponds to normal sinus rhythm (shown in green outline in panel B), and the slope of the curve is found to be less than 1. At higher heart rates or lower Activation intervals, the slope of the restitution curve becomes greater than 1 and this was found to correlate with an unstable myocardial substrate, and may manifest as APD alternans as depicted in Red action potentials in panel A. Wave-front analysis of the myocardium may have a spiral wave which is seen on surface ECG as ventricular tachycardia (VT), and when the slope is steep ( $>1$ ) may show aperiodic rhythms like alternans (not shown here) or deteriorate into Ventricular fibrillation (VF). Modified from (Gilmour 2003)

Choi *et al* illustrated the relationship between an index AP and its preceding APs (known as stimulation history) by using a random restitution protocol. They showed that the duration of the index AP was governed by the APDs and DIs of the preceding 3-6 beats and was modulated by a feedback control mechanism (Choi, Liu et al. 2004). The evidence from other modeling and experimental studies has shown that sodium and calcium currents contribute to the steepness of the slope. However, the mechanisms underlying APD rate adaptation are complex, and involve many factors (Qu, Weiss et al. 1999; Baker, Wolk et al. 2004; Carmeliet 2004). (Also see discussion section of this chapter)

There is also evidence to suggest that the restitution kinetics may vary in the same model if the experimental and stimulation protocols are different (Koller, Riccio et al. 1998; Banville and Gray 2002; Goldhaber, Xie et al. 2005). For example, Goldhaber et al showed the dynamic restitution protocol showed a shallower slope than standard restitution protocol (discussed elsewhere). However, there is no data to yet to characterize the RK in near physiological ranges of heart rates.

#### **4.2.1.1 Autonomics and Restitution**

There are several studies that showed a link between increased sympathetic activity and arrhythmias (Han, Garcidejalon et al. 1964; La Rovere, Bigger et al. 1998; Nolan, Batin et al. 1998; Schwartz 1998). Sympathetic stimulation has been shown to increase the slope of restitution in both animals and in humans (Taggart, Sutton et al. 1990; Taggart, Sutton et al. 2003). There is recent data from GA Ng's group showing the effect of sympathetic nerve stimulation on the slope of standard restitution curves. They showed that sympathetic nerve stimulation increased the slope of standard restitution to greater than 1 and also lowered ventricular fibrillation threshold (Ng, Brack et al. 2007). However, there is no data about APD restitution kinetics during physiological heart rate changes following sympathetic nerve stimulation.

#### **4.2.2 Relevance of Physiological Restitution**

The Autonomic neuro-regulation of the heart has been shown to execute a complex stochastic beat-to-beat control of the heart at various levels of the neuronal hierarchy especially

at level of the peripheral nervous system. The role of intrinsic cardiac ganglia in the sympathetic neuronal modulation of cardiac electrophysiology was studied in detail and characterized in the past (Armour 2004). However, repolarization properties, important as they are, in arrhythmogenesis and physiological restitution under sympathetic neuronal activation have not been studied. Studying restitution kinetics at physiological rate changes is particularly important because initiation of clinical arrhythmias tend to occur at much higher CLs than seen in restitution studies (for references see the experimental protocols in above studies).

In 2001, Andre Ng *et al* were first to develop and describe the isolated innervated heart preparation. In this preparation, the intrinsic cardiac ganglia, extra cardiac intra thoracic neuro-ganglionic plexus are not surgically intersected. Thus, the beat-to-beat regulation of cardiac electrophysiology by the complex neuronal nested feedback control is preserved (Ardell JL. Ardell JL. Neuronal regulation of cardiac function In: Armour JA 2004). As mentioned in the methods chapter, it is a modified Langendorff perfused rabbit heart preparation with intact dual autonomic innervations including the proximal spinal cord. This preparation enables one to study the direct effects of both sympathetic and vagal nerve stimulation individually and differentially on the whole heart. In this study, the ‘nerve prep’ was adapted and conjoined with optical mapping to effectively study electrophysiology over the surface of the heart during sympathetic nerve stimulation.

The aim of this study was to examine the rate adaptation pattern of APD restitution during changes in heart rate obtained with sympathetic nerve stimulation as its APD time course would be unique when compared to any previous pacing protocols studying restitution. Secondly, we aim to try and understand its restitution kinetics SNS vis-à-vis Pacing, by mimicking the activation interval time course obtained from sympathetic neuronal stimulation with pacing alone but without actually stimulating the sympathetic nerves. This, we hypothesized, may bring out the features of the repolarization characteristics that is neuronally modulated.

## 4.3 METHODS

Experiments to study the physiological restitution were performed with the isolated innervated heart preparation and optical mapping using voltage sensitive dye Di 4 ANNEPS. A brief account of the procedure and specific nerve stimulation protocols are described below.

### 4.3.1 Nerve stimulation protocols and measurements

The surgical technique of the isolated innervated rabbit heart preparation has been described in the Methods chapter. Briefly, adult New Zealand White rabbits (3.5-4 kg,  $n = 10$ ) were premedicated with Ketamine HCl (Hospira Inc USA;  $0.1 \text{ mg kg}^{-1}$ , s.c.) and Medetomidine (Pfizer,  $1 \text{ mg s.c.}$ ). General anaesthesia was induced and maintained by Diprivan (Astra Zeneca  $1\text{-}2 \text{ mg kg}^{-1}$ , i.v.) Rabbits were ventilated, after tracheotomy, using a small-animal ventilator (Harvard Apparatus Ltd, Edenbridge, Kent, UK, 60 breaths per min) with an  $\text{O}_2$ /air mixture. The vagus nerves were isolated and the blood vessels leading to and from the ribcage were ligated and dissected. The rabbit was permanently anaesthetised with an overdose of Pentobarbitone ( $60 \text{ mg i.v.}$ ) with  $500 \text{ IU heparin i.v.}$  The anterior and lateral portion of the rib cage was removed and descending aorta cannulated. The pericardium was cut and ice-cold Tyrode solution applied to the surface of the beating heart to preserve myocardial function. The preparation extending from the neck to thorax was dissected from surrounding tissues as described previously (Ng, Brack et al. 2001). For optical mapping purposes dual cannulation method was used where two separate peristaltic pumps were used a) to perfuse the spinal cord via descending aorta - spinal artery route and b) to perfuse the heart in a langendorff fashion via the ascending aorta route, using a balloon catheter which when inflated separates the two systems. This method helped to optimize the dye and drug delivery while achieving excellent perfusion pressures to the heart and the spinal cord. Perfusing solution was Tyrode solution with (in mM):  $130 \text{ NaCl}$ ,  $24 \text{ NaHCO}_3$ ,  $1.0 \text{ CaCl}_2$ ,  $1.0 \text{ MgCl}_2$ ,  $4.0 \text{ KCl}$ ,  $1.2 \text{ NaH}_2\text{PO}_4$ ,  $20 \text{ dextrose}$  at pH 7.4, and was gassed with 95%  $\text{O}_2$  and 5%  $\text{CO}_2$ . This investigation conformed to the current *Guide for Care and Use of Laboratory Animals* published by the National Institutes of Health. Temperature was maintained at  $37.0^\circ\text{C} \pm 0.2^\circ\text{C}$  and perfusion pressure was adjusted to  $\approx 65 \text{ mmHg}$  with peristaltic pumps. Hearts were stained with a voltage sensitive dye (di-4 ANEPPS,  $40 \mu\text{L}$  of  $1 \text{ mg/mL}$  dimethyl sulfoxide,

DMSO). A combination of two methods were used to reduce motion artifact during experiments 1) mechanical immobilization using a custom made tray with adjustable slide-strap arrangement was used to hold the heart in place for imaging during nerve stimulation and 2) Cytochalasin D was used in a novel dose of a short infusion of 2  $\mu\text{mol}$  for a period of 10 min. Use of Cytochalasin- D in this fashion helped to reduce the contractile motion and at the same time did not significantly alter the conduction velocity (which was one of the early electrophysiological features shown to change followed by changes in calcium transients in earlier studies (Baker, Wolk et al. 2004)).

The optical apparatus was previously described in Methods chapter (Baker, London et al. 2000). Briefly, light from two 100-W tungsten-halogen lamps was collimated and passed through  $520 \pm 30$  nm interference filters. Fluorescence emitted from the stained heart was collected with a camera lens. Fluorescence emission from the anterior region of heart (see figure 21) was passed through a cutoff filter (610 nm, Omega Optical, Brattleboro, VT, USA) and focused on a  $16 \times 16$  elements photodiode array (C4675-103, Hamamatsu Corp., Bridgewater, NJ, USA). Outputs from the photodiode array were amplified, digitized (14-bit) at 2,000 frames/second (Microstar Laboratories, Inc., Bellevue, WA, USA) for at least 40 seconds for data analysis. Voltage sensitive dye di 4 ANNEPS was used for these experiments.

SNS was performed with stimulation at the thoracic outflow of the spinal cord (N=10) at a strength of 15V and 15 Hz using custom made stimulus generator and analogue stimulus isolator (AM systems model 2000) and a quadripolar electrode in the spinal canal. With SNS, there was an increase in heart rate (observed by using ADL Power lab/4SP software) or decrease in activation interval (AI), which reached a plateau at the peak heart rate. When the peak heart rate or the lowest AI was maintained, the stimulation was stopped and the heart was allowed to recover to baseline. The optical action potential signals were recorded continuously from anterior surface of the left ventricle. Custom written software using Interactive data language (IDL) platform was used to measure APD using the 2<sup>nd</sup> derivative (described in detail in the Methods section). Beat-to-beat activation intervals (AI) acquired by SNS and APDs were measured during stimulation and recovery Diastolic intervals (DIs) were calculated from AI and APD. For each cardiac cycle,  $DI = AI - APD$ . Restitution curves were plotted with APDs and preceding DIs over the course of heart rate change with sympathetic stimulation and during recovery. A straight line was plotted at maximum heart rate when a plateau is reached and  $APD + DI$  become constant at

shortest AI with the equation:  $APD = \text{shortest AI} - DI$ . The same hearts were paced, with right ventricular endocardial electrodes, using the same pattern of change of AI with time using a computer generated pacing protocol. Changes in APD and DI with pacing were plotted in a similar way as mentioned above. See figure 30 below for the scheme of protocol.

A second set of experiments were conducted to study the effect of the inhibitors of key repolarizing ion currents on restitution loops. The above experimental protocol was repeated during the infusion of the ion channel blocker after the appropriate control restitution loops were obtained.

The effect of  $I_{Ks}$  inhibition was tested by administrating HMR1556 at a concentration of  $0.5\mu\text{M}$  ( $ic_{50}$   $10.5\text{nM}$ ). HMR has been shown to be relatively more specific for  $I_{Ks}$  than other available  $I_{Ks}$  inhibitors. However, it is not entirely specific and inhibits calcium currents,  $I_{to}$  and  $I_{Kr}$  (Thomas, Gerlach et al. 2003). In our pilot experiments with 1 and 5  $\mu\text{M}$ , HMR caused shortening of APD. Also, the restitution curves were not formed due to severe impairment of APD adaptation to SNS. The optimal dosage which allowed prolongation of APD and maintained APD adaptation was  $0.5\mu\text{M}$ . Data is presented in the results section.

E4031 is a potent, specific  $I_{Kr}$  inhibitor which is widely used for specific  $I_{Kr}$  inhibition. This also posed its share of problems. In our pilot experiments we found that E4031 at concentrations of 1.0, 0.5, 0.25  $\mu\text{M}$  severely prolonged the APDs; the actual problem in studying APD restitution kinetics at these dosages was that APD adaptation was lost and AI did not change or changed minimally to produce any appreciable restitution loops. The optimum dose that avoided those problems was 0.05  $\mu\text{M}$ . At this dose APD prolonged significantly and the APD adaptation to SNS was present. This dose was above the reported  $ic_{50}$  of 7.7nM in cell studies. (Zhou, Gong et al. 1998)

Sea anemone toxin Anthopleurin-A, is a widely used and a potent inhibitor of slow inactivation of sodium current by binding to a specific domain on the channel (Benzinger, Drum et al. 1997). We used APA at 10nM concentration as an infusion. An earlier study in dogs used a higher dose of APA in their experiments (Restivo, Caref et al. 2004). Our pilot studies in traditional Langendorff perfused rabbit hearts showed that a lower dose (10nM) was effective in prolonging APD and also produced torsade de pointes (Liu T 2001).

## 4.3.2 Data Analysis

Maximum and minimum activation intervals (AI) and action potential durations (APD), were measured in milliseconds. The range and percentage change of AI and APD during SNS and pacing were calculated and expressed as mean and standard error of the mean. The loops shown in the figures in this chapter are based on data from single pixels. The percentage change of APD and range of change (maximum minus minimum) were then compared between sympathetic stimulation and with pacing using paired t-test of the mean data from four adjacent pixels. When the ion channel blockers were used, these parameters were compared to their controls using paired t-test. Mathematical curve fitting was not applied as the physiological geometry of the curves and the APD adaptation was not preserved, when attempted.

## 4.3.3 Results

### 4.3.3.1 APD adaptation during sympathetic nerve stimulation

Stimulation of the spinal canal at the thoracic outflow resulted in sympathetic neuro-stimulation of the heart and the heart rate increased. The activation interval decreased from  $444 \pm 18$  ms to  $284 \pm 9$  ms ( $\Delta AI\% = 35 \pm 2.5$ ) and the APD shortened from a max of  $216 \pm 9$  ms to minimum of  $154 \pm 7$  ms;  $\% \Delta APD = 29 \pm 2$  (n=10). When the physiological restitution curves with SNS were compared to that obtained by pacing alone (n=10), the percentage change in AI as one would expect, was identical in both neuro-stimulation and pacing groups. For the given  $\Delta AI$ , the  $\Delta APD$  was significantly different between the two groups  $62 \pm 5$  ms ( $29 \pm 2\%$ ) in SNS vs.  $46 \pm 3$  ms ( $21 \pm 1\%$ ) during pacing with  $P < 0.05$  (Table 4).

When the APD was plotted against the preceding DI for the entire stimulation and recovery periods, complete loops were formed and showed the same characteristics seen in all experiments. For the sake of description, a loop is divided arbitrarily into 4 phases (a-d). (See figure 31)

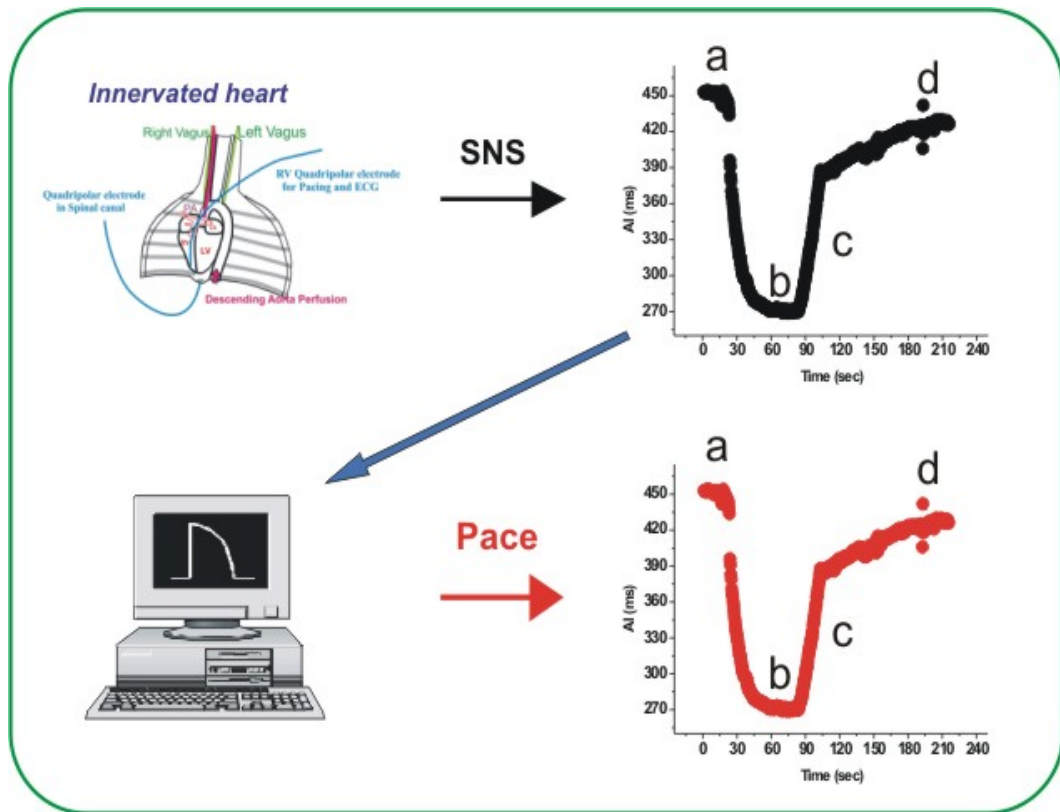


**Figure 30: Scheme of stimulation protocol for comparisons of APD Restitution Loops**

The sympathetic nerves were stimulated and the heart rate was allowed to reach the Peak (or AI reaches its lowest) then the stimulation was stopped and the heart was allowed to recover. The AI vs. Time graph was obtained for SNS (shown in black) and was fed into the computer. The heart was then paced using custom-made computer software (without SNS) with exactly the same AI vs. Time (shown in red). Then the APD vs. DI curves were plotted and superimposed for comparison (shown in Figure 31). To study the effect of ion channel blockers the same protocol was repeated during the infusion of drug. a),b),c) and d) refers to the stages of heart rate (or AI) change with time during SNS or during pacing of the heart. Corresponding APD changes are depicted in figure 31.

During phase 'a' the relationship between APD and DI was shallow and shortening of the AI predominantly led to a shortening of DI with little change in APD. As AI shortens following SNS, the slope of the curve steepened compared to phase 'a'. At peak heart rates during (phase 'b') or low AIs, the slope of the restitution curve became negative. This was due to increasing DI and shortening of APD. At plateau heart rates with constant AI, there was continued decrease in the APD which was associated with an increase in the DI. When stimulation was stopped after reaching the plateau heart rate, DI increased more than the APD (phase 'c') after which there is a reduction of APD to reach the baseline during phase 'd'. The main focus of our study was phase 'b' as it was where that the effect sympathetic activity was at its peak. Here, APD shortening during SNS was much more than seen during pacing alone. Examples of typical physiological restitution loops (both SNS and Pacing), with raw data of the traces of action potentials from all four phases is shown in figure 31.

On comparing the restitution curves from the apex and the base of the heart, very interesting data emerged. The SNS-restitution curves at the base were different from that of pacing-restitution curves for the reasons mentioned above. But, this difference was not observed at the apex. Where, the loops appeared similar (n=6). For the same change in AI ( $\Delta AI\% = 32 \pm 3\%$ ) between the SNS and Pacing loops in all regions, in the base region, the maximum and minimum APDs during SNS, were  $218 \pm 8$  ms and  $154 \pm 8$  respectively. The percentage change APD was  $29 \pm 3\%$ . In the same region, during pacing, the maximum, minimum and APD change were  $222 \pm 10$  ms,  $173 \pm 8$  ms and  $22 \pm 3\%$ , respectively. While there was no significant difference in the Max APD between the SNS and pacing loops, there was significant difference ( $p < 0.05$ ) in the minimum APD and the total change in the APDs. In sharp contrast, at the apex of the heart there was no significant difference between the SNS and Pacing loops (Max APD, Min APD and  $\Delta APD\%$  SNS vs. Pacing:  $206 \pm 12$  vs  $206 \pm 12$ ;  $158 \pm 7$  vs  $157 \pm 6$ ;  $23 \pm 3$  vs  $23 \pm 3\%$ ) (See Table 5 and Figure 31).

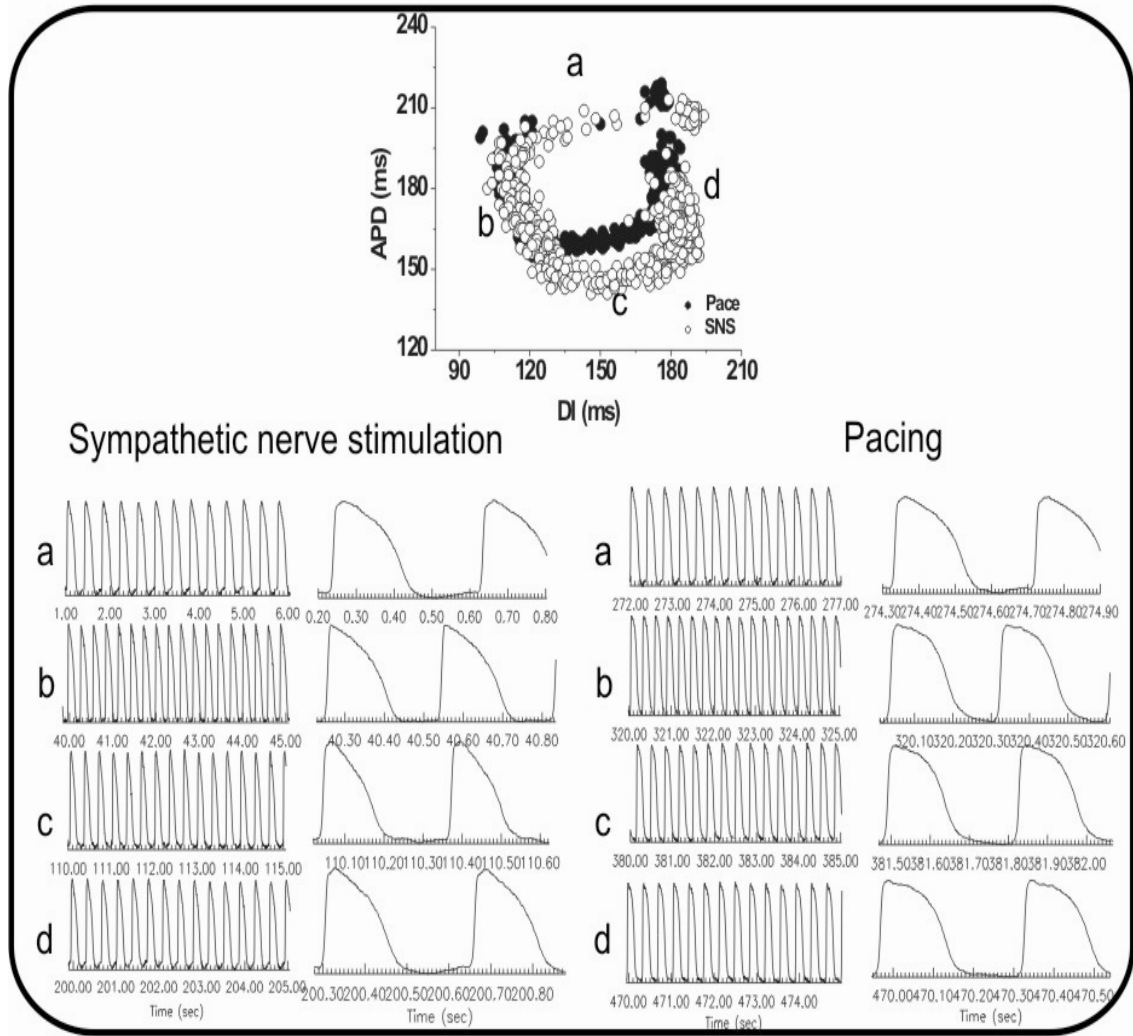


**Figure 31 : APD Samples and physiological Restitution loops**

This Figure above shows Physiological APD Restitution curves with and without SNS for identical heart rate changes. Shown in the figure are typical restitution curves obtained during sympathetic nerve stimulation (SNS) (unfilled circles); and pacing (filled circles) for identical activation interval changes. When the heart was stimulated via SNS the heart rate increased from 'a' to 'b' and recovered back to the base line via 'c' and 'd' (see the coloured inset of the AI vs T time course graph of a typical SNS figure 30). At peak heart rate (b) the Action potential duration (APD) continues to shorten and diastolic interval (DI) increases leading to a negative slope. APD shortening was much more significant during SNS than pacing. APD samples taken at various phases of the physiological restitution are shown.

**Table 4: Comparisons between Activation intervals and Action Potential durations SNS vs. Pacing**

	SNS	Pace	t-test
AI <sub>(max)</sub> (ms)	444±18		-
AI <sub>(min)</sub> (ms)	284±9		-
ΔAI (ms)	159±16		-
ΔAI %	35±2		-
APD <sub>(max)</sub> (ms)	216±9	216±8	NS
APD <sub>(min)</sub> (ms)	154±7	170±6	P<0.05 <sup>*</sup>
ΔAPD (ms)	62±5	46±3	P<0.05 <sup>*</sup>
ΔAPD %	29±2	21±1	P<0.05 <sup>*</sup>

SNS: sympathetic nerve stimulation, AI: Activation interval, APD: Action potential duration, ΔAPD is maximum minus minimum; ΔAPD% is the percentage change in APD; on Paired samples, P value less than 0.05 was considered statistically significant (\*); NS: refers to data not significant by Student's t-test.

**Table 5: Apex-base heterogeneity of physiological restitution**

<b>AI Max (ms)</b>	<b>395 ± 5</b>					
<b>AI Min (ms)</b>	<b>270 ± 14</b>					
<b>Δ AI %</b>	<b>32 ± 3</b>					
	<b>Base SNS</b>	<b>Base Pace</b>	<b>t-Test</b>	<b>Apex SNS</b>	<b>Apex Pace</b>	<b>t-Test</b>
<b>APD Max (ms)</b>	<b>218 ± 8</b>	<b>222 ± 10</b>	<b>NS</b>	<b>206 ± 12</b>	<b>206 ± 12</b>	<b>NS</b>
<b>APD Min (ms)</b>	<b>154 ± 8</b>	<b>173 ± 8</b>	<b>P&lt;0.05*</b>	<b>158 ± 7</b>	<b>157 ± 6</b>	<b>NS</b>
<b>Δ APD %</b>	<b>29 ± 3</b>	<b>22 ± 3</b>	<b>P&lt;0.05*</b>	<b>23 ± 3</b>	<b>23 ± 3</b>	<b>NS</b>

The Table shows data of physiological restitution from apex and base regions of the LV. SNS: sympathetic nerve stimulation, AI: Activation interval, APD: Action potential duration, ΔAPD is maximum minus minimum; ΔAPD% is the percentage change in APD; on Paired samples, P value less than 0.005 was considered statistically significant(\*); NS: not significant by Student's t-test

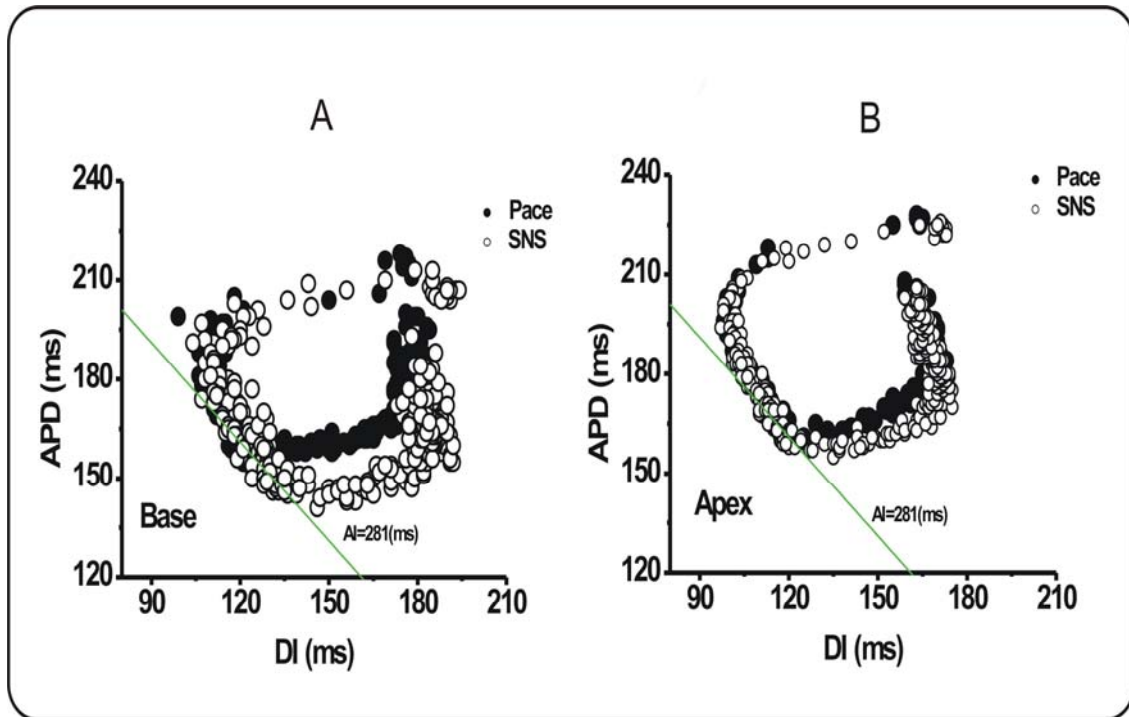


**Figure 32 : Apex-base heterogeneity of Physiological Restitution curves**

This figure clearly shows the differences in restitution curves at the apex and base regions of the heart. At the Base, the SNS loops were significantly larger than the ones driven by pacing alone. This was because, in the sympathetically driven loops, the APD adaptation was much more than during pacing. At the Apex, the loops appeared identical. The green line indicates the plateau heart rate where the APDs shorten at a constant heart rate. Also see the text (and figure below) for further details.

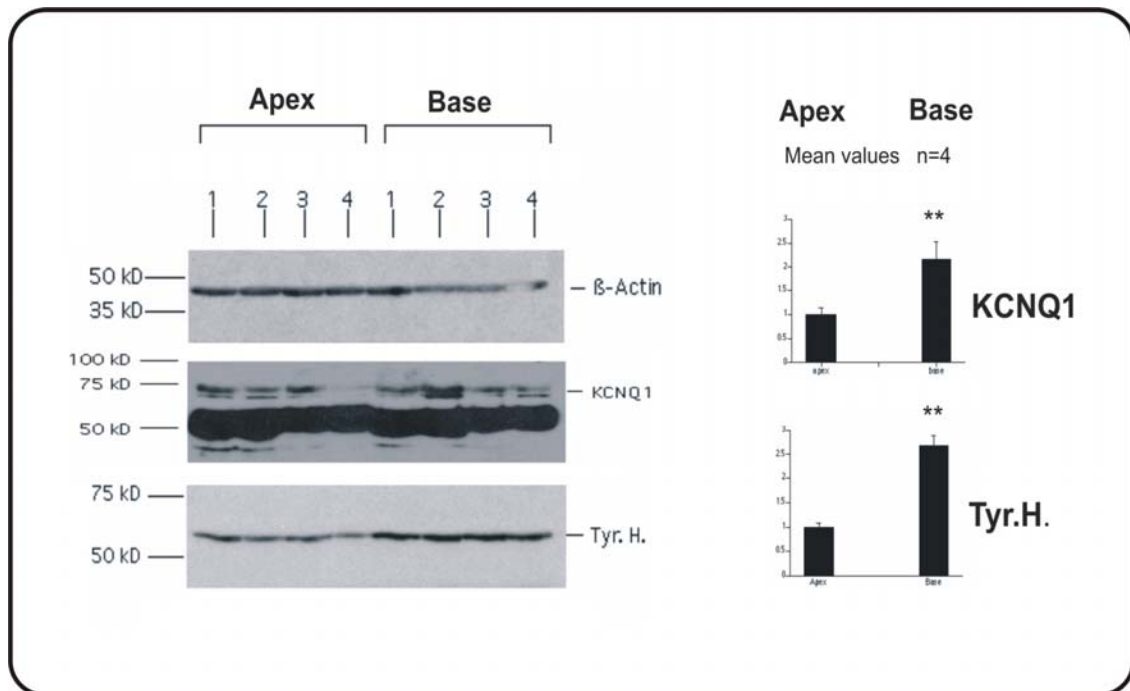


**Figure 33 : Western blot data of two key Repolarization factors**

The figure shows comparative protein expression of Tyr.H and KCNQ1 at the apex and base in four rabbit hearts. Tyr.H refers to Tyrosine hydroxylase a surrogate marker for sympathetic nerve endings. KCNQ1 is the pore forming subunit of the  $I_{Ks}$  channel. The figure shows a clear increase in the expression of these proteins at the base as depicted on the right hand side panel. Lanes 1-4 are protein expressions in different rabbit hearts. This may provide early evidence of an increased probability of an interaction leading to an increased local APD adaptation at the base. \*\*: represents  $P < 0.05$  using paired t-test.

In order to explain selective APD shortening at the base region during SNS, we explored to see if there was any difference in the distributions of sympathetic nerve ending and  $I_{Ks}$  channel protein over apex and base. Western blot analysis of tyrosine hydroxylase and KCNQ1 protein expression over apex and base regions of the heart (n=4), provided early explanations. Compared to  $\beta$ -Actin controls, the expression of Tyrosine hydroxylase was significantly higher at the base compared to apex. The KCNQ1 protein expression was about two times higher at the base and the tyrosine hydroxylase expression was two and a half times higher at the base. See figure 33.

#### 4.3.3.2 Physiological Restitution in LQT1 models

To understand the role of  $I_{Ks}$  participation in the physiological restitution, the experiments were conducted with the  $I_{Ks}$  inhibitor HMR 1556 (0.5 $\mu$ M) (n=5). The effect of  $I_{Ks}$  inhibition was tested by administrating HMR1556 at a concentration of 0.5 $\mu$ M (ic50 10.5nM). HMR has been shown to be relatively more specific for  $I_{Ks}$  than other available  $I_{Ks}$  inhibitors. However, it is not entirely specific and inhibits calcium currents,  $I_{to}$  and  $I_{Kr}$  (Thomas, Gerlach et al. 2003). In our pilot experiments with 1 and 5  $\mu$ M, HMR caused shortening of APD. Also, the restitution curves were not formed due to severe impairment of APD adaptation to SNS. The optimal dosage which allowed prolongation of APD and maintained APD adaptation was 0.5 $\mu$ M. Data is presented in the results section. Under  $I_{Ks}$  inhibition, baseline AI increased from 459 $\pm$ 19 to 484 $\pm$ 40 ms (P=NS) and the minimum AI from 261 $\pm$ 16 to 276 $\pm$ 16 ms (P=NS). At the base, HMR 1556 significantly changed maximum APD from 228 $\pm$ 11ms to 251 $\pm$ 15 for SNS loops; and from 227 $\pm$ 11 ms to 248 $\pm$ 16 for pacing (P<0.05). The minimum APD between the SNS and Paced loops were significantly different in the control situation (SNS vs. Pace: 178 $\pm$ 9 and 185 $\pm$ 10ms; P<0.05), as seen in the previous experiments. During HMR infusion this difference in minimum APDs was abolished (HMR SNS vs. HMR Pace: 170 $\pm$ 8 vs.169 $\pm$ 7; P=NS) (See Table 6 and figure 34). After the hearts were treated with  $I_{Ks}$  inhibitor, the loops shifted upward and outward due to an increase in APD. Importantly, the differences in the loops seen in control were lost in the same region of the heart. This was because the APD adaptation under SNS could not exceed that of the Pacing-a feature of physiological restitution normally seen in controls at the base region of the heart. There was no change in the slope of the restitution curves after treating the hearts with HMR. Also, there were no arrhythmias seen during the infusion.

#### 4.3.3.3 Physiological Restitution in LQT2 models:

In another set of experiments, the physiological restitution curves were obtained under  $I_{Kr}$  inhibition. E4031 is a potent, specific  $I_{Kr}$  inhibitor which is widely used for specific  $I_{Kr}$  inhibition. This also posed its share of problems. As mentioned before, in our pilot experiments we found that E4031 at concentrations of 1.0, 0.5, 0.25  $\mu\text{M}$  severely prolonged the APDs; the actual problem in studying APD restitution kinetics at these dosages was that APD adaptation was lost and AI did not change or changed minimally to produce any appreciable restitution loops. The optimum dose that avoided those problems was 0.05  $\mu\text{M}$ . At this dose APD prolonged significantly and the APD adaptation to SNS was present. This dose was above the reported  $\text{ic}_{50}$  of 7.7nM in cell studies. (Zhou, Gong et al. 1998)

In controls, AI changed from  $391 \pm 24$  to  $280 \pm 15$ ms ( $\Delta\text{AI}\% = 28 \pm 3$ ). The Max and Min APD during SNS vs. Pace were  $193 \pm 14$  vs  $193 \pm 17$  (P=NS) and  $151 \pm 15$  vs  $161 \pm 13$  (P<0.05) with a significant difference in the  $\Delta\text{APD}$  between SNS and pacing. When the hearts were treated with E4031 (at 0.01  $\mu\text{M}$ ) the baseline APD prolonged from  $193 \pm 14$  to  $256 \pm 15$  ms (P<0.05); during SNS, the AI reduced by about 28%. Under E4031, the APD reduced to  $217 \pm 21$  during SNS and to  $229 \pm 23$  during pacing. This difference was not statistically significant (P=NS; by paired t-test N=5) (Table 7 and Figure 35). After the hearts were treated with  $I_{Kr}$  inhibitor, the loops shifted upward and outward due to an increase in APD. Importantly, the differences in the loops (seen in control) were changed following E4031 in the base region of the heart. This was because the APD adaptation under SNS could not exceed that of the pacing -a feature of physiological restitution normally seen in controls at the base region of the heart. Also, the SNS loops showed a tendency to be smaller than the pacing loops in 3/5 hearts.

#### 4.3.3.4 Physiological Restitution in LQT3 models:

In the next set of experiments (n=5), the hearts were perfused with APA (Anthopleurin-A) at 10nM concentration. We used APA at 10nM concentration as an infusion. An earlier study in dogs used a higher dose of APA in their experiments (Restivo, Caref et al. 2004). Our pilot studies in traditional Langendorff perfused rabbit hearts showed that a lower dose (10nM) was effective in prolonging APD and also produced torsade de pointes (Liu T 2001). In controls, the AI decreased from  $376 \pm 12$  to  $245 \pm 12$  ( $\Delta\text{AI}\% = 34 \pm 3$ ) this was not significantly changed by APA (AI max to AI min:  $380 \pm 17$  to  $261 \pm 24$  ms). Application of APA increased the baseline APD

modestly. In controls, the max and min APD for SNS and Pace were:  $198 \pm 15$  &  $142 \pm 8$  vs.  $201 \pm 17$  &  $158 \pm 10$  ms respectively ( $\Delta$ APD% SNS vs. Pace:  $28 \pm 4$  vs.  $21 \pm 2$ ;  $P < 0.05$ ). When APA was administered, the Max & Min APD SNS vs. Pace changed from  $206 \pm 7$  vs.  $146 \pm 14$  to  $207 \pm 5$  vs.  $150 \pm 14$  ms ( $\Delta$ APD% APA SNS vs. APA pace:  $29 \pm 6$  vs.  $28 \pm 6$ ;  $P = \text{NS}$ ). The differences between the SNS and pacing seen in control were lost in same base region of the heart. This was because the APD adaptation under SNS could not exceed that of the pacing -a feature of physiological restitution normally seen in controls at the base region of the heart. See table 8 and figure 36.

classical restitution, reveals a negative slope at peak plateau heart rate due to continuing APD adaptation and prolongation of DI b) Physiological restitution also demonstrated additional APD shortening with SNS over and above changes incurred by pacing alone accounting for the difference in the loops c) This difference was eliminated by treating the hearts with drugs known to inhibit the key repolarization currents ( $I_{Ks}$ ,  $I_{Kr}$  and inactivation of slow  $I_{Na}$ ). Further, the differences between the SNS and pacing loops may represent repolarization reserve at an organ level. d) Most interestingly, the analysis of restitution loops at the base and apex regions have revealed heterogeneity. Preliminary data from the protein expressions in the base and apex regions of the left ventricle suggests the probability of a multiple neurocardiac factors modulating the repolarization of the ventricle, especially at the base. Improvements in experimental techniques have enabled studies of dynamic properties of repolarization such as APD Restitution to gain additional insights.

**Table 6 AI and APD changes (at Base) in control and after HMR1556 (0.5 $\mu$ M infusion)**

	Ctrl SNS	Ctrl Pace	t-test	HMR SNS	HMR Pace	t-test
AI <sub>(max)</sub> (ms)	459 $\pm$ 19		-	484 $\pm$ 40		-
AI <sub>(min)</sub> (ms)	261 $\pm$ 16			276 $\pm$ 16		
$\Delta$ AI %	43 $\pm$ 3			42 $\pm$ 4		
APD <sub>(max)</sub> (ms)	228 $\pm$ 11	227 $\pm$ 11	NS	251 $\pm$ 15	248 $\pm$ 16	NS
APD <sub>(min)</sub> (ms)	178 $\pm$ 9	185 $\pm$ 10	P< 0.05*	170 $\pm$ 8	169 $\pm$ 7	NS
$\Delta$ APD %	28 $\pm$ 2	22 $\pm$ 2	P< 0.05*	32 $\pm$ 2	31 $\pm$ 2	NS

Ctrl: control, SNS: sympathetic nerve stimulation, AI: Activation interval, APD: Action potential duration, NS: not significant by Student t-test on Paired samples, HMR1556- selective I<sub>Ks</sub> (slow delayed rectifier channel inhibitor), AI: Activation interval, APD: Action potential duration,  $\Delta$ APD is maximum minus minimum;  $\Delta$ APD% is the percentage change in APD; on Paired samples, P value less than 0.05 was considered statistically significant (\*). NS: not significant by Student's t-test. (n=5)

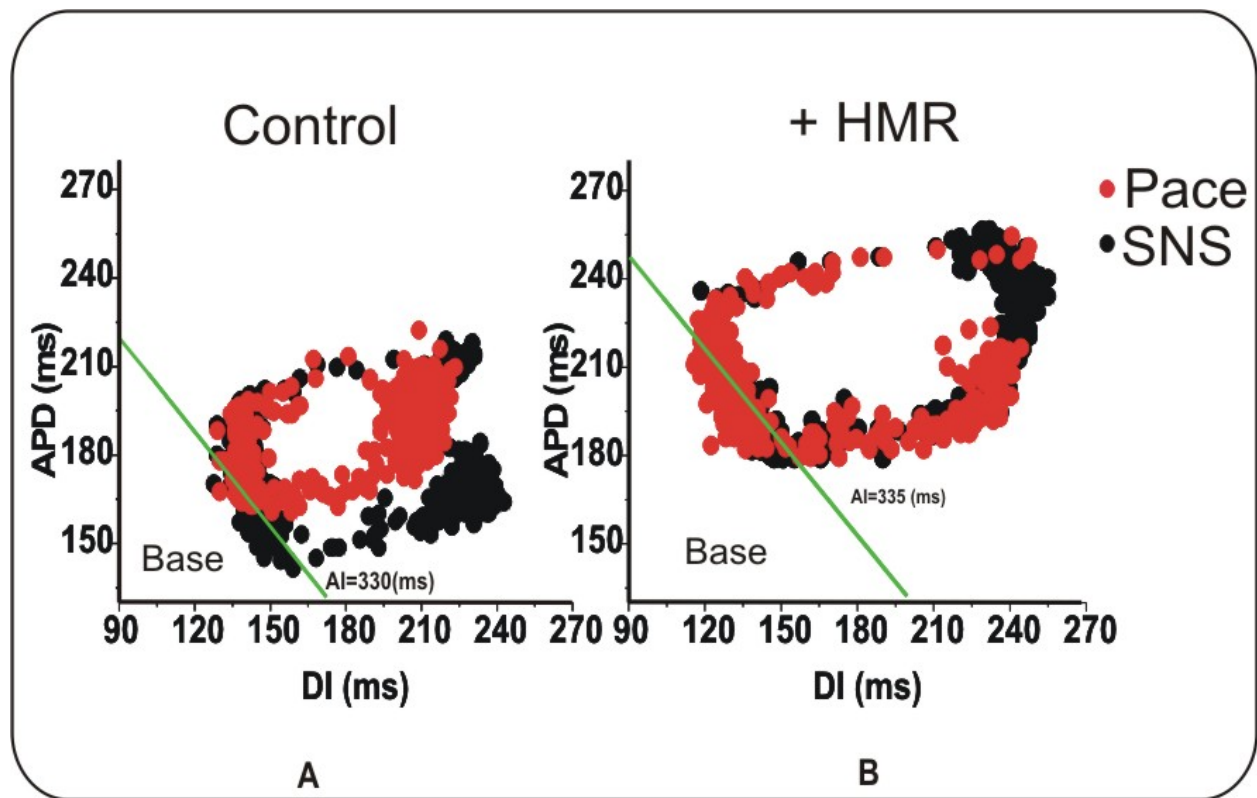


**Figure 34: Comparison between APD restitution loops without and with HMR infusion**

SNS: sympathetic nerve stimulation, AI: Activation interval, APD: Action potential duration, HMR1556- selective inhibitor of  $I_{Ks}$  (slow delayed rectifier channel). The green line passes through the plateau heart rate (peak) and the symbols falling on the line indicate the APD changes occurring at that constant heart rate. Also note the slope of curve is negative.

**Table 7 AI and APD changes at Base before and during E4031 infusion (0.01 $\mu$ M)**

	Ctrl SNS	Ctrl Pace	t-test	E4031SNS	E4031Pace	t-test
AI <sub>(max)</sub> (ms)	391 $\pm$ 24		-	399 $\pm$ 17		-
AI <sub>(min)</sub> (ms)	280 $\pm$ 15			288 $\pm$ 22		
$\Delta$ AI %	28 $\pm$ 3			28 $\pm$ 5		
APD <sub>(max)</sub> (ms)	193 $\pm$ 14	193 $\pm$ 17	NS	256 $\pm$ 16	261 $\pm$ 17	NS
APD <sub>(min)</sub> (ms)	151 $\pm$ 15	161 $\pm$ 13	P < 0.05*	217 $\pm$ 21	229 $\pm$ 23	NS
$\Delta$ APD %	21 $\pm$ 3	16 $\pm$ 2	P < 0.05*	22 $\pm$ 4	18 $\pm$ 5	NS

This table summarizes the influence of E4031 on physiological restitution. Ctrl: control, SNS: sympathetic nerve stimulation, AI: Activation interval, APD: Action potential duration, NS: not significant by Student t-test on Paired samples, E4031- selective I<sub>Kr</sub> (Rapid delayed rectifier channel inhibitor), AI: Activation interval, APD: Action potential duration,  $\Delta$ APD is maximum minus minimum;  $\Delta$ APD% is the percentage change in APD; on Paired samples, P value less than 0.05 was considered statistically significant (\*). NS: not significant by Student t-test.

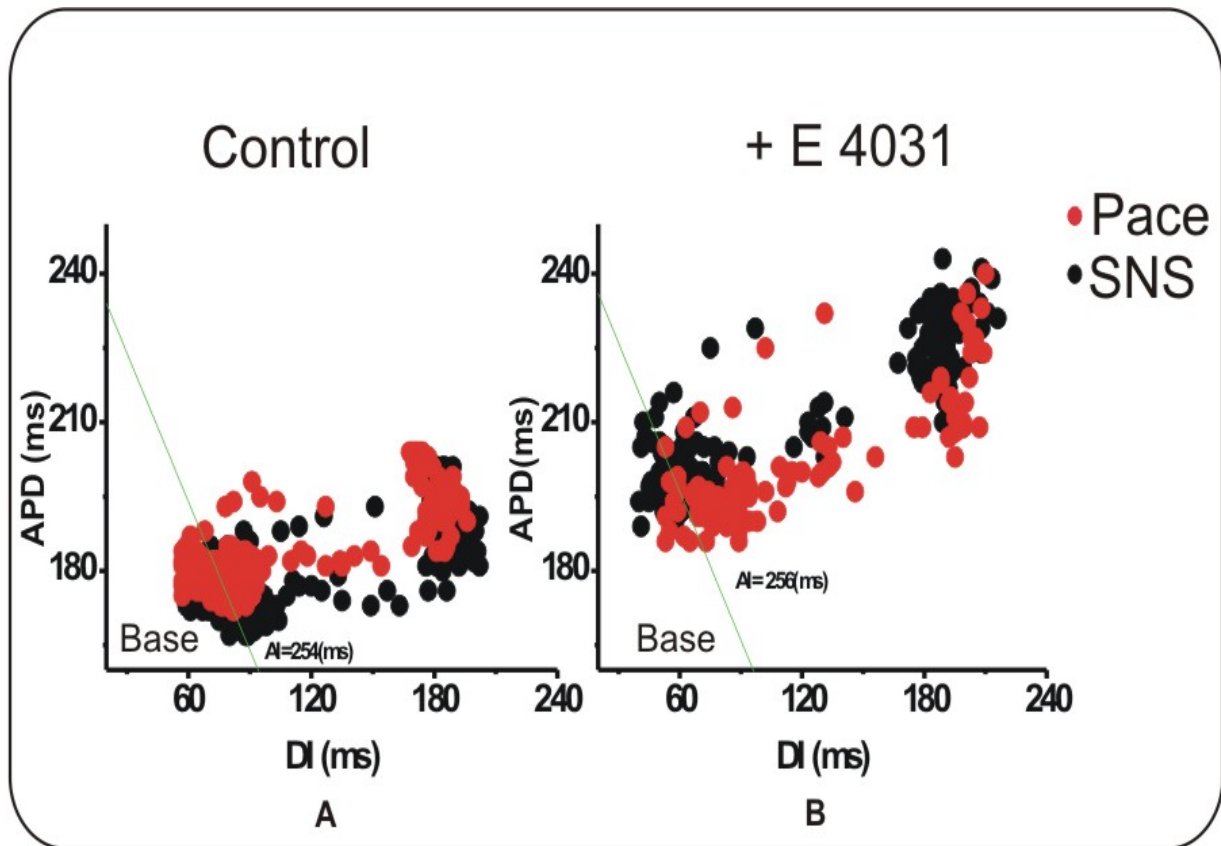


**Figure 35: Physiological Restitution under E4031 (0.01 $\mu$ M)**

SNS: sympathetic nerve stimulation, AI: Activation interval, APD: Action potential duration, E4031-selective inhibitor of  $I_{Kr}$  (Rapid type of delayed rectifier channel). The green line represents the plateau heart rate (peak) and the symbols falling on the line indicate the APD changes occurring at that constant heart rate. Also note the slope of curve is negative.

**Table 8 AI and APD changes at Base before and during APA infusion (10nM)**

	Ctrl SNS	Ctrl Pace	t-test	APA SNS	APA Pace	t-test
AI <sub>(max)</sub> (ms)	376±12		-	380±17		-
AI <sub>(min)</sub> (ms)	245±12			261±24		
ΔAI %	34±3			31±5		
APD <sub>(max)</sub> (ms)	198±15	201±17	NS	206±7	207±5	NS
APD <sub>(min)</sub> (ms)	142±8	158±10	P< 0.05*	146±14	150±14	NS
ΔAPD %	28±4	21±2	P< 0.05*	29±6	28±6	NS

The table 7 summarizes the influence of APA on physiological restitution. Ctrl: control, SNS: sympathetic nerve stimulation, AI: Activation interval, APD: Action potential duration, NS: not significant by Student t-test on Paired samples, APA- a selective I<sub>Na</sub> inactivation inhibitor. AI: Activation interval, APD: Action potential duration, ΔAPD is maximum minus minimum; ΔAPD% is the percentage change in APD; on Paired samples, P value less than 0.05 was considered statistically significant (\*). NS: not significant by Student t-test.

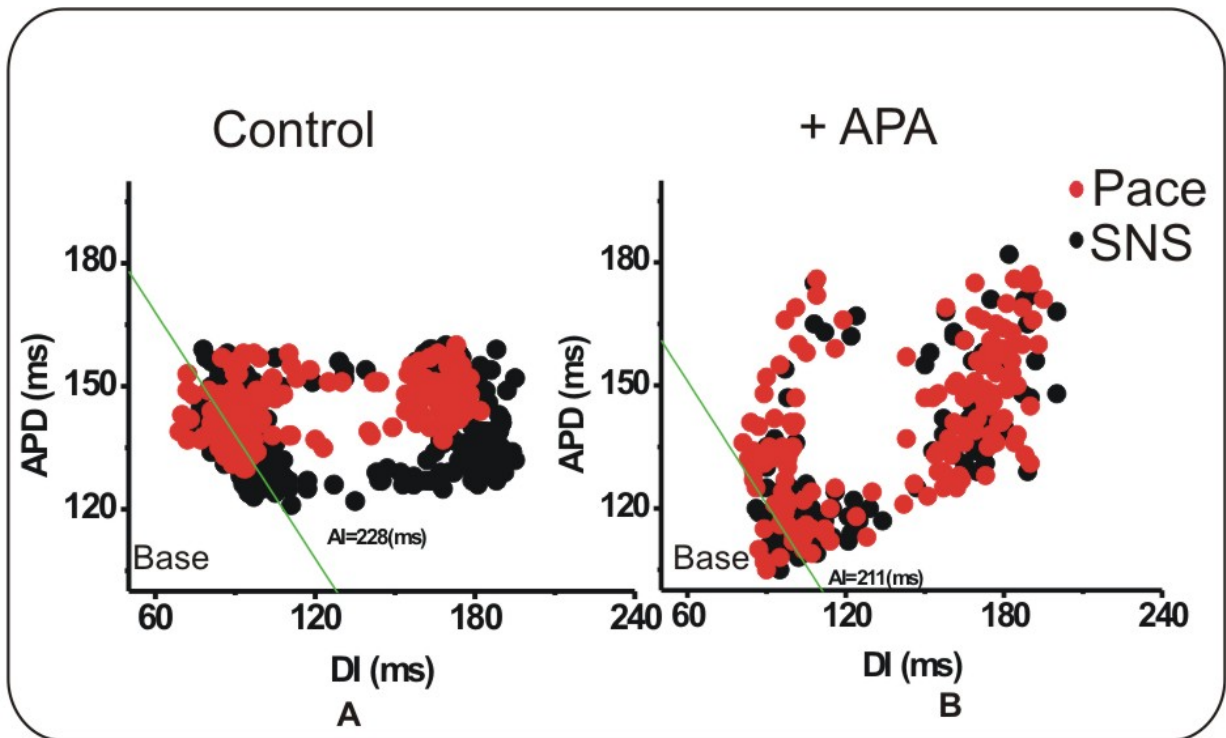


**Figure 36 : Physiological restitution under APA**

SNS: sympathetic nerve stimulation, AI: Activation interval, APD: Action potential duration, APA- selective inhibitor of slow  $I_{Na}$  current inactivation. The green line passing through the curves indicate the plateau (max) heart rate and the symbols falling on the line indicate the APD changes occurring at that constant heart rate. With APA differences between the SNS and pacing seen in control were lost in same region (base) of the heart.

#### 4.3.4 Discussion

These novel neurocardiological experiments have yielded interesting findings that are being reported for the first time. The main findings were a) physiological restitution, contrary to

Slopes of APD Restitution curves have been shown to be linked with the occurrence and behavior of unstable arrhythmia i.e. alternans and ventricular fibrillation. It has been experimentally shown by a number of researchers that the maximum slope of restitution-curve, when greater than one, made the myocardial substrate prone to electrically aperiodic rhythms i.e. alternans and ventricular fibrillation. Analysis of wave dynamics (Panfilov 1998; Witkowski, Leon et al. 1998) also revealed a correlation of wave patterns and the heart rhythm. Normal sinus rhythm corresponds to regular planar wave. A spiral wave was seen at higher heart rates (an optical or modeling equivalent of regular periodic rhythm). When slope of the restitution curve was more than 1, the spiral wave disintegrated more easily into multiple wavelets, after colliding with each other in a disorderly manner. These wavelets did not allow synchronized conduction of the electrical currents and prevented the mechanical ejection of blood from the ventricle (Benzinger, Drum et al. 1997; Koller, Riccio et al. 1998; Panfilov 1998; Lee, Lin et al. 2001; Fox, Riccio et al. 2002).

In vivo, the autonomic control of the heart is two pronged: neuronal and humoral. In this study, the main focus of interest is on the neuromodulation of ventricular repolarization. The local neural component involves intra-thoracic neuronal ganglia, intrinsic cardiac neuronal ganglia. When intact, the neurons by the continuous cross talk and feedback mechanisms organize a beat to beat control of the heart rate. The feedback is such that there is two way information processing between the mechanical activity generated by the heart and sensory inputs into the neuronal ganglia and efferent controls inputs back to the heart via short-loop mechano-sensory reflexes (Armour). On the other hand, humoral component comprises mainly of the catecholamine output from the adrenal medulla. This is governed by stimulus from the lumbar out flow of the sympathetic nerves. Both components of sympathetic system together produce a net effect on the cardiovascular system (Dubin 2003). Some data suggest that circulating catecholamines levels did not reflect the cardiac interstitial fluid levels of catecholamines and neuronal release of norepinephrine from intrinsic cardiac nerve terminals yielded much higher levels of norepinephrine in the cardiac interstitial fluid than medullary catecholamine release

(Farrell, Wei et al. 2001). The roles of individual components have not been characterized fully as there were no models, until lately, to study these components independently (Ng, Brack et al. 2001). The confounding influence of humoral component is eliminated in the isolated innervated heart preparation by retrograde perfusion of Tyrode solution through the aorta to study the influence of local autonomic neuronal input on the heart without confounding influence of circulating catecholamines.

Testing two arms of autonomic control together is beyond the scope of present work but may be an interesting future endeavour.

It is common clinical observation that arrhythmia starts mostly when the heart rates are in or near physiological ranges often initiated by a pause (Viswanathan and Rudy 1999; El-Sherif and Turitto 2003; Liu and Laurita 2005). Cardiac restitution studies, done in the past, used programmed stimulation protocols by pacing alone. As a result, the behavior of restitution kinetics was often analyzed with CL shorter than physiological. Further, the characteristics of restitution kinetics depend on rate of change in CL, which depended on the protocols. This has resulted in several 'models' of restitutions (Berger 2004; Wu and Patwardhan 2004).

Restitution is the result of changes to repolarization during heart rate change; which in turn is the net result of dynamic changes in the underlying repolarizing ion currents and channel kinetics. Hence it is obvious that a mono-exponential APD response would be impossible as the ion channel conductances differ from each other and not follow mono exponential time courses. For example, the key ion currents have either abrupt on off kinetics as seen in ( $I_{Na}$ ) or have rectifier kinetics as in the case of potassium currents (Franz 2003). Therefore, the complexity of the physiological restitution curves may be a more 'realistic depiction' of the dynamic changes in ventricular repolarization.

An important feature of this experimental protocol is that the changes of APD and DI occurred with heart rates in the physiological range (not very short or very long cycle lengths seen in experimental studies); and the AI was not controlled by the investigator but rather by the SNS. When the central sympathetic outflow was stimulated, the local circuit neurons and their ganglia together with the efferent sympathetic arm and intrinsic cardiac ganglia participate in the neurotransmission to allow tachycardia (decrease in Activation interval) which reaches a plateau at peak heart rate as shown by Ng GA et al (Ng, Brack et al. 2001).

Physiological restitution, showed an inverse relationship between the AI and APD where the Max APD was when the AI was at baseline, and was shortest when the AI was the least. Physiological restitution describes the complex relationship between APD and DI in a consistent manner. The relationship is not linear or curvilinear but more complex (Figures 31) described as phases 'a-d'. The response to SNS initially, was similar to the unimodal APD restitution described by other studies (Berger 2004). But at peak heart rates, the slope of the restitution was intriguingly different (from any previous studies) in that there was not only continued shortening of the APD but this was associated with prolongation of the DI (phase 'b'). The negative slope may be a result of ventricular myocardial effect of SNS lagging behind sino-atrial effect i.e. SNS effects on SAN & heart rate is fast and peaks before maximum effect on ventricular myocardium and ventricular APD. Although, there are reports in the literature suggesting the APD-DI relationship to be complex (Franz 2003), there has been no previous report describing a negative slope of the restitution curve.

When the physiological restitution curves are compared with classical restitution curves, the phase b of the physiological restitution curve shows the following features- the restitution slope is initially steep, but contrary to what was expected, the slope shifted to minus one at peak heart rates. This may be a physiologic adaptive phenomenon to 'stabilize' the normal myocardium against arrhythmias at these physiological heart rates.

When the stimulation was stopped, the physiological restitution curves showed hysteresis (phases c and d), where the return path of APD to baseline was not identical to its path to peak adaptation. Hysteresis may be due to differences in recoveries of APD and DI. The APD recovery lags behind DI recovery, as the heart rate reduces. This feature of hysteresis is not unique to this study. It has been seen in several other classical restitution studies (Berger 2004; Wu and Patwardhan 2004).

The underlying mechanisms for the complex APD-DI relationship in restitution have been studied by several groups. The roles of individual ion channel kinetics in the adaptation process and the results of various ion current modifications on the effect on the APD restitution are discussed below.

#### **4.3.4.1 Alterations in ion channel kinetics in APD adaptation in the context of APD restitution.**

Functional alteration of ion channels kinetics seems to cause the APD to shorten at higher heart rates. The APD adaptation to rate and autonomic influences is complex, multifactorial, and probably under explored (Carmeliet 2004) .

Sodium channel inhibitors have been shown to flatten the slope of the restitution curve and reduce the window for arrhythmias. This was mainly due to its effect on conduction velocity (Qu, Weiss et al. 1999). There is no data yet on the effect of increased sodium current by delayed inactivation. However, sodium current kinetics are intimately related to that of calcium current because of its voltage and calcium dependent kinetics. (See below)

The  $I_{Ks}$  and  $I_{Kr}$  currents (the slow and rapid components of delayed rectifier potassium currents), in general, and particularly the  $I_{Ks}$  currents accumulate under the influence of catecholamines via both beta and alpha receptor stimulation via the PKA and PKC activation respectively (Walsh and Kass 1988). Also, at steeper slopes (seen in phase 'b' and 'd' in the physiological restitution loops) may be partly due to  $I_{Ks}$  tail current modification (accumulation in phase 'b' and recovery in phase 'd') and current enhancement due to rise in intra cellular calcium (Cheng, Kamiya et al. 1999); (Tohse, Kameyama et al. 1987).

$I_{Kr}$  current is thought to be activated indirectly via PKA, increase in calcium current and PKC (Heath and Terrar 2000). This may also contribute to the shortening of APD at higher rates e.g. phase 'b' of the restitution loop. The governing principles of channel kinetics controlling the slope of the restitution curve is not yet fully understood. At present, all we know is that potassium and calcium channel blockers flatten the slope of the restitution curve and prevent arrhythmias (Garfinkel, Kim et al. 2000, Riccio, Koller et al. 1999, Koller, Riccio et al.2000).

During steady increase in heart rate, L-type calcium current kinetics plays an important part. The facilitation of L-type calcium channel under PKA and recovery of the channel probably may not contribute to the shape of phase 'a' of the restitution loop, as we found no initial prolongation of the APD seen by other groups (Carmeliet 2004). It has been suggested that at steady heart rates, there is slow gating of L- type calcium channels (delayed or slow recovery from inactivation). This limits the amount of calcium entering the cell the via L- type calcium channel. Facilitation of the L-type calcium current or its voltage dependent recovery, alone, may not also explain APD shortening during phase 'b' (Taggart, Sutton et al. 2003). An increase in

intracellular calcium would, by itself, lead to prolongation of the action potential duration but not shortening. Also, voltage patch clamp studies have shown that increase in peak  $I_{CaL}$  is associated with faster rates of inactivation permitting shorter APD. (McDonald, Pelzer et al. 1994; Carmeliet 2004) As a matter of fact, at no time during sympathetic nerve stimulation was prolongation of APD observed in the study.

Figure 37, presents a summary of the kinetics of a number of ion channels which can affect APD e.g. rectifier potassium currents, L-type calcium current.

During peak heart rate, there is data to suggest increase in extracellular potassium due to increased stimulation (Kline and Morad 1978). This increases in potassium conductance via  $I_{K1}$  which may contribute to shortening of the action potential (Kline and Morad 1978). There is evidence to suggest that accumulation of intracellular sodium ions at a sub-sarcolemmal region setting sodium potassium exchange pump into activity leading to hyperpolarization of the membrane in diastole and enhancing the repolarization. Even though increase in potassium conductance and sodium accumulation may be competing in terms of their opposing influence on sodium potassium exchanger, sodium ions have been shown to have a more influential effect in driving the sodium potassium exchanger (Loew, Cohen et al. 1992; Taggart, Sutton et al. 2003).

Calcium handling alterations occur during higher heart rates (achieved either by increasing beta and alpha adrenergic receptor agonist or by simply pacing the heart at higher frequencies). This again is multi factorial and complex. When the heart rate is high, there is an increase in the cytosolic calcium loading purely by the virtue of the increased frequency of the  $I_{CaL}$  activation. This loading is however offset by several mechanisms- a relatively slow-acting NCX in forward mode, increased calcium dependent inactivation of the L-type calcium channel, PKA induced or simply CaM Kinase II induced phosphorylation of the phospholamban (PLB) and or SERCA 2 (Sarcolemmal reticulum calcium ATPase). The later plays a pivotal role in pushing extra cytosolic calcium back into the SR (Schouten 1990). This 'sucking out' of cytosolic calcium may shorten the APD. APD shortening also occurs by other factors including activation of calcium dependent chloride current and activation of calcium dependent potassium currents.

Recent data suggest that the hysteresis of restitution is influenced by  $I_{Ks}$ ,  $I_{Kr}$ ,  $I_{Ca-L}$  and rate of calcium transfer into the Junctional SR (JSR). It was found that  $I_{Ks}$  and  $I_{Kr}$  had opposing

effects on hysteresis. Interestingly, it was also found that it was the rate of transfer of calcium into the JSR, more than  $I_{Ca-L}$ , which influenced the hysteresis (Wu and Patwardhan 2007).

Early data from protein expression analyses suggest that not only is the heart being controlled by its own ion channel kinetics but also modulated by local neuronal innervations. The Tyrosine hydroxylase expression showed that sympathetic nerve distribution could be heterogeneous over the myocardium. An earlier study also showed that the innervational patterns are also regionally heterogeneous (Kawano, Okada et al. 2003). There are studies including the present study which found the distribution of the major repolarizing currents to be heterogeneously distributed. Regional modulation of repolarization should not come as a surprise. The differences in the restitution loops from apex and base (shown in figure 32) exemplifies the multilevel interaction of at least two factors i.e. the sympathetic nerve ending and increased density of  $I_{Ks}$  at the base of the heart. The result of an increased APD adaptation during SNS is supportive of this hypothesis (Cheng, Kamiya et al. 1999; Kawano, Okada et al. 2003; Mantravadi, Gabris et al. 2007). It must be stated that data are preliminary and further exploration into this important issue is required.

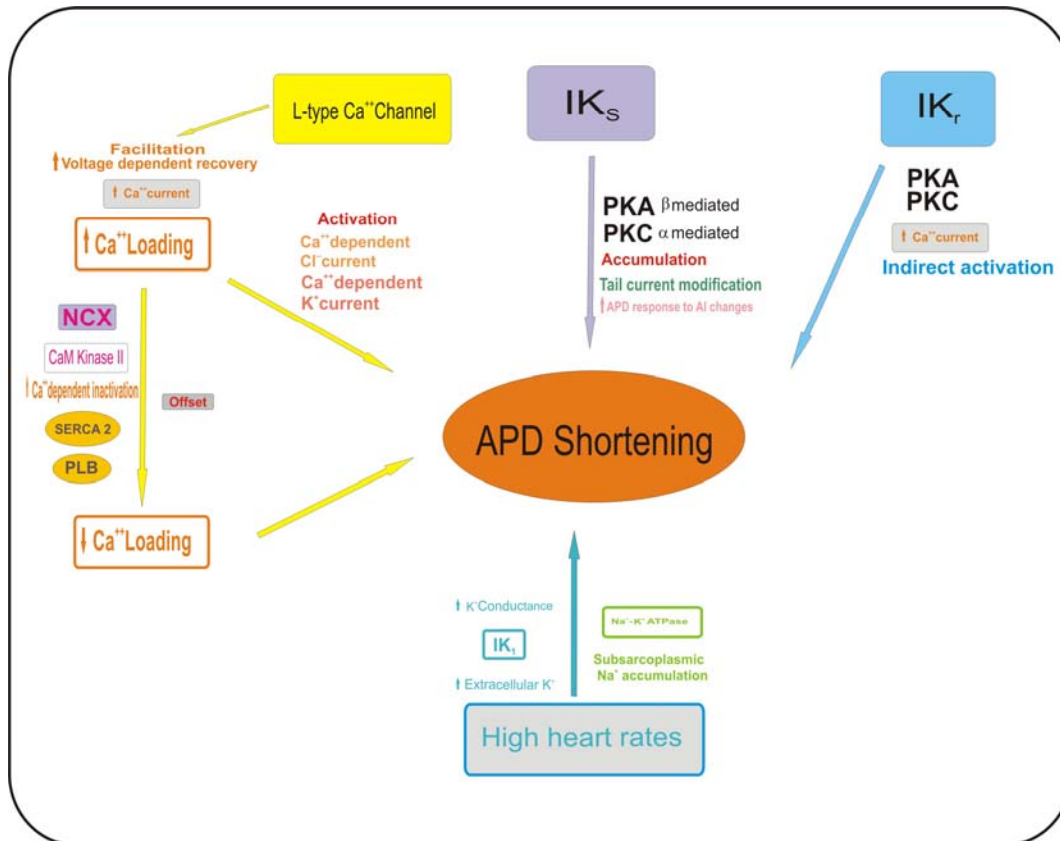


**Figure 37: Factors controlling APD rate adaptation with changes in Heart rate**

The figure summarizes the complex factors influencing the shortening of APD with an increase in heart rate. These can be arbitrarily divided into calcium cycling factors and ion channel interactions. All these factors play their part resulting in the net result of reduction of APD. At higher sympathetic stimulation increase the cytosolic  $\text{Ca}^{2+}$  concentration, which activates  $\text{Ca}^{2+}$ /calmodulin-dependent protein kinase (CaMKII). CaMKII is thought to phosphorylate L-type calcium channel, and phospholamban (PLB). Activation of  $\alpha$  adrenoceptor activates phospholipase C (PLC) via G proteins, which in turn activate protein kinase C (PKC  $\alpha$ ). PKC  $\alpha$ , directly phosphorylates protein phosphatase inhibitor-1 (I-1), enhancing the activity of the protein phosphatase-1 (PP1) and causing hypo phosphorylation of PLB; SERCA2a, sarcoplasmic reticulum ATP-ase;  $\text{I}_{\text{Ks}}$ : slow type of delayed rectifier potassium current;  $\text{I}_{\text{Kr}}$ : rapid type of delayed rectifier potassium current;  $\text{I}_{\text{K2.1}}$ : Inward rectifier potassium current. PKA: Protein kinase A,  $\text{Na}^+/\text{Ca}^{2+}$  exchanger (NCX).

Given the complex effects of multiple ion currents and calcium cycling proteins on restitution, the final effect on APD adaptation seems to be a sum of all these factors in a particular species. Therefore a unified approach to repolarization may be a sensible way of understanding arrhythmia vulnerability. Even in normal hearts, there may be arrhythmogenic windows in the early phases of classical restitution at physiological ranges (Franz 2003).

Recent concepts like repolarization reserve have become relevant especially at an organ level. The data on physiological restitution and ion channel inhibition is discussed below in this context.

#### **4.3.4.2 Repolarization Reserve and Restitution curves**

Restitution primarily describes repolarization alterations during heart rate changes. We studied the effect of individual ion channel blockers on restitution. When loops obtained by SNS were compared to loops by obtained by pacing simulation of the former's heart rate change, the main differences were that the ranges of APD were significantly different. SNS had greater APD adaptation (shortening) at higher heart rates than during pacing.

From the discussion in the previous sections it may be clear that repolarization (hence restitution) is governed by complex kinetics of numerous ion channels. It is possible that a decrease in function of one of the repolarizing currents may alter effectiveness of the overall repolarization (hence the restitution) of the myocardium. Recently, a single and unified paradigm to evaluate the arrhythmogenic factors was conceived by Roden et al (Brink, Crotti et al. 2005). It was proposed that no individual ion channel lesion was sufficient to produce full manifestation of the LQT phenotype; but contribute in part to a reduction in a normal repolarization reserve. This reserve, believed to be formed by multiple redundant mechanisms, normally exist in the heart to constitute normal repolarization. Silva et al demonstrated this phenomenon in KCNQ1 and KCNQ1+ KCNE1 models where they showed the existence of such a reserve by studying the subunit interactions (Silva and Rudy 2005). They have shown that these subunit interactions (thereby the channel functions) vary in degree and rates depending on the sympathetic states. This autonomic depended variance allowed formation of a 'reserve functional capacity' or repolarization reserve. There are other studies suggesting changes of repolarization reserve by number of factors e.g. increase in  $IK_r$  current by drugs like NS1643 (Diness, Hansen et al. 2006), and ion channel cross-cover ( $IK_s$  providing reserve function to  $IK_r$  dysfunction) (Viswanathan

and Rudy 1999). There have been no studies in the literature at an organ level to directly demonstrate the repolarization reserve by APD restitution. We hypothesized that the differences between SNS and pacing loops may be used to demonstrate repolarization reserve as it primarily depicts APD adaptation which is a sum effect of repolarizing currents.

The differences between the SNS and Pacing restitution loops normally seen at the base were abolished by inhibition of  $I_{Ks}$ . When HMR was administered, APD prolonged without a significant change in the heart rate. When the heart was driven by SNS, the net repolarizing currents in the presence of  $I_{Ks}$  inhibition may not be adequate to shorten the APD as well as in controls. In LQT1 symptoms mostly occur during peak sympathetic stress. APD adaptation at peak heart rate is significantly more during SNS than during Pacing. This difference is lost during infusion of HMR1556, which indicates a reduction of APD adaptation under sympathetic stress.

When the hearts were treated with  $I_{Kr}$  and slow  $I_{Na}$  inactivation inhibitors, similar observations were made; where the net repolarizing currents were inadequate to control APD adaptation during SNS. In these experiments, only one of the repolarizing currents at a time was reduced by pharmacological inhibition. This allows the other repolarizing currents to maintain the overall restitution curve characteristic; suggesting a ‘repolarization cross- cover’ to maintain normal periodic rhythm.

Thus Physiological Restitution Kinetics studies during SNS suggested that  $\beta$ -adrenergic activity produced an additional APD shortening over and above that of pacing at high rates. When these loops were studied during drug induced LQT, a possible decrease in repolarization reserve abolished differences between SNS and pacing restitution kinetics curves and suggested that a common cellular signalling mechanism may be involved, which was altered by the 3 drugs that impeded the extra APD shortening seen with SNS. Further studies are required to elucidate these observations further.

#### **4.3.4.3 Conclusion**

Isolated innervated heart preparation was successfully adapted for optical mapping, for the first time.

The present study suggests that it is possible to measure physiological restitution during SNS and study the restitution characteristics of these curves. The physiological restitution curves have shown an unique 'four-phase' characteristic features, different from classical restitution studies.

Comparisons of restitution curves obtained by SNS and Pacing reveals an apex to base heterogeneity of restitution. Protein expression studies show an increase in protein density of both  $I_{Ks}$  channel and sympathetic innervation in the base region compared to the apex.

This may be early evidence of a heterogeneous neurocardiological interaction at the base causing the increased regional shortening of APD at the base (see chapter 4 and 5).

Finally, early results of physiological restitution under repolarizing current inhibitors suggested the presence of repolarization reserve which had only been shown only in cellular and modeling studies, primarily.

#### **4.3.4.4 Limitations**

Optical mapping used in the present study allows electrophysiological data to be obtained from the surface of the heart. The physiological restitution characteristics from within the walls of the ventricle are not available in these studies.

Motion artifacts were resolved using excitation-contraction uncouplers. These uncouplers have their effects on cardiac electrophysiology as discussed in detail in the Methods section. Great care was taken to use a minimal dose of the cyto-D along with physical restraint to reduce motion.

Confounding electrophysiological effects from cyto-D on restitution cannot be completely ruled out for the following reasons: early experiments were done with larger hearts, in vertical position to accommodate them in the immobilization chamber. The APD adaptation was slightly higher but the overall restitution characteristics remained unchanged. Further, the heart sizes were not identical in the same aged rabbits. Therefore dose of cyto-D per gram of

tissue may not be identical. This limitation was minimized by using paired data for statistical analysis.

The limitations of pharmacological ion channel blockers are well known. They do not cause the exact molecular defects in the ion channels as seen in disease mutation. The pharmacological agents may have collateral inhibitions of other ion channels.

Doses of ion channel blockers were chosen such that manifestation of the inhibition was obvious. Higher doses were avoided as they produced significant unwanted side effects especially on heart rate and APD adaptation. Also, it may be impossible to estimate the optimal level of inhibition given the limitations of the pharmaco-kinetics and pharmaco-dynamics of the specific ion channel inhibitors.

No arrhythmias were seen in these studies. Several reasons could account for this. Most importantly, the resting CL were lower (heart rates were faster) in this preparation than seen in other LQT experiments where the Langendorff perfused hearts were treated with higher doses of inhibitors and the AV nodes were destroyed and the hearts were paced with desired CL (not necessarily physiological) such that arrhythmias were produce at very low or very high CLs. In the present study the CL and heart rates were always in the physiological range by neuronal manipulation. A way to circumvent this problem would be to use transgenic rabbits (which are recently made available) and/or use realistic three dimensional whole heart models to study arrhythmias. It is important to study arrhythmias in a realistic setting in order to understand clinical arrhythmia mechanisms and develop possible treatment.

The data obtained from this novel preparation is preliminary observational data and not mechanistic, as not all of the neurocardiological factors modulating restitution were analysed in this study. It must be said that the ion channel kinetics seen during classical restitution studies may not be directly applicable to these experiments as the protocols are significantly different (e.g. extra stimulus, steady state, CL).

No corroborative in-silico modeling studies were done to reproduce this phenomenon of physiological restitution. This would provide an opportunity to manipulate individual factors at will and study the changes more closely.

#### **4.3.4.5 Future directions**

As mentioned before, the exciting novel data obtained in this study is preliminary and observational. Further experimental testing and in-silico validation is required; especially, to understand the individual factors controlling the phenomenon of physiological restitution and its heterogeneity.

It is easy to verify the validity of physiological restitution in patients by measuring the QT vs. TQ intervals on an exercise stress test.

The four-phase restitution characteristic and typical APD adaptations were lost in pilot experiments when the hearts were tested with higher doses of the inhibitors; or high doses of uncouplers especially BDM; or use of CaM kinase II inhibitors or when AI interval was increased dramatically by any other means for example: temperature reductions, hypoxia, bradycardia due to vagal compression etc. The reason for this is not known yet and will require further experimentation to tease out the effects of various factors and pinpoint the underlying reasons.

Although ion channel inhibitors at the concentrations studied did not alter restitution characteristics dramatically, major disturbances of physiological milieu like the aforementioned ones, could potentially derail the restitution kinetics altogether.

Further, physiological restitution studies in various pathological conditions like myocardial infarction, and heart failure may invoke avid interest in the future.

## **5.0 DISPERSION OF REPOLARIZATION**

### **5.1 ABSTRACT**

Increase in dispersion of repolarization (DOR) is linked to arrhythmogenesis and is modulated by autonomic inputs. However there is no the effect of autonomic neuronal stimulation on the DOR of the ventricle. We used a recently described neurocardiology mode of the isolated innervated rabbit heart preparation model with voltage sensitive dyes and optical mapping technique to measure apex-base spatial DOR over the left ventricle before during and after sympathetic nerve stimulation and vagal stimulation separately and together. We found the normal dispersion of repolarization without neuronal stimulation was in apex to base direction and during SNS DOR increased significantly and repolarization sequence changed to base to apex direction. On stopping SNS repolarization returned to its baseline direction. During individual vagal nerve stimulation there was no change direction of the repolarization but when both vagii were stimulated, DOR increased and the direction inversed to base to apex direction. Herein, observations obtained from the novel neuro-cardiological model in the context of existing data on apex-base heterogeneity of ion channels and the autonomic ventricular innervation are discussed and compared with the changes in DOR during autonomic stimulation of the heart by pharmacological means.

## 5.2 INTRODUCTION

There has been extensive research and information on cardiac repolarization over the past four decades but the full picture is still not completely understood. Repolarization is a cumulative result of ion channel kinetics occurring during the second and third phases of the cardiac action potential. Repolarization has been shown to be independent of the activation sequence of the ventricle, not uniform over the ventricle, and is dependent on the differences in action potential duration over the ventricle. (Efimov, Huang et al. 1994).

The changes in the kinetics of individual ion channels, mainly, the delayed rectifier potassium channels, sodium channels and L-Type calcium channels have a direct effect on repolarization (Curran, Splawski et al. 1995; Yan, Wu et al. 2001; Splawski, Timothy et al. 2005).

Repolarization and its dynamic characteristics like action potential duration restitution (APDR), dispersion of repolarization (DOR), cardiac memory and electrical remodeling have been shown to strongly influence the genesis of arrhythmias. Data from animals and humans has shown that alteration of repolarization makes the myocardial substrate more vulnerable to arrhythmias. There is also extensive data to suggest that autonomic drugs like isoproterenol, epinephrine etc, modulate ion channel kinetics and influence the APD regionally and therefore the effects of repolarization dynamics (Conrath and Opthof 2006).

Dispersion of repolarization is a measure of the non-uniformity of repolarization over and across the myocardium. It is known that there are regional differences in ion channel distribution from endocardium to epicardium and from Apex to Base on the surface of the ventricle. These fundamental differences result in the regional differences in APDs. The role of transmural dispersion of repolarization has been studied in depth and its role in arrhythmogenesis has been well elucidated (Antzelevitch 2007). Optical mapping has allowed the study of DOR over Apex-Base regions of the ventricle. There is clear evidence that increase in DOR over the surface of the ventricle increases the vulnerability of the myocardium to re-entry and arrhythmia (Baker, London et al. 2000). There are a number of factors which affect DOR, including ion channel distribution and their kinetics, autonomic status, hypoxia and hypothermia (Shimizu and Antzelevitch 2000), (Salama G 1993). However, there are no in vitro studies, to our knowledge, describing the effects of neuro-modulation on apex-base DOR.

In this study the isolated innervated rabbit heart preparation was used- a Langendorff perfused heart with intact dual autonomic innervations- to study the effects of neurostimulation of sympathetic and vagal nerves, on apex-base dispersion of repolarization of the anterior surface of left ventricle, using optical mapping technique and voltage sensitive dyes.

### 5.3 METHODS

The surgical technique of the isolated innervated rabbit heart preparation has been described in the Methods chapter. Briefly, adult New Zealand White rabbits (3.5-4 kg,  $n = 8$ ) were premedicated with Ketamine Hcl (Hospira Inc USA;  $0.1 \text{ mg kg}^{-1}$ , s.c.) and Medetomidine (Pfizer, 1mg s.c). General anaesthesia was induced and maintained by Diprivan (Astra Zeneca 1-2  $\text{mg kg}^{-1}$ , i.v.) Rabbits were ventilated, after tracheotomy, using a small-animal ventilator (Harvard Apparatus Ltd, Edenbridge, Kent, UK, 60 breaths per min) with an  $\text{O}_2$ /air mixture. The vagus nerves were isolated and the blood vessels leading to and from the ribcage were ligated and dissected. The rabbit was terminally anaesthetized with an overdose of Pentobarbitone (60 mg i.v.) with 500 IU Heparin i.v. The anterior and lateral portion of the rib cage was removed and descending aorta cannulated. The pericardium was cut and ice-cold Tyrode solution applied to the surface of the beating heart to preserve myocardial function. The preparation extending from the neck to thorax was dissected from surrounding tissues as described previously (Ng, Brack et al. 2001). For optical mapping purposes a dual cannulation method was used where two separate peristaltic pumps were used a) to perfuse the spinal cord via the descending aorta - spinal artery route and b) to perfuse the heart in a Langendorff fashion via the ascending aorta route, using a balloon catheter which when inflated separates the two systems. This method helped to optimize dye and drug delivery while achieving excellent perfusion pressures to the heart and the spinal cord. Perfusing solution was Tyrode solution with (in mM): 130 NaCl, 24  $\text{NaHCO}_3$ , 1.0  $\text{CaCl}_2$ ; 1.0  $\text{MgCl}_2$ ; 4.0 KCl; 1.2  $\text{NaH}_2\text{PO}_4$ ; 20 dextrose at pH 7.4; and gassed with 95%  $\text{O}_2$  and 5%  $\text{CO}_2$ . This investigation conformed to the current *Guide for Care and Use of Laboratory Animals* published by the National Institutes of Health and animal scientific procedures Act 1986 in the UK. Temperature was maintained at  $37.0^\circ\text{C} \pm 0.2^\circ\text{C}$  and perfusion pressure was adjusted to  $\sim 65$  mmHg with peristaltic pumps. Hearts were stained with a voltage

sensitive dye (di-4 ANEPPS, 40  $\mu$ L of 1 mg/mL dimethyl sulfoxide, DMSO). A combination of two methods were used to reduce motion artifact during experiments 1) Mechanical immobilization using a custom made tray with adjustable slide-strap arrangement (see Figs 24,25) was used to hold the heart in place for imaging during nerve stimulation and 2) Cytochalasin D was used in a novel dose of a short infusion of 2  $\mu$ mol for a period of 10 min. Use of Cytochalasin- D in this fashion helped to reduce the contractile motion and at the same time did not significantly alter conduction velocity (which was one of the early electrophysiological features shown to change followed by changes in calcium transients in earlier studies (Baker, Wolk et al. 2004)).

The optical apparatus has been previously described (Baker, London et al. 2000). Briefly, light from two 100-W tungsten-halogen lamps was collimated and passed through  $520 \pm 30$  nm interference filters. Fluorescence emitted from the stained heart was collected with a camera lens. Fluorescence emission from the anterior region of heart (see figure 21) was passed through a cutoff filter (610 nm, Omega Optical, Brattleboro, VT, USA) and focused on a  $16 \times 16$  elements photodiode array (C4675-103, Hamamatsu Corp., Bridgewater, NJ, USA). Outputs from the photodiode array were amplified and digitized (14-bit) at 2,000 frames/second (Microstar Laboratories, Inc., Bellevue, WA, USA) for at least 40 seconds for data analysis. Voltage sensitive dye Di 4 ANNEPS was used for these experiments.

### **5.3.1 Stimulation protocols**

**Sympathetic Nerve Stimulation:** A Quadripolar electrode was inserted at the 12th thoracic vertebra and the tip of the wire was advanced to the level of the 2nd thoracic vertebra to allow stimulation of both sides of the cardiac sympathetic outflow. A sub-maximal stimulus (Ng, Brack et al. 2001) of 15V 15Hz strength was used obtain maximum heart rate response (details discussed in the Methods chapter) till the heart rate reached a peak and then the stimulus was turned off allowing the heart rate to return to baseline. Vagus nerve stimulation was done using custom-made silver chloride bipolar electrodes. Individual vagus nerves (Right and Left) were stimulated separately and together with the sub-maximal stimulus strength (15v 15Hz for a period of 5 seconds) each producing a significant drops in heart rate. Stimulus generator was

made in the electronic shop of University of Pittsburgh, which allowed a choice of stimulating strength from a range of 1-20 volts and 1-20 Hz.

## 5.4 RESULTS

### 5.4.1 Neuro-Modulation of apex-base DOR

#### *Control VS.Sympathetic nerve stimulation*

Stimulation of the spinal canal to induce SNS increased heart rate gradually (see figure 37) from  $143 \pm 6.3$  (AI=  $427 \pm 18.3$  ms) to a peak rate of  $229 \pm 12.3$  beats /min (AI= $265 \pm 13.2$ ms) and changed the direction of repolarization from apex towards the base (in control: CTRL) to base towards the apex (Table 9, n=7), during SNS. Figure 39A illustrates a map of repolarization gradient and a series of 16 superimposed APs from apex to base at slow and fast sweep speeds, during sinus rhythm (CTRL) prior to SNS. Figure 39B shows the same measurement from the same heart after 50 s of SNS at 15 Hz. The reversal of the direction of repolarization during SNS was due to difference of its effects at the base and apex of the ventricles. As shown in Table 9, SNS did not significantly change APDs at the apex (Control: APD= $159 \pm 4$ , during SNS APD= $155 \pm 12$  ms; p= NS) whereas SNS caused a marked shortening of APDs at the base ( $134 \pm 9$  ms) compared to sinus rhythm (APD = $176 \pm 4$  ms; p< 0.001; n=7). DOR during sinus rhythm (APD base-APD apex) was  $17 \pm 1$  ms and during SNS, DOR changed to  $-22 \pm 1.6$  ms; (p < 0.001), (n=7); meaning that the direction of repolarization was reversed due to heterogeneities of the effects of SNS being more pronounced at the base than at the apex.

#### *Sinus Rhythm vs. Isoproterenol Infusion*

Isoproterenol infusion (100nM) increased heart rate to  $204 \pm 13.1$  beats/min (n=6) (p<0.05) and DOR to  $23 \pm 2$  ms (p<0.05 n=5) but did not change the direction of repolarization, which remained from apex to base. Figure 40 A and B compares maps of APDs recorded from the same heart first in sinus rhythm (CTRL) and 2 min after perfusion with 100 nM isoproterenol (ISO).

### *Time course of DOR changes Caused by SNS*

Upon SNS, DOR reversed from apex → base to base → apex by 15 s and when SNS stimulation was stopped, heart rate returned to baseline and DOR returned to control values and to its original orientation (i.e. apex to base) with a latency of 130-140 s. Figure 41 depicts the changes in DOR as a function of time for 4 hearts where DOR was mapped before, during 50 s of SNS and 150 s after the interruption of SNS. The slower recovery of DOR of  $135 \pm 23$  s implicates a cellular signaling process.

### *Vagus Nerve Stimulation (VNS)*

Right vagus nerve stimulation (VNS), caused a significant drop in heart rate to  $95 \pm 5$  beats/min ( $n=6$ ) and DOR did not change significantly in magnitude or direction (Table 1). Left VNS caused a significant similar drop in heart rate as for right VNS ( $96 \pm 6$  beats/min), failed to produce a statistically significant change DOR and did not reverse the orientation of repolarization (Table 1). In contrast, bilateral VNS reversed the direction of repolarization from apex → base to base → apex with  $\Delta APD = -16 \pm 2$  ms during bilateral VNS. Figure 39 compares maps of repolarization from the same during sinus rhythm (CTRL), right VNS (VNSR), left VNS (VNSL) and bilateral VNS (VNSBL). Bilateral VNS reversed the repolarization sequence due to its different effects at the base and apex of the ventricles. APDs at the apex increased significantly during bilateral VNS compared to sinus rhythm, from  $159 \pm 4.2$  to  $195 \pm 14$  ms ( $n=6$ ;  $p < 0.02$ ) which may be attributed in large part to the decrease in heart rate from  $143 \pm 6.3$  to  $91 \pm 6.6$  beats/min (Table 9). At the base, however, bilateral VNS did not cause a statistically significant APD prolongation from  $176 \pm 4.0$  ms in sinus rhythm to  $178 \pm 13.8$  ms with bilateral VNS (Table 1). When compared to the anticipated APD prolongation observed by pacing at long cycle lengths, bilateral VNS failed to produce the APD prolongation expected from the slower heart rate when compared with earlier experimental data (Liu and Laurita 2005).

### *Sinus Rhythm vs. Acetylcholine infusion*

Perfusion with acetylcholine ( $1 \mu\text{M}$ ) to mimic parasympathetic nerve activity decreased heart rate to  $105 \pm 10$  beats/min with significant increase in (DOR  $32 \pm 3.0$  ms) but without any change in the direction of repolarization sequence (Table 8).

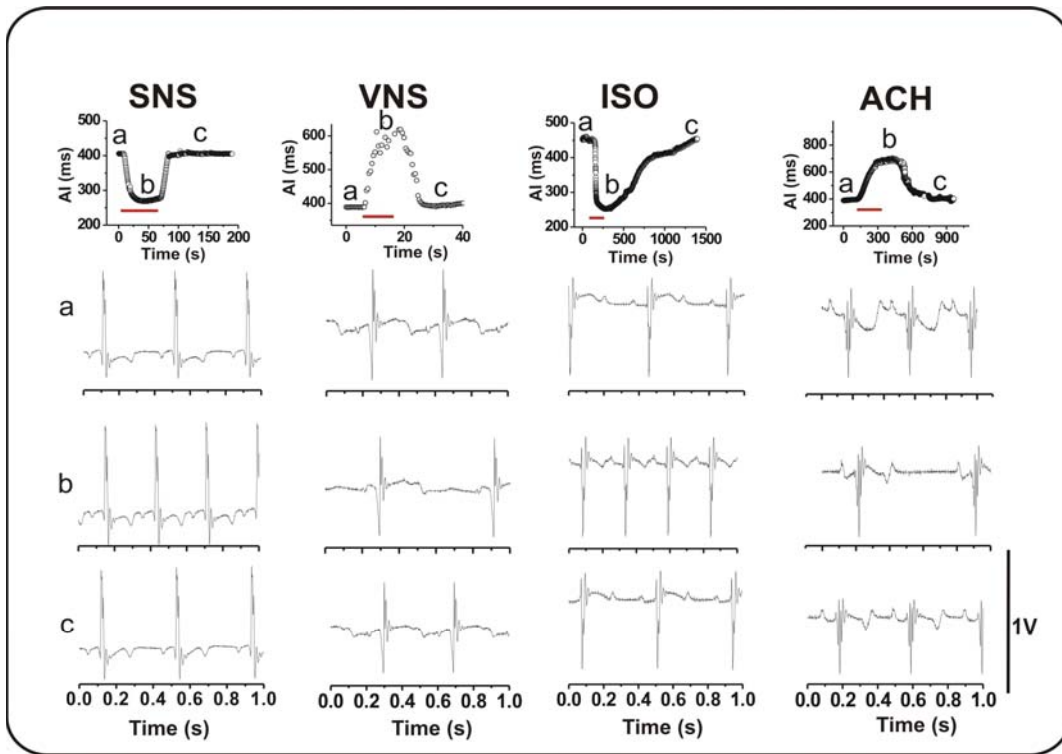


**Figure 38 : Summary of heart rate changes and electrograms during Autonomic Modulation**

The figure shows the changes in heart rate and the rhythm before (a), during (b) and after (c) autonomic stimulations. AI: Activation interval (milliseconds); SNS: Sympathetic nerve stimulation; VNS: bilateral vagus nerve stimulation; ISO: isoproterenol (100nM) infusion; ACH Acetylcholine (1  $\mu$ M). The red line indicates the duration of stimulation or agonist application. The top panels show Activation interval vs time course and the lower panel shows examples of electrograms during corresponding times.

**Table 9: Changes in APD and DOR during Autonomic stimulation**

	<b>HR (beats/min)</b>	<b>APD APEX (ms)</b>	<b>APD Base (ms)</b>	<b>DOR (ms)</b>
<b>Control n=14</b>	143±6	159±4	176±4	17±1
<b>SNS n=7</b>	229±13*	155±12	134±9*	-22±2*
<b>ISO n=5</b>	204±13*	115±4*	138±5*	23±2*
<b>VNS L n=6</b>	96±6*	165±14	182±12	17±2
<b>VNS R n=6</b>	95±5*	170±11	185±10	13±2
<b>VNS BL n=6</b>	91±7*	195±14*	178±14	-16±2.0*
<b>ACH n=6</b>	105±10*	178±19	204±18	32±3*

This table shows changes during autonomic stimulation of the heart SNS: sympathetic nerve stimulation, VNSL: Left vagus nerve stimulation; VNSR: Right vagus nerve stimulation; VNSBL: Bilateral vagus nerve stimulation; ACH Acetylcholine infusion (1µ mol); Isoproterenol (100nmol), APD: Action potential duration; DOR: Dispersion of repolarization (measured as the difference in APD (Base-Apex)). Also, see figure 39, which displays the repolarization maps during autonomic nerve stimulation (\*: p<0.05 vs. controls).

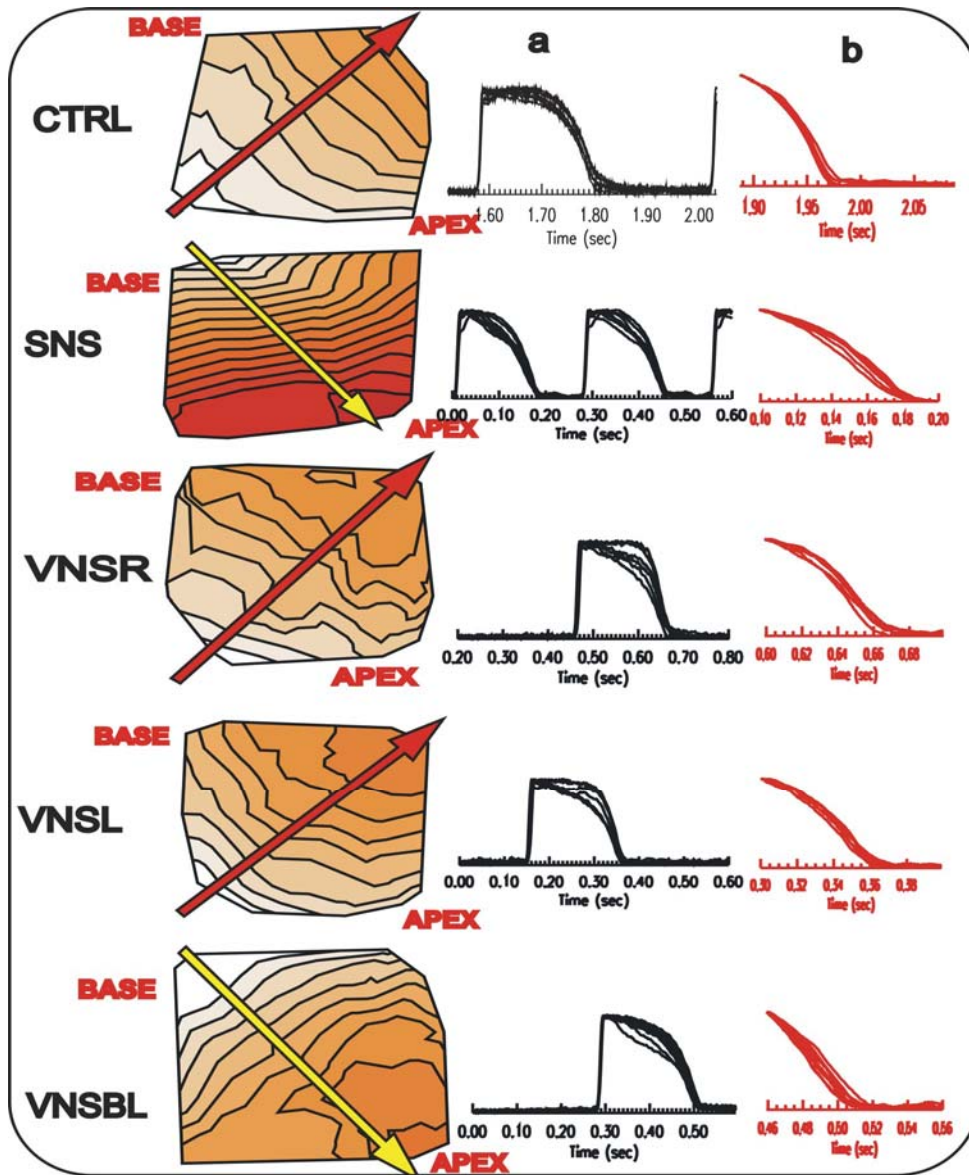


**Figure 39 : Summary of changes of DOR during Autonomic Nerve stimulation**

CTRL: control; SNS: Sympathetic nerve stimulation; VNSR: Right vagus stimulation; VNSL: left vagus stimulation; VNSBL: bilateral vagus nerve stimulation. Dispersion of repolarization is mapped with isochronal lines of 2 ms duration. The lightest shade indicates earliest and darkest indicates the latest. The direction of the arrow summarizes the overall direction of repolarization. Panel 'a' displays the superimposed plots of the APD maps across the surface. Panel 'b' displays the zoomed view of the terminal repolarization phase of the APD. Note these are dispersion of repolarization maps and not APD dispersion maps in that the APs are not aligned.

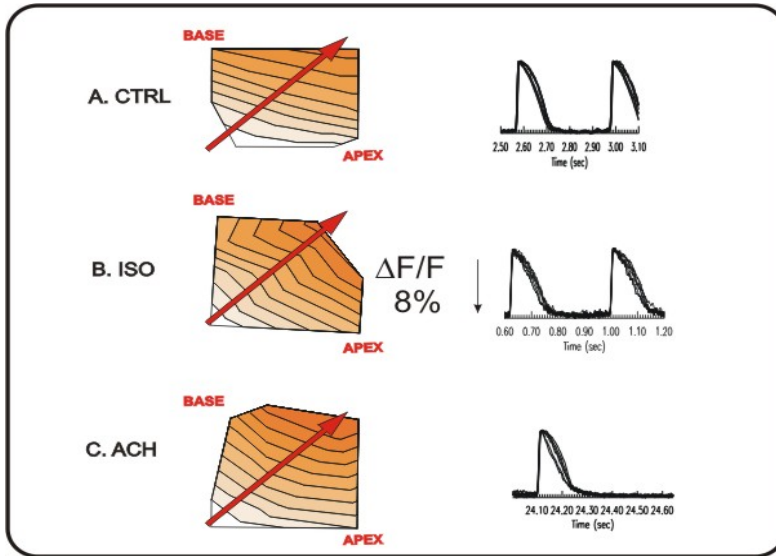


**Figure 40 : Pharmacological modulation of (apex-base) DOR**

CTRL: control; ISO: Isoproterenol; ACH: Acetylcholine infusion. DOR is mapped with isochronal lines (2 ms apart). Light to dark shades represent early to late repolarization time-points. Arrow points to the direction of repolarization. Note there is no change in the direction of the repolarization sequence caused by the adrenergic or muscarinic agonists.

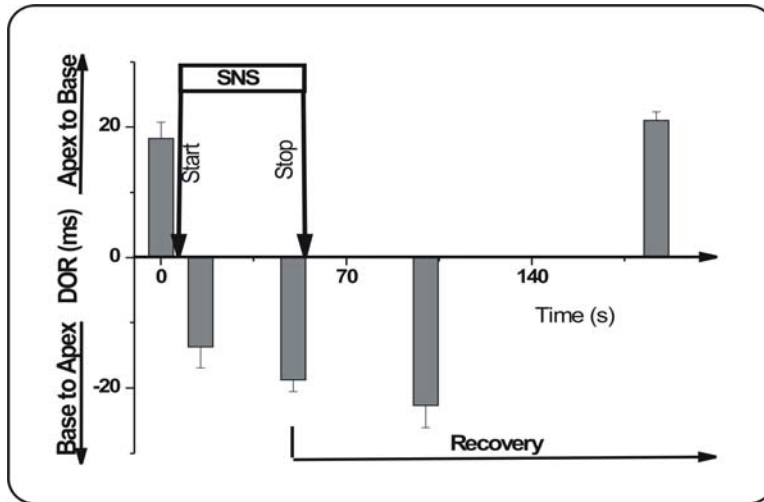


**Figure 41: Dynamic changes of DOR during SNS and recovery**

Time-course of changes in DOR before, during and after sympathetic nerve stimulation (n=4 hearts). DOR was inverted within 15 s after SNS and remained inverted in some experiments for as long as 30 min (not shown) whereas recovery had a longer latency of 130-140 s after the interruption of SNS.

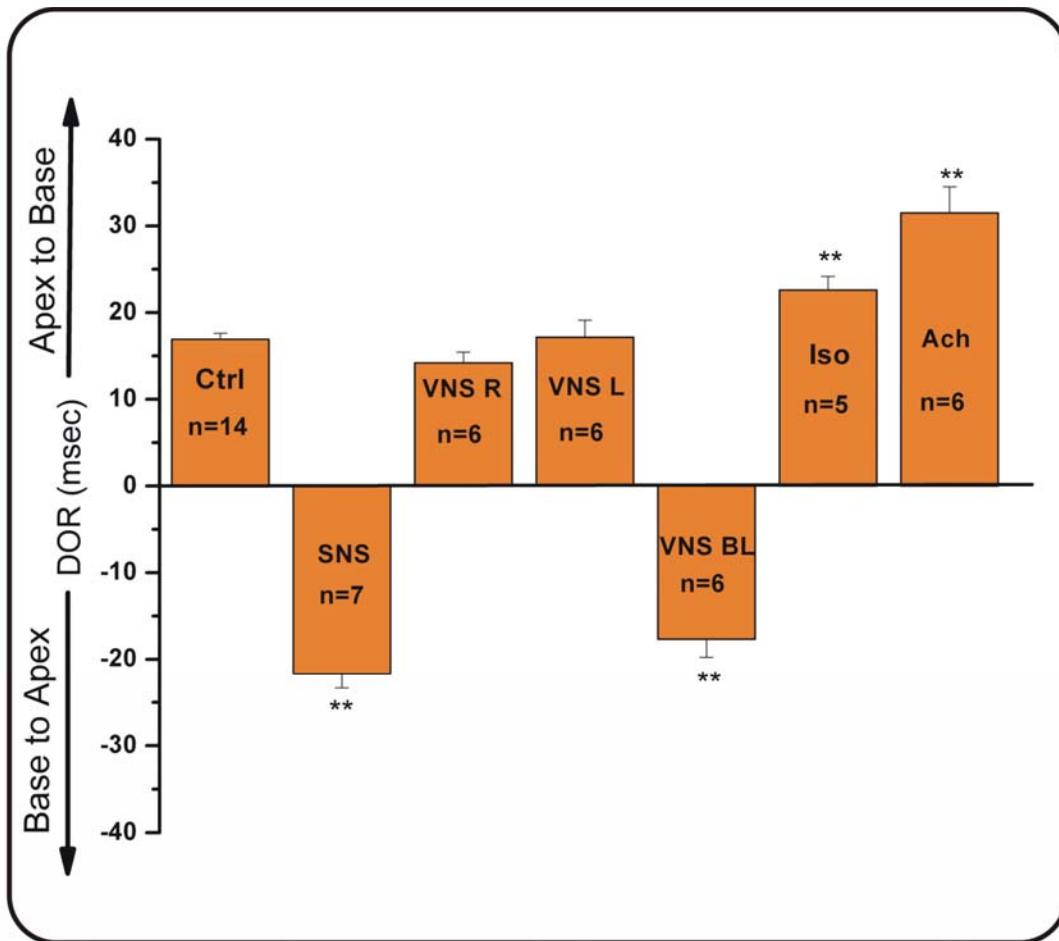


**Figure 42: Overall DOR changes during Autonomic interventions**

The overall DOR (dispersion of Repolarization) changes during autonomic interventions show that sympathetic nerve stimulation (SNS) and bilateral vagus nerve stimulation (VNS BL) reverse the direction of repolarization from control Apex to base direction to Base to Apex direction. Although, pharmacological drugs like Isoproterenol (Iso) a beta adrenergic agonist, and Acetylcholine (Ach) a muscarinic agonist produced significant changes; (\*\* P<0.05) in DOR compared to control, the overall direction of repolarization sequence did not change.

Figure 40 C illustrates a repolarization map and the superposition of APs (apex → base) that were recorded during perfusion with Ach (1  $\mu$ M). As shown in Figure 40 C, repolarization was from apex to base, similar to repolarization sequence recorded in the absence of autonomic nerve activity.

#### 5.4.2 Apex-base DOR under ion channel inhibition

When the hearts were treated with HMR1556 (0.5 $\mu$ M), APD increased more at the apex ( $P<0.05$ ); where control apex: base vs. HMR apex: base was 175 $\pm$ 12:188 $\pm$ 12 vs. 212 $\pm$ 8: 184 $\pm$ 8; the DOR increased significantly (control vs. HMR: 13 $\pm$ 2 vs. -27 $\pm$ 4;  $P<0.05$ ). When sympathetic nerves were stimulated after treating the hearts with HMR1556, the APD changes at peak response was thus: SNS apex: base vs. HMR SNS apex: base 178 $\pm$ 10:156 $\pm$ 13 vs. 198 $\pm$ 9:167 $\pm$ 8; DOR showed a tendency to increase but the differences were not significant. The individual vagus nerves did not change the APD or DOR significantly but bilateral vagus nerve stimulations had changed the DOR to -14 $\pm$ 2 (also see table 9). When vagus nerves were stimulated in the HMR treated hearts; the DOR remained significantly changed compared to controls. (See table 10). Application of HMR reversed the DOR sequence from apex-base to base-apex directions. In order to study the effects of inhibition of the major repolarizing current  $I_{Kr}$ , specific  $I_{Kr}$  inhibitor E4031, a methanesulfonamide, was used at 0.01 $\mu$ M as described elsewhere in the thesis. In controls, as before, the dispersion of repolarization increased from 11 $\pm$ 1 to -13 $\pm$ 1 and -14 $\pm$ 1 ms during SNS and BLVNS respectively, due to the dominant changes in APDs at the base and apex respectively. The APD prolongation was more dramatic by  $I_{Kr}$  inhibition. This could partly be due to the fact that  $I_{Kr}$  is a larger current in the rabbit heart. When the hearts were treated with E 4031, the APD prolonged from 171 $\pm$ 7 and 182 $\pm$ 7 at apex and base to 280 $\pm$ 20 and 260 $\pm$ 21 ms ( $P<0.05$ ). When these hearts were sympathetically stimulated APD shortened ( $P<0.05$ ) to 203 $\pm$ 11 at apex and 182  $\pm$ 12 at base but the DOR did not change significantly compared to the baseline  $I_{Kr}$  inhibited state. Vagus nerve stimulation increased the DOR compared to baseline controls but did not differ from the baseline  $I_{Kr}$  inhibited states. (See table 11 and figure 44).

**Table 10: Neuromodulation of APEX-Base DOR during HMR 1556 (0.5 $\mu$ M)**

Control AI=484 $\pm$ 13 ms			SNS AI=307 $\pm$ 22 ms			RVNS AI=671 $\pm$ 36 ms			LVNS AI=684 $\pm$ 69 ms			BLVNS AI=839 $\pm$ 90 ms		
APEX	BASE	DOR	APEX	BASE	DOR	APEX	BASE	DOR	APEX	BASE	DOR	APEX	BASE	DOR
175 $\pm$ 12	188 $\pm$ 12	13 $\pm$ 2	178 $\pm$ 10	156 $\pm$ 13	-22 $\pm$ 3*	189 $\pm$ 7	202 $\pm$ 6	12 $\pm$ 2	183 $\pm$ 7	197 $\pm$ 7	14 $\pm$ 1	201 $\pm$ 11	187 $\pm$ 9	-14 $\pm$ 2*
HMR 1556 AI=484 $\pm$ 32 ms			HMR SNS AI=392 $\pm$ 34 ms			HMR RVNS AI=683 $\pm$ 125 ms			HMR LVNS AI=752 $\pm$ 90 ms			HMR BLVNS AI=705 $\pm$ 155 ms		
APEX	BASE	DOR	APEX	BASE	DOR	APEX	BASE	DOR	APEX	BASE	DOR	APEX	BASE	DOR
212 $\pm$ 5	184 $\pm$ 8	-27 $\pm$ 4**	198 $\pm$ 9	167 $\pm$ 8	-31 $\pm$ 2**	228 $\pm$ 9	208 $\pm$ 9	-19 $\pm$ 8**	214 $\pm$ 18	197 $\pm$ 17	-17 $\pm$ 2**	194 $\pm$ 12	175 $\pm$ 10	-19 $\pm$ 4**

Table 9 summarizes the changes in the activation interval (AI), action potential duration (in ms at specific regions i.e. apex and base of the heart) and dispersion of repolarization (DOR) during SNS: Sympathetic nerve stimulation; RVNS: Right vagus stimulation; LVNS: left vagus stimulation; BLVNS: bilateral vagus nerve stimulation; HMR1556:  $I_{Ks}$  inhibition.; DOR changes highlighted by \* shows  $P < 0.05$  compared to controls without nerve stimulation; and \*\* shows  $P < 0.05$  compared with no HMR (N=4).

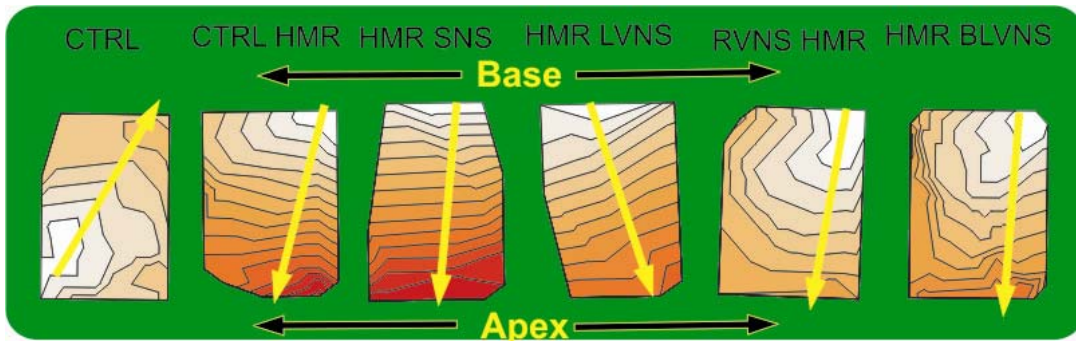


**Figure 43 : Neuromodulation of Apex-Base DOR under  $I_{Ks}$  inhibition**

The figure presents DOR maps taken from a heart at control, treatment with HMR1556 and nerve stimulation. Note the change in sequence of repolarization after the hearts were treated with HMR1556. The DOR increased considerably when the  $I_{Ks}$  were inhibited. There is also evidence to suggest that  $I_{Ks}$  inhibition decreases the repolarization reserve (Silva and Rudy 2005). See chapter 3. DOR is mapped with isochronal lines (2 ms apart). Light to dark shades represent early to late repolarization time-points. Arrow points to the direction of repolarization.

**Table 11: Neuromodulation of Apex-Base DOR during E 4031 (0.01 $\mu$ M)**

Control AI=396 $\pm$ 20 ms			SNS AI=289 $\pm$ 17ms			RVNS AI=623 $\pm$ 31 ms			LVNS AI=680 $\pm$ 60 ms			BLVNS AI=718 $\pm$ 72 ms		
APEX	BASE	DOR	APEX	BASE	DOR	APEX	BASE	DOR	APEX	BASE	DOR	APEX	BASE	DOR
171 $\pm$ 7	182 $\pm$ 7	11 $\pm$ 1	174 $\pm$ 5	161 $\pm$ 5	-13 $\pm$ 1*	196 $\pm$ 14	208 $\pm$ 15	13 $\pm$ 2	197 $\pm$ 14	208 $\pm$ 14	14 $\pm$ 2	213 $\pm$ 14	199 $\pm$ 14	-14 $\pm$ 1*
E 4031 AI=413 $\pm$ 19 ms			E SNS AI=261 $\pm$ 4 ms			E RVNS AI=623 $\pm$ 31 ms			E LVNS AI=771 $\pm$ 73 ms			E BLVNS AI=813 $\pm$ 88 ms		
APEX	BASE	DOR	APEX	BASE	DOR	APEX	BASE	DOR	APEX	BASE	DOR	APEX	BASE	DOR
280 $\pm$ 20	260 $\pm$ 21	-20 $\pm$ 4**	203 $\pm$ 11	182 $\pm$ 12	-21 $\pm$ 1**	281 $\pm$ 20	260 $\pm$ 18	-23 $\pm$ 2**	274 $\pm$ 14	251 $\pm$ 17	-24 $\pm$ 3**	293 $\pm$ 17	271 $\pm$ 17	-22 $\pm$ 4**

Table summarizes the changes in the activation interval (AI), Action potential duration in ms, from apex and base of the heart and dispersion of repolarization (DOR), during SNS: Sympathetic nerve stimulation; RVNS: Right vagus stimulation; LVNS: left vagus stimulation; BLVNS: bilateral vagus nerve stimulation; E4031:  $I_{Kr}$  inhibition; DOR changes highlighted by \*shows ( $P < 0.05$ ) compared with controls without nerve stimulation; and \*\* shows  $P < 0.05$  compared with no E4031 (N=4).

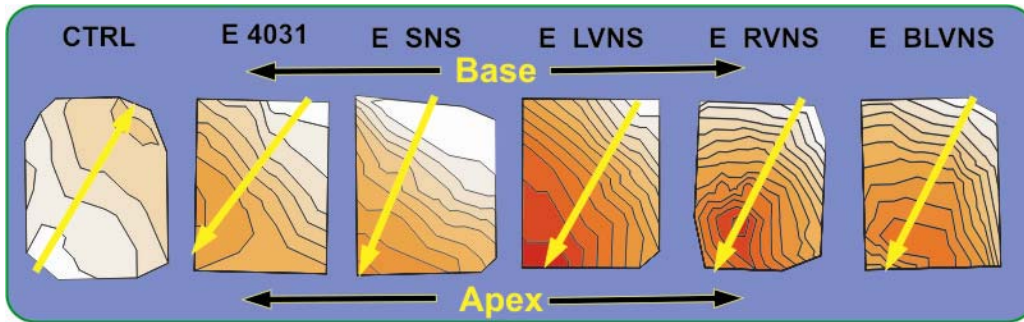


**Figure 44: Neuromodulation of DOR under E4031**

This figure shows the changes to dispersion of repolarization (DOR), when the heart was treated with  $I_{Kr}$  blocker E4031. DOR is mapped with isochronal lines (2 ms apart). Light to dark shades represent early to late repolarization time-points. Arrow points to the direction of repolarization.

A third key contributor to the repolarization was the timely inactivation of the sodium current. When this was delayed, APD and QT interval prolonged, and the hearts were more prone to arrhythmias especially at rest or during sleep (LQT3). (See earlier chapters for details) Anthopleurin A, a sea anemone toxin is a specific blocker of the inactivation of the sodium current. It is used widely to study the LQT3 physiology in the laboratory. In the present study, APA was infused at 10nM concentration and the Apex base DOR was studied during infusion (table12). APA prolonged the action potential duration at the apex more than at the base and the DOR increased and the sequence of repolarization reversed as seen with other inhibitors (see tables 9-11).

The baseline APDs were as follows- control baseline apex: base, DOR vs. APA baseline apex: base, DOR were  $179\pm 4$ : $193\pm 4$  ms,  $14\pm 2$  ms vs.  $232\pm 16$ :  $202\pm 15$  ms,  $-30\pm 2$  ms respectively. During SNS, the repolarization characteristics changed with APDs being shorter at both apex from  $179\pm 4$  to  $152\pm 4$  ms and base  $193\pm 4$  to  $136\pm 3$  ms ( $P<0.05$ ); but APDs were significantly shorter at the base than the apex and reversed the direction of sequence of repolarization ( $-16\pm 3$  ms). When the hearts were stimulated by SNS under APA, the APDs showed a tendency to shorten at the apex and the base (from  $232\pm 16$  to  $189\pm 7$  ms and from  $202\pm 15$  to  $162\pm 8$  ms, ( $P=NS$ )). The dispersion did not change significantly from baseline state under APA ( $-30\pm 2$  vs.  $-27\pm 1$  ( $P=NS$ )). When vagus nerves were stimulated, individual vagus nerves did not change the DOR significantly both in the APA and the control groups. Bilateral vagus nerve stimulation changed the DOR from  $14\pm 2$  to  $-16\pm 3$  ms in the control group but did not change the DOR under APA ( $-30\pm 2$  to  $-29\pm 7$  ms;  $P=NS$ ).

**Table 12: Neuromodulation of APEX-Base DOR during Anthopleurin A (10nM)**

Control AI=406±14ms			SNS AI=239±11 ms			RVNS AI=600±13 ms			LVNS AI=670±102 ms			BLVNS AI=685±72 ms		
APEX	BASE	DOR	APEX	BASE	DOR	APEX	BASE	DOR	APEX	BASE	DOR	APEX	BASE	DOR
179±4	193±4	14±2	152±4	136±3	-16±3*	184±1	196±2	12±2	184±12	199±14	15±2	189±4	177±2	-16±3*
APA AI=400±8ms			APA SNS AI=309±23ms			APA RVNS AI=512±118ms			APA LVNS AI=609±60ms			APA BLVNS AI=690±80ms		
APEX	BASE	DOR	APEX	BASE	DOR	APEX	BASE	DOR	APEX	BASE	DOR	APEX	BASE	DOR
232±16	202±15	-30±2**	189±7	162±8	-27±1**	265±39	239±40	-26±4**	302±37	279±36	-24±3**	333±46	304±41	-29±7**

Table summarizes the changes in the activation interval (AI), action potential duration in ms, from apex and base of the heart and dispersion of repolarization (DOR), during SNS: Sympathetic nerve stimulation; RVNS: Right vagus stimulation; LVNS: left vagus stimulation; BLVNS: bilateral vagus nerve stimulation; Anthopleurin A (APA):  $I_{Na}$  inactivation inhibitor without nerve stimulation DOR changes highlighted by \*shows ( $P<0.05$ ) compared with controls without nerve stimulation; and \*\* shows  $P<0.05$  compared with no APA ( $N=4$ ).

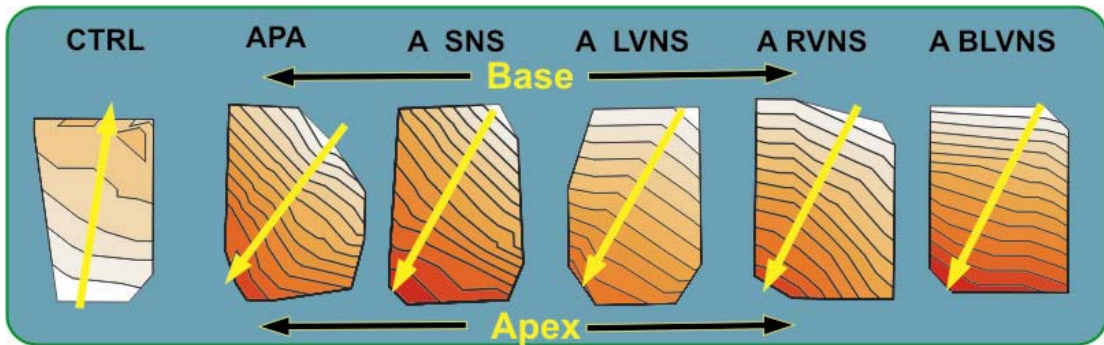


**Figure 45: Neuromodulation of DOR under APA**

This figure shows the changes to dispersion of repolarization (DOR) when a heart was treated with  $I_{Na}$  inactivation blocker Anthopleurin A. DOR is mapped with isochronal lines (2 ms apart). Light to dark shades represent early to late repolarization time-points. Arrow points to the direction of repolarization.

## 5.5 DISCUSSION

The main findings in these sets of experiments are that autonomic (bilateral either sympathetic or parasympathetic) nerve stimulation changes DOR across the epicardial surface of LV in a manner distinct from perfusion with a  $\beta$ -adrenergic or cholinergic agonist (see Figure 42). In particular, autonomic nerve stimulation was found to bring about a reversal of the direction of repolarization along the apex to base axis of the heart. The reversal of DOR had a rapid onset of  $< 15$  s after SNS and upon stopping SNS, DOR reversed back to sinus rhythm with a latency of  $\sim 2$  min. Perfusion with isoproterenol produced similar increases in heart rate as those obtained by SNS, yet there was no reversal of DOR. Similarly, bilateral VNS produced the expected decrease in heart rate and reversed the direction of repolarization whereas perfusion with Ach produced a similar decrease in heart rate but did not reverse DOR.

It is important to emphasize that the stimulation of the autonomic nerves described in this study followed previous protocols that were shown to be physiological with respect to a) changes in heart rate and b) left ventricular developed pressure.

Changes during SNS were entirely blocked by a selective  $\beta_1$  adrenergic antagonist, Metoprolol ( $1.8 \mu\text{M}$ ) and during VNS by a muscarinic antagonist, Atropine ( $0.1 \mu\text{M}$ ) (Ng, Brack et al. 2001) indicating that autonomic nerve stimulation modulated the heart by the standard neurotransmitters. In the current experiments, autonomic nerve stimulation produced changes in heart rate in the physiological range that were highly reproducible from heart-to-heart and were reversible upon interruption of nerve stimulation. In addition, we were able to obtain multiple repetitions (3-4) of SNS and VNS on the same heart without significant run down of the autonomic nerves based on the cardiac responses.

Multisite optical mapping is a powerful way to study the changes in DOR across the ventricular surface. There have been a number of studies, which used optical mapping to study the direction of impulse propagation and DOR. Here in this study we tried to study DOR without pacing but during the stimulation of autonomic nerves. The combinational approach of using the 'minimal' dosage of Cytochalasin D with physical immobilization has helped to get accurate images of action potentials not only during control situations but also during nerve stimulation. The signals to noise ratios were very good throughout the experiments.

### *Ventricular Repolarization*

Ventricular activation sequences have been extensively characterized in intact hearts by mapping the time delays of QRS spikes measured from closely spaced extracellular bipolar electrodes (Burgess, Baruffi et al. 1986). In contrast, the repolarization sequence or recovery to baseline has been poorly defined in large part due to technical difficulties and the sensitivity of that process to numerous variables. Changes in heart rate, temperature, depth of anesthesia, sympathetic tone and electrolyte balance all influence the action potential duration locally and thus, ventricular repolarization. Action potentials can be recorded from the epicardial surface with microelectrodes or suction electrodes but only from a limited number of sites, leaving surface electrograms as the most practical method to track activation and repolarization sequences (Burgess, Baruffi et al. 1986). However, unlike activation, there is no electrogram deflection that accurately identifies the onset or termination of repolarization. Nevertheless, local activation recovery intervals (ARI) measured with surface electrodes (i.e. activation time point (minimum  $dV/dt$  of the QRS complex) to the recovery (maximum  $dV/dt$  of the T-wave) time-point) were used as a surrogate for APDs measured with an intracellular electrode. In early studies on dog hearts, ventricular repolarization determined from ARI produced opposite findings; with repolarization sequence proceeding from base to apex (Pipberger, Schwartz et al. 1957) or apex to base (Haas 1960). Although there was a good correlation between ARI and refractory periods and APDs, most ARI were shorter than refractory periods (Millar, Kralios et al. 1985) and differed from APDs by as much as 24 ms (Haws and Lux 1990). Alternatively, repolarization sequences determined from the local refractory periods indicated that repolarization and APD gradients proceeds from base to apex APDs) *in situ* dog hearts (Burgess, Green et al. 1972; Autenrieth, Surawicz et al. 1975). A more recent study on canine and human hearts reported the opposite result that APDs are shorter in ventricular myocytes from the apex than the base due to higher densities of  $K^+$  currents involved in ventricular repolarization (Szentadrassy, Banyasz et al. 2005). The advent of voltage sensitive dyes and optical mapping techniques has provided new tools to characterize ventricular repolarization (Salama and Choi 2000). In isolated perfused hearts, ventricular repolarization was found to proceed from apex to base in a wide range of species: a) mouse, (Baker, London et al. 2000; London, Baker et al. 2007), b) rat, (Wan, Doumen et al. 1993) c) guinea pig, (Salama, Lombardi et al. 1987) d) rabbit, (Choi, Burton et al. 2002). In all these species, repolarization is driven by a different set of ion

channels yet their spatial distribution preserve short to long APDs in going from apex to base so as to guide the sequence of repolarization and relaxation.

#### *Anatomical Distribution of Autonomic Nerves to the Heart*

Sympathetic outflow to the heart emerges from the thoracic intermedio-lateral horns of the spinal cord. Pre-ganglionic neurons in the spinal cord project to the heart via axons to postganglionic neurons to innervate the heart via paravertebral ganglia and the various thoracic and cardiac ganglia (Armour 2004). Studies on dogs reported that different branches of the sympathetic nerves innervated distinct regions of the ventricles but there is a controversy regarding such specific anatomical nerve distribution. In our experiment, spinal canal stimulation at the level of T2 vertebrae allowed us to broadly activate bilaterally the sympathetic nerves thus, circumventing potential controversies, inaccuracies and animal-to-animal variability of cardiac nerve distribution. (Gillespie and Muir 1967; Opthof, Misier et al. 1991)

#### *Effects and Mechanism of Sympathetic Activity on DOR*

The humoral effect on ventricular electrophysiology was extensively studied whilst the effects of the autonomic nerve stimulation are less well studied. Sympathetic outflow to the heart is from the thoracic intermedio-lateral horns of the spinal cord, via the cardiac plexus and sympathetic efferent pre-ganglionic neurons in the spinal cord project axons to postganglionic neurons that innervate the heart via paravertebral ganglia and the various thoracic and cardiac ganglia (Vincent 1998; Armour 2004). Most of the studies thus far, concerning ventricular repolarization were done in dogs. Changes in APD during SNS were heterogeneous and striking. Initially, there were reports that different limbs of the sympathetic nerves innervate distinct parts of the ventricle but more recent studies did not clearly agree with such specific anatomical distribution in all hearts. In our experiments we used spinal canal stimulation at the level of T2 vertebrae where the both limbs of the sympathetic outflow were stimulated to study the broad effect of sympathetic nerve stimulation on the DOR ventricle, circumventing the inaccuracies and large inter-individual variability of distribution (Gillespie and Muir 1967; Opthof, Misier et al. 1991).

During SNS, DOR not only increased across the ventricle but its direction was inverted. Under control conditions, APDs were longer at the base than the apex whereas during SNS, APDs at the base were significantly shorter than at the apex. Changes of DOR upon SNS occurred rapidly in 5-15 s and DOR reversed back to control orientation but with a slower time-

course of 130 to 140 s. These findings are consistent with current concepts in the literature. The autonomic nerves and of delayed rectifying K<sup>+</sup> channels involved in the repolarization of the heart are heterogeneously distributed along the apex to base axis of the heart.

In human hearts, autonomic nerves (both sympathetic and parasympathetic) are considerably more abundant at the base than the apex of left ventricles. (Kawano, Okada et al. 2003) The delayed rectifying K<sup>+</sup> currents are non-uniform on the surface of the heart, with the slow component, I<sub>Ks</sub> being more abundant at the base and the fast component I<sub>Kr</sub> being more abundant at the apex of the rabbit left ventricle (Cheng, Kamiya et al. 1999; Choi, Burton et al. 2002).

Moreover, I<sub>Ks</sub> tends to be a small amplitude current, difficult to measure until activated by a β-adrenergic agonist such as isoproterenol which decreases the refractory period by a protein kinase A-dependent phosphorylation of I<sub>Ks</sub>. but has no effect on I<sub>Kr</sub> (Sanguinetti, Jurkiewicz et al. 1991; Volders, Stengl et al. 2003). However, there is emerging evidence, that I<sub>Kr</sub> is also regulated by beta adrenergic stimulation (Thomas, Zhang et al. 1999; Kagan, Melman et al. 2002; Choe, Schulze-Bahr et al. 2006). I<sub>Kr</sub> unlike I<sub>Ks</sub> is prominent even when there is no sympathetic activity and may play an important role in repolarization during normal states. Thus may contribute to the direction of repolarization sequence from apex to base.

In contrast, during SNS, activation of I<sub>Ks</sub> is more abundant at the base resulting in greater APD shortening at the base than at the apex and a reversal of the repolarization sequence. The preferential shortening of APDs at the base under sympathetic influence occurred in ~ 15 s (i.e. time to phosphorylate I<sub>Ks</sub>) and was reversible upon interruption of SNS with a latency of 180s consistent with the time-course of I<sub>Ks</sub> dephosphorylation (Sanguinetti, Jurkiewicz et al. 1991).

Interestingly, perfusion of the heart with isoproterenol had a tendency to enhance DOR (Table 9) by shortening APDs slightly more at the apex than the base but the direction of repolarization was not reversed. These data highlight the complexity of the system because SNS releases norepinephrine, a β- and α-adrenergic agonist that stimulates nearly all ionic currents and their kinetics, (see figure 37). In addition, SNS may activate afferent as well efferent nerves and release other neurotransmitters such as neuropeptide Y, ATP and substance P.

Nevertheless, the results from isoproterenol perfusion allows us to reasonably infer that in normal hearts, regional (apex-base) heterogeneities of sympathetic innervation (efferent and/or afferent nerves) is the dominant factor responsible for the reversal of DOR during SNS rather

than  $I_{Kr}$ ,  $I_{Ks}$  or  $\beta 1$  adrenergic receptor distribution across the ventricle (Conrath and Opthof 2006).

#### *Effects and Mechanism of Parasympathetic Activity on DOR*

Right or left VNS did not change the DOR significantly but bilateral VNS reversed the direction of DOR (see tables 8-11), this time by prolonging APD more at the apex than the base. All 3 methods of VNS decreased heart rate to the similar extent so that differences in APD caused by the 3 conditions cannot be attributed to heart rate alone but to enhanced recruitment of parasympathetic and acetylcholine release during bilateral VNS. Acetylcholine released by vagus nerves may shorten ventricular APDs by increasing the  $K^+$  conductance via the muscarinic receptors in the ventricle (Koumi, Sato et al. 1997). Immuno-histochemistry (Kawano, Okada et al. 2003) of parasympathetic nerve distribution to the ventricle suggests a greater density of nerves at the base than the apex which may explain the lack of APD prolongation at the base despite the slow heart rate during bilateral VNS. Thus, as for SNS, the effects of VNS on DOR are most likely due to heterogeneities in nerve distribution resulting in the modulation of the repolarization sequence.

Individual vagal nerve (right, left) stimulation did not change the DOR significantly but the bilateral vagal nerve stimulation significantly changed the DOR. This may be possibly explained by the effect of stimulus summation seen in some studies (Armour 2004). It has been known for many years that the vagal nerves may be controlling the ventricular action potential via muscarinic receptors on the ventricle. Immuno-histochemistry data of the vagal distribution on the ventricle supports the view that heterogeneity in distribution contributes to heterogeneity of modulation of repolarization (Kawano, Okada et al. 2003). When the heart rate reduced during bilateral vagal stimulation there was an increase in the action potential duration at the apex but there was no such response seen at the base. APD prolongation with reduction in heart rate could simply be a response to change in cycle length. But, when one compares with earlier data, the APD prolongation with similar changes in heart rate at the base was at least 50% less when bilateral vagus nerves were stimulated. This may indicate that this lack of anticipated APD prolongation at the base region may indeed be due to vagus induced APD ‘shortening’ at the base. Also, neuromodulation of the repolarization seems to be dynamic i.e. the changes occurring only during stimulation. DOR returns to control position as heart rate returns to baseline.

Thus neuronal modulation of ventricular repolarization is unique and distinct from pharmacological modulation. In order to understand the role of neuromodulation under altered myocardial substrates, we conducted early observational studies, by reducing the repolarizing currents for a start. The findings are discussed below.

#### *Effects of inhibition of key repolarizing currents on DOR*

Apex base DOR analysis using  $I_{Ks}$ ,  $I_{Kr}$  and  $I_{Na}$  inactivation inhibitors (i.e. LQT physiology) showed several similarities. When the hearts were treated with pharmacological agents known to inhibit key repolarizing currents and contributors to repolarization (i.e.  $I_{Na}$  inactivation), the ABDOR increased significantly. This has been shown in separate experiments by several other groups that dispersion of repolarization increases with ion channel inhibition (discussed previously in this chapter). The exact mechanism underlying this observation is not yet understood. The changes of DOR observed in this study can be explained by a ‘multifactorial summative effect’ rather than a ‘single-channel-single-pathway mediated response’ of individual ion channel inhibition. Several lines of evidence from current literature are discussed below.

Links between pharmacological inhibition of one channel and down regulation of another other was shown in the late nineties (Vos, Verduyn et al. 1995; Vos, de Groot et al. 1998). However, the characteristics of the interactions between different ion channels are not clearly established yet. Several early observations have been made in this regard. The induction of EADs in LQT seems to require an initiation or a conditioning phase formed by the net membrane currents during the plateau phase. In experiments involving specific ion channel inhibition, heterogeneity of distribution of other (uninhibited) ion channels seemed to play a role in DOR and genesis of torsade de pointes. Different layers of the myocardium contributed to the dispersion of repolarization and torsadogenesis differently, based on their ion channel composition and cell to cell coupling (Viswanathan and Rudy 1999; Emori and Antzelevitch 2001; Yan, Wu et al. 2001; Burashnikov and Antzelevitch 2002).

Ion currents control repolarization via their individual kinetic properties. Biological redundancy in their kinetics allow a functional overlap among these channels. This enables the heart to have a reserve during ‘exigencies’. A loss of function defect in one of the channels is partially rectified by the ‘cross-cover’ provided by other channels thus minimizing the vulnerability of the myocardium to arrhythmogenic triggers (Roden 1998). This has also been shown experimentally in single cell/modeling studies (Silva and Rudy 2005).

As mentioned in earlier chapters, calcium plays an important, if not dominant role in LQT physiology.  $I_{Ca2+}$  increases during prolongation of action potential (i.e. during repolarizing current inhibition) following secondary activation and recovery from inactivation (January and Riddle 1989; Luo and Rudy 1994). Recently, heterogeneity of calcium channels in the heart has come into the lime light. Epicardial cells had a greater calcium current magnitude, were capable of second activation (unlike endocardial cells) and the  $I_{Ca2+}$  was strongly coupled to the changes in kinetics of  $I_{to}$  during the plateau phase (Banyasz, Fulop et al. 2003; Cordeiro, Greene et al. 2004). Another important player, NCX or the sodium calcium exchanger has been shown to be heterogeneously distributed in the wall of the ventricle; and has been shown to contribute to APD prolongation and predispose the ventricle to arrhythmias (Zygmunt, Goodrow et al. 2000). Very recent data from Donald Bers group have shown calcium-calmodulin protein kinase II (CaMKII) to have a bimodal effect (loss of function effects: CaMKII shifts  $Na(+)$  current availability to more negative voltage, enhances intermediate inactivation, and slows recovery from inactivation; and gain of function effects: enhances late noninactivating of  $I_{Na}$ ) on sodium channel kinetics and action potential duration. In their in silico model, it was shown that CaMKII also increases  $I_{CaL}$  and calcium dependent potassium currents. Further, individual current increases of  $I_{CaL}$  and  $I_{Na}$ , increased the duration of action potentials (Grandi, Puglisi et al. 2007). Emerging data from Salama's group show that  $I_{CaL}$  current densities are significantly higher at the base of the ventricle in adult female and pre-pubertal male ventricles. Incorporation of these differences into a silicon models produced regional alterations of APDs and lead to the production of EADs (Sims 2007). Recent evidence from Yoram Rudy's group confirms that oscillation of the calcium subsystem, which includes: SR calcium load; SR calcium fluxes; SR calcium release via Ryanodine receptors; CaMKII activity; calcium transient induced NCX activation, has a dominant modulatory effect on APDs (Livshitz and Rudy 2007).

Autonomic nerve stimulation did not significantly change the DOR over and above the ion channel inhibitors in any of the groups and may suggest that myocardial substrate alterations overshadow neuromodulation in LQT physiology.

Therefore, from the above discussion, it may be apparent that there is a complex multifactorial regulation of the APD across the myocardium.

The exact mechanism of DOR regulation is not yet understood and may be an exciting future research project. A comprehensive realistic model (experimental or insilico) with detailed

characterization of all the neurocardiological factors is necessary gain deeper insights into the complex phenomenon of repolarization.

### **5.5.1.1 Conclusions**

Neuronal modulation of ventricular repolarization is unique and distinct from pharmacological modulation.

Neuromodulation underscores neurocardiological heterogeneity involved in the regulation of physiological repolarization.

These findings reveal that under physiological conditions autonomic activity has a marked impact on cardiac repolarization and broaden our views on why and how ‘autonomic imbalance’ may be an important factor contributing to arrhythmia vulnerability during physical or emotional stress.

Reduction of net repolarizing currents produced an increase in DOR and reversal of the sequence of repolarization. This did not appear to be specific to inhibition of an individual repolarizing current but rather seemed to be a generic effect.

Substrate modulation by ion channel inhibition seems to be a dominant component of the two neurocardiological components.

Broader characterization studies are required to fully understand the role of each individual player in the overall control of APD adaptation and neuromodulation of ventricular repolarization.

### 5.5.1.2 Limitations

The limitation of the techniques used in this work has been discussed in detail in the previous chapter but may warrant repetition.

Optical mapping used in the present study allows electrophysiological data to be obtained from the surface of the heart. The DOR characteristics from within the walls of the ventricle are not available in these studies.

Motion artifacts were resolved using excitation contraction uncouplers and physical restraints. However, this method could not prevent all motion artifacts.

However, the use of a combinational approach has limited the motion artifacts to the minimum.

The limitation of pharmacological blockers is well known. They do not cause the exact molecular defects in the ion channels as seen in disease mutation. The pharmacological agents may have collateral inhibitions of other ion channels.

Doses of ion channel inhibitors were chosen such that manifestation of the inhibition was obvious. Higher doses were avoided as they produced significant unwanted side effects especially on heart rate and APD adaptation. Also, it may be impossible to estimate the optimal level of inhibition given the limitations of the pharmaco-kinetics and pharmaco-dynamics of the specific ion channel inhibitors with the channel.

No arrhythmias were seen in these studies. Several reasons could account for this. Most importantly, the resting CL were higher in this preparation than seen in other LQT experiments where the Langendroff perfused hearts were treated with higher doses of inhibitors, the AV nodes were destroyed and the hearts were paced with desired CL (not necessarily physiological) such that arrhythmias were produced at very low or very high CLs. In the present study the CL were obtained only by neuronal manipulation. A way to circumvent this problem would be to use transgenic rabbits (which are recently made available) and/or use realistic three dimensional whole heart models to study arrhythmias.

The data obtained from this novel preparation is preliminary observational data and not as mechanistic, the data available for mechanistic insights are limited.

No corroborative in-silico modeling studies were done to verify the roles of individual ion channels and calcium cycling proteins in the modulation of DOR.

### **5.5.1.3 Future directions**

The exact mechanism of DOR regulation will be a fascinating future endeavour. This may involve the following steps.

Firstly, ion channel distribution heterogeneity has to be characterized experimentally, in a species, in both apex base and transmural axes.

Secondly, the ion currents, calcium cycling kinetics and action potentials has to be studied from these specific regions and their heterogeneity has to be characterized. Further, neuronal hierarchy and heterogeneity of nerve distribution has to be clarified.

Finally, all the above data (including heterogeneity) has to be incorporated into an in-silico, three-dimensional, neurocardiological model. This may set the paradigm for a deeper and more realistic understanding of the APD adaptation and arrhythmogenesis at an organ level.

## 6.0 SUMMARY AND FUTURE DIRECTIONS

### **Summary:**

This work describes an attempt to answer a need for a novel neurocardiological model that enables one to study the autonomic neuronal effects on cardiac electrophysiology. The model, which is a combination of isolated innervated heart preparation and optical mapping, offers an opportunity to study complex electrical changes during the time of nerve stimulation in great detail. The dual cannulation technique allows the study of differential effects of factors on the heart and nerves independently.

The different sets of experiments have been done using this model to begin the initial exploration into the complexity of neuromodulation of ventricular repolarization. In this study, two main repolarization properties, which have been shown in other studies to be involved in arrhythmia mechanisms i.e. dispersion of repolarization and restitution kinetics, were studied.

During analysis of restitution kinetics in normal hearts, novel physiological findings like the negative slope during peak heart rates were seen. The characteristics of these loops also showed apex base heterogeneity. Preliminary protein expression studies suggest that at least two neurocardiological factors contribute to this heterogeneity. Further, restitution data during ion channel inhibition seemed to suggest that changes in physiological restitution loops may represent a loss of repolarization reserve - a feature shown for the first time which points to final common pathways in arrhythmia mechanisms in three different LQT models.

Dispersion of repolarization studies have shown that neuromodulation of ventricular repolarization is distinct from pharmacological autonomic modulation. Further, early data from ion channel inhibition studies using this model; also suggest that neuromodulation of dispersion of repolarization may be a less dominant factor when ion channels are inhibited.

### **Future directions:**

Although this work has attempted to improve on the scope of this model, several issues have to be addressed in future.

The complete neurophysiology of the cardiovascular system in rabbit is still not fully understood. The elucidation of the role of individual ganglia in neuromodulation will be an exciting future endeavour. Neuronal firing data from transgenic rabbits will throw more light into quantitative aspects of neuromodulation, especially in LQTS models. Also, this model opens the door to study illnesses like diabetes which have a neuropathic component involving autonomic nerves and sudden cardiac death.

It is possible to verify the feasibility studying physiological restitution in humans, non-invasively by measuring the QT vs. TQ intervals on an exercise stress test. Pilot studies are underway.

Further research to mechanistically understand the physiological restitution curves may be inspired by observations made during pilot and failed experiments. Extreme disturbances of physiological milieu derailed the restitution kinetics altogether. The four-phase restitution characteristics and typical APD adaptations were lost in pilot experiments when the hearts were tested with higher doses of ion channel inhibitors, high doses of uncouplers especially BDM and use of CaM kinase II inhibitors. Also, the loops were not formed when the experimental temperatures were too low, with cardiac hypoxia, bradycardia due to vagal compression, etc. It was beyond the scope of the present work to study these factors in detail. It may be an exciting future endeavour as further controlled experimentation will be required to reproduce these observations, to tease out the effects of various factors and to pinpoint the underlying reasons.

The exact mechanisms of DOR and Restitution regulation will be a fascinating future endeavour. This may involve the following steps.

Firstly, ion channel distribution heterogeneity has to be characterized experimentally, in a species, in both apex-base and transmural axes, as out lined above.

Secondly, the ion currents, calcium cycling kinetics and action potentials have to be studied from these specific regions and their heterogeneity characterized. Further, neuronal hierarchy and heterogeneity of nerve distribution has to be clarified.

All the above data (including heterogeneity) should be incorporated into an in-silico, three-dimensional, neurocardiological model. One of the ways to achieve this would be to adopt a ‘three-dimensional, brick-by-brick reconstruction’ approach to characterizing the ion channel distribution, kinetics and neuronal heterogeneity of the heart; and then build an in-silico model based on the species specific kinetics data from the cellular studies. This may help in developing a realistic model which may in turn help in understanding complex arrhythmia mechanisms. This may set the paradigm for a deeper and more realistic understanding of the APD adaptation and arrhythmogenesis at an organ level.

To conclude, the exciting novel data obtained in this study is preliminary and observational. Further experimental testing using this model and in-silico validation is required, especially, to understand the individual factors controlling the phenomenon of physiological restitution and dispersion of repolarization.

## BIBLIOGRAPHY

- Abbott GW, S. F., Splawski I, Buck ME, Lehmann MH, Timothy KW, Keating MT, Goldstein SA. (1999). "MiRP1 forms IKr potassium channels with HERG and is associated with cardiac arrhythmia." Cell **97**(2): 175-87.
- Allingham, J. S., R. Smith, et al. (2005). "The structural basis of blebbistatin inhibition and specificity for myosin II." Nat Struct Mol Biol **12**(4): 378-9.
- An RH, W. X., Kerem B, Benhorin J, Medina A, Goldmit M, Kass RS (1998). "Novel LQT-3 mutation affects Na<sup>+</sup> channel activity through interactions between alpha- and beta1-subunits." Circ Res **83**(2): 141-146.
- Antzelevitch, C. (2007). "Heterogeneity and cardiac arrhythmias: an overview." Heart Rhythm **4**(7): 964-72.
- Ardell JL1. Ardell JL. Neuronal regulation of cardiac function In: Armour JA, A. J., eds. Neurocardiology. Oxford university press 2004 pp 118-152 (2004). Intrathoracic Neuronal Regulation of Cardiac Function. Oxford, Oxford university press.
- Armour J.A., M. D. A., Yuan B.X, Macdonald S, Hopkins D.A. (1997). "Gross and microscopic anatomy of the human intrinsic nervous system." Anat Rec(247): 289-298.
- Armour, J. A. (2004). "Cardiac neuronal hierarchy in health and disease." Am J Physiol Regul Integr Comp Physiol **287**(2): R262-71.
- Arora RC, W. M., Hopkins DA, and Armour JA (2003). "Porcine intrinsic cardiac ganglia." Anat Rec(271): 249-258.
- Ashcroft, F. M. (2000). Ion channels and disease. New York, Academic Press.
- Autenrieth, G., B. Surawicz, et al. (1975). "Sequence of repolarization on the ventricular surface in the dog." Am Heart J **89**(4): 463-9.
- Baker, L. C., B. London, et al. (2000). "Enhanced dispersion of repolarization and refractoriness in transgenic mouse hearts promotes reentrant ventricular tachycardia." Circ Res **86**(4): 396-407.
- Baker, L. C., R. Wolk, et al. (2004). "Effects of mechanical uncouplers, diacetyl monoxime, and cytochalasin-D on the electrophysiology of perfused mouse hearts." Am J Physiol Heart Circ Physiol **287**(4): H1771-9.
- Balligand, J. L. (1999). "Regulation of cardiac beta-adrenergic response by nitric oxide." Cardiovasc Res **43**(3): 607-20.
- Balligand JL, U.-L. D., Simmons WW, Kobzik L, Lowenstein CJ, Lamas S, Kelly RA, Smith TW, Michel T. (1995). "Induction of NO synthase in rat cardiac microvascular endothelial cells by IL-1 beta and IFN-gamma." Am J Physiol **268**((3 Pt 2)): H1293-303.
- Banville, I. and R. A. Gray (2002). "Effect of action potential duration and conduction velocity restitution and their spatial dispersion on alternans and the stability of arrhythmias." J Cardiovasc Electrophysiol **13**(11): 1141-9.

- Banyasz, T., L. Fulop, et al. (2003). "Endocardial versus epicardial differences in L-type calcium current in canine ventricular myocytes studied by action potential voltage clamp." Cardiovasc Res **58**(1): 66-75.
- Bartel, S., P. Karczewski, et al. (1993). "Protein phosphorylation and cardiac function: cholinergic-adrenergic interaction." Cardiovasc Res **27**(11): 1948-53.
- Bass, B. G. (1975). "Restitution of the action potential in cat papillary muscle." Am J Physiol **228**(6): 1717-24.
- Belardinelli, L. and G. Isenberg (1983). "Isolated atrial myocytes: adenosine and acetylcholine increase potassium conductance." Am J Physiol **244**(5): H734-7.
- Benzinger, G. R., C. L. Drum, et al. (1997). "Differences in the binding sites of two site-3 sodium channel toxins." Pflugers Arch **434**(6): 742-9.
- Berger, R. D. (2004). "Electrical restitution hysteresis: good memory or delayed response?" Circ Res **94**(5): 567-9.
- Biermann, M., M. Rubart, et al. (1998). "Differential effects of cytochalasin D and 2,3 butanedione monoxime on isometric twitch force and transmembrane action potential in isolated ventricular muscle: implications for optical measurements of cardiac repolarization." J Cardiovasc Electrophysiol **9**(12): 1348-57.
- Blanchard, E. M., G. L. Smith, et al. (1990). "The effects of 2,3-butanedione monoxime on initial heat, tension, and aequorin light output of ferret papillary muscles." Pflugers Arch **416**(1-2): 219-21.
- Boyett, M. R. and B. R. Jewell (1980). "Analysis of the effects of changes in rate and rhythm upon electrical activity in the heart." Prog Biophys Mol Biol **36**(1): 1-52.
- Brink, P. A., L. Crotti, et al. (2005). "Phenotypic variability and unusual clinical severity of congenital long-QT syndrome in a founder population." Circulation **112**(17): 2602-10.
- Burashnikov, A. and C. Antzelevitch (2002). "Prominent I(Ks) in epicardium and endocardium contributes to development of transmural dispersion of repolarization but protects against development of early afterdepolarizations." J Cardiovasc Electrophysiol **13**(2): 172-7.
- Burdon-Sanderson, J. (1880). "On the Time-Relations of the Excitatory Process in the Ventricle of the Heart of the Frog." J Physiol **2**(5-6): 384-435.
- Burgess, M. J., S. Baruffi, et al. (1986). "Determination of activation and recovery sequences and local repolarization durations from distant electrocardiographic leads." Jpn Heart J **27 Suppl 1**: 205-16.
- Burgess, M. J., L. S. Green, et al. (1972). "The sequence of normal ventricular recovery." Am Heart J **84**(5): 660-9.
- Cao, J. M., Z. Qu, et al. (1999). "Spatiotemporal heterogeneity in the induction of ventricular fibrillation by rapid pacing: importance of cardiac restitution properties." Circ Res **84**(11): 1318-31.
- cardiology, E. s. o. "FONDAZIONE SALVATORE MAUGERI." Istituto di Ricovero e Cura a Carattere Scientifico(<http://pc4.fsm.it:81/cardmoc/index.html>).
- Carmeliet, E. (2004). "Intracellular Ca(2+) concentration and rate adaptation of the cardiac action potential." Cell Calcium **35**(6): 557-73.
- Cheng, J., K. Kamiya, et al. (1999). "Heterogeneous distribution of the two components of delayed rectifier K+ current: a potential mechanism of the proarrhythmic effects of methanesulfonanilideclass III agents." Cardiovasc Res **43**(1): 135-47.
- Chiang, C. E. (2004). "Congenital and acquired long QT syndrome. Current concepts and management." Cardiol Rev **12**(4): 222-34.

- Choe, C. U., E. Schulze-Bahr, et al. (2006). "C-terminal HERG (LQT2) mutations disrupt IKr channel regulation through 14-3-3epsilon." Hum Mol Genet **15**(19): 2888-902.
- choi, B.-R. (2001). Mechanisms underlying LongQT related arrhythmias. Gaduate school of Medicine University of Pittsburgh. Pittsburgh, University of Pittsburgh. **PhD**.
- Choi, B. R., F. Burton, et al. (2002). "Cytosolic Ca<sup>2+</sup> triggers early afterdepolarizations and Torsade de Pointes in rabbit hearts with type 2 long QT syndrome." J Physiol **543**(Pt 2): 615-31.
- Choi, B. R., T. Liu, et al. (2004). "Adaptation of cardiac action potential durations to stimulation history with random diastolic intervals." J Cardiovasc Electrophysiol **15**(10): 1188-97.
- Conrath, C. E. and T. Opthof (2006). "Ventricular repolarization: an overview of (patho)physiology, sympathetic effects and genetic aspects." Prog Biophys Mol Biol **92**(3): 269-307.
- Cooper, J. A. (1987). "Effects of cytochalasin and phalloidin on actin." J Cell Biol **105**(4): 1473-8.
- Cordeiro, J. M., L. Greene, et al. (2004). "Transmural heterogeneity of calcium activity and mechanical function in the canine left ventricle." Am J Physiol Heart Circ Physiol **286**(4): H1471-9.
- Curran, M. E., I. Splawski, et al. (1995). "A molecular basis for cardiac arrhythmia: HERG mutations cause long QT syndrome." Cell **80**(5): 795-803.
- De Ferrari, G. M., M. C. Viola, et al. (1995). "Distinct patterns of calcium transients during early and delayed afterdepolarizations induced by isoproterenol in ventricular myocytes." Circulation **91**(10): 2510-5.
- Del Nido, P. J., P. Glynn, et al. (1998). "Fluorescence measurement of calcium transients in perfused rabbit heart using rhod 2." Am J Physiol **274**(2 Pt 2): H728-41.
- Dessertenne, F. (1961). "La tachycardie ventriculaire à deux foyers opposés variables." Arch Mal Coeur(59): 263-272.
- Dessertenne, F., Fabiato, A., and Coumel, P (1966). "Un chapitre nouveau d'électrocardiographie: les variations progressives de l'amplitude de l'électrocardiogramme." Actual Cariol Angeiol Int **15**: 241-258.
- Dillon, S. and M. Morad (1981). "A new laser scanning system for measuring action potential propagation in the heart." Science **214**(4519): 453-6.
- Diness, T. G., R. S. Hansen, et al. (2006). "Frequency-dependent modulation of KCNQ1 and HERG1 potassium channels." Biochem Biophys Res Commun **343**(4): 1224-33.
- Dittrich, M., J. Jurevicius, et al. (2001). "Local response of L-type Ca(2+) current to nitric oxide in frog ventricular myocytes." J Physiol **534**(Pt 1): 109-21.
- Dubin, D. (2003). Ion adventure in the Heartland. Tampa, Florida, Cover Publishing company.
- Edes, I., Kranias, E.G (1997). Ca<sup>2+</sup>ATPases/pumps. San Diego, CA, Academic press.
- Efimov, I. R., D. T. Huang, et al. (1994). "Optical mapping of repolarization and refractoriness from intact hearts." Circulation **90**(3): 1469-80.
- Efimov, I. R., V. P. Nikolski, et al. (2004). "Optical imaging of the heart." Circ Res **95**(1): 21-33.
- El-Sherif, N. and G. Turitto (2003). "Torsade de pointes." Curr Opin Cardiol **18**(1): 6-13.
- Emori, T. and C. Antzelevitch (2001). "Cellular basis for complex T waves and arrhythmic activity following combined I(Kr) and I(Ks) block." J Cardiovasc Electrophysiol **12**(12): 1369-78.

- Entcheva, E. and H. Bien (2006). "Macroscopic optical mapping of excitation in cardiac cell networks with ultra-high spatiotemporal resolution." Prog Biophys Mol Biol **92**(2): 232-57.
- Farrell, D. M., C. C. Wei, et al. (2001). "Angiotensin II modulates catecholamine release into interstitial fluid of canine myocardium in vivo." Am J Physiol Heart Circ Physiol **281**(2): H813-22.
- Fedorov, V. V., I. T. Lozinsky, et al. (2007). "Application of blebbistatin as an excitation-contraction uncoupler for electrophysiologic study of rat and rabbit hearts." Heart Rhythm **4**(5): 619-26.
- Fischmeister R, H. H. (1987). "Cyclic guanosine 3',5'-monophosphate regulates the calcium current in single cells from frog ventricle." J Physiol **387**: 453-72.
- Fleming, J. W., R. A. Strawbridge, et al. (1987). "Muscarinic receptor regulation of cardiac adenylate cyclase activity." J Mol Cell Cardiol **19**(1): 47-61.
- Fogoros, R. N. (2006). Electrophysiologic Testing. Malden, Blackwell Publisher.
- Fontaine, G., Frank, R., Welti, J. J., and Grospegat, Y (1979). "Electrophysiology of torsade de pointes. In Proceedings of the VIth world symposium on cardiac pacing." Pacesymp Montreal.
- Fox, J. J., M. L. Riccio, et al. (2002). "Spatiotemporal transition to conduction block in canine ventricle." Circ Res **90**(3): 289-96.
- Fozzard, H. A., Hanck, D.A. (1992). The Heart and Cardiovascular system: Scientific Foundations. New York, Raven Press Ltd.
- Franz, M., M. Schottler, et al. (1980). "Simultaneous recording of monophasic action potentials and contractile force from the human heart." Klin Wochenschr **58**(24): 1357-9.
- Franz, M. R. (1983). "Long-term recording of monophasic action potentials from human endocardium." Am J Cardiol **51**(10): 1629-34.
- Franz, M. R. (1991). "Method and theory of monophasic action potential recording." Prog Cardiovasc Dis **33**(6): 347-68.
- Franz, M. R. (1999). "Current status of monophasic action potential recording: theories, measurements and interpretations." Cardiovasc Res **41**(1): 25-40.
- Franz, M. R. (2003). "The electrical restitution curve revisited: steep or flat slope--which is better?" J Cardiovasc Electrophysiol **14**(10 Suppl): S140-7.
- Franz MR, B. D., Lakatta EG, Weisfeldt ML. (1989). Monophasic action potential recording by contact electrode technique: In vitro validation and clinical applications. London, Farrand Press.
- Franz, M. R., D. Burkhoff, et al. (1986). "In vitro validation of a new cardiac catheter technique for recording monophasic action potentials." Eur Heart J **7**(1): 34-41.
- Gbadebo, T. D., R. W. Trimble, et al. (2002). "Calmodulin inhibitor W-7 unmasks a novel electrocardiographic parameter that predicts initiation of torsade de pointes." Circulation **105**(6): 770-4.
- Gillespie, J. S. and T. C. Muir (1967). "A method of stimulating the complete sympathetic outflow from the spinal cord to blood vessels in the pithed rat." Br J Pharmacol Chemother **30**(1): 78-87.
- Gilmour, R. F., Jr. (2003). "A novel approach to identifying antiarrhythmic drug targets." Drug Discov Today **8**(4): 162-7.
- Gilmour, R. F., Jr. and D. R. Chialvo (1999). "Electrical restitution, critical mass, and the riddle of fibrillation." J Cardiovasc Electrophysiol **10**(8): 1087-9.

- Gilmour, R. F., Jr., N. F. Otani, et al. (1997). "Memory and complex dynamics in cardiac Purkinje fibers." Am J Physiol **272**(4 Pt 2): H1826-32.
- Girouard, S. D., K. R. Laurita, et al. (1996). "Unique properties of cardiac action potentials recorded with voltage-sensitive dyes." J Cardiovasc Electrophysiol **7**(11): 1024-38.
- Goldhaber, J. I., L. H. Xie, et al. (2005). "Action potential duration restitution and alternans in rabbit ventricular myocytes: the key role of intracellular calcium cycling." Circ Res **96**(4): 459-66.
- Grandi, E., J. L. Puglisi, et al. (2007). "Simulation of Ca/Calmodulin-dependent protein kinase II on rabbit ventricular myocyte ion currents and action potentials." Biophys J.
- Grant, A. O. W., D.W.,Wendt,D.J. (1995). Cardiac Electrophysiology,Cell to Bedside. Philadelphia, WB Saunders Company.
- Gullo, F., E. Ales, et al. (2003). "ERG K<sup>+</sup> channel blockade enhances firing and epinephrine secretion in rat chromaffin cells: the missing link to LQT2-related sudden death?" Faseb J **17**(2): 330-2.
- Gupta, A., A. T. Lawrence, et al. (2007). "Current concepts in the mechanisms and management of drug-induced QT prolongation and torsade de pointes." Am Heart J **153**(6): 891-9.
- Haas, H. G. (1960). "[Contribution to the theory of the ventricular gradient.]." Cardiologia **36**: 321-36.
- Han, J., P. Garciadejalon, et al. (1964). "Adrenergic Effects on Ventricular Vulnerability." Circ Res **14**: 516-24.
- Hartzell, H. C. (1988). "Regulation of cardiac ion channels by catecholamines, acetylcholine and second messenger systems." Prog Biophys Mol Biol **52**(3): 165-247.
- Haws, C. W. and R. L. Lux (1990). "Correlation between in vivo transmembrane action potential durations and activation-recovery intervals from electrograms. Effects of interventions that alter repolarization time." Circulation **81**(1): 281-8.
- Hayashi, H., Y. Miyauchi, et al. (2003). "Effects of cytochalasin D on electrical restitution and the dynamics of ventricular fibrillation in isolated rabbit heart." J Cardiovasc Electrophysiol **14**(10): 1077-84.
- Heath, B. M. and D. A. Terrar (2000). "Protein kinase C enhances the rapidly activating delayed rectifier potassium current, I<sub>Kr</sub>, through a reduction in C-type inactivation in guinea-pig ventricular myocytes." J Physiol **522 Pt 3**: 391-402.
- Hille, B. (1992). Ionic channels of Excitable Membranes. Massachusetts, Sinauer Associate Inc.
- Hirano, Y., H. A. Fozzard, et al. (1989). "Characteristics of L- and T-type Ca<sup>2+</sup> currents in canine cardiac Purkinje cells." Am J Physiol **256**(5 Pt 2): H1478-92.
- Hoffman, B. F., P. F. Cranefield, et al. (1959). "Comparison of cardiac monophasic action potentials recorded by intracellular and suction electrodes." Am J Physiol **196**(6): 1297-301.
- Hoorntje, T., M. Alders, et al. (1999). "Homozygous premature truncation of the HERG protein : the human HERG knockout." Circulation **100**(12): 1264-7.
- Hoshi, T., W. N. Zagotta, et al. (1990). "Biophysical and molecular mechanisms of Shaker potassium channel inactivation." Science **250**(4980): 533-8.
- Ino, T., H. S. Karagueuzian, et al. (1988). "Relation of monophasic action potential recorded with contact electrode to underlying transmembrane action potential properties in isolated cardiac tissues: a systematic microelectrode validation study." Cardiovasc Res **22**(4): 255-64.

- Ishihara, K., T. Mitsuiye, et al. (1989). "The Mg<sup>2+</sup> block and intrinsic gating underlying inward rectification of the K<sup>+</sup> current in guinea-pig cardiac myocytes." J Physiol **419**: 297-320.
- January, C. T. and J. M. Riddle (1989). "Early afterdepolarizations: mechanism of induction and block. A role for L-type Ca<sup>2+</sup> current." Circ Res **64**(5): 977-90.
- Jervell, A. and F. Lange-Nielsen (1957). "Congenital deaf-mutism, functional heart disease with prolongation of the Q-T interval and sudden death." Am Heart J **54**(1): 59-68.
- Kagan, A., Y. F. Melman, et al. (2002). "14-3-3 amplifies and prolongs adrenergic stimulation of HERG K<sup>+</sup> channel activity." Embo J **21**(8): 1889-98.
- Karma, A. (1994). "Electrical alternans and spiral wave breakup in cardiac tissue." Chaos **4**(3): 461-472.
- Katz, A. (1992). Physiology of the Heart. New York, NY, Raven Press.
- Kawano, H., R. Okada, et al. (2003). "Histological study on the distribution of autonomic nerves in the human heart." Heart Vessels **18**(1): 32-9.
- Keating, M. T. and M. C. Sanguinetti (2001). "Molecular and cellular mechanisms of cardiac arrhythmias." Cell **104**(4): 569-80.
- Kenneth Jochim, L. N. K., and Walter Mayne (1935). "The Monophasic Electrogram obtained from the Mammalian Heart " Am J Physiol(111): 187-191.
- Kenneth R Laurita, I. L. (2001). Optics and detectors used in Optical mapping. Armonk, Futura.
- Kenneth R Laurita, J. M. P. a. D. S. R. (2001). Mapping of Arrhythmia Substrates Related to Repolarization. Armonk NY, Futura publishing company.
- Keren, A., D. Tzivoni, et al. (1981). "Etiology, warning signs and therapy of torsade de pointes. A study of 10 patients." Circulation **64**(6): 1167-74.
- Kettlewell, S., N. L. Walker, et al. (2004). "The electrophysiological and mechanical effects of 2,3-butane-dione monoxime and cytochalasin-D in the Langendorff perfused rabbit heart." Exp Physiol **89**(2): 163-72.
- Kihara, Y., W. Grossman, et al. (1989). "Direct measurement of changes in intracellular calcium transients during hypoxia, ischemia, and reperfusion of the intact mammalian heart." Circ Res **65**(4): 1029-44.
- Kline, R. P. and M. Morad (1978). "Potassium efflux in heart muscle during activity: extracellular accumulation and its implications." J Physiol **280**: 537-58.
- Knisley, S. B. (1995). "Transmembrane voltage changes during unipolar stimulation of rabbit ventricle." Circ Res **77**(6): 1229-39.
- Knisley, S. B., R. K. Justice, et al. (2000). "Ratiometry of transmembrane voltage-sensitive fluorescent dye emission in hearts." Am J Physiol Heart Circ Physiol **279**(3): H1421-33.
- Kobayashi, O., H. Nagashima, et al. (1987). "Direct evidence that pancuronium and gallamine enhance the release of norepinephrine from the atrial sympathetic nerve by inhibiting prejunctional muscarinic receptors." J Auton Nerv Syst **18**(1): 55-60.
- Koller, M. L., M. L. Riccio, et al. (1998). "Dynamic restitution of action potential duration during electrical alternans and ventricular fibrillation." Am J Physiol **275**(5 Pt 2): H1635-42.
- Kondo, M., V. Nesterenko, et al. (2004). "Cellular basis for the monophasic action potential. Which electrode is the recording electrode?" Cardiovasc Res **63**(4): 635-44.
- Koumi, S., R. Sato, et al. (1997). "Activation of inwardly rectifying potassium channels by muscarinic receptor-linked G protein in isolated human ventricular myocytes." J Membr Biol **157**(1): 71-81.

- Koumi, S. and J. A. Wasserstrom (1994). "Acetylcholine-sensitive muscarinic K<sup>+</sup> channels in mammalian ventricular myocytes." Am J Physiol **266**(5 Pt 2): H1812-21.
- La Rovere, M. T., J. T. Bigger, Jr., et al. (1998). "Baroreflex sensitivity and heart-rate variability in prediction of total cardiac mortality after myocardial infarction. ATRAMI (Autonomic Tone and Reflexes After Myocardial Infarction) Investigators." Lancet **351**(9101): 478-84.
- Laflamme, M. A. and P. L. Becker (1996). "Ca<sup>2+</sup>-induced current oscillations in rabbit ventricular myocytes." Circ Res **78**(4): 707-16.
- Lankipalli, R. S., T. Zhu, et al. (2005). "Mechanisms underlying arrhythmogenesis in long QT syndrome." J Electrocardiol **38**(4 Suppl): 69-73.
- LazzaraR, S. B., Robinson MJ, and Samet P (1973). "Selective in situ parasympathetic control of the canine sinoatrial and atrioventricular nodes." Circ Res(32): 393-401.
- Lee, M. H., S. F. Lin, et al. (2001). "Effects of diacetyl monoxime and cytochalasin D on ventricular fibrillation in swine right ventricles." Am J Physiol Heart Circ Physiol **280**(6): H2689-96.
- Levi, A. J., G. R. Dalton, et al. (1997). "Role of intracellular sodium overload in the genesis of cardiac arrhythmias." J Cardiovasc Electrophysiol **8**(6): 700-21.
- Lindemann, J. P. and A. M. Watanabe (1985). "Muscarinic cholinergic inhibition of beta-adrenergic stimulation of phospholamban phosphorylation and Ca<sup>2+</sup> transport in guinea pig ventricles." J Biol Chem **260**(24): 13122-9.
- Liu, D. W. and C. Antzelevitch (1995). "Characteristics of the delayed rectifier current (I<sub>Kr</sub> and I<sub>Ks</sub>) in canine ventricular epicardial, midmyocardial, and endocardial myocytes. A weaker I<sub>Ks</sub> contributes to the longer action potential of the M cell." Circ Res **76**(3): 351-65.
- Liu, J. and K. R. Laurita (2005). "The mechanism of pause-induced torsade de pointes in long QT syndrome." J Cardiovasc Electrophysiol **16**(9): 981-7.
- Liu T, C. B. a. S. G. (2001). "Simultaneous maps of optical action potentials (APs) and intracellular Ca<sup>2+</sup> transients (Cai) in a rabbit model of LQT3: Role of Cai handling in the initiation of early afterdepolarization and arrhythmias." Circulation **104**(SUPPLS): 515.
- Liu, Y., C. Cabo, et al. (1993). "Effects of diacetyl monoxime on the electrical properties of sheep and guinea pig ventricular muscle." Cardiovasc Res **27**(11): 1991-7.
- Livshitz, L. M. and Y. Rudy (2007). "Regulation of Ca<sup>2+</sup> and electrical alternans in cardiac myocytes: role of CAMKII and repolarizing currents." Am J Physiol Heart Circ Physiol **292**(6): H2854-66.
- Loew, L. M., L. B. Cohen, et al. (1992). "A naphthyl analog of the aminostyryl pyridinium class of potentiometric membrane dyes shows consistent sensitivity in a variety of tissue, cell, and model membrane preparations." J Membr Biol **130**(1): 1-10.
- Loew, L. M., L. B. Cohen, et al. (1985). "Charge-shift probes of membrane potential. Characterization of aminostyrylpyridinium dyes on the squid giant axon." Biophys J **47**(1): 71-7.
- Loew, L. M. and L. L. Simpson (1981). "Charge-shift probes of membrane potential: a probable electrochromic mechanism for p-aminostyrylpyridinium probes on a hemispherical lipid bilayer." Biophys J **34**(3): 353-65.
- Loffelholz, K. and E. Muscholl (1969). "A muscarinic inhibition of the noradrenaline release evoked by postganglionic sympathetic nerve stimulation." Naunyn Schmiedebergs Arch Pharmakol **265**(1): 1-15.

- London, B., L. C. Baker, et al. (2007). "Dispersion of repolarization and refractoriness are determinants of arrhythmia phenotype in transgenic mice with long QT." *J Physiol* **578**(Pt 1): 115-29.
- Lopatin, A. N., E. N. Makhina, et al. (1994). "Potassium channel block by cytoplasmic polyamines as the mechanism of intrinsic rectification." *Nature* **372**(6504): 366-9.
- Luo, C. H. and Y. Rudy (1994). "A dynamic model of the cardiac ventricular action potential. II. Afterdepolarizations, triggered activity, and potentiation." *Circ Res* **74**(6): 1097-113.
- Lupoglazoff, J. M., T. Cheav, et al. (2001). "Homozygous SCN5A mutation in long-QT syndrome with functional two-to-one atrioventricular block." *Circ Res* **89**(2): E16-21.
- M.Loew, L. (2001). *Mechanisms and Principles of Voltage sensitive Fluorescence*. Armonk, Futura.
- MacGowan, G. A., C. Du, et al. (2001). "Rhod-2 based measurements of intracellular calcium in the perfused mouse heart: cellular and subcellular localization and response to positive inotropy." *J Biomed Opt* **6**(1): 23-30.
- Mantravadi, R., B. Gabris, et al. (2007). "Autonomic nerve stimulation reverses ventricular repolarization sequence in rabbit hearts." *Circ Res* **100**(7): e72-80.
- Marban, E., M. Kitakaze, et al. (1987). "Intracellular free calcium concentration measured with <sup>19</sup>F NMR spectroscopy in intact ferret hearts." *Proc Natl Acad Sci U S A* **84**(16): 6005-9.
- Mark Anderson, D. R. (2004). *Cardiology*. Philadelphia, Elsevier.
- Marx, S. O., J. Kurokawa, et al. (2002). "Requirement of a macromolecular signaling complex for beta adrenergic receptor modulation of the KCNQ1-KCNE1 potassium channel." *Science* **295**(5554): 496-9.
- McDonald, T. F., S. Pelzer, et al. (1994). "Regulation and modulation of calcium channels in cardiac, skeletal, and smooth muscle cells." *Physiol Rev* **74**(2): 365-507.
- Medeiros-Domingo, A., T. Kaku, et al. (2007). "SCN4B-encoded sodium channel beta4 subunit in congenital long-QT syndrome." *Circulation* **116**(2): 134-42.
- Millar, C. K., F. A. Kralios, et al. (1985). "Correlation between refractory periods and activation-recovery intervals from electrograms: effects of rate and adrenergic interventions." *Circulation* **72**(6): 1372-9.
- Miura, M., N. Ishide, et al. (1995). "Diversity of early afterdepolarizations in guinea pig myocytes: spatial characteristics of intracellular Ca<sup>2+</sup> concentration." *Heart Vessels* **10**(5): 266-74.
- Miura, M., N. Ishide, et al. (1993). "Spatial features of calcium transients during early and delayed afterdepolarizations." *Am J Physiol* **265**(2 Pt 2): H439-44.
- Mohler, P. J., J. J. Schott, et al. (2003). "Ankyrin-B mutation causes type 4 long-QT cardiac arrhythmia and sudden cardiac death." *Nature* **421**(6923): 634-9.
- Mohler, P. J. and X. H. Wehrens (2007). "Mechanisms of human arrhythmia syndromes: abnormal cardiac macromolecular interactions." *Physiology (Bethesda)* **22**: 342-50.
- Moore, H. J. and M. R. Franz (2007). "Monophasic action potential recordings in humans." *J Cardiovasc Electrophysiol* **18**(7): 787-90.
- Moss, A. J., P. J. Schwartz, et al. (1985). "The long QT syndrome: a prospective international study." *Circulation* **71**(1): 17-21.
- Moss, A. J., P. J. Schwartz, et al. (1991). "The long QT syndrome. Prospective longitudinal study of 328 families." *Circulation* **84**(3): 1136-44.
- Murray KT, S. D., Bennett PB (1990). "Isoproterenol increases the cardiac sodium current in the presence of buffered Ca<sup>++</sup>." *Circulation* **82**((suppl III):III-522).

- Naik, A. (2007). "Long QT syndrome revisited." J Assoc Physicians India **55 Suppl**: 58-61.
- Nathan, D. and G. W. Beeler, Jr. (1975). "Electrophysiologic correlates of the inotropic effects of isoproterenol in canine myocardium." J Mol Cell Cardiol **7**(1): 1-15.
- Nerbonne, J. M. and R. S. Kass (2005). "Molecular physiology of cardiac repolarization." Physiol Rev **85**(4): 1205-53.
- Ng, G. A., K. E. Brack, et al. (2001). "Effects of direct sympathetic and vagus nerve stimulation on the physiology of the whole heart--a novel model of isolated Langendorff perfused rabbit heart with intact dual autonomic innervation." Exp Physiol **86**(3): 319-29.
- Ng, G. A., K. E. Brack, et al. (2007). "Autonomic modulation of electrical restitution, alternans and ventricular fibrillation initiation in the isolated heart." Cardiovasc Res **73**(4): 750-60.
- Nichols, C. G. and A. N. Lopatin (1997). "Inward rectifier potassium channels." Annu Rev Physiol **59**: 171-91.
- Nichols, C. G., E. N. Makhina, et al. (1996). "Inward rectification and implications for cardiac excitability." Circ Res **78**(1): 1-7.
- Nolan, J., P. D. Batin, et al. (1998). "Prospective study of heart rate variability and mortality in chronic heart failure: results of the United Kingdom heart failure evaluation and assessment of risk trial (UK-heart)." Circulation **98**(15): 1510-6.
- Nolasco, J. B. and R. W. Dahlen (1968). "A graphic method for the study of alternation in cardiac action potentials." J Appl Physiol **25**(2): 191-6.
- Nordin, C. (1997). "Computer model of electrophysiological instability in very small heterogeneous ventricular syncytia." Am J Physiol **272**(4 Pt 2): H1838-56.
- Ono, K. and W. Trautwein (1991). "Potentiation by cyclic GMP of beta-adrenergic effect on Ca<sup>2+</sup> current in guinea-pig ventricular cells." J Physiol **443**: 387-404.
- Opthof, T., A. R. Misier, et al. (1991). "Dispersion of refractoriness in canine ventricular myocardium. Effects of sympathetic stimulation." Circ Res **68**(5): 1204-15.
- P.Haugland, R. Handbook of fluorescent Probes and research chemicals Molecular Probes.
- Panfilov, A. V. (1998). "Spiral breakup as a model of ventricular fibrillation." Chaos **8**(1): 57-64.
- Pauza DH, S. V., Puzine N, and Stropus R. (2000). "Morphology, distribution, and variability of epicardial neural ganglionated subplexus in the human heart." Anat Rec(259): 353-382.
- Pipberger, H., L. Schwartz, et al. (1957). "Studies on the nature of the repolarization process." Ann N Y Acad Sci **65**(6): 924-31.
- Poelzing, S., F. G. Akar, et al. (2004). "Heterogeneous connexin43 expression produces electrophysiological heterogeneities across ventricular wall." Am J Physiol Heart Circ Physiol **286**(5): H2001-9.
- Poelzing, S. and D. S. Rosenbaum (2004). "Altered connexin43 expression produces arrhythmia substrate in heart failure." Am J Physiol Heart Circ Physiol **287**(4): H1762-70.
- Pourrier, M., S. Zicha, et al. (2003). "Canine ventricular KCNE2 expression resides predominantly in Purkinje fibers." Circ Res **93**(3): 189-91.
- Priori, S. G., P. J. Schwartz, et al. (1998). "A recessive variant of the Romano-Ward long-QT syndrome?" Circulation **97**(24): 2420-5.
- Priori, S. G., P. J. Schwartz, et al. (2003). "Risk stratification in the long-QT syndrome." N Engl J Med **348**(19): 1866-74.
- Qu, Z., J. N. Weiss, et al. (1999). "Cardiac electrical restitution properties and stability of reentrant spiral waves: a simulation study." Am J Physiol **276**(1 Pt 2): H269-83.

- Quan, X. Q., R. Bai, et al. (2007). "Increasing Gap Junction Coupling Reduces Transmural Dispersion of Repolarization and Prevents Torsade de Pointes in Rabbit LQT3 Model." J Cardiovasc Electrophysiol.
- Randall, W. a. A., JL. (1985). "Selective parasympathectomy of automatic and conductile tissues of the canine heart." Am J Physiol(248): H61-H68.
- Ratzlaff, E. H. and A. Grinvald (1991). "A tandem-lens epifluorescence microscope: hundred-fold brightness advantage for wide-field imaging." J Neurosci Methods **36**(2-3): 127-37.
- Remme, C. A. and C. R. Bezzina (2007). "Genetic modulation of cardiac repolarization reserve." Heart Rhythm **4**(5): 608-10.
- Restivo, M., E. B. Caref, et al. (2004). "Spatial dispersion of repolarization is a key factor in the arrhythmogenicity of long QT syndrome." J Cardiovasc Electrophysiol **15**(3): 323-31.
- Roden, D. M. (2006). "Long QT syndrome: reduced repolarization reserve and the genetic link." J Intern Med **259**(1): 59-69.
- Roden, D. M. (2008). "Clinical practice. Long-QT syndrome." N Engl J Med **358**(2): 169-76.
- Rohde, G. K., B. M. Dawant, et al. (2005). "Correction of motion artifact in cardiac optical mapping using image registration." IEEE Trans Biomed Eng **52**(2): 338-41.
- Rohr, S. and J. P. Kucera (1998). "Optical recording system based on a fiber optic image conduit: assessment of microscopic activation patterns in cardiac tissue." Biophys J **75**(2): 1062-75.
- Romano C, G. G., Pongiglione R (1963). "Aritmie cardiache rare dell'eta' pediatrica." Clin Pediatr(45): 656-683
- Rosati, B., Z. Pan, et al. (2001). "Regulation of KChIP2 potassium channel beta subunit gene expression underlies the gradient of transient outward current in canine and human ventricle." J Physiol **533**(Pt 1): 119-25.
- Rosenbaum, D. S. (2001). Optical Mapping of Cardiac Excitation and Arrhythmias. Armonk, Futura publisher
- Rosenbaum, D. S., D. T. Kaplan, et al. (1991). "Repolarization inhomogeneities in ventricular myocardium change dynamically with abrupt cycle length shortening." Circulation **84**(3): 1333-45.
- Saffitz, J. E., L. M. Davis, et al. (1995). "The molecular basis of anisotropy: role of gap junctions." J Cardiovasc Electrophysiol **6**(6): 498-510.
- Salama, G. (2001). Historical perspective of optical mapping. Armonk, Futura Publishing Company.
- Salama, G. and B. R. Choi (2000). "Images of Action Potential Propagation in Heart." News Physiol Sci **15**: 33-41.
- Salama G, H. D., Efimov IR (1993). "Changes in activation and repolarization patterns during cardiac hypoxia, no-flow ischemia, and partial-flow ischemia measured with voltage-sensitive dyes and imaging techniques." Prog Int Union Physiol Sci(3): 174-198.
- Salama, G., R. Lombardi, et al. (1987). "Maps of optical action potentials and NADH fluorescence in intact working hearts." Am J Physiol **252**(2 Pt 2): H384-94.
- Salama, G. and M. Morad (1976). "Merocyanine 540 as an optical probe of transmembrane electrical activity in the heart." Science **191**(4226): 485-7.

- Sanguinetti, M. C., N. K. Jurkiewicz, et al. (1991). "Isoproterenol antagonizes prolongation of refractory period by the class III antiarrhythmic agent E-4031 in guinea pig myocytes. Mechanism of action." Circ Res **68**(1): 77-84.
- Sanguinetti, M. C., Jurkiewicz, N.K. (1993). Delayed rectifier Potassium channels of Cardiac muscle. New York, Futura Publishing Co., Inc.
- Sasaki, S., K. Daitoku, et al. (2000). "NO is involved in MCh-induced accentuated antagonism via type II PDE in the canine blood-perfused SA node." Am J Physiol Heart Circ Physiol **279**(5): H2509-18.
- Schouten, V. J. (1990). "Interval dependence of force and twitch duration in rat heart explained by Ca<sup>2+</sup> pump inactivation in sarcoplasmic reticulum." J Physiol **431**: 427-44.
- Schwartz, P. J. (1998). "The autonomic nervous system and sudden death." Eur Heart J **19 Suppl F**: F72-80.
- Schwartz, P. J. (2005). "Management of long QT syndrome." Nat Clin Pract Cardiovasc Med **2**(7): 346-51.
- Schwartz, P. J., A. J. Moss, et al. (1993). "Diagnostic criteria for the long QT syndrome. An update." Circulation **88**(2): 782-4.
- Schwartz, P. J., S. G. Priori, et al. (2001). "Genotype-phenotype correlation in the long-QT syndrome: gene-specific triggers for life-threatening arrhythmias." Circulation **103**(1): 89-95.
- Sesti, F., G. W. Abbott, et al. (2000). "A common polymorphism associated with antibiotic-induced cardiac arrhythmia." Proc Natl Acad Sci U S A **97**(19): 10613-8.
- Shimizu, W. and C. Antzelevitch (2000). "Differential effects of beta-adrenergic agonists and antagonists in LQT1, LQT2 and LQT3 models of the long QT syndrome." J Am Coll Cardiol **35**(3): 778-86.
- Silva, J. and Y. Rudy (2005). "Subunit interaction determines IKs participation in cardiac repolarization and repolarization reserve." Circulation **112**(10): 1384-91.
- Sims, C., Viswanathan P.C., Colflesh D., Reisenweber, S., Walker W., Salama, G (2007). "Sex, Age, and regional differences in I<sub>CaL</sub> modulates EAD vulnerability in a rabbit Model of LQT2." Heart Rhythm **4**(5S): S156 (PO2-42).
- Sperelakis, N., Y. Katsube, et al. (1996). "Regulation of the slow Ca<sup>++</sup> channels of myocardial cells." Mol Cell Biochem **163-164**: 85-98.
- Splawski, I., K. W. Timothy, et al. (2005). "Severe arrhythmia disorder caused by cardiac L-type calcium channel mutations." Proc Natl Acad Sci U S A **102**(23): 8089-96; discussion 8086-8.
- Steenbergen, C., E. Murphy, et al. (1987). "Elevation in cytosolic free calcium concentration early in myocardial ischemia in perfused rat heart." Circ Res **60**(5): 700-7.
- Sulakhe, P. V. and X. T. Vo (1995). "Regulation of phospholamban and troponin-I phosphorylation in the intact rat cardiomyocytes by adrenergic and cholinergic stimuli: roles of cyclic nucleotides, calcium, protein kinases and phosphatases and depolarization." Mol Cell Biochem **149-150**: 103-26.
- Szentadrassy, N., T. Banyasz, et al. (2005). "Apico-basal inhomogeneity in distribution of ion channels in canine and human ventricular myocardium." Cardiovasc Res **65**(4): 851-60.
- Taggart, N. W., C. M. Haglund, et al. (2007). "Diagnostic miscues in congenital long-QT syndrome." Circulation **115**(20): 2613-20.
- Taggart, P., P. Sutton, et al. (2003). "Effect of adrenergic stimulation on action potential duration restitution in humans." Circulation **107**(2): 285-9.

- Taggart, P., P. Sutton, et al. (1990). "Interplay between adrenaline and interbeat interval on ventricular repolarisation in intact heart in vivo." Cardiovasc Res **24**(11): 884-95.
- Tai, D. C., B. J. Caldwell, et al. (2004). "Correction of motion artifact in transmembrane voltage-sensitive fluorescent dye emission in hearts." Am J Physiol Heart Circ Physiol **287**(3): H985-93.
- Thomas, D., W. Zhang, et al. (1999). "Deletion of protein kinase A phosphorylation sites in the HERG potassium channel inhibits activation shift by protein kinase A." J Biol Chem **274**(39): 27457-62.
- Thomas, G. P., U. Gerlach, et al. (2003). "HMR 1556, a potent and selective blocker of slowly activating delayed rectifier potassium current." J Cardiovasc Pharmacol **41**(1): 140-7.
- Thomsen, M. B., A. Oros, et al. (2007). "Proarrhythmic electrical remodelling is associated with increased beat-to-beat variability of repolarisation." Cardiovasc Res **73**(3): 521-30.
- Tohse, N., M. Kameyama, et al. (1987). "Intracellular Ca<sup>2+</sup> and protein kinase C modulate K<sup>+</sup> current in guinea pig heart cells." Am J Physiol **253**(5 Pt 2): H1321-4.
- Tristani-Firouzi, M., J. L. Jensen, et al. (2002). "Functional and clinical characterization of KCNJ2 mutations associated with LQT7 (Andersen syndrome)." J Clin Invest **110**(3): 381-8.
- van Opstal JM, S. M., Verduyn SC "Chronic Amiodarone evokes no Torsade de Pointes arrhythmias despite QT lengthening in an animal model of acquired Long-QT Syndrome." Circulation **104**: 2722-7.
- Vandecasteele, G., T. Eschenhagen, et al. (1998). "Role of the NO-cGMP pathway in the muscarinic regulation of the L-type Ca<sup>2+</sup> current in human atrial myocytes." J Physiol **506 ( Pt 3)**: 653-63.
- Vatta, M., M. J. Ackerman, et al. (2006). "Mutant caveolin-3 induces persistent late sodium current and is associated with long-QT syndrome." Circulation **114**(20): 2104-12.
- Veldkamp, M. W., R. Wilders, et al. (2003). "Contribution of sodium channel mutations to bradycardia and sinus node dysfunction in LQT3 families." Circ Res **92**(9): 976-83.
- Verrecchia, F. and J. C. Herve (1997). "Reversible blockade of gap junctional communication by 2,3-butanedione monoxime in rat cardiac myocytes." Am J Physiol **272**(3 Pt 1): C875-85.
- Vincent, G. M. (1998). "The molecular genetics of the long QT syndrome: genes causing fainting and sudden death." Annu Rev Med **49**: 263-74.
- Viskin, S. (1999). "Long QT syndromes and torsade de pointes." Lancet **354**(9190): 1625-33.
- Viswanathan, P. C. and Y. Rudy (1999). "Pause induced early afterdepolarizations in the long QT syndrome: a simulation study." Cardiovasc Res **42**(2): 530-42.
- Volders PG, K. A., Vos MA, Sipido KR, Wellens HJ, Lazzara R, Szabo B. (1997). "Similarities between early and delayed afterdepolarizations induced by isoproterenol in canine ventricular myocytes." Cardiovasc Res **34**(2): 348-59.
- Volders, P. G., M. Stengl, et al. (2003). "Probing the contribution of IKs to canine ventricular repolarization: key role for beta-adrenergic receptor stimulation." Circulation **107**(21): 2753-60.
- Vos, M. A., S. H. de Groot, et al. (1998). "Enhanced susceptibility for acquired torsade de pointes arrhythmias in the dog with chronic, complete AV block is related to cardiac hypertrophy and electrical remodeling." Circulation **98**(11): 1125-35.
- Vos, M. A., S. C. Verduyn, et al. (1995). "Reproducible induction of early afterdepolarizations and torsade de pointes arrhythmias by d-sotalol and pacing in dogs with chronic atrioventricular block." Circulation **91**(3): 864-72.

- Wainger, B. J., M. DeGennaro, et al. (2001). "Molecular mechanism of cAMP modulation of HCN pacemaker channels." Nature **411**(6839): 805-10.
- Walsh, K. B. and R. S. Kass (1988). "Regulation of a heart potassium channel by protein kinase A and C." Science **242**(4875): 67-9.
- Wan, B., C. Doumen, et al. (1993). "Effects of cardiac work on electrical potential gradient across mitochondrial membrane in perfused rat hearts." Am J Physiol **265**(2 Pt 2): H453-60.
- Ward, O. C. (1964). "A New Familial Cardiac Syndrome In Children." J Ir Med Assoc **54**: 103-6.
- Watanabe, M. A. and M. L. Koller (2002). "Mathematical analysis of dynamics of cardiac memory and accommodation: theory and experiment." Am J Physiol Heart Circ Physiol **282**(4): H1534-47.
- WC, A. J. a. R. (1986). "Selective vagal innervation of sinoatrial and atrioventricular nodes in the canine heart." Am J Physiol(251): H764-H773.
- Wehrens, X. H. and A. R. Marks (2004). "Novel therapeutic approaches for heart failure by normalizing calcium cycling." Nat Rev Drug Discov **3**(7): 565-73.
- Witkowski, F. X., L. J. Leon, et al. (1998). "Spatiotemporal evolution of ventricular fibrillation." Nature **392**(6671): 78-82.
- Wu, R. and A. Patwardhan (2004). "Restitution of action potential duration during sequential changes in diastolic intervals shows multimodal behavior." Circ Res **94**(5): 634-41.
- Wu, R. and A. Patwardhan (2007). "Effects of rapid and slow potassium repolarization currents and calcium dynamics on hysteresis in restitution of action potential duration." J Electrocardiol **40**(2): 188-99.
- Yan, G. X., Y. Wu, et al. (2001). "Phase 2 early afterdepolarization as a trigger of polymorphic ventricular tachycardia in acquired long-QT syndrome : direct evidence from intracellular recordings in the intact left ventricular wall." Circulation **103**(23): 2851-6.
- Yang, Z. K., M. R. Boyett, et al. (1996). "Regional differences in the negative inotropic effect of acetylcholine within the canine ventricle." J Physiol **492 ( Pt 3)**: 789-806.
- Zhou, M., J. H. Morais-Cabral, et al. (2001). "Potassium channel receptor site for the inactivation gate and quaternary amine inhibitors." Nature **411**(6838): 657-61.
- Zhou, Z., Q. Gong, et al. (1998). "Properties of HERG channels stably expressed in HEK 293 cells studied at physiological temperature." Biophys J **74**(1): 230-41.
- Zygmunt, A. C., R. J. Goodrow, et al. (2000). "I(NaCa) contributes to electrical heterogeneity within the canine ventricle." Am J Physiol Heart Circ Physiol **278**(5): H1671-8.